

University of Groningen

Role of proteoglycans in renal chronic transplant dysfunction

Katta, Kirankumar

IMPORTANT NOTE: You are advised to consult the publisher's version (publisher's PDF) if you wish to cite from it. Please check the document version below.

Document Version

Publisher's PDF, also known as Version of record

Publication date:

2012

[Link to publication in University of Groningen/UMCG research database](#)

Citation for published version (APA):

Katta, K. (2012). *Role of proteoglycans in renal chronic transplant dysfunction*. s.n.

Copyright

Other than for strictly personal use, it is not permitted to download or to forward/distribute the text or part of it without the consent of the author(s) and/or copyright holder(s), unless the work is under an open content license (like Creative Commons).

The publication may also be distributed here under the terms of Article 25fa of the Dutch Copyright Act, indicated by the "Taverne" license. More information can be found on the University of Groningen website: <https://www.rug.nl/library/open-access/self-archiving-pure/taverne-amendment>.

Take-down policy

If you believe that this document breaches copyright please contact us providing details, and we will remove access to the work immediately and investigate your claim.

Downloaded from the University of Groningen/UMCG research database (Pure): <http://www.rug.nl/research/portal>. For technical reasons the number of authors shown on this cover page is limited to 10 maximum.

Role of Proteoglycans in Renal Chronic Transplant Dysfunction

Kirankumar Katta

Printing of this thesis was financially supported by:

GUIDE

University of Groningen

Novartis

Amgen

Astellas

Fresenius Medical Care Nederland BV

K. Katta

Role of Proteoglycans in Renal Chronic Transplant Dysfunction

Proefschrift Groningen, met literatuuropgave en samenvatting in het Nederlands

ISBN: 978-90-367-5538-2

ISBN electronic version: 978-90-367-5539-9

© Copyright 2012 K. Katta

All rights are reserved.

No part of this publication may be reproduced, stored in retrieval system, or transmitted in any form or by any means, without permission of the author.

Cover design: A. Reznichenko

Layout: C.R.C. Doorenbos

Printing: CPI Wöhrmann Print Service B.V., ZUTPHEN



**rijksuniversiteit
groningen**

Role of Proteoglycans in Renal Chronic Transplant Dysfunction

Proefschrift

ter verkrijging van het doctoraat in de
Medische Wetenschappen
aan de Rijksuniversiteit Groningen
op gezag van de
Rector Magnificus, dr. E. Sterken,
in het openbaar te verdedigen op
maandag 21 mei 2012
om 12.45 uur

door

Kirankumar Katta

geboren op 15 augustus 1984
te Vemulawada, India

Promotores:

Prof. dr. G. Navis
Prof. dr. J.L. Hillebrands

Copromotor:

Dr. J. van den Born

Beoordelingscommissie:

Prof. dr. R.A. Bank
Prof. dr. J. H. M. Berden
Prof. dr. L. Schaefer

ఈ రురిశోధన వ్యాసం అమ్మ నాన్న కి అంకితం

Paranimfen:

Pramod Kumar Agarwal
Miriam Boersema

Contents

Chapter 1	9
General introduction	
Chapter 2	31
Differential expression of proteoglycans in tissue remodeling and lymphangiogenesis after experimental renal transplantation in rats <i>PLoS One. 2010 Feb 5;5(2):e9095</i>	
Chapter 3	57
Renal heparan sulfate proteoglycans modulate FGF2 signaling in experimental chronic transplant dysfunction	
Chapter 4	79
Non-anticoagulant heparinoid reduces renal inflammation in experimental renal transplant dysfunction	
Chapter 5	97
Local medial microenvironment directs phenotypic modulation of smooth muscle cells after experimental renal transplantation <i>Am J Transplant. 2012 Mar 15. doi: 10.1111/j.1600-6143.2012.04001.x.</i>	
Chapter 6	125
Tubular epithelial syndecan-1 maintains renal function in murine ischemia/reperfusion and human transplantation <i>Kidney Int. 2012 Apr;81(7):651-61</i>	
Chapter 7	151
General discussion and future perspectives	
Nederlandse samenvatting voor niet-ingewijden	163
Dankwoord	169
Curriculum vitae	175

Chapter 1

General introduction

Renal transplantation

Kidney transplantation is the best treatment for patients with end stage renal failure, in terms of quality of life and life expectancy. Due to many reasons, such as increasing age of the general population and growing incidence of obesity and diabetes, the number of patients with end stage renal disease is increasing world-wide, and consequently, the demand for donor kidneys remains increasing. In 2010, in the Netherlands >800 kidney transplantations have been performed, half of them with donor kidneys from living donors. Within the Netherlands the waiting list for renal transplantation is >900 patients, with a waiting time for post-mortal kidneys of over 4 years (<http://www.renine.nl> and <http://www.nierstichting.nl>). Over the last decades the use of several potent new immune suppressive drugs after renal transplantation has led to a sharp decline in the incidence of acute rejection. Therefore, the focus of transplantation research moved towards long term graft survival, which remains sub-optimal because of progressive damage culminating in chronic transplant dysfunction, which has barely improved over the last 30 years (1).

Chronic transplant dysfunction

Chronic transplant dysfunction (CTD) is associated with decline in kidney function over time and is related to progressive tissue remodeling in the transplanted kidney. CTD is the second leading risk for graft loss (after death) and has an incidence of >70% already 2 years after transplantation based on biopsies without clear functional loss (2,3). The pathogenesis of CTD is multifactorial. It is believed that long term graft survival reflects the dual impact of immunologic and non-immunologic injury (4). Non-immunological risk factors include hypertension, hyperlipidemia, hyperfiltration, calcineurin inhibitor toxicity (side effect of immunosuppressive drug), urological complications, smoking, and viral or bacterial infections (5). A close correlation has been found between the presence of proteinuria and worse allograft survival (6). Fibrosis/sclerosis is a major morphological characteristic occurring in most intrarenal microstructures, including the glomeruli, arteries and tubulo-interstitium, leading to glomerulosclerosis, transplant vasculopathy with neointima formation, and interstitial fibrosis, respectively (7).

Histopathological hallmarks of CTD

Focal segmental glomerulosclerosis (FSGS) - The sclerotic lesions of FSGS are characterized by diffuse effacement of podocyte foot processes, detachment and loss of podocytes from the glomerular basement membrane, obliterated capillaries, mesangial proliferation and matrix expansion (8,9). FSGS is the result of structural and functional abnormalities of podocytes, the glomerular epithelial cells that are involved in glomerular ultrafiltration (10). Thus, malfunctioning of podocytes results in proteinuria as well as

flattening of these cells with segmental sclerosis in FSGS. FSGS might be induced by various pathogenetic mechanisms including mutations in proteins that are specific to podocytes, steroid toxicities, bacterial and viral infections and glomerular hypertension (12). De novo FSGS has been reported after renal transplantation and is associated with transplant dysfunction and early graft loss (11-14).

Transplant Vasculopathy - Upon renal transplantation, the host immune system primarily responds to the renal vasculature of the allograft. In the arteries this results in progressive intimal thickening of the arteries, referred as transplant vasculopathy or arteriopathy, which contributes to renal allograft failure. The pathological features of transplant vasculopathy include the accumulation of migrated vascular smooth muscle cells (VSMCs) as well as immune cells such as macrophages and T-cells and extracellular matrix components within the neointimal lesions (15). In response to allo-transplantation, activation of VSMCs occurs, which in turn leads to the phenotypic modulation of VSMCs from a 'contractile and quiescent' into a 'synthetic and proliferative' phenotype. This phenotypic change is characterized by the production of extracellular matrix components and the loss of VSMC marker genes (16). Both macrophages and activated T cells are able to initiate and induce the proliferation or apoptosis of intimal cells, and can alter the synthesis of extracellular matrix components in the newly-formed intima (17,18). However, the precise mechanism underlying the pathogenesis of TV remains elusive.

Tubulo-interstitial damage - Interstitial fibrosis/tubular atrophy (IF/TA) is a main characteristic of chronic transplant dysfunction, and is often associated with progression to late graft loss (1). Interstitial fibrosis is characterized by excessive deposition of extracellular matrix in the tubular interstitium by myofibroblasts characterized by the expression of alpha-smooth muscle actin (α -SMA) (19). Tubular atrophy refers to flattening and loss of tubular epithelium and increased luminal size of the tubules, and is furthermore characterized by thickening of the tubular basement membranes (20,21). IF/TA is an irreversible histopathological entity that can be induced already early after transplantation and which is chronic, progressive and non-specific (22). Myofibroblasts are crucial cells which are involved in interstitial fibrosis due to their excessive production of extracellular matrix. In the kidney, myofibroblasts are derived from multiple cell types, including activated resident interstitial fibroblasts, bone marrow-derived cells, perivascular fibroblasts and pericytes, endothelial and tubular epithelial cells (19,23,24). Epithelial to mesenchymal transition (EMT) of tubular epithelium is also playing an important role in chronic allograft related interstitial fibrosis (25). Calcineurin inhibitors may result in interstitial fibrosis, and in particular cyclosporine A has been associated with the development of interstitial fibrosis (26). Many studies showed the role of infiltrating renal macrophages as mediators of interstitial fibrosis (27), indicating a role of influxed interstitial macrophages by directing the myofibroblasts.

Taken together, in CTD endothelial and epithelial activation is followed by the recruitment of inflammatory cells, mainly macrophages, which in turn activate mesenchymal cells such as vascular smooth muscle cells, mesangial cells and interstitial fibroblasts leading to renal tissue remodeling. In general, a large number of mediators such as cytokines, chemokines, growth factors and adhesion molecules are involved in tissue remodeling. Many of these mediators will only evoke cellular signaling in the presence of a proteoglycan co-receptor by the formation of a ternary signaling complex composed of mediator, high affinity receptor and low-affinity proteoglycan co-receptor. Indeed, proteoglycans have been highly implicated in tissue remodeling such as development, adhesion, migration, growth, wound healing and repair processes, proliferation and fibrosis (28,29). This implies that targeting proteoglycan function might provide a strategy to combat CTD-associated tissue remodeling. Therefore in the next paragraphs we further focus on proteoglycans in general and renal proteoglycans more specific.

Proteoglycans and glycosaminoglycans

Proteoglycans (PGs) are constituted by various core proteins to which linear, anionic polysaccharide, glycosaminoglycan (GAG) side chains are covalently conjugated (30). GAGs consist of repeating hexosamine and hexuronic acid disaccharide units (except keratan sulfate that comprise of repeating hexosamine and galactose disaccharides), with variable -N and/or -O sulfation. PGs are ubiquitously expressed and can be found throughout the extracellular matrix (ECM) including basement membranes and on virtually all cell surfaces (31). Based on their ability to interact with various proteins (see below), PGs mediate biological processes such as cell-cell and cell-matrix interactions, growth factor signaling cascades, chemokine and cytokine activation, tissue morphogenesis during development, cell migration and proliferation, and wound healing (28,29).

Based on the presence of different types of GAGs, PGs are mainly classified as heparan sulfate PGs (HSPGs), chondroitin sulfate PGs, dermatan sulfate PGs and keratan sulfate PGs. Hyaluronic acid (HA), unlike the other GAGs, is synthesized as a free GAG chain and is not linked to a core protein. HA is synthesized at the cytoplasmic surface of the plasma membrane rather than the endoplasmic reticulum and Golgi (32). Heparin is a highly modified HS produced by mast cells. During its biosynthesis heparin becomes attached to the serglycin protein core but is released as free heparin GAG chain (33). Since most of the studies in this thesis deal with HSPGs, the various HSPG families, HS biosynthesis and formation of functional domains is explained below.

Heparan sulfate proteoglycans

Depending on their core protein, the major HSPGs are classified as syndecans and glypicans (cell –surface HSPGs), and perlecan, agrin and collagen type XVIII (extracellular matrix HSPGs). The cell surface HSPGs consists of two major families: Firstly, the family of syndecans (members 1-4) belongs to the transmembrane cell surface HSPGs, consisting of ecto, transmembrane and cytoplasmic domains. Virtually all cell types, with the exception of erythrocytes, express at least one syndecan. Syndecans have pivotal roles during development, wound healing, inflammation, angiogenesis and tumor progression (28,34). Secondly, glypicans (members 1-6) are linked with a glycosyl-phosphatidylinositol anchor to the cell membrane. Glypicans display cell-type and development-stage-specific expression and are involved in various biological processes such as cell proliferation, differentiation and morphogenesis (35).

Agrin, perlecan and collagen type XVIII are the major extracellular HSPGs, which are abundantly present in basement membranes. Agrin, known to be expressed in the specialized basement membranes of the neuromuscular junction plays an important role in the development of synaptic apparatus (36,37). Apart from the neuromuscular junction, agrin is also widely expressed in the basement membranes of the kidney, lung and microvasculature (38-41). Perlecan plays a key role in the vasculature and angiogenesis (42). The HS residues on perlecan are able to interact with fibroblast growth factor-2 (FGF2), and were shown to participate in mitogenesis and angiogenesis *in vitro*, CHO cells and *in vivo* rabbit ear model respectively. Perlecan-HS bound FGF2 is presented to its high affinity receptor located on the cell surface (43,44). Collagen type XVIII, another basement membrane HSPG, has structural properties of both a collagen and a proteoglycan (45). Upon proteolytic cleavage of the C-terminus of collagen type XVIII, a domain called endostatin is released, which displays strong antiangiogenic effects (46). Generally collagen type XVIII is present in the basement membranes of the lung, retina, kidney and blood vessels (47,48) often in conjunction with perlecan (49).

Heparan sulfate biosynthesis and structural heterogeneity of Heparan sulfates

Proteoglycan synthesis starts by cellular uptake of building blocks (i.e. monosaccharides and sulphate) for GAG synthesis through specialized transporter complexes. By nucleotide metabolism in the cytoplasm, sugars and sulphates are then activated to form UDP-sugars and 3'-phosphoadenosine 5'-phosphosulphate (PAPs) respectively. The formed UDP-sugars and PAPs are translocated into the endoplasmic reticulum and Golgi by specific transporters (50,51). HS biosynthesis initiates by the assembly of a so-called linkage tetrasaccharide on specific serine residues (GlcA-Gal-Gal-Xyl-Ser) of the protein core molecule. The chain polymerizes by the alternating addition of two monosaccharide units

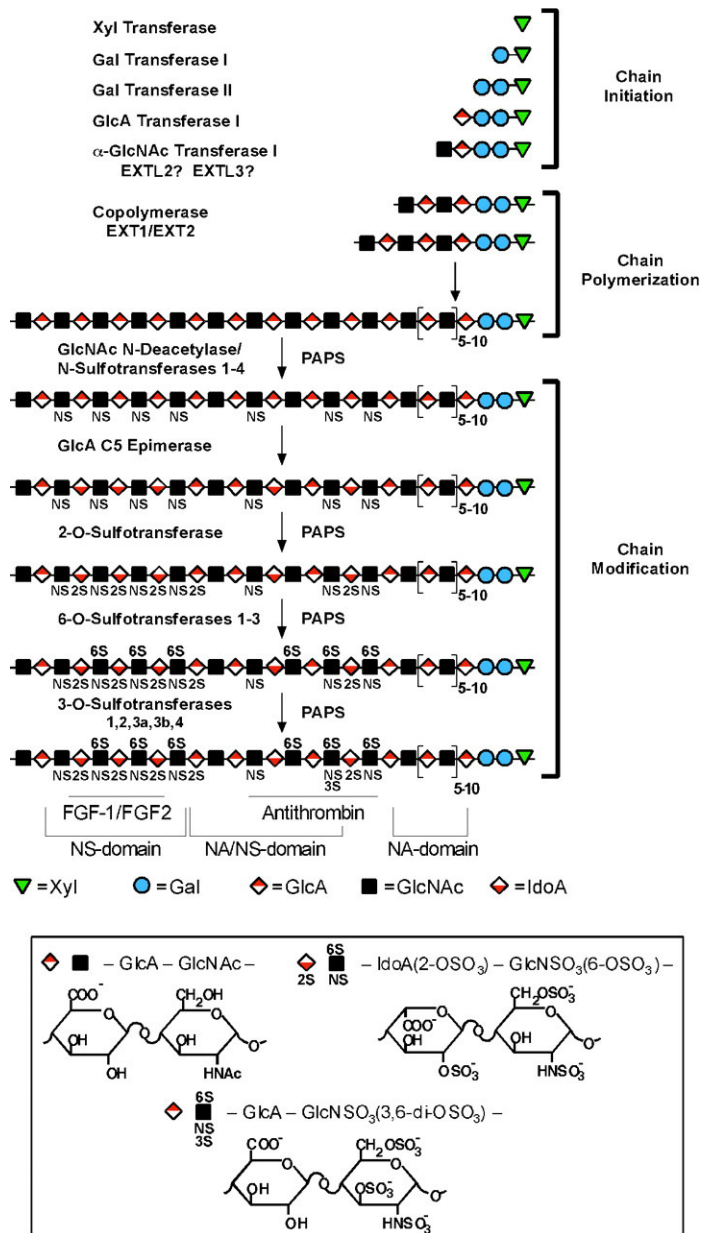


Figure 1. Schematic representation of Heparan sulfate biosynthesis that includes chain initiation, polymerization and modification. Each monosaccharide unit is represented by a geometric symbol and named accordingly. NA, NA/NS, NS domains are shown with specific binding domains for the ligands, such as FGF-1/FGF2 and antithrombin (from 30). Figure reproduced with permission of the publisher from Annual Review of Biochemistry 2002;71:435-471.

forming heparosan, composed of repeating α -linked N-acetyl-glucosamine (GlcNAc) and β -linked glucuronic acid (GlcA). Subsequently, a series of modifications might occur in the chain that involves partial N-deacetylation of GlcNAc units, followed by N-sulfation of the unsubstituted amino groups to form GlcNS residues, 5-epimerization of GlcA to form iduronic acid (IdoA), O-sulfation of IdoA at C-2 and O-sulfation of GlcNSO₃⁻ at C-6 and C-3 (52,53). The various biosynthetic enzymes that are involved in the chain modification procedure act non-uniformly along the chain, and form specific domains. In particular, N-acetylated (NA) domains that are rich in GlcA and GlcNAc derivatives, N-sulfated (NS) domains rich in IdoA and GlcNS derivatives with a high density of O-sulfates, and in between domains that contain alternating NA and NS units of glucosamine (NA/NS domains) with variable degree of O-sulfation (54) as shown in the figure 1 (30). Extracellularly, HS chains can be modified by heparanase (55), an enzyme that specifically cleaves HS chains to deliver free HS oligosaccharide fragments (eventually with HS-bound proteins). SULF1 and SULF2 are extracellularly acting HS endo-6-O-sulfatases that can remove 6-O sulfates at specific positions along the HS chain. Latter enzymes may thus regulate protein binding to HSs that is critically dependent on 6-O sulfate units (56,57).

Heparan sulfate – protein interaction

Due to their vast structural heterogeneity HS are able to bind and interact with a myriad of proteins, such as growth factors, chemokines, cytokines and extra cellular matrix components. Table 1 shows different proteins that might interact with HSs and modulate various processes. The interaction of a certain protein with HS depends on a number of critical requirements, namely i) degree of sulfation and formation of patches with high charge density; ii) the length of the HS chain and the spacing of the N-sulfated domains; iii) 3-dimensional confirmation and flexibility of the HS chain. Studies in mice that were knocked out for different enzymes in HS biosynthesis unexpectedly revealed that many HS-protein interactions appear to depend more on the overall organization of HS domains than on their fine structure. Nowadays it is generally accepted that polymer modification in HS biosynthesis is primarily regulated with regard to domain distribution and degree of sulfation. The resultant clusters of negative charge will determine interactions with proteins that may be relative nonselective with sharing/overlap of saccharide target sequences between different protein ligands. More selective interactions would require either sequences containing rare components (like 3-O-sulfates and/or unsubstituted GlcNH₃⁺ units) or precise spacing of the N-sulfated domains (58).

From the list of HS-binding proteins it can be anticipated that HSPGs are involved in adhesion and migration, cell growth and survival, angiogenesis, fibrosis and inflammation. HSPGs fulfil these functions via a number of different mechanisms. i) HSPGs bind and concentrate/store protein ligands on cell surfaces and in extracellular matrices; ii) HSPGs

Chapter 1

function as high abundant low affinity receptors that modulate the quality of chemokine, cytokine and growth factor responses (such as amplitude and kinetics of activation/inactivation); iii) HSPGs stabilize chemokine/morphogen gradients, thereby guiding directed cell migration; iv) HSPGs stabilize extracellular matrices by cross-linking to matrix components; v) HSPGs regulate internalization of receptor complexes; vi) HSPG ectodomain shedding or HS degradation by heparanase may release HS-bound ligands from the cell surface or from the matrix (59). This implies that HSPGs orchestrate tissue plasticity and remodelling and as such might be crucial in tissue remodelling associated with CTD in transplanted kidneys. In the next paragraphs we will further highlight renal involvement of PGs.

Table 1. Examples of glycosaminoglycan binding proteins and their biological activity

<i>Class</i>	<i>Examples</i>	<i>Physiological/pathophysiological effects of binding</i>
Enzymes	Glycosaminoglycan biosynthetic enzymes, thrombin and coagulation factors (proteases), complement proteins(esterases, extracellular superoxide dismutase, topoisomerase	Multiple
Enzyme inhibitors	Antithrombin III, Heparin cofactor II, secretory leukocyte proteinase inhibitor, esterase inhibitor	Coagulation, inflammation, complement regulation
Cell adhesion proteins	P-selectins, L-selectin, neural cell adhesion molecule (N-CAM), Platelet endothelial cell adhesion molecule (PECAM-1), Heparin interaction protein (HIP), Monocyte adhesion molecule(MAC-1)	Cell adhesion and migration
Extracellular matrix proteins	Laminin, Fibronectin, collagens, thrombospondin, tenascin, vitronectin	Matrix organisation
Chemokines	CCL-2 (MCP1), CCL-5 (RANTES), CXCL12, platelet factor 4	Chemotaxis
Growth factors	Fibroblast growth factors (FGF), heparin binding epidermal growth factor (HB-EGF),	Proliferation

	Vascular endothelial growth factor (VEGF), Hepatocyte growth factor, Transforming growth factor- β (TGF- β)	
Morphogen	Hedgehogs, Bone morphogenic protein (BMP)	Development
Tyrosine kinase grov receptors	Fibroblast growth factors receptors, vascular endothelium growth factor receptor	Proliferation
Lipid proteins	Apolipoprotein E and B, Lipoprotein Lipase, Hepatic lipase, annexins	Lipid metabolism

Table 1 shows the list of the glycosaminoglycan binding proteins that modulate different biological processes through this interaction

Renal involvement of proteoglycans

Proteoglycans in normal kidney

Kidney development - In normal renal tissue a number of PGs are expressed. With a focus on HSPGs, in basement membranes three HSPGs are abundantly present, namely agrin, perlecan and collagen type XVIII (60). The expression of cell surface HSPG (Syndecans 1-4, Glypicans 1-6, CD44V3 variant) is less well described. Syndecan-1 seems to be the major epithelial HSPG during development and in renal cell lines, but is barely expressed in adult kidney (61). At the mRNA level it has been shown that cell surface syndecan-4 is abundantly expressed (62). It also has been shown that in the developing kidney various growth factors are involved in the activation of their specific cell surface receptors in growth and branching morphogenesis of the isolated ureteric bud (63), and also these processes are regulated by sulfated proteoglycans (64). Syndecan-1 expression showed both spatial and temporal correlation with kidney morphogenesis, thus suggesting the important role for this cellular proteoglycan in development (65). Mice deficient in the HS2st showed developmental anomalies that include skeletal malformation and kidney agenesis (66,67). Thus, proteoglycans are likely to play major roles in the development of the kidney.

Proteoglycans in glycocalyx - The glycocalyx is a thick carbohydrate-rich layer lining the vascular endothelium and considered to be attached to the endothelium through several “backbone” molecules that include proteoglycans and also glycoproteins. A dynamic equilibrium exists between soluble components of the glycocalyx and the flowing blood, continuously affecting composition and thickness of the glycocalyx (68,69). Under healthy physiological conditions the glycocalyx acts as an anti-thrombotic, anti-proliferative, anti-adhesive and anti-inflammatory sheath (69). However, in inflammatory state the glycocalyx can be shed into the circulation leaving denuded endothelial cells with activated apical membranes. Studies in healthy mouse cremaster muscle venules show that upon breakdown

of heparan sulfate side chains by heparitinase an increased leukocyte adhesion to the endothelium occurs in a dose-dependent manner (70). HSPG expression may alter in the glycocalyx as the endothelial expression of proteoglycans as well as the fine composition of the HS side chains depend on various stimuli. As an example, syndecan-1 has a tightly regulated expression pattern which alters with activation of endothelial cell or stimulation with various chemokines (71). Heterogeneity of the GAG chain gives rise to an array of binding sites on GAGs for various plasma-derived molecules. The roles of proteoglycans in the glycocalyx of glomerular endothelial cells strongly suggest a role in charge-dependent permeability (72), but this concept has been challenged recently, as outlined below.

Proteoglycans in glomerular ultrafiltration - The filtration barrier of the glomerular capillary wall is made up of three specialized layers which determine its permselective properties, namely the fenestrated endothelium, the glomerular basement membrane (GBM) and the glomerular epithelial cells or podocytes (73). Within the kidney, HSPG research has focussed for 30 years on the role of HSPGs in glomerular filtration. It is assumed that the highly anionic HSPGs in the glomerular basement membrane contribute to electrostatic repulsion of albumin and thereby keep the formed primary urine free of protein (74). Studies in mice have shed new light on this classical dogma. Collagen type XVIII knockout mice (*col18a1^{-/-}*) have no lethal phenotype and display mild mesangial expansion and slightly elevated serum creatinine levels compared to controls (75). Agrin and perlecan knockout mice showed neuromuscular defects and have an embryonic or perinatal lethal phenotype respectively (76,77). Mice lacking the GAG attachment sites in the N-terminal domain I of perlecan (*Hspg2 Δ 3/ Δ 3*) showed normal glomerular ultrastructure and GBM charge, and no evidence of kidney disease (78). Podocyte-specific agrin knockout mice (conditional knockout) revealed normal glomerular filtration barrier even when these mice were challenged with bovine serum albumin overload (79). Also the podocyte-specific EXT-1 knockout mice showed fully normal glomerular ultrafiltration (80). The generation of these conditional HSPG-deficient mice has questioned the role of HSPG in charge selective permeability, and made this concept very controversial.

Proteoglycans in the diseased kidney

Inflammation - Tissue injury results in inflammatory responses that primarily involve the recruitment of leukocytes to the site of injury. Immune cells, such as macrophages, release TNF-alpha and interleukin-1 immediately after injury and further activate nearby endothelial cells. During the process of inflammation and leukocyte extravasation, HSPGs play several important roles (81). GAG chains are mainly involved in three major steps during the migration of leukocytes into the site of inflammation: L-selectin-mediated cell rolling, chemokine-mediated activation and transmigration between the endothelial cells, and stabilization of chemokine gradients in extracellular matrix to facilitate directed

migration of the leukocytes (80,82,84). Recent studies of endothelium specific N-deacetylase/sulfotransferase-1 knockout mice revealed that decreasing HS sulfation by ~60% significantly reduced neutrophil infiltration. Alterations in N-deacetylase/sulfotransferase-1 expression in leukocytes did not affect neutrophil recruitment or T-cell mediated responses, indicating that endothelial HS dominates in the system (82). It also has been demonstrated *in vitro* that culturing microvascular brain endothelial cells in medium containing chlorate (inhibiting GAG sulfation) or treatment with heparitinase (HS degradation) resulted in reduced transendothelial migration of monocytes (83). In contrast, the role of leukocyte HSPGs in leukocyte extravasation was evidenced by syndecan-1 knockout mice, which show increased leukocyte-endothelial adhesion (84). This effect was shown to be mostly due to the lack of syndecan-1 on leukocytes (85). Rops et al. showed increased leukocyte recruitment in syndecan-1 knockout mice following induction of experimental anti-glomerular basement membrane nephritis (86). Celie et al. showed that L-selectin binding HSPGs are detected at the abluminal side of peritubular capillaries in both experimental and human renal inflammatory conditions and these basement membrane HSPGs contribute to the influx of inflammatory cells (87,88). *In vivo*, collagen type XVIII/endostatin knockout mice with anti-GBM disease developed more severe glomerular and tubulointerstitial injury than wild-type mice. The Collagen XVIII/endostatin knockout mice showed altered matrix remodeling, induced inflammatory responses, and vascular endothelial cell damage suggesting that collagen type XVIII/endostatin plays major role in maintaining the integrity of the extracellular matrix and capillaries in the kidney, protecting against progressive glomerulonephritis (89). Another type of proteoglycans named Small Leucine-Rich proteoglycans (SLRPs; such as decorin, biglycan, fibromodulin and lumican) are very much involved in the regulation of inflammatory kidney disorders. The basic concept comprises activation of inflammatory routes via Toll-like receptor activation by fragments of these small PGs upon matrix degradation by MMPs. The roles of SLRPs in the normal and diseased kidney were reviewed in detail recently by Schaefer et al (90).

Fibrosis - Fibrosis is the result of continuous wound healing upon severe/chronic injury, in which there is progression rather than resolution of scarring. Myofibroblasts are the cells that play a crucial role in the pathogenesis of fibrosis. Myofibroblasts are terminally differentiated cells, responsible for the synthesis and accumulation of interstitial ECM components during wound healing and at sites of scarring and fibrosis (91). GAGs can bind a variety of ligands depending on their composition and FGF-2 is known to be one of the GAG binding proteins involved in fibrosis (92). It was demonstrated in renal interstitial fibroblasts, that HSPGs are essential for the control of the proliferative response to FGF-2 (93-95). Hepatocyte Growth Factor (HGF) is a clinically important pleiotropic factor with therapeutic potential for the treatment of interstitial fibrosis and chronic renal failure. It has been suggested that HGF plays an important role in the regulation of proteoglycan synthesis in rat renal interstitial fibroblasts (NRK-49F cells) (96).

In addition, VSMCs have been shown to express FGF-2, which act as a autocrine/paracrine mitogen. Its effect on VSMCs *in vivo* is only present in case of vascular injury, since quiescent medial VSMCs are unresponsive to FGF-2 due to the lack of FGF-2 binding domains in their HSs (97). Recently, it has been shown that syndecan 4, a cell surface proteoglycan, ameliorates neointimal formation after vascular injury by regulating VSMC proliferation and vascular progenitor cell mobilization (98). The well-known heparan binding growth factor HB-EGF is mitogenic for several cell types. It has been shown that HB-EGF is synthesized and expressed by mesangial cells and in an autocrine fashion stimulates mesangial cell proliferation and collagen synthesis *in vitro* (99). Our own data (chapter3) show the involvement of mesangial HSPGs in FGF2-driven mesangial proliferation. These data indicate that HSPGs are involved in renal mesenchymal cell proliferation and matrix expansion.

Regeneration - We recently observed upregulation of syndecan-1 expression in tubular epithelial cells in functioning human renal allografts. Interestingly, the level of syndecan-1 expression was positively correlated with graft function and survival as well as with binding of HB-EGF. Using the HK-2 proximal tubular epithelial cell line, we were able to demonstrate a functional role for syndecan 1 in TEC proliferation. In line with this, *in vitro* knockdown of syndecan-1 in HK2 cells reduced cell proliferation. Moreover, after renal ischemia/reperfusion, tubular repair was hampered in syndecan-1 KO mice (Kidney Int 2012: in press; chapter 6 of this thesis). Previously it has been shown that growth factors such as HGF and HB-EGF and follistatin are involved in renal repair and regeneration (100-105). For these growth factors, HSPGs serve as co-receptors and mediate the cell signaling cascades. Thus proteoglycans are most likely involved in renal regeneration and repair.

Heparinoids as therapeutic modalities to reduce tissue remodeling

According the abovementioned previous findings HSPGs play major roles in tissue remodeling in renal CTD. This fuels the hypothesis that exogenously administered heparinoids as decoy molecules for growth factors, selectins and chemokines can interfere with the endogenous HS-mediated growth factor signaling cascades and the process of inflammatory cell recruitment that characterizes the development of CTD. Such an approach would potentially be a useful adjunct to the current treatment strategies in CTD that are mainly based on immunosuppressive regimens, that have substantial side effects such as increased susceptibility to infections, chronic calcineurin inhibitor toxicity (106), and increased risk for metabolic syndrome and diabetes. So far, adjunct treatment in renal transplant recipients addressed the control of hypertension, proteinuria and metabolic abnormalities. No therapy directly targeting renal remodeling is available. As mentioned before heparin/HS GAGs have great structural heterogeneity and are involved in various

cellular processes. Most of the biological activities of these polysaccharides are associated with complexation with proteins involved in tissue remodeling and inflammation. Therefore these glycans could be interesting therapeutic decoy molecules to retard CTD.

Heparin is a molecule specifically well known for its anticoagulant activity and which has a very broad spectrum of actions that include anti-inflammatory and anti-tumor properties. The anti-inflammatory and anti-angiogenic properties of heparin are thought to be largely associated with the influence on pathophysiological functions of HS chains of HSPGs (107,108). Treatment with exogenous heparin and low-molecular-weight heparins have been shown to exert beneficial outcomes in inflammation(109-111). However, prolonged heparin therapy leads to significant complications that includes bleeding, heparin-induced osteoporosis and heparin-induced thrombocytopenia (112-114). Thus, prolonged administration of heparin to transplanted patients might results in impaired coagulative function and other undesirable side effects. To date, many efforts have been made to design heparin derivatives with specific, predictable binding properties. Non-anticoagulant heparins are used in several experimental renal disease models and demonstrated that these heparin-like glycomimetica are able to reduce the inflammation after renal ischemia/reperfusion. It was demonstrated that N-desulfated heparin, which has a strongly reduced anti-coagulant activity compared to normal heparin, is able to reduce the renal damage significantly in a rat renal I/R model(115). These results were supported by findings which show that treatment with non-anticoagulant hypersulfated heparin and low molecular weight heparin reduced inflammation after renal ischemia/reperfusion, and renal allograft rejection, and CTD in the Fisher to Lewis rat model of renal transplantation (109,116). Recently it has been demonstrated that intervention with a LMWH, sulodexide, was not renoprotective in patients with type 2 diabetes, renal impairment, and macroalbuminuria (117). Although sulodexide has similar structure as unfractionated heparin, it has a lower degree of sulfation and shorter polysaccharide length compared to normal unfractionated heparin and RO-heparin (118). Together, exogenously administered heparin-like glycomimetica might be potential therapeutics to retard development of CTD upon renal transplantation.

Aim of the Thesis

The aim of this thesis focuses on the role of proteoglycans in renal CTD. The general introduction (chapter 1) of this thesis briefly outlines kidney transplantation, the histopathological lesions of CTD, potential involvement of proteoglycans in CTD-related tissue remodeling and potential beneficial therapeutic effects of heparinoids. Most of the experiments in this thesis are performed in a rat kidney transplantation model for CTD. This rat model was previously used and well described in which kidney transplantation occurs from Dark Agouti donor to Wistar Furth recipient (119). However, whether and how

proteoglycans mediate tissue remodeling in CTD was unanswered. Therefore in chapter 2 we characterize differential heparan sulfate proteoglycans (collagen type XVIII, perlecan and agrin) and chondroitin sulfate proteoglycan (Versican) expression in transplant vasculopathy, glomerulosclerosis and interstitial fibrosis in rat renal allografts with chronic transplant dysfunction. Later we continued to unravel the functional importance of the upregulated proteoglycans in CTD, so in chapter 3, we investigate the glomerular and neointimal induction of perlecan and FGF2 in allografted kidneys. In addition, we characterize the heparan sulfate (HS) polysaccharide side chains by anti-HS mAbs and their binding capacity for FGF2. Finally, we evaluate the functional role of HSPG by *in vitro* cell culture assays to demonstrate the HSPG dependency of FGF2-driven mesangial proliferation. According to the results obtained in chapter 2 and 3, proteoglycans most likely involved in tissue remodelling in CTD. Therefore in chapter 4, we test the therapeutic effects of exogenously administered heparin and two non-anticoagulant heparin derivatives (N-acetyl-heparin and Reduced/oxidized-heparin) to ameliorate CTD in the experimental transplantation model. As the molecular mechanisms behind the neointima formation is still unclear in the arteries of the kidneys effected with CTD. So in chapter 5 we specifically focus on the vascular component of CTD, namely transplant vasculopathy in the rat CTD model. In addition, we investigate genes indicative of (de)differentiation of medial SMCs in rat renal allografts with transplant vasculopathy by micro dissection of neointimal and medial layers using laser dissection microscopy and gene expression was analyzed with a low density array, and expressions of the corresponding proteins in renal allograft tissue sections and their function in an *in vitro* SMC functional assay.

Lastly in chapter 6, we test the hypothesis that syndecan-1 is involved in tubular survival and repair upon renal transplantation. To this purpose we study the expression of syndecan-1 in human renal allograft biopsies, including protocol biopsies and biopsies taken at indication, and correlated syndecan-1 expression to allograft function and survival, and to the binding of relevant growth factors. To show the functional role of syndecan-1, we study the effect of syndecan-1 knockdown (*in vitro*) on TEC proliferation. In addition, we perform bilateral renal IRI in syndecan-1 versus wildtype mice and studied functional and histological outcome.

In chapter 7 the experimental data presented in chapters 2-6 are discussed in their context and perspectives for future research are indicated.

References

1. Colvin RB. Chronic allograft nephropathy. *N Engl J Med* 2003 Dec 11;349(24):2288-2290.
2. Chapman JR, O'Connell PJ, Nankivell BJ. Chronic renal allograft dysfunction. *J Am Soc Nephrol* 2005 Oct;16(10):3015-3026.
3. Solez K, Vincenti F, Filo RS. Histopathologic findings from 2-year protocol biopsies from a U.S. multicenter kidney transplant trial comparing tacrolimus versus cyclosporine: a report of the FK506 Kidney Transplant Study Group. *Transplantation* 1998 Dec 27;66(12):1736-1740.
4. Nankivell BJ, Borrows RJ, Fung CL, O'Connell PJ, Allen RD, Chapman JR. The natural history of chronic allograft nephropathy. *N Engl J Med* 2003 Dec 11;349(24):2326-2333.
5. Najafian B, Kasiske BL. Chronic allograft nephropathy. *Curr Opin Nephrol Hypertens* 2008 Mar;17(2):149-155.
6. Amer H, Fidler ME, Myslak M, Morales P, Kremers WK, Larson TS, et al. Proteinuria after kidney transplantation, relationship to allograft histology and survival. *Am J Transplant* 2007 Dec;7(12):2748-2756.
7. Solez K, Colvin RB, Racusen LC, Sis B, Halloran PF, Birk PE, et al. Banff '05 Meeting Report: differential diagnosis of chronic allograft injury and elimination of chronic allograft nephropathy ('CAN'). *Am J Transplant* 2007 Mar;7(3):518-526.
8. Verani RR, Hawkins EP. Recurrent focal segmental glomerulosclerosis. A pathological study of the early lesion. *Am J Nephrol* 1986;6(4):263-270.
9. Shi SF, Wang SX, Zhang YK, Zhao MH, Zou WZ. Ultrastructural features and expression of cytoskeleton proteins of podocyte from patients with minimal change disease and focal segmental glomerulosclerosis. *Ren Fail* 2008;30(5):477-483.
10. LeHir M, Kriz W. New insights into structural patterns encountered in glomerulosclerosis. *Curr Opin Nephrol Hypertens* 2007 May;16(3):184-191.
11. Cosio FG, Frankel WL, Pelletier RP, Pesavento TE, Henry ML, Ferguson RM. Focal segmental glomerulosclerosis in renal allografts with chronic nephropathy: implications for graft survival. *Am J Kidney Dis* 1999 Oct;34(4):731-738.
12. Hariharan S, Adams MB, Brennan DC, Davis CL, First MR, Johnson CP, et al. Recurrent and de novo glomerular disease after renal transplantation: a report from Renal Allograft Disease Registry (RADR). *Transplantation* 1999 Sep 15;68(5):635-641.
13. Ivanyi B. A primer on recurrent and de novo glomerulonephritis in renal allografts. *Nat Clin Pract Nephrol* 2008 Aug;4(8):446-457.
14. Takeda A, Morozumi K, Koyama K, Yoshida A, Uchida K, Tominaga Y, et al. Severe cyclosporine arteriopathy with focal segmental glomerulosclerosis is not a fatal finding in chronic renal allograft failure after year 5 of transplantation using cyclosporine. *Transplant Proc* 1997 Feb-Mar;29(1-2):96-99.
15. Xu Q. Stem cells and transplant arteriosclerosis. *Circ Res* 2008 May 9;102(9):1011-1024.
16. Owens GK, Kumar MS, Wamhoff BR. Molecular regulation of vascular smooth muscle cell differentiation in development and disease. *Physiol Rev* 2004 Jul;84(3):767-801.
17. de Boer OJ, Becker AE, van der Wal AC. T lymphocytes in atherogenesis-functional aspects and antigenic repertoire. *Cardiovasc Res* 2003 Oct 15;60(1):78-86.
18. Lepage S, Cailhier JF. Chronic transplant vasculopathy microenvironment present in the renal allograft reprograms macrophage phenotype. *Transplant Proc* 2009 Oct;41(8):3311-3313.
19. Strutz F, Heeg M, Kochsiek T, Siemers G, Zeisberg M, Muller GA. Effects of pentoxifylline, pentifylline and gamma-interferon on proliferation, differentiation, and matrix synthesis of human renal fibroblasts. *Nephrol Dial Transplant* 2000 Oct;15(10):1535-1546.
20. Solez K, Colvin RB, Racusen LC, Haas M, Sis B, Mengel M, et al. Banff 07 classification of renal allograft pathology: updates and future directions. *Am J Transplant* 2008 Apr;8(4):753-760.
21. Racusen LC, Solez K, Colvin RB, Bonsib SM, Castro MC, Cavallo T, et al. The Banff 97 working classification of renal allograft pathology. *Kidney Int* 1999 Feb;55(2):713-723.

Chapter 1

22. Halloran PF, Melk A, Barth C. Rethinking chronic allograft nephropathy: the concept of accelerated senescence. *J Am Soc Nephrol* 1999 Jan;10(1):167-181.
23. Strutz F, Zeisberg M. Renal fibroblasts and myofibroblasts in chronic kidney disease. *J Am Soc Nephrol* 2006 Nov;17(11):2992-2998.
24. Lin SL, Kisseleva T, Brenner DA, Duffield JS. Pericytes and perivascular fibroblasts are the primary source of collagen-producing cells in obstructive fibrosis of the kidney. *Am J Pathol* 2008 Dec;173(6):1617-1627.
25. Djamali A, Reese S, Yracheta J, Oberley T, Hullett D, Becker B. Epithelial-to-mesenchymal transition and oxidative stress in chronic allograft nephropathy. *Am J Transplant* 2005 Mar;5(3):500-509.
26. Liptak P, Ivanyi B. Primer: Histopathology of calcineurin-inhibitor toxicity in renal allografts. *Nat Clin Pract Nephrol* 2006 Jul;2(7):398-404; quiz following 404.
27. Anders HJ, Ryu M. Renal microenvironments and macrophage phenotypes determine progression or resolution of renal inflammation and fibrosis. *Kidney Int* 2011 Aug 3.
28. Bernfield M, Gotte M, Park PW, Reizes O, Fitzgerald ML, Lincecum J, et al. Functions of cell surface heparan sulfate proteoglycans. *Annu Rev Biochem* 1999;68:729-777.
29. Iozzo RV. Basement membrane proteoglycans: from cellar to ceiling. *Nat Rev Mol Cell Biol* 2005 Aug;6(8):646-656.
30. Esko JD, Selleck SB. Order out of chaos: assembly of ligand binding sites in heparan sulfate. *Annu Rev Biochem* 2002;71:435-471.
31. Ly M, Laremore TN, Linhardt RJ. Proteoglycomics: recent progress and future challenges. *OMICS* 2010 Aug;14(4):389-399.
32. Fraser JR, Laurent TC, Laurent UB. Hyaluronan: its nature, distribution, functions and turnover. *J Intern Med* 1997 Jul;242(1):27-33.
33. Prydz K, Dalen KT. Synthesis and sorting of proteoglycans. *J Cell Sci* 2000 Jan;113 Pt 2:193-205.
34. Choi Y, Chung H, Jung H, Couchman JR, Oh ES. Syndecans as cell surface receptors: Unique structure equates with functional diversity. *Matrix Biol* 2011 Mar;30(2):93-99.
35. Filmus J, Capurro M, Rast J. Glypicans. *Genome Biol* 2008;9(5):224.
36. Ruegg MA, Bixby JL. Agrin orchestrates synaptic differentiation at the vertebrate neuromuscular junction. *Trends Neurosci* 1998 Jan;21(1):22-27.
37. Denzer AJ, Gesemann M, Schumacher B, Ruegg MA. An amino-terminal extension is required for the secretion of chick agrin and its binding to extracellular matrix. *J Cell Biol* 1995 Dec;131(6 Pt 1):1547-1560.
38. Godfrey EW. Comparison of agrin-like proteins from the extracellular matrix of chicken kidney and muscle with neural agrin, a synapse organizing protein. *Exp Cell Res* 1991 Jul;195(1):99-109.
39. Biroc SL, Payan DG, Fisher JM. Isoforms of agrin are widely expressed in the developing rat and may function as protease inhibitors. *Brain Res Dev Brain Res* 1993 Sep 17;75(1):119-129.
40. Barber AJ, Lieth E. Agrin accumulates in the brain microvascular basal lamina during development of the blood-brain barrier. *Dev Dyn* 1997 Jan;208(1):62-74.
41. Groffen AJ, Buskens CA, van Kuppevelt TH, Veerkamp JH, Monnens LA, van den Heuvel LP. Primary structure and high expression of human agrin in basement membranes of adult lung and kidney. *Eur J Biochem* 1998 May 15;254(1):123-128.
42. Segev A, Nili N, Strauss BH. The role of perlecan in arterial injury and angiogenesis. *Cardiovasc Res* 2004 Sep 1;63(4):603-610.
43. Aviezer D, Hecht D, Safran M, Eisinger M, David G, Yaron A. Perlecan, basal lamina proteoglycan, promotes basic fibroblast growth factor-receptor binding, mitogenesis, and angiogenesis. *Cell* 1994 Dec 16;79(6):1005-1013.
44. Guillonneau X, Tassin J, Berrou E, Bryckaert M, Courtois Y, Mascarelli F. *In vitro* changes in plasma membrane heparan sulfate proteoglycans and in perlecan expression participate in the regulation of fibroblast growth factor 2 mitogenic activity. *J Cell Physiol* 1996 Jan;166(1):170-187.
45. Halfter W, Dong S, Schurer B, Cole GJ. Collagen XVIII is a basement membrane heparan sulfate proteoglycan. *J Biol Chem* 1998 Sep 25;273(39):25404-25412.

46. Marneros AG, Olsen BR. Physiological role of collagen XVIII and endostatin. *FASEB J* 2005 May;19(7):716-728.
47. Dong S, Cole GJ, Halfter W. Expression of collagen XVIII and localization of its glycosaminoglycan attachment sites. *J Biol Chem* 2003 Jan 17;278(3):1700-1707.
48. Li Q, Olsen BR. Increased angiogenic response in aortic explants of collagen XVIII/endostatin-null mice. *Am J Pathol* 2004 Aug;165(2):415-424.
49. Miosge N, Simniok T, Sprysch P, Herken R. The collagen type XVIII endostatin domain is co-localized with perlecan in basement membranes *in vivo*. *J Histochem Cytochem* 2003 Mar;51(3):285-296.
50. Hirschberg CB, Snider MD. Topography of glycosylation in the rough endoplasmic reticulum and Golgi apparatus. *Annu Rev Biochem* 1987;56:63-87.
51. Hirschberg CB, Robbins PW, Abeijon C. Transporters of nucleotide sugars, ATP, and nucleotide sulfate in the endoplasmic reticulum and Golgi apparatus. *Annu Rev Biochem* 1998;67:49-69.
52. Salmivirta M, Lidholt K, Lindahl U. Heparan sulfate: a piece of information. *FASEB J* 1996 Sep;10(11):1270-1279.
53. Casu B, Petitou M, Provasoli M, Sinay P. Conformational flexibility: a new concept for explaining binding and biological properties of iduronic acid-containing glycosaminoglycans. *Trends Biochem Sci* 1988 Jun;13(6):221-225.
54. Maccarana M, Sakura Y, Tawada A, Yoshida K, Lindahl U. Domain structure of heparan sulfates from bovine organs. *J Biol Chem* 1996 Jul 26;271(30):17804-17810.
55. Marchetti D. Specific degradation of subendothelial matrix proteoglycans by brain-metastatic melanoma and brain endothelial cell heparanases. *J Cell Physiol* 1997 Sep;172(3):334-342.
56. Dhoot GK, Gustafsson MK, Ai X, Sun W, Standiford DM, Emerson CP, Jr. Regulation of Wnt signaling and embryo patterning by an extracellular sulfatase. *Science* 2001 Aug 31;293(5535):1663-1666.
57. Morimoto-Tomita M, Uchimura K, Werb Z, Hemmerich S, Rosen SD. Cloning and characterization of two extracellular heparin-degrading endosulfatases in mice and humans. *J Biol Chem* 2002 Dec 20;277(51):49175-49185.
58. Kreuger J, Spillmann D, Li JP, Lindahl U. Interactions between heparan sulfate and proteins: the concept of specificity. *J Cell Biol* 2006 Jul 31;174(3):323-327.
59. Bishop JR, Schuksz M, Esko JD. Heparan sulphate proteoglycans fine-tune mammalian physiology. *Nature* 2007 Apr 26;446(7139):1030-1037.
60. Rienstra H, Katta K, Celie JW, van Goor H, Navis G, van den Born J, et al. Differential expression of proteoglycans in tissue remodeling and lymphangiogenesis after experimental renal transplantation in rats. *PLoS One* 2010 Feb 5;5(2):e9095.
61. Kim CW, Goldberger OA, Gallo RL, Bernfield M. Members of the syndecan family of heparan sulfate proteoglycans are expressed in distinct cell-, tissue-, and development-specific patterns. *Mol Biol Cell* 1994 Jul;5(7):797-805.
62. Plisov SY, Ivanov SV, Yoshino K, Dove LF, Plisova TM, Higinbotham KG, et al. Mesenchymal-epithelial transition in the developing metanephric kidney: gene expression study by differential display. *Genesis* 2000 May;27(1):22-31.
63. Qiao J, Bush KT, Steer DL, Stuart RO, Sakurai H, Wachsman W, et al. Multiple fibroblast growth factors support growth of the ureteric bud but have different effects on branching morphogenesis. *Mech Dev* 2001 Dec;109(2):123-135.
64. Steer DL, Shah MM, Bush KT, Stuart RO, Sampogna RV, Meyer TN, et al. Regulation of ureteric bud branching morphogenesis by sulfated proteoglycans in the developing kidney. *Dev Biol* 2004 Aug 15;272(2):310-327.
65. Vainio S, Lehtonen E, Jalkanen M, Bernfield M, Saxen L. Epithelial-mesenchymal interactions regulate the stage-specific expression of a cell surface proteoglycan, syndecan, in the developing kidney. *Dev Biol* 1989 Aug;134(2):382-391.

66. Bullock SL, Fletcher JM, Beddington RS, Wilson VA. Renal agenesis in mice homozygous for a gene trap mutation in the gene encoding heparan sulfate 2-sulfotransferase. *Genes Dev* 1998 Jun 15;12(12):1894-1906.
67. Merry CL, Wilson VA. Role of heparan sulfate-2-O-sulfotransferase in the mouse. *Biochim Biophys Acta* 2002 Dec 19;1573(3):319-327.
68. Lipowsky HH. Microvascular rheology and hemodynamics. *Microcirculation* 2005 Jan-Feb;12(1):5-15.
69. Reitsma S, Slaaf DW, Vink H, van Zandvoort MA, oude Egbrink MG. The endothelial glycocalyx: composition, functions, and visualization. *Pflugers Arch* 2007 Jun;454(3):345-359.
70. Constantinescu AA, Vink H, Spaan JA. Endothelial cell glycocalyx modulates immobilization of leukocytes at the endothelial surface. *Arterioscler Thromb Vasc Biol* 2003 Sep 1;23(9):1541-1547.
71. Tkachenko E, Rhodes JM, Simons M. Syndecans: new kids on the signaling block. *Circ Res* 2005 Mar 18;96(5):488-500.
72. Jeansson M, Haraldsson B. Morphological and functional evidence for an important role of the endothelial cell glycocalyx in the glomerular barrier. *Am J Physiol Renal Physiol* 2006 Jan;290(1):F111-6.
73. Brenner BM, Hostetter TH, Humes HD. Glomerular permselectivity: barrier function based on discrimination of molecular size and charge. *Am J Physiol* 1978 Jun;234(6):F455-60.
74. Raats CJ, Van Den Born J, Berden JH. Glomerular heparan sulfate alterations: mechanisms and relevance for proteinuria. *Kidney Int* 2000 Feb;57(2):385-400.
75. Utriainen A, Sormunen R, Kettunen M, Carvalhaes LS, Sajanti E, Eklund L, et al. Structurally altered basement membranes and hydrocephalus in a type XVIII collagen deficient mouse line. *Hum Mol Genet* 2004 Sep 15;13(18):2089-2099.
76. Costell M, Gustafsson E, Aszodi A, Morgelin M, Bloch W, Hunziker E, et al. Perlecan maintains the integrity of cartilage and some basement membranes. *J Cell Biol* 1999 Nov 29;147(5):1109-1122.
77. Gautam M, Noakes PG, Moscoso L, Rupp F, Scheller RH, Merlie JP, et al. Defective neuromuscular synaptogenesis in agrin-deficient mutant mice. *Cell* 1996 May 17;85(4):525-535.
78. Rossi M, Morita H, Sormunen R, Airene S, Kreivi M, Wang L, et al. Heparan sulfate chains of perlecan are indispensable in the lens capsule but not in the kidney. *EMBO J* 2003 Jan 15;22(2):236-245.
79. Harvey SJ, Jarad G, Cunningham J, Rops AL, van der Vlag J, Berden JH, et al. Disruption of glomerular basement membrane charge through podocyte-specific mutation of agrin does not alter glomerular permselectivity. *Am J Pathol* 2007 Jul;171(1):139-152.
80. Chen S, Wassenhove-McCarthy DJ, Yamaguchi Y, Holzman LB, van Kuppevelt TH, Jenniskens GJ, et al. Loss of heparan sulfate glycosaminoglycan assembly in podocytes does not lead to proteinuria. *Kidney Int* 2008 Aug;74(3):289-299.
81. Parish CR. The role of heparan sulphate in inflammation. *Nat Rev Immunol* 2006 Sep;6(9):633-643.
82. Wang L, Fuster M, Sriramapo P, Esko JD. Endothelial heparan sulfate deficiency impairs L-selectin- and chemokine-mediated neutrophil trafficking during inflammatory responses. *Nat Immunol* 2005 Sep;6(9):902-910.
83. Floris S, van den Born J, van der Pol SM, Dijkstra CD, De Vries HE. Heparan sulfate proteoglycans modulate monocyte migration across cerebral endothelium. *J Neuropathol Exp Neurol* 2003 Jul;62(7):780-790.
84. Gotte M, Joussen AM, Klein C, Andre P, Wagner DD, Hinkes MT, et al. Role of syndecan-1 in leukocyte-endothelial interactions in the ocular vasculature. *Invest Ophthalmol Vis Sci* 2002 Apr;43(4):1135-1141.
85. Gotte M, Bernfield M, Joussen AM. Increased leukocyte-endothelial interactions in syndecan-1-deficient mice involve heparan sulfate-dependent and -independent steps. *Curr Eye Res* 2005 Jun;30(6):417-422.
86. Rops AL, Jacobs CW, Linssen PC, Boezeman JB, Lensen JF, Wijnhoven TJ, et al. Heparan sulfate on activated glomerular endothelial cells and exogenous heparinoids influence the rolling and adhesion of leucocytes. *Nephrol Dial Transplant* 2007 Apr;22(4):1070-1077.
87. Celie JW, Rutjes NW, Keuning ED, Soininen R, Heljasvaara R, Pihlajaniemi T, et al. Subendothelial heparan sulfate proteoglycans become major L-selectin and monocyte chemoattractant protein-1 ligands upon renal ischemia/reperfusion. *Am J Pathol* 2007 Jun;170(6):1865-1878.

Chapter 1

88. Celie JW, Reijmers RM, Slot EM, Beelen RH, Spaargaren M, Ter Wee PM, et al. Tubulointerstitial heparan sulfate proteoglycan changes in human renal diseases correlate with leukocyte influx and proteinuria. *Am J Physiol Renal Physiol* 2008 Jan;294(1):F253-63.
89. Hamano Y, Okude T, Shirai R, Sato I, Kimura R, Ogawa M, et al. Lack of collagen XVIII/endostatin exacerbates immune-mediated glomerulonephritis. *J Am Soc Nephrol* 2010 Sep;21(9):1445-1455.
90. Schaefer L. Small leucine-rich proteoglycans in kidney disease. *J Am Soc Nephrol* 2011 Jul;22(7):1200-1207.
91. Meran S, Steadman R. Fibroblasts and myofibroblasts in renal fibrosis. *Int J Exp Pathol* 2011 Jun;92(3):158-167.
92. Guimond S, Maccarana M, Olwin BB, Lindahl U, Rapraeger AC. Activating and inhibitory heparin sequences for FGF-2 (basic FGF). Distinct requirements for FGF-1, FGF-2, and FGF-4. *J Biol Chem* 1993 Nov 15;268(32):23906-23914.
93. Clayton A, Thomas J, Thomas GJ, Davies M, Steadman R. Cell surface heparan sulfate proteoglycans control the response of renal interstitial fibroblasts to fibroblast growth factor-2. *Kidney Int* 2001 Jun;59(6):2084-2094.
94. Evans RA, Tian YC, Steadman R, Phillips AO. TGF-beta1-mediated fibroblast-myofibroblast terminal differentiation-the role of Smad proteins. *Exp Cell Res* 2003 Jan 15;282(2):90-100.
95. Thomas G, Clayton A, Thomas J, Davies M, Steadman R. Structural and functional changes in heparan sulfate proteoglycan expression associated with the myofibroblastic phenotype. *Am J Pathol* 2003 Mar;162(3):977-989.
96. Kobayashi E, Sasamura H, Mifune M, Shimizu-Hirota R, Kuroda M, Hayashi M, et al. Hepatocyte growth factor regulates proteoglycan synthesis in interstitial fibroblasts. *Kidney Int* 2003 Oct;64(4):1179-1188.
97. Ross R, Masuda J, Raines EW. Cellular interactions, growth factors, and smooth muscle proliferation in atherogenesis. *Ann N Y Acad Sci* 1990;598:102-112.
98. Ikesue M, Matsui Y, Ohta D, Danzaki K, Ito K, Kanayama M, et al. Syndecan-4 deficiency limits neointimal formation after vascular injury by regulating vascular smooth muscle cell proliferation and vascular progenitor cell mobilization. *Arterioscler Thromb Vasc Biol* 2011 May;31(5):1066-1074.
99. Takemura T, Murata Y, Hino S, Okada M, Yanagida H, Ikeda M, et al. Heparin-binding EGF-like growth factor is expressed by mesangial cells and is involved in mesangial proliferation in glomerulonephritis. *J Pathol* 1999 Nov;189(3):431-438.
100. Matsumoto K, Mizuno S, Nakamura T. Hepatocyte growth factor in renal regeneration, renal disease and potential therapeutics. *Curr Opin Nephrol Hypertens* 2000 Jul;9(4):395-402.
101. Derksen PW, Keehnen RM, Evers LM, van Oers MH, Spaargaren M, Pals ST. Cell surface proteoglycan syndecan-1 mediates hepatocyte growth factor binding and promotes Met signaling in multiple myeloma. *Blood* 2002 Feb 15;99(4):1405-1410.
102. Aviezer D, Yayon A. Heparin-dependent binding and autophosphorylation of epidermal growth factor (EGF) receptor by heparin-binding EGF-like growth factor but not by EGF. *Proc Natl Acad Sci U S A* 1994 Dec 6;91(25):12173-12177.
103. Vaidya VS, Shankar K, Lock EA, Dixon D, Mehendale HM. Molecular mechanisms of renal tissue repair in survival from acute renal tubule necrosis: role of ERK1/2 pathway. *Toxicol Pathol* 2003 Nov-Dec;31(6):604-618.
104. Nakamura T, Sugino K, Titani K, Sugino H. Follistatin, an activin-binding protein, associates with heparan sulfate chains of proteoglycans on follicular granulosa cells. *J Biol Chem* 1991 Oct 15;266(29):19432-19437.
105. Maeshima A, Miya M, Mishima K, Yamashita S, Kojima I, Nojima Y. Activin A: autocrine regulator of kidney development and repair. *Endocr J* 2008 Mar;55(1):1-9.
106. Kuypers DR. Influence of interactions between immunosuppressive drugs on therapeutic drug monitoring. *Ann Transplant* 2008;13(3):11-18.
107. Lindahl U. Heparan sulfate-protein interactions--a concept for drug design? *Thromb Haemost* 2007 Jul;98(1):109-115.
108. Lindahl U, Li JP. Interactions between heparan sulfate and proteins-design and functional implications. *Int Rev Cell Mol Biol* 2009;276:105-159.

109. Gottmann U, Mueller-Falcke A, Schnuelle P, Birck R, Nickeleit V, van der Woude FJ, et al. Influence of hypersulfated and low molecular weight heparins on ischemia/reperfusion: injury and allograft rejection in rat kidneys. *Transpl Int* 2007 Jun;20(6):542-549.
110. Shin CS, Han JU, Kim JL, Schenarts PJ, Traber LD, Hawkins H, et al. Heparin attenuated neutrophil infiltration but did not affect renal injury induced by ischemia reperfusion. *Yonsei Med J* 1997 Jun;38(3):133-141.
111. Braun C, Schultz M, Fang L, Schaub M, Back WE, Herr D, et al. Treatment of chronic renal allograft rejection in rats with a low-molecular-weight heparin (reviparin). *Transplantation* 2001 Jul 27;72(2):209-215.
112. Andrew M, Mitchell L, Vegh P, Ofosu F. Thrombin regulation in children differs from adults in the absence and presence of heparin. *Thromb Haemost* 1994 Dec;72(6):836-842.
113. Sackler JP, Liu L. Heparin-induced osteoporosis. *Br J Radiol* 1973 Jul;46(547):548-550.
114. Newall F, Barnes C, Ignjatovic V, Monagle P. Heparin-induced thrombocytopenia in children. *J Paediatr Child Health* 2003 May-Jun;39(4):289-292.
115. Zhou T, Chen JL, Song W, Wang F, Zhang MJ, Ni PH, et al. Effect of N-desulfated heparin on hepatic/renal ischemia reperfusion injury in rats. *World J Gastroenterol* 2002 Oct;8(5):897-900.
116. Braun C, Schultz M, Schaub M, Fang L, Back WE, Herr D, et al. Effect of treatment with low-molecular-weight heparin on chronic renal allograft rejection in rats. *Transplant Proc* 2001 Feb-Mar;33(1-2):363-365.
117. Packham DK, Wolfe R, Reutens AT, Berl T, Heerspink HL, Rohde R, et al. Sulodexide Fails to Demonstrate Renoprotection in Overt Type 2 Diabetic Nephropathy. *J Am Soc Nephrol* 2011 Oct 27.
118. Callas DD, Hoppensteadt DA, Jeske W, Iqbal O, Bacher P, Ahsan A, et al. Comparative pharmacologic profile of a glycosaminoglycan mixture, Sulodexide, and a chemically modified heparin derivative, Suleparoides. *Semin Thromb Hemost* 1993;19 Suppl 1:49-57.
119. Rienstra H, Boersema M, Onuta G, Boer MW, Zandvoort A, van Riezen M, et al. Donor and recipient origin of mesenchymal and endothelial cells in chronic renal allograft remodeling. *Am J Transplant* 2009 Mar;9(3):463-472.

Chapter 2

Differential Expression of Proteoglycans in Tissue Remodeling and Lymphangiogenesis after Experimental Renal Transplantation in Rats

PLoS One. 2010 Feb 5;5(2):e9095.

Heleen Rienstra*
Kirankumar Katta*
Johanna W.A.M. Celie
Harry van Goor
Gerjan Navis
Jacob van den Born
Jan-Luuk Hillebrands

* Contributed equally

Abbreviations

BM	basement membrane
collXVIII	collagen type XVIII
CS	chondroitin sulfate
CTD	chronic transplant dysfunction
DA	Dark Agouti
FGS	focal glomerulosclerosis
HS	heparan sulfate
IF	interstitial fibrosis
TV	transplant vasculopathy
SMC	smooth muscle cell
WF	Wistar Furth

Abstract

Background: Chronic transplant dysfunction explains the majority of late renal allograft loss and is accompanied by extensive tissue remodeling leading to transplant vasculopathy, glomerulosclerosis and interstitial fibrosis. Matrix proteoglycans mediate cell-cell and cell-matrix interactions and play key roles in tissue remodeling. The aim of this study was to characterize differential heparan sulfate proteoglycan and chondroitin sulfate proteoglycan expression in transplant vasculopathy, glomerulosclerosis and interstitial fibrosis in renal allografts with chronic transplant dysfunction.

Methods: Renal allografts were transplanted in the Dark Agouti (DA)-to-Wistar Furth (WF) rat strain combination. DA-to-DA isografts and non-transplanted DA kidneys served as controls. Allograft and isograft recipients were sacrificed 81 and 66 days (mean) after transplantation, respectively. Heparan sulfate proteoglycan (collXVIII, perlecan and agrin) and chondroitin sulfate proteoglycan (versican) expression, as well as CD31 and LYVE-1 (vascular and lymphatic endothelium, respectively) expression were (semi-)quantitatively analyzed using immunofluorescence.

Findings: Arteries with transplant vasculopathy and sclerotic glomeruli in allografts displayed pronounced neo-expression of collXVIII and perlecan. In contrast, in interstitial fibrosis expression of the chondroitin sulfate proteoglycan versican dominated. In the cortical tubular basement membranes in both iso- and allografts, induction of collXVIII was detected. Allografts presented with extensive lymphangiogenesis ($p < 0.01$ compared to isografts and non-transplanted controls) which was associated with induced perlecan expression underneath the lymphatic endothelium ($p < 0.05$ and $p < 0.01$ compared to isografts and non-transplanted controls, respectively). The magnitude of lymphangiogenesis correlated with severity of interstitial fibrosis ($R^2 = 0.7634$, $p = 0.0002$) and reduced graft function (proteinuria: $R^2 = 0.4350$, $p = 0.0002$; plasma creatinine: $R^2 = 0.4350$, $p = 0.0347$).

Interpretation: Our results reveal that changes in the extent of expression and the type of proteoglycans being expressed are tightly associated with tissue remodeling after renal transplantation. Therefore, proteoglycans might be potential targets for clinical intervention in renal chronic transplant dysfunction.

Introduction

Chronic transplant dysfunction (CTD) explains the majority of long-term loss of transplanted kidneys [1,2]. Although considerable improvement has been made in overall graft survival due to improved prevention and treatment of acute rejection, the rate of long-term renal graft loss has remained unchanged over more than a decade. CTD is the overall outcome of tissue remodeling processes in multiple intrarenal structures (i.e. the intrarenal arteries, the glomeruli and the interstitium leading to transplant vasculopathy (TV), focal glomerulosclerosis (FGS) and interstitial fibrosis (IF), respectively [2-4] and is the resultant of various underlying causes [5]. TV is presumed to result from activation of the vascular endothelium, leading to the activation and migration of vascular smooth muscle cells (SMCs) and the development of an occlusive neointima in the lumen of the arteries [6]. The neointima consists of smooth muscle cells, extracellular matrix and inflammatory cells [7]. FGS presumably results from defects in the filtration barrier, which is formed by podocytes, the glomerular basement membrane (BM) and endothelial cells [8]. IF results from the accumulation of extracellular matrix synthesized by infiltrating and proliferating interstitial myofibroblasts. To date, due to the lack of knowledge on the pathogenesis of tissue remodeling leading to CTD, no effective therapies are available to prevent or treat CTD. The identification of molecules involved in pathological tissue remodeling after renal transplantation might provide novel targets for intervention.

Proteoglycans are glycoconjugates that play an important role in tissue remodeling. They consist of a core protein with one or more carbohydrate side chains (i.e. glycosaminoglycans, GAGs) attached. Depending on the composition of these GAGs, different types of proteoglycans can be distinguished: heparan sulfate (HS), chondroitin sulfate (CS), dermatan sulfate (DS), and keratan sulfate proteoglycans. The extracellular matrix HS proteoglycans collagen type XVIII (collXVIII), perlecan and agrin are components of BMs of various tissues [9-11]. The CS/DS proteoglycan versican is a major extracellular matrix component which is not expressed in BMs. Depending on the sulfation patterns of the carbohydrate side chains, HS and CS/DS proteoglycans are capable of binding and presenting a variety of proteins like chemokines and growth factors and are involved in various cell-cell and cell-matrix interactions [12].

Using a rat renal transplant model for chronic transplant dysfunction [13-15], we sought to determine the spatial expression of HS (collXVIII, perlecan, agrin) and CS/DS (versican) proteoglycans and its association with lymphangiogenesis. We used specific (semi-)quantitative immunofluorescent (double)labeling to identify the spatial expression of proteoglycans and lymphatics in non-transplanted kidney, isografts and allografts. We established a clear spatial relationship between the presence of HS and CS/DS proteoglycans in allografts and the development of CTD. Allografts were characterized by marked tubulointerstitial lymphangiogenesis coinciding with enhanced perlecan expression.

Both the magnitude of lymphangiogenesis and perlecan expression correlated with IF development and impaired graft function.

Methods

Rats

Inbred female (175-210 gram) and male (200-225 gram) Dark Agouti (DA) rats were obtained from Harlan (Horst, the Netherlands) and inbred male Wistar Furth (WF) rats (240-295 gram) from Charles River Laboratories Inc. (l'Arbresle, Cedex, France).

Ethics statement

All animals received care in compliance with the Principles of Laboratory Animal Care (NIH Publication No.86-23, revised 1985), the University of Groningen guidelines for animal husbandry (University of Groningen, the Netherlands), and the Dutch Law on Experimental Animal Care.

Kidney transplantation and experimental groups

Female DA kidneys were orthotopically transplanted into male recipients as described previously [14]. Cold ischemic time ranged from 16 to 38 min. Warm ischemic time ranged from 19 to 32 min. Recipients received cyclosporine A (5 mg/kg bodyweight) (Sandimmune, Novartis, the Netherlands) subcutaneously on the first 10 days after transplantation. The contralateral native kidney was removed 8 to 14 days after transplantation. Total follow-up was 12 wks or shorter in case animals had to be sacrificed due to graft failure. The following experimental groups were included: control (non-transplanted) DA kidneys (n=5), DA-to-DA isografts (n=5), and DA-to-WF allografts (n=11). Clinical variables of recipients within these groups have been described in detail elsewhere [14;15]. Briefly, isograft recipients were sacrificed at day 81 [70-84] (mean [range]) and allograft recipients at day 66 [40-84] after transplantation. The allograft recipients showed significantly increased plasma creatinine levels measured at time of sacrifice compared with isograft recipients (119 [93-139] $\mu\text{mol/L}$ vs. 42 [34-50] $\mu\text{mol/L}$, respectively, $p < 0.005$ Mann-Whitney test). In addition, allograft recipients developed severe proteinuria compared with isograft recipients (110 [9-262] vs. 18 [9-43] mg/day, respectively, $p < 0.05$ Mann-Whitney test).

Immunofluorescence

Four-micron frozen sections fixed in acetone or 4% formaldehyde were blocked for endogenous peroxidase activity with 0.03% H_2O_2 if appropriate. For some stainings the

sections were blocked with normal goat, rabbit or mouse serum. Sections were incubated for 1 hr with the following primary antibodies: rabbit anti-mouse collagen XVIII (NC11, kindly provided by Dr. T. Sasaki, Shrines Hospital for Children, Portland, OR, USA), mouse anti-rat perlecan (10B2, kindly provided by Dr. Couchman, Biomedicine Institute, University of Copenhagen, Denmark), sheep anti-rat agrin (Gr14) [16], mouse anti-heparan sulfate stub region (F69-3G10, Tokyo, Japan), mouse anti-HS (JM-403) [17,18], mouse anti-rat CD31 (TLD-3A12, BD Pharmingen, the Netherlands), and rabbit anti-LYVE-1 (Millipore, USA). Binding of primary antibodies was detected by incubating the sections for 30 min with secondary antibodies diluted in PBS with normal rat serum: rabbit anti-mouse HRP (DAKO, Belgium), goat anti-rabbit FITC (SouthernBiotech, USA), and rabbit anti-sheep HRP (DAKO). HRP activity was visualized using the TSATM Tetramethylrhodamine System (PerkinElmer LAS Inc., USA). Nuclei were stained with DAPI.

L-selectin binding assay with enzymatic pre-treatments

L-selectin-IgM chimeric protein, consisting of the extracellular domain of human L-selectin linked to an IgM Fc-tail [19] was allowed to bind for 1hr. L-selectin binding was detected by incubation with rabbit anti-human IgM HRP (DAKO) for 30 min, followed by the use of the TSATM Tetramethylrhodamine System. Heparitinase I (EC4.2.2.8), and chondroitinase ABC (EC4.2.2.4) (both from Seikagaku, Tokyo, Japan) were used to digest the side chains of the heparan sulfate and chondroitin sulfate proteoglycans, respectively. To this end, prior to some L-selectin binding assays, enzymatic pretreatments were performed with heparitinase I (0.05 U/ml) and/or chondroitinase ABC (1 U/ml) in acetate buffer (50 mM $C_2H_3O_2Na$, 5 mM $CaCl_2 \cdot 2H_2O$, 5 mM $MgCl_2 \cdot 6H_2O$, [pH 7.0 for heparitinase I, pH 8.0 for chondroitinase ABC]) for 1 hr at 37°C.

Fluorescence microscopy

Fluorescence microscopy was performed using a Leica DMLB microscope (Leica Microsystems, Rijswijk, the Netherlands) equipped with a Leica DC300F camera and LeicaQWin 2.8 software. Confocal imaging was performed with a Leica TCS SP2 confocal laser scanning microscope equipped with the Leica Confocal Software package (version 2.61).

Quantification of protein expression in stained tissue sections

Semiquantitative scoring of proteoglycan expression was performed independently by two observers (HR and KK) and the mean value of both observers was used. In the rare cases

discrepancies were identified between the values of both observers, the respective sections were re-evaluated in the presence of a third observer (JvdB) until consensus was reached. Both intensity of the staining as well as the stained surface area of the structures in the specific renal compartments (i.e. intima, media, neointima, Bowman's capsule, glomerular BM, mesangial matrix, interstitial matrix and tubular BMs) were scored separately in a semi-quantitative manner on a scale ranging from 0-4. For staining intensity the following grading was used (relative to the strongest staining observed in a specific renal compartment of interest): 0= no staining, 1=weak staining, 2=moderate staining, 3=strong staining, 4= most intense staining observed. For surface area stained the following grading system was used (relative to the total area of the specific renal compartment of interest): 0= no staining, 1= 0-25% area positive, 2= 26-50% area positive, 3= 51-75% area positive, 4= 76-100% area positive. Quantification of perlecan, CD31 and LYVE-1 in the outer medulla was performed in four overview photomicrographs of randomly selected fields (magnification 320x). The total area stained was quantified using ImageJ 1.41 (Rasband, W.S., ImageJ, U.S. National Institutes of Health, Bethesda, Maryland, USA) which was downloaded from <http://rsb.info.nih.gov/ij/download.html>).

Statistics

Differences between non-transplanted control kidneys, isografts and allografts in total area stained for perlecan, CD31 and LYVE-1 were tested with a Mann-Whitney test. Spearman correlation analysis was performed to correlate the magnitude of lymphangiogenesis to interstitial fibrosis and renal function parameters. $p < 0.05$ was considered statistically significant. Statistics were performed using GraphPad Prism 5.00 for Windows (GraphPad Software Inc., USA).

Results

Chronic tissue remodeling in renal grafts

The rat renal allografts showed severe CTD with transplant vasculopathy (TV), focal glomerulosclerosis (FGS) and interstitial fibrosis (IF) (Figure 1), as reported previously [14,15]. The isografts developed some interstitial remodeling characterized by tubular atrophy and IF, but to a much lesser extent than observed in the allografts (not shown) [14,15]. Development of TV and FGS was minimal in isografts.

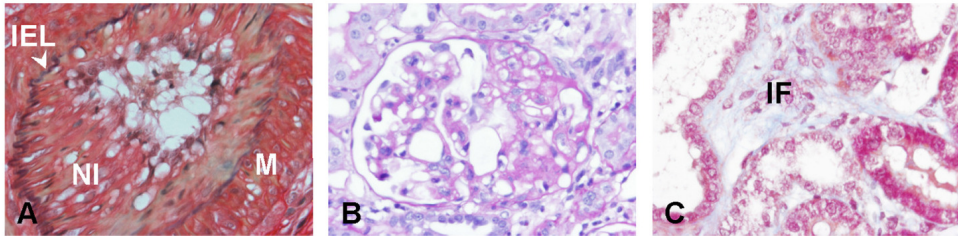


Figure 1. Allografts present severe development of transplant vasculopathy (A), focal glomerulosclerosis (B) and interstitial fibrosis (C). (A) Intrarenal artery with a neointima (Verhoeff staining [elastic laminae: black; collagen: red; smooth muscle cells: yellow]). (B) Glomerulus with a sclerotic lesion (periodic acid-Schiff staining [glycogen in connective tissue: purple-magenta]). (C) Part of the tubulointerstitium with a fibrotic area (Masson's trichrome staining [collagen: blue]). Stainings were performed on 2 μ m formalin-fixed paraffin sections. Abbreviations: IEL: internal elastic lamina; IF: interstitial fibrosis; M: media; NI: neointima. Magnification 400x.

Heparan sulfate proteoglycan expression in non-transplanted control kidneys

In non-transplanted DA control kidneys, the HS proteoglycans collXVIII, perlecan, and agrin, as well as the CS/DS proteoglycan versican were strongly expressed in the intima of the arteries (Figure 2A-D). More specifically, the HS proteoglycans were located in the subendothelial BM whereas versican was located in the apical endothelial cell membrane (Figure 2D, insert). The BM of vascular SMCs in the media were characterized by a strong expression of collXVIII and a patchy expression of perlecan (Figure 2A and B). The arterial expression of proteoglycans was similar in arteries in isografts and arteries without TV in allografts (not shown).

In the glomerular BM of non-transplanted control kidneys, expression of collXVIII was moderate whereas perlecan was virtually absent (Figure 2E and F). In contrast to collXVIII and perlecan, agrin was abundantly present (Figure 2G). All three HS proteoglycans were strongly expressed in the Bowman's capsule but only minimally in the mesangial matrix (Figure 2E-G). A patchy glomerular versican expression pattern was observed suggesting non-glomerular BM staining (Figure 2H).

Double labeling for versican and the mesangial cell marker CD90 (Thy-1) [20] did not reveal co-localization indicating non-mesangial versican origin (not shown). Double labeling for versican and CD31 revealed minor co-localization of versican and glomerular ECs (not shown). Since the limited endothelial versican expression could not account for the majority of glomerular versican expression, these data suggest podocyte origin of glomerular versican. These observations are in line with previous data showing that glomerular versican is expressed by both podocytes and glomerular endothelium [21,22].

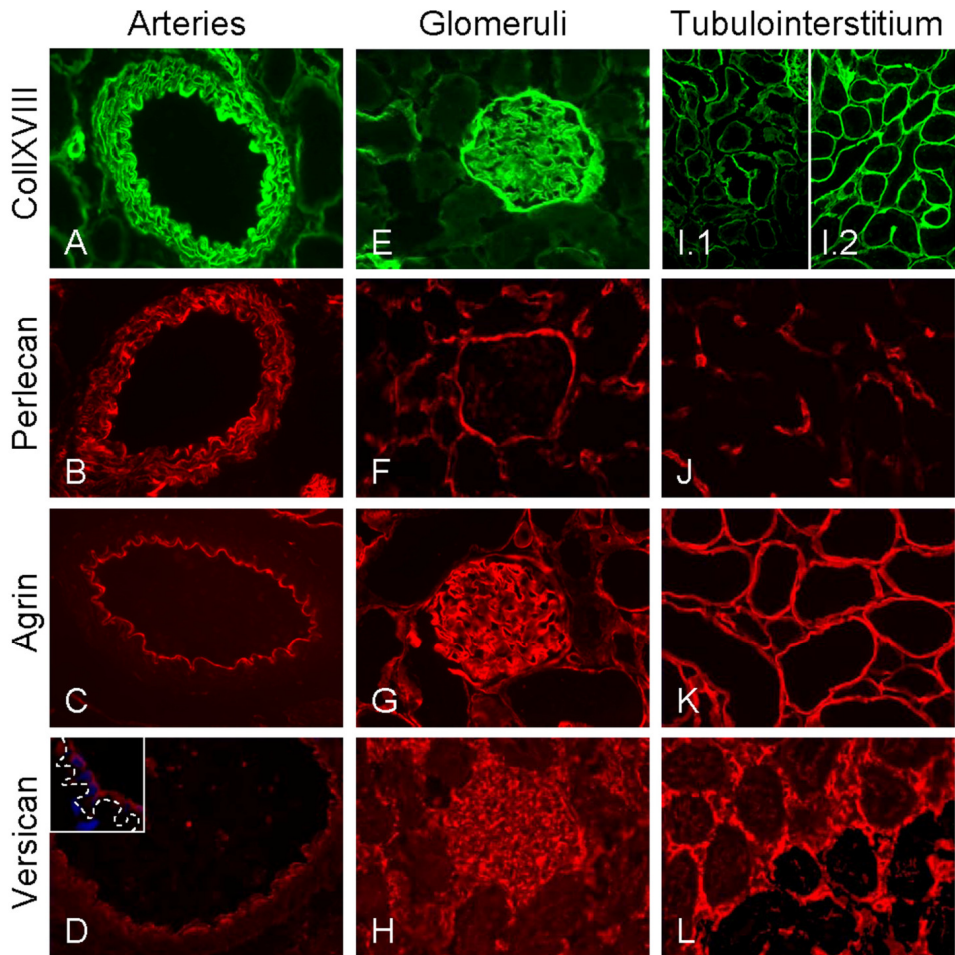


Figure 2. Proteoglycan expression in arteries, glomeruli and tubulo-interstitium of non-transplanted control kidneys. All proteoglycans were strongly expressed in the intima of arteries (A-D). HS proteoglycans were located in the subendothelial BM while versican was located in the endothelial cell membrane (insert D, confocal image, magnification 3780x). The BMs of vascular SMCs in the media showed a strong expression of collXVIII and a patchy expression of perlecan (A and B). In the glomeruli (E-H), the glomerular BM moderately expressed collXVIII (E) while perlecan was virtually absent (F) whereas agrin was abundantly present (G). All HS proteoglycans were expressed in Bowman's capsule but only minimally in the mesangial matrix (E-G). Dotted staining pattern for versican suggested expression by podocytes (H). In the tubulo-interstitium (I-L), tubular BMs minimally expressed collXVIII and perlecan in the cortex (I.1 and J). Compared with the cortex, collXVIII expression was increased in medullary tubular BMs (I.2). Perlecan was moderately to strongly expressed in peritubular capillaries (J). Agrin was uniformly expressed in tubular BMs (K). Versican was not present in tubular BMs but strongly expressed in the tubulointerstitial matrix (L). Magnifications: A-G, H & J: 640x; I: 320x.

In the tubular BM, expression of collXVIII was only minimal in the cortical regions (Figure 2I.1) but more pronounced in the medullary regions (Figure 2I.2). Agrin was strongly expressed in all tubular BMs in a uniform fashion (Figure 2K). The tubular BMs were virtually devoid of perlecan expression but we observed moderate to strong expression of

perlecan in the peritubular capillaries (Figure 2J) as well as in larger vessels (Figure 2B). Although versican was not present in the tubular BM, it was strongly expressed in the interstitial matrix (Figure 2L), where all three HS proteoglycans were absent.

Table 1 summarizes the semi-quantitative scoring of proteoglycan expression (both intensity and surface area) in the intrarenal arteries, glomeruli and interstitium. Below we describe the significant changes in expression of HS proteoglycans and versican in renal isografts, and allografts with CTD.

Differential proteoglycan expression in isografts compared with control kidneys

Table 1. Proteoglycan expression in the specific renal compartments in non-transplanted control kidneys, isografts, and allografts.

	Artery			Glomerulus			Tubulointerstitium		
	Intima	Media	NI	BC	GBM	MM	Matrix	TBM	
								cortex	med
CollXVIII									
control	3 (3)	2 (4)		3 (4)	2 (4)	1 (4)	0	½ (4)	1½ (4)
isograft	3 (3)	2 (4)		3 (4)	2 (4)	1 (4)	½ (1)	2 (4)	2 (4)
allograft	3 (3)	2 (4)	3 (4)	3 (4)	1-3 (4)	1-3 (4)	½ (1)	2 (4)	2 (4)
Perlecan									
control	3 (2)	1-3 (4)		1-3 (3)	½ (1)	½ (1)	0	½ (1)	½ (1)
isograft	3 (2)	1-3 (4)		1-3 (3)	2-3 (2)	1-3 (2)	1 (1)	1 (2)	1 (2)
allograft	3 (2)	1-3 (4)	3 (4)	1-3 (3)	3 (4)	1-3 (4)	1 (1)	1 (2)	1 (2)
Agtrin									
control	3 (4)	½ (1)		1-3 (3)	3 (4)	1 (2)	0	2½ (4)	3 (4)
isograft	3 (4)	½ (1)		1-2 (3)	3 (4)	1 (2)	0	2-3 (4)	2-3 (4)
allograft	3 (4)	1-2 (1)	1-3 (2)	1-3 (3)	3½ (4)	1 (2)	0	2-3 (4)	2-3 (4)
Versican									
control	2 (4)	1 (3)		0	0	0	3 (4)	0	0
isograft	2 (4)	1-2 (3)		0	0	0	2-3 (4)	0	0
allograft	2 (4)	1-2 (3)	2 (1)	0	0	0	2-3 (4)	0	0

Semi-quantitative scores (ranging from 0-4) of proteoglycan expression presented as the staining intensity and, between parentheses, the surface area stained (as described in detail in the Methods section). Scores given are the group means of the different grafts analyzed. Numbers of grafts analyzed are: non-transplanted control, n=5; isografts, n=5; allografts, n=11. The framed values indicate differentially expressed proteoglycans in the various groups as discussed in more detail in the Results section. Abbreviations: NI, neointima; BC, Bowman's capsule; GBM, glomerular basement membrane; MM, mesangial matrix; TBM, tubular basement membrane; med, medulla.

The expression profile of proteoglycans in renal isografts was mostly similar to the expression profile in control kidneys except for changes in the glomerular and tubular BMs (Table 1). In the glomerular BM, perlecan expression was increased compared with control kidneys, but to a far lesser extent than observed in allografts (described below). In the tubular BM of isografts, an increased cortical expression of collXVIII and slight induction of perlecan was observed. The expression of agrin in the tubular BM remained strong alike control kidneys, although after transplantation the expression was slightly interrupted. In regions with IF (only limited present compared with allografts), an increased expression of versican was observed.

Differential proteoglycan expression in neointima and FGS versus IF in allografts

In arteries with TV in allografts, strong expression of collXVIII and perlecan was observed in the newly-formed neointima (Figure 3A and B). The expression of agrin and versican in the neointima was less prominent than collXVIII and perlecan, and varied in intensity within a single neointima. Agrin and versican expression in the media was slightly upregulated compared with non-transplanted control kidneys (Figure 3C and D).

In sclerotic lesions of FGS, we also observed a strong expression of collXVIII and perlecan (Figure 3E and F). Within a single glomerulus differential expression of collXVIII expression was detected and contained both areas with decreased or strongly increased expression compared with control kidneys and isografts (Figure 3E). Agrin was not differently expressed in these lesions (Figure 3G) compared with glomerular BM staining in control kidneys. Compared with control kidneys and isografts, no altered expression of versican was observed in the glomeruli of allografts (Figure 3H). In the glomerular BM, and probably also podocytes of allografts, an impressive induction of perlecan expression was detected compared with its expression in control kidneys and isografts (Figure 3F).

In contrast to the neointima and glomerulosclerotic lesions, collXVIII and perlecan were minimally expressed in IF with complete absence of agrin (Figure 3I-K). However, collXVIII/agrin and perlecan were clearly expressed in the tubular BM and peritubular capillaries, respectively (Figure 3I-K) as described in more detail below. In contrast to the HS proteoglycans, we observed a massive expression of versican in IF (Figure 3L). These data indicate that in neointimal and glomerular lesions HS proteoglycans dominate, whereas in regions with IF CS/DS proteoglycans are more prominent.

Increased expression of collXVIII in cortical tubular basement membranes in allografts

The expression profile of proteoglycans in the cortical tubular BM was similar in allografts and isografts (Table 1). In the allografts, increased expression of collXVIII and a slight

induction of perlecan was detected (Figure 3I and J). Increased collXVIII expression was observed in both cortical (Figure 3 I.1) and medullary (Figure 3 I.2) tubular BMs. Agrin remained strongly expressed; however, in a less homogeneous pattern compared with control kidneys (Figures 2K and 3K).

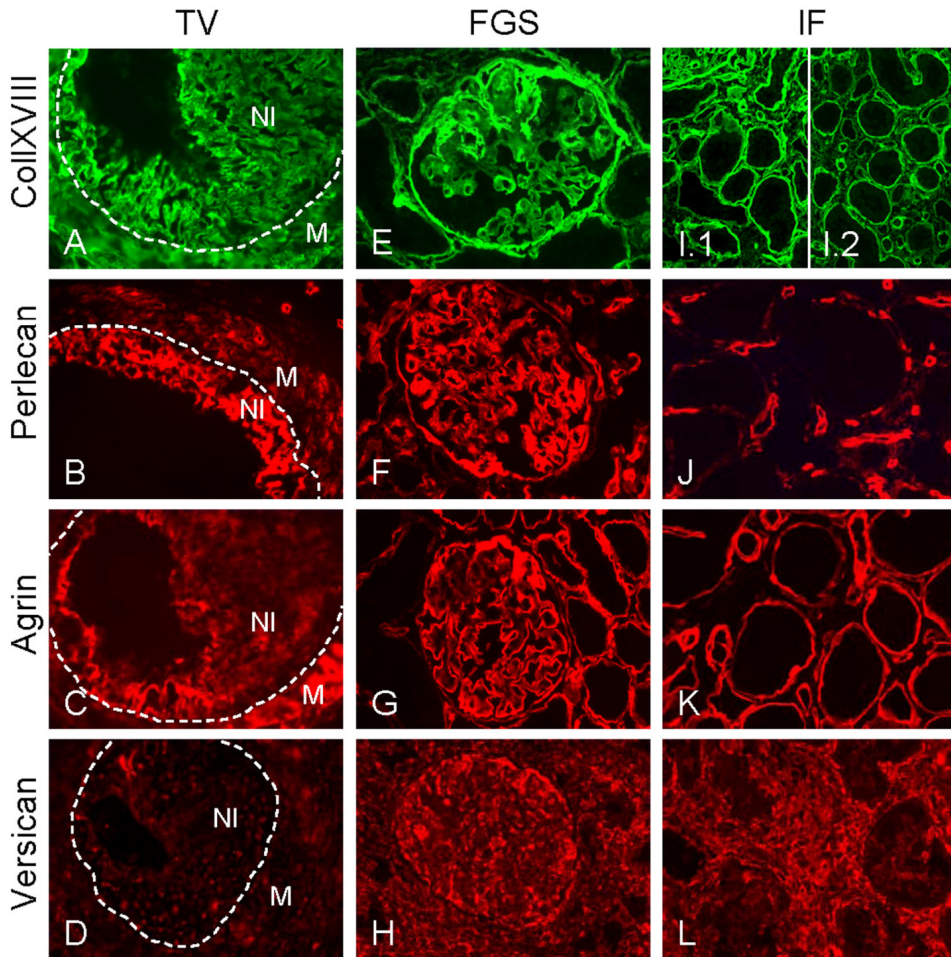


Figure 3. Proteoglycan expression in transplant vasculopathy (TV), focal glomerulo-sclerosis (FGS) and tubulointerstitial fibrosis (IF) in allografts. In the neointima in TV, collXVIII and perlecan were strongly expressed (A and B). Expression of agrin and versican was less prominent in the neointima but their expression was slightly upregulated in the media (compared with non-transplanted control tissue) (C and D). Dotted lines indicate the internal elastic lamina. In the glomeruli (E-H), expression of collXVIII in the glomerular BM was variable with strong expression in glomerulosclerotic lesions (E). Perlecan was strongly induced in the glomerular BM (F). Agrin expression remained similar to its expression in glomerular BMs in non-transplanted control tissue (G). Versican staining was comparable with non-transplanted control tissue (H). In the tubulointerstitium (I-L), collXVIII (I) and perlecan (J) were minimally present in IF in which agrin expression was absent (K). CollXVIII was clearly expressed by tubular BMs in cortical (I.1) and medullary (I.2) regions at similar levels. Versican was strongly expressed in IF (L). In the cortical tubular BM, collXVIII was strongly expressed with a strong, but slightly interrupted, expression of agrin (I and K). Perlecan was only weakly expressed in the tubular BM but strongly expressed in peritubular capillaries (J). Magnification 640x.

Proteoglycan core proteins expressed in allografts contain functional glycosaminoglycan side chains

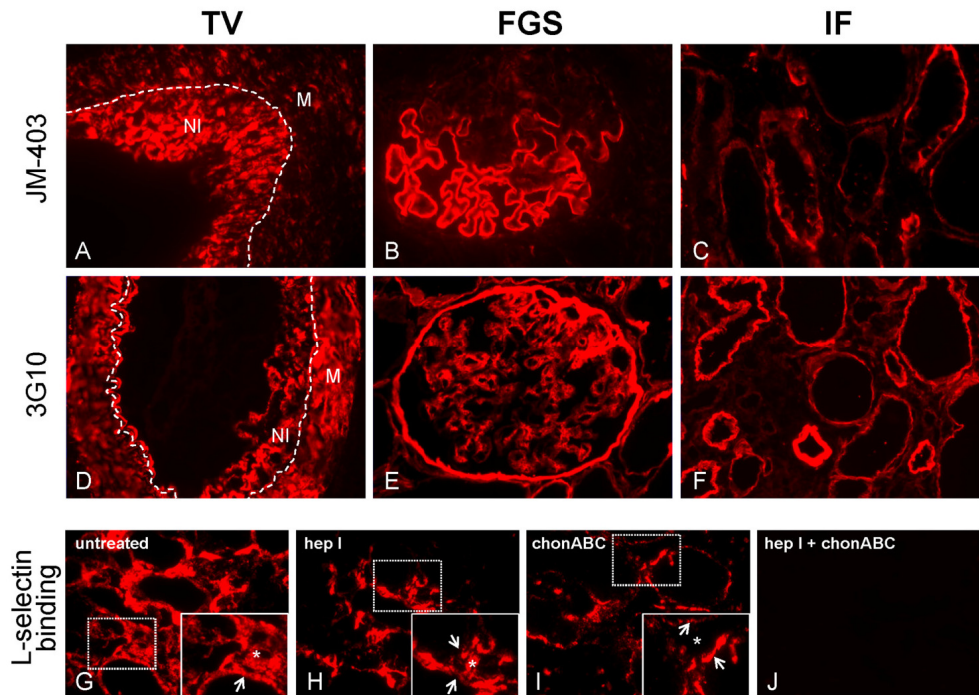


Figure 4. Proteoglycan core proteins expressed in transplant vasculopathy, glomerulosclerosis and interstitial fibrosis in allografts contain functional glycosaminoglycan side chains. Neointimal cells in TV (A), glomerular BMs in non-sclerotic areas (B) and tubular BMs in IF (C) express heparan sulfate domains with N-unsubstituted glucosamine residues as recognized by antibody JM-403. Following heparitinase treatment presence of heparan sulfate stub regions was identified in medial and neointimal cells in TV (D), in glomerular BMs (E) and in tubular BMs (F) using antibody F69-3G10. Dotted line in panel A and D represents the internal elastic lamina. Abbreviations: M: media; NI: neointima. L-selectin-IgM chimeric protein binding in the tubulointerstitial in no pre-treated sections (G), sections pre-treated with heparitinase I [hep I] (H), sections pre-treated with chondroitinase ABC [chonABC] (I) and sections pre-treated with both heparitinase I and chondroitinase ABC (J). Insets show high power magnifications of the framed areas. Arrow: tubular BMs, asterisk: interstitium.

In order to determine whether the proteoglycans (differentially) expressed in allografts contain HS glycosaminoglycan side chains, stainings with the antibodies JM-403 and 3G10 were performed. JM-403 recognizes heparan sulfate domains with N-unsubstituted glucosamine residues [17,18]. As shown in Figure 4 A-C, neointimal cells in TV (A), glomerular BMs in non-sclerotic areas of glomeruli (B) and tubular BMs in IF (C) indeed expressed heparan sulfate domains with N-unsubstituted glucosamine residues, thereby confirming the presence of HS side chains. As JM-403 only recognizes a specific subset of HS side chains, not all HS glycosaminoglycans present will be detected using JM-403. Therefore, we additionally performed stainings using antibody F69-3G10. F69-3G10

recognizes HS stubs that remain attached to the proteoglycan core protein following heparitinase treatment. As shown in Figure 4 D-F, F69-3G10 staining revealed presence of HS stubs in medial and neointimal cells in TV (D), in glomerular BMs (E) as well as tubular BMs (F), also confirming presence of HS glycosaminoglycans on the proteoglycan core proteins.

Finally, to demonstrate that the glycosaminoglycan side chains are capable of binding L-selectin (as an example of a natural ligand), L-selectin binding assays were performed. As shown in Figure 4G, L-selectin binding in the tubulointerstitium was detected on the tubular BMs as well as in the interstitium. To determine whether L-selectin preferentially binds to HS or CS/DS proteoglycans, sections were pre-incubated with heparitinase I and/or chondroitinase ABC. Following heparitinase I pre-treatment, only interstitial L-selectin binding was preserved indicating preferential binding of L-selectin to HS proteoglycans in tubular BMs (Figure 4H). Following chondroitinase ABC pre-treatment, only L-selectin binding to tubular BMs was preserved indicating preferential binding of L-selectin to CS/DS proteoglycans in the interstitium (Figure 4I). Sections pre-treated with both heparitinase I and chondroitinase ABC were completely devoid of L-selectin binding (Figure 4J).

Abundant lymphangiogenesis is related to increased expression of perlecan

In the interstitium of allografts we observed a significant increase in expression of perlecan in a capillary-like pattern (Figure 5A-C). Since perlecan has been related to angiogenesis [23-26], we analyzed whether the increased perlecan expression was associated with the formation of new peritubular capillaries. However, quantification of interstitial CD31 staining revealed that allografts do not contain an increased number of peritubular capillaries (Figure 5D-F). Instead, we observed a non-significant decrease in area stained positively for CD31 per given surface area in both allografts and isografts, which might be associated with enlargement of the renal graft after transplantation due to removal of the contralateral kidney [15]. When staining for the lymphatic marker LYVE-1 [27], we observed a marked increase in the number of lymph vessels in the allografts (Figure 4G-I) indicative of lymphangiogenesis. In isografts, we also observed an increase in LYVE-1 staining but to a significant lesser extent than observed in allografts (Figure 5I). Double labeling for perlecan and LYVE-1 revealed that the newly-formed lymph vessels all express perlecan in their BM (Figure 5J-L). In addition, allografts also displayed abundant presence of capillary-like structures that were strongly positive for perlecan but LYVE-1 negative, indicating an overall upregulation of perlecan in pre-existing peritubular capillaries as well (Figure 5J-L). The observed increase in perlecan expression in isografts and allografts positively correlated with the severity of IF (Spearman $r=0.5580$, $p=0.0475$)

as well as serum creatinine levels (Spearman $r=0.7770$, $p=0.0004$ [8 wk] and Spearman $r=0.8182$, $p=0.0011$ [12 wk]) and proteinuria (Spearman $r=0.6714$, $p=0.0061$ [8 wk] and Spearman $r=0.7510$, $p=0.0031$ [12 wk]).

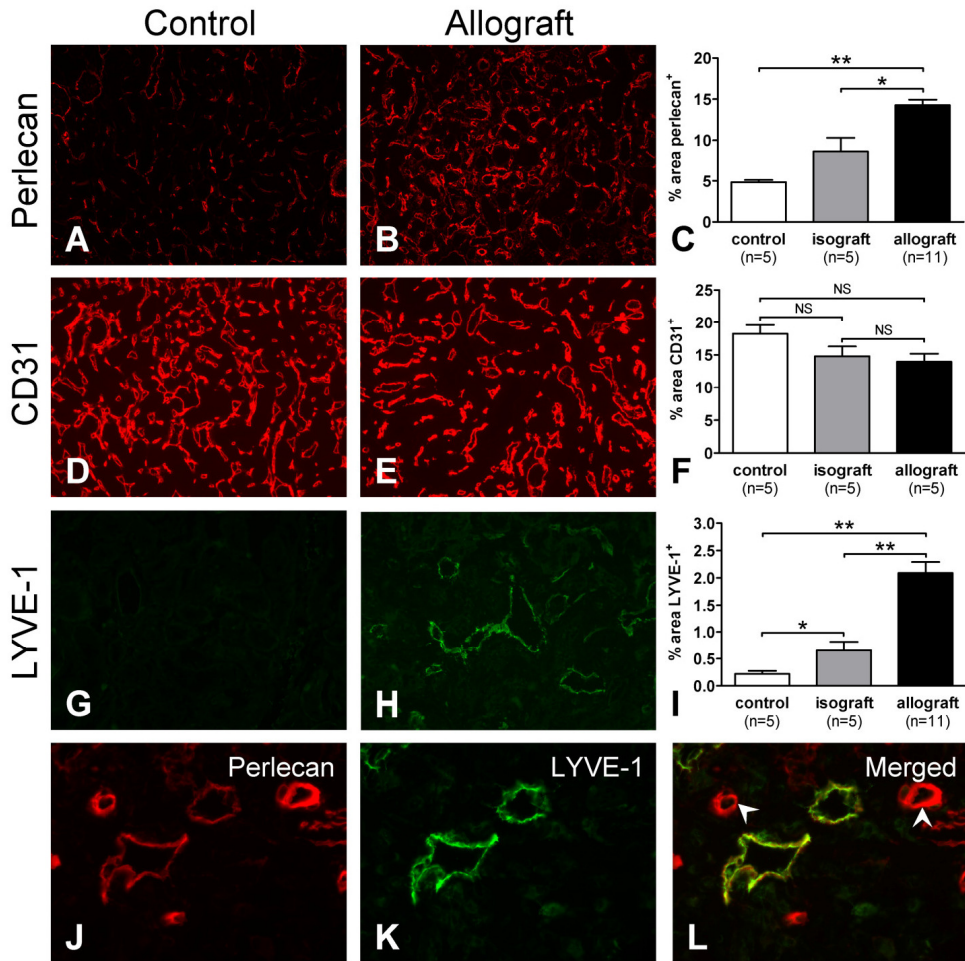


Figure 5. Lymphangiogenesis in the tubulo-interstitium is associated with perlecan expression. Expression of perlecan in allografts was significantly increased compared with non-transplanted control kidneys and isografts (A-C). After transplantation (of both iso- and allografts), the area with CD31 expression slightly decreased (D-F) (NS: not significant). In allografts, LYVE-1 expression was significantly increased compared with non-transplanted control kidneys and isografts (G-I). Double staining for perlecan and LYVE-1 revealed that perlecan is expressed in association with lymphatic endothelium in the newly-formed lymphatics (J-L). Arrowheads indicate peritubular capillaries strongly positive for perlecan but negative for LYVE-1. C, F and I represent the quantification of surface area stained for perlecan, CD31 and LYVE-1, respectively. Magnification A, B, D, E, G, H: 320x; J-L: 640x. * $p<0.05$, ** $p<0.01$

Lymphangiogenesis in renal grafts correlate with IF and impaired graft function.

In order to analyze whether the magnitude of tubulointerstitial lymphangiogenesis correlates with the severity of IF and graft function, Spearman correlation analyses were performed in which data from both the isografts and allografts were included. As shown in Figure 6A, the magnitude of lymphangiogenesis showed a significant positive correlation with the severity of IF. When analyzing proteinuria and plasma creatinine levels (measured at 8 wks after transplantation), also these functional variables turned out to be positively correlated with the magnitude of lymphangiogenesis at sacrifice (Figures 6B & C, respectively). Similarly, plasma creatinine levels at sacrifice positively correlated with lymphangiogenesis (Spearman $r=0.8571$, $p=0.0137$). Increased plasma creatinine levels translated into reduced creatinine clearance, which was inversely correlated with the magnitude of lymphangiogenesis (Figure 6D).

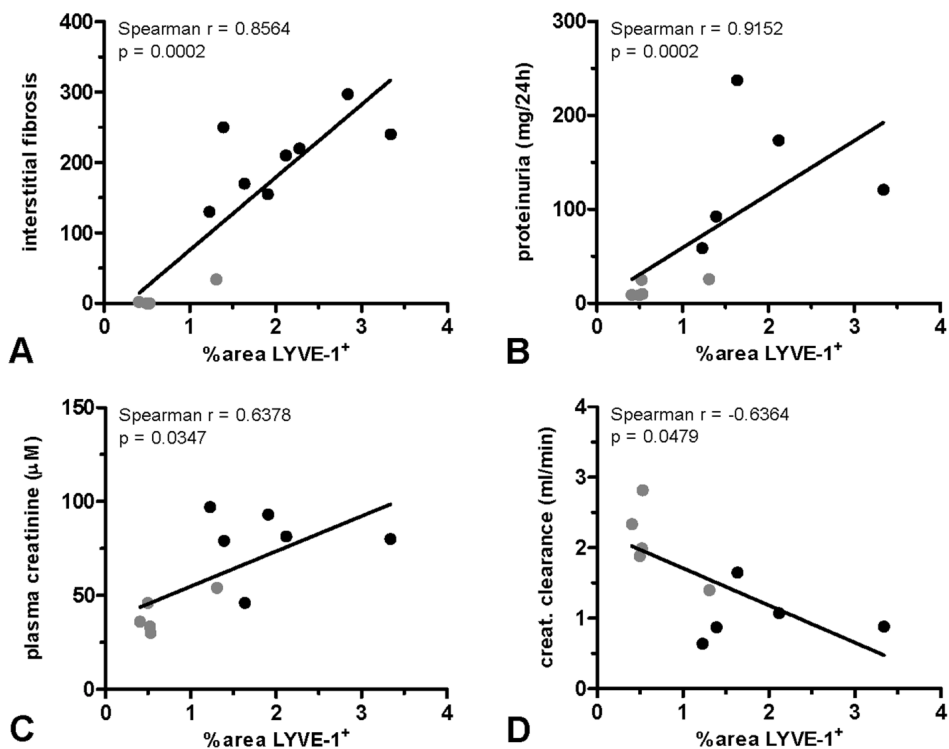


Figure 6. Lymphangiogenesis in the tubulo-interstitium correlates with severity of interstitial fibrosis (A), proteinuria (B), plasma creatinine levels (C) and creatinine clearance (D). Interstitial fibrosis, proteinuria (8 wks post transplantation), plasma creatinine levels (8 wks post transplantation) and creatinine clearance (8 wks post transplantation) were determined as recently described [14;15]. LYVE-1 expression was quantified as described in the Methods section. (● isografts, ● allografts)

Discussion

This study is the first to demonstrate the extensive involvement of proteoglycans in tissue remodeling in experimental CTD, demonstrating marked changes in proteoglycan expression in the intrarenal arteries, glomeruli and interstitium. The following key observations were made. First, whereas heparan sulfate (HS) proteoglycans dominate in neointimal lesions in transplant vasculopathy (TV) and in focal glomerulosclerosis (FGS), the chondroitin sulfate/dermatan sulfate (CS/DS) proteoglycan versican dominates in interstitial fibrosis (IF). Second, glomerular remodeling is associated with an impressive induction of perlecan expression in the glomerular BM. Third, the HS proteoglycan content becomes increased in cortical tubular BMs, especially due to increased collXVIII expression. Finally, allografts are characterized by marked tubulointerstitial lymphangiogenesis which correlates with IF development and impaired graft function.

Some earlier work demonstrated increased HS polysaccharides in fibrotic and sclerotic lesions in vessels, interstitium and mesangium of chronic renal transplant dysfunction [28], along with increased glycosaminoglycan-mediated chemokine binding [29,30]. However, proteoglycan core-proteins were not identified in those studies. In non-transplant renal diseases, tubular upregulation of collagen XVIII/endostatin was reported in a number of experimental models [31-33]. Mesangial expression of perlecan and agrin was reported in human diffuse mesangial sclerosis [34], in diabetic nephropathy [35,36], and some other human glomerulopathies with mesangial expansion [37]. Concerning proteoglycan expression in the neointima, both perlecan and versican have been shown to be present in neointimal lesions formed after experimental or human stenting or denudation or related to atherosclerosis [38-40]. The neointima in arteries of human cardiac allograft contain versican [41]. The striking similarities in proteoglycan expression in transplantation unrelated kidney diseases and chronic renal allograft dysfunction suggest comparable matrix remodeling programmes. This might indicate that anti-fibrotic treatments in various kidney diseases might also reduce chronic transplant dysfunction.

We showed differential expression of HS proteoglycans in neointimal lesions and FGS on one hand, and CS/DS proteoglycans in IF on the other, suggesting the existence of spatial (i.e. compartment-specific) proteoglycan responses during the development of CTD with potentially variable biological effects. Expression of the CS/DS proteoglycan versican in IF is likely involved in leukocyte recruitment and infiltration by its L-selectin-binding capacity [30,42]. The abundant versican expression in IF supports our previous finding demonstrating that L-selectin in the interstitium binds to CS/DS side chains and not HS side chains [43] which was supported by preliminary data obtained in our experimental transplant model in rats revealing virtual absence of L-selectin binding following chondroitinase treatment (not shown). Moreover, the high L-selectin-binding capacity of CS/DS proteoglycans in IF fits well with our observation that most leukocyte infiltration was observed in interstitial regions and to a far lesser extent in neointimal lesions and FGS.

The marked expression of versican in IF is probably produced by interstitial myofibroblasts [44,45]. Tubulointerstitial versican might contribute to the activation and proliferation of intra- and extrarenal myofibroblasts and may also mediate their recruitment. In line with this, we recently demonstrated that ~53% of interstitial myofibroblasts in IF are derived from extrarenal sources [14] and may originate from a population of recirculating fibrocytes. Fibrocytes are mesenchymal progenitor cells exhibiting morphological characteristics of hematopoietic stem cells, monocytes and fibroblasts and have the capacity to differentiate into α -SMA-expressing myofibroblasts which is promoted by TGF- β [46]. Although HS proteoglycans have been shown to modulate hematopoietic progenitor cell homing [47] this needs to be experimentally proven for CS/DS proteoglycans.

In contrast to interstitial myofibroblasts in IF, neointimal SMCs in experimental renal allografts are solely derived from an intrarenal source, probably the arterial media [14]. In the current study, we observed a strong expression of perlecan in the neointima. Perlecan expression in arteries has been associated with inhibition of SMC proliferation and reduced intimal hyperplasia [25,39,48-50] which favours for a role of perlecan in neointima stabilization. However, data reported by others indicate that arterial HS proteoglycans can actually activate SMC proliferation by modulating the function of basic fibroblast growth factor (bFGF/FGF2) [51]. Although clear expression of collXVIII was observed in the neointima, its potential role in neointima formation is as yet unknown.

After transplantation, we observed a strong induction of perlecan in the glomerular and peritubular capillary BMs. Peritubular capillaries play an essential role in graft rejection [52]. Upon capillary inflammation, endothelial cells become activated and changes occur in the BM, like splitting and multi-layering [53,54]. The response in peritubular capillaries is similar to that observed in glomerular capillaries, and the thickened BM might be the resultant of processes associated with endothelial cell death and regeneration [53,54]. Capillary BM changes are related to our previous data indicating endothelial chimerism (i.e. presence of recipient-derived endothelial cells) in glomerular and peritubular capillaries in CTD [14]. Both endothelial chimerism and perlecan expression in capillaries could be essential in capillary endothelial regeneration [23]. Perlecan in capillary BM might thus play a role in maintaining the capillary endothelial integrity but also contribute to the inflammatory response [30].

We observed a major increase of collXVIII expression in the tubular BM after renal transplantation in both iso- and allografts. The integrity of the tubular BM and its changes are involved in inflammation, phenotypic changes of tubular epithelial cells, and the development of IF and tubular atrophy [29,55-57]. Tubular epithelial cells can contribute to IF via epithelial-to-mesenchymal transition (EMT) in which epithelial cells transdifferentiate into interstitial myofibroblasts [58-60]. CollXVIII and (weakly expressed) perlecan in the tubular BM could play a role in the EMT process by binding of chemokines and growth factors resulting in a concentration gradient in the tubular BM [61]. This gradient might then direct migration of tubular epithelial cells into the interstitium during

EMT. In line with this, preliminary data indeed suggest increased binding capacity of HS proteoglycans for HB-EGF in the tubular BM in allografts (not shown).

The more interrupted and less uniform expression of agrin in tubular BMs after transplantation supports the assumption that agrin normally plays a role in anchoring tubular epithelial cells and focal loss of agrin could therefore be related to migration of transdifferentiated tubular cells in EMT or tubular atrophy [62,63]. In addition to tubular atrophy and EMT, proteoglycan expression in the tubular BM could be involved in binding of L-selectin, thereby facilitating inflammatory responses in tubules [30,64]. The potential causal role of BM HS proteoglycans in tubular atrophy or EMT are under current investigation in HS proteoglycan mutant mice.

We showed a marked induction of lymphangiogenesis in allografts, which was accompanied by the expression of perlecan at the abluminal side of lymphatic endothelium. Recovery of renal lymph drainage is shown to occur as early as 24 hours after renal transplantation [65], suggesting that lymph drainage and the process of lymphangiogenesis after renal transplantation is of potential functional relevance. However, it is still a matter of debate whether lymphangiogenesis and potential development of lymphoid structures in renal grafts is beneficial or detrimental to clinical outcome. Lymph vessels could be beneficial by mediating the drainage of extravasated fluid and the export of leukocytes [66-68]. On the other hand, lymph vessels and additional development of lymphoid structures could also perpetuate the inflammatory response [66,67,69-71]. We observed a clear correlation between the magnitude of lymphangiogenesis and severity of IF, suggesting that new lymph vessel formation may enhance the fibrotic process by stimulating the inflammatory process. This is supported by recent findings in diabetic nephropathy indicating that lymphangiogenesis is associated with inflammatory cell infiltration and progression of IF [72]. In our study, increased lymphangiogenesis correlated with reduced graft function suggesting that therapies that target de novo lymphatic formation might contribute to improved graft function. The existence of a causal relation between lymphangiogenesis and loss of graft function, however, needs to be established in future studies. The expression of perlecan in close proximity of lymphatic endothelial cells suggests a functional role for perlecan in lymphangiogenesis. This is supported by results from studies performed in a mouse model for regenerating skin which suggest that perlecan is involved in lymphatic endothelial cell migration, lymphatic organization and maturation [73]. In addition, also versican, which was abundantly present in the interstitium, might play a role in lymphangiogenesis [74].

In conclusion, we identified increased spatial expression of HS and CS/DS proteoglycans in the intrarenal arteries, glomeruli and tubulointerstitium undergoing extensive tissue remodeling associated with CTD in renal allografts. Compartment-specific expression of proteoglycans in CTD might translate into compartment-specific responses to therapy. In line with this concept, we recently reported a differential response in renal allograft

remodeling to aldosterone receptor blockade using spironolactone in which spironolactone ameliorated TV and FGS but not IF [15]. The potential role of proteoglycans in the spironolactone-induced effects are currently under investigation.

Although our results are descriptive in nature, the observed differential expression of proteoglycans in renal allografts most likely also have functional consequences as the proteoglycan core proteins were shown to have GAGs that were able to bind L-selectin. Preliminary data furthermore suggest altered endogenous expression of natural proteoglycan ligands (such as FGF-2, HB-EGF and L-selectin). As a result, the bioavailability of these ligands, which are key in driving tissue remodeling and inflammation, is most likely modulated due to altered proteoglycan expression as well as glycosaminoglycan side chain modifications.

Based on our results we propose that proteoglycans could be targets for intervention to ameliorate CTD. As an example, antibodies recognizing, and thereby blocking, specific HS-motifs/domains may inhibit leukocyte extravasation resulting in reduced inflammation. Also generated small inactive chemokine fragments might be used to block the HS proteoglycan-binding sites of their *in vivo* active counterparts thereby making the HS proteoglycans less bioactive. Alternatively, we suggest the possibility to produce small HS-mimetics which may target more specifically a particular component of HS/heparin bioactivity [75]. Therefore, focus should now be on the identification of the precise functional role of proteoglycans in chronic tissue remodeling after renal transplantation followed by exploration of the feasibility to use proteoglycans as targets for therapeutic intervention to ameliorate the development of CTD.

Acknowledgments

Financial disclosure: This study was supported by a Career Stimulation Program Grant from the Dutch Kidney Foundation (C03.6015, JLH and HR) and the University Medical Center Groningen (KK). The funders had no role in study design, data collection and analysis, decision to publish, or preparation of the manuscript.

Author contributions

Conceived and designed the experiments: HR, KK, JvdB, JLH. Performed the experiments: HR, KK, JvdB, JLH. Analyzed the data: HR, KK, JWAMC, HvG, GN, JvdB, JLH. Wrote the paper: HR, KK, JWAMC, HvG, GN, JvdB, JLH.

References

1. Kouwenhoven EA, IJzermans JN, de Bruin RW (2000) Etiology and pathophysiology of chronic transplant dysfunction. *Transpl Int* 13: 385-401.
2. Chapman JR, O'Connell PJ, Nankivell BJ (2005) Chronic renal allograft dysfunction. *J Am Soc Nephrol* 16: 3015-3026.
3. Solez K, Colvin RB, Racusen LC, Sis B, Halloran PF et al. (2007) Banff '05 Meeting Report: differential diagnosis of chronic allograft injury and elimination of chronic allograft nephropathy ('CAN'). *Am J Transplant* 7: 518-526.
4. Solez K, Colvin RB, Racusen LC, Haas M, Sis B et al. (2008) Banff 07 classification of renal allograft pathology: updates and future directions. *Am J Transplant* 8: 753-760.
5. El Zoghby ZM, Stegall MD, Lager DJ, Kremers WK, Amer H et al. (2009) Identifying specific causes of kidney allograft loss. *Am J Transplant* 9: 527-535.
6. Ross R (1993) The pathogenesis of atherosclerosis: a perspective for the 1990s. *Nature* 362: 801-809.
7. Hillebrands JL, Klatter FA, Rozing J (2003) Origin of vascular smooth muscle cells and the role of circulating stem cells in transplant arteriosclerosis. *Arterioscler Thromb Vasc Biol* 23: 380-387.
8. Lavin PJ, Gbadegesin R, Damodaran TV, Winn MP (2008) Therapeutic targets in focal and segmental glomerulosclerosis. *Curr Opin Nephrol Hypertens* 17: 386-392.
9. Celie JW, Keuning ED, Beelen RH, Drager AM, Zweegman S et al. (2005) Identification of L-selectin binding heparan sulfates attached to collagen type XVIII. *J Biol Chem* 280: 26965-26973.
10. Iozzo RV (2005) Basement membrane proteoglycans: from cellar to ceiling. *Nat Rev Mol Cell Biol* 6: 646-656.
11. Iozzo RV (1998) Matrix proteoglycans: from molecular design to cellular function. *Annu Rev Biochem* 67: 609-652.
12. Esko JD, Lindahl U (2001) Molecular diversity of heparan sulfate. *J Clin Invest* 108: 169-173.
13. Kunter U, Floege J, von Jurgenson AS, Stojanovic T, Merkel S et al. (2003) Expression of A20 in the vessel wall of rat-kidney allografts correlates with protection from transplant arteriosclerosis. *Transplantation* 75: 3-9.
14. Rienstra H, Boersema M, Onuta G, Walther Boer M, Zandvoort A et al. (2009) Donor and recipient origin of mesenchymal and endothelial cells in chronic renal allograft remodeling. *Am J Transplant* 9: 463-472.
15. Waanders F, Rienstra H, Walther Boer M, Zandvoort A, Rozing J et al. (2009) Spironolactone ameliorates transplant vasculopathy in renal chronic transplant dysfunction in rats. *Am J Physiol Renal Physiol*
16. Raats CJ, Bakker MA, Hoch W, Tamboer WP, Groffen AJ et al. (1998) Differential expression of agrin in renal basement membranes as revealed by domain-specific antibodies. *J Biol Chem* 273: 17832-17838.
17. van den Born J, van den Heuvel LP, Bakker MA, Veerkamp JH, Assmann KJ et al. (1992) A monoclonal antibody against GBM heparan sulfate induces an acute selective proteinuria in rats. *Kidney Int* 41: 115-123.
18. van den Born J, Gunnarsson K, Bakker MA, Kjellen L, Kusche-Gullberg M et al. (1995) Presence of N-unsubstituted glucosamine units in native heparan sulfate revealed by a monoclonal antibody. *J Biol Chem* 270: 31303-31309.
19. Celie JW, Beelen RH, van den Born J (2005) Effect of fixation protocols on in situ detection of L-selectin ligands. *J Immunol Methods* 298: 155-159.
20. Paul LC, Renneke HG, Milford EL, Carpenter CB (1984) Thy-1.1 in glomeruli of rat kidneys. *Kidney Int* 25: 771-777.
21. Bjornson A, Moses J, Ingemansson A, Haraldsson B, Sorensson J (2005) Primary human glomerular endothelial cells produce proteoglycans, and puromycin affects their posttranslational modification. *Am J Physiol Renal Physiol* 288: F748-F756.
22. Bjornson Granqvist A, Ebefors K, Saleem MA, Mathieson PW, Haraldsson B et al. (2006) Podocyte proteoglycan synthesis is involved in the development of nephrotic syndrome. *Am J Physiol Renal Physiol* 291: F722-F730.

23. Sephel GC, Kennedy R, Kudravi S (1996) Expression of capillary basement membrane components during sequential phases of wound angiogenesis. *Matrix Biol* 15: 263-279.
24. Jiang X, Couchman JR (2003) Perlecan and tumor angiogenesis. *J Histochem Cytochem* 51: 1393-1410.
25. Segev A, Nili N, Strauss BH (2004) The role of perlecan in arterial injury and angiogenesis. *Cardiovasc Res* 63: 603-610.
26. Whitelock JM, Melrose J, Iozzo RV (2008) Diverse cell signaling events modulated by perlecan. *Biochemistry* 47: 11174-11183.
27. Banerji S, Ni J, Wang SX, Clasper S, Su J et al. (1999) LYVE-1, a new homologue of the CD44 glycoprotein, is a lymph-specific receptor for hyaluronan. *J Cell Biol* 144: 789-801.
28. Born J, Jann K, Assmann KJ, Lindahl U, Berden JH (1996) N-Acetylated domains in heparan sulfates revealed by a monoclonal antibody against the Escherichia coli K5 capsular polysaccharide. Distribution of the cognate epitope in normal human kidney and transplant kidney with chronic vascular rejection. *J Biol Chem* 271: 22802-22809.
29. Ali S, Malik G, Burns A, Robertson H, Kirby JA (2005) Renal transplantation: examination of the regulation of chemokine binding during acute rejection. *Transplantation* 79: 672-679.
30. Celie JW, Rutjes NW, Keuning ED, Soininen R, Heljasvaara R et al. (2007) Subendothelial heparan sulfate proteoglycans become major L-selectin and monocyte chemoattractant protein-1 ligands upon renal ischemia/reperfusion. *Am J Pathol* 170: 1865-1878.
31. Maciel TT, Coutinho EL, Soares D, Achar E, Schor N et al. (2008) Endostatin, an antiangiogenic protein, is expressed in the unilateral ureteral obstruction mice model. *J Nephrol* 21: 753-760.
32. Bellini MH, Coutinho EL, Filgueiras TC, Maciel TT, Schor N (2007) Endostatin expression in the murine model of ischaemia/reperfusion-induced acute renal failure. *Nephrology (Carlton)* 12: 459-465.
33. Stoessel A, Paliege A, Theilig F, Addabbo F, Ratliff B et al. (2008) Indolent course of tubulointerstitial disease in a mouse model of suppressor, low-dose nitric oxide synthase inhibition. *Am J Physiol Renal Physiol* 295: F717-F725.
34. Yang Y, Zhang SY, Sich M, Beziau A, van den Heuvel LP et al. (2001) Glomerular extracellular matrix and growth factors in diffuse mesangial sclerosis. *Pediatr Nephrol* 16: 429-438.
35. Tamsma JT, van den Born J, Bruijn JA, Assmann KJ, Weening JJ et al. (1994) Expression of glomerular extracellular matrix components in human diabetic nephropathy: decrease of heparan sulphate in the glomerular basement membrane. *Diabetologia* 37: 313-320.
36. van den Born J, Pisa B, Bakker MA, Celie JW, Straatman C et al. (2006) No change in glomerular heparan sulfate structure in early human and experimental diabetic nephropathy. *J Biol Chem* 281: 29606-29613.
37. van den Born J, van den Heuvel LP, Bakker MA, Veerkamp JH, Assmann KJ et al. (1993) Distribution of GBM heparan sulfate proteoglycan core protein and side chains in human glomerular diseases. *Kidney Int* 43: 454-463.
38. Talusan P, Bedri S, Yang S, Kattapuram T, Silva N et al. (2005) Analysis of intimal proteoglycans in atherosclerosis-prone and atherosclerosis-resistant human arteries by mass spectrometry. *Mol Cell Proteomics* 4: 1350-1357.
39. Kinsella MG, Tran PK, Weiser-Evans MC, Reidy M, Majack RA et al. (2003) Changes in perlecan expression during vascular injury: role in the inhibition of smooth muscle cell proliferation in the late lesion. *Arterioscler Thromb Vasc Biol* 23: 608-614.
40. Farb A, Kolodgie FD, Hwang JY, Burke AP, Tefera K et al. (2004) Extracellular matrix changes in stented human coronary arteries. *Circulation* 110: 940-947.
41. Lin H, Wilson JE, Roberts CR, Horley KJ, Winters GL et al. (1996) Biglycan, decorin, and versican protein expression patterns in coronary arteriopathy of human cardiac allograft: distinctness as compared to native atherosclerosis. *J Heart Lung Transplant* 15: 1233-1247.
42. Kawashima H, Li YF, Watanabe N, Hirose J, Hirose M et al. (1999) Identification and characterization of ligands for L-selectin in the kidney. I. Versican, a large chondroitin sulfate proteoglycan, is a ligand for L-selectin. *Int Immunol* 11: 393-405.

43. Celie JW, Reijmers RM, Slot EM, Beelen RH, Spaargaren M et al. (2008) Tubulointerstitial heparan sulfate proteoglycan changes in human renal diseases correlate with leukocyte influx and proteinuria. *Am J Physiol Renal Physiol* 294: F253-F263.
44. Ricciardelli C, Brooks JH, Suwiat S, Sakko AJ, Mayne K et al. (2002) Regulation of stromal versican expression by breast cancer cells and importance to relapse-free survival in patients with node-negative primary breast cancer. *Clin Cancer Res* 8: 1054-1060.
45. Sakko AJ, Ricciardelli C, Mayne K, Tilley WD, LeBaron RG et al. (2001) Versican accumulation in human prostatic fibroblast cultures is enhanced by prostate cancer cell-derived transforming growth factor beta1. *Cancer Res* 61: 926-930.
46. Bellini A, Mattoli S (2007) The role of the fibrocyte, a bone marrow-derived mesenchymal progenitor, in reactive and reparative fibroses. *Lab Invest* 87: 858-870.
47. Netelenbos T, van den BJ, Kessler FL, Zweegman S, Huijgens PC et al. (2003) *In vitro* model for hematopoietic progenitor cell homing reveals endothelial heparan sulfate proteoglycans as direct adhesive ligands. *J Leukoc Biol* 74: 1035-1044.
48. Bingley JA, Hayward IP, Campbell JH, Campbell GR (1998) Arterial heparan sulfate proteoglycans inhibit vascular smooth muscle cell proliferation and phenotype change *in vitro* and neointimal formation *in vivo*. *J Vasc Surg* 28: 308-318.
49. Tran PK, Agardh HE, Tran-Lundmark K, Ekstrand J, Roy J et al. (2007) Reduced perlecan expression and accumulation in human carotid atherosclerotic lesions. *Atherosclerosis* 190: 264-270.
50. Tran PK, Tran-Lundmark K, Soininen R, Tryggvason K, Thyberg J et al. (2004) Increased intimal hyperplasia and smooth muscle cell proliferation in transgenic mice with heparan sulfate-deficient perlecan. *Circ Res* 94: 550-558.
51. Kinsella MG, Irvin C, Reidy MA, Wight TN (2004) Removal of heparan sulfate by heparinase treatment inhibits FGF-2-dependent smooth muscle cell proliferation in injured rat carotid arteries. *Atherosclerosis* 175: 51-57.
52. Shimizu A, Colvin RB, Yamanaka N (2000) Rejection of peritubular capillaries in renal allo- and xeno-graft. *Clin Transplant* 14 Suppl 3: 6-14.
53. Mazzucco G, Motta M, Segoloni G, Monga G (1994) Intertubular capillary changes in the cortex and medulla of transplanted kidneys and their relationship with transplant glomerulopathy: an ultrastructural study of 12 transplantectomies. *Ultrastruct Pathol* 18: 533-537.
54. Monga G, Mazzucco G, Messina M, Motta M, Quaranta S et al. (1992) Intertubular capillary changes in kidney allografts: a morphologic investigation on 61 renal specimens. *Mod Pathol* 5: 125-130.
55. Aresu L, Rastaldi MP, Scanziani E, Baily J, Radaelli E et al. (2007) Epithelial-mesenchymal transition (EMT) of renal tubular cells in canine glomerulonephritis. *Virchows Arch* 451: 937-942.
56. Suzuki T, Kimura M, Asano M, Fujigaki Y, Hishida A (2001) Role of atrophic tubules in development of interstitial fibrosis in microembolism-induced renal failure in rat. *Am J Pathol* 158: 75-85.
57. Sinniah R, Khan TN (1999) Renal tubular basement membrane changes in tubulointerstitial damage in patients with glomerular diseases. *Ultrastruct Pathol* 23: 359-368.
58. Iwano M, Plieth D, Danoff TM, Xue C, Okada H et al. (2002) Evidence that fibroblasts derive from epithelium during tissue fibrosis. *J Clin Invest* 110: 341-350.
59. Liu Y (2004) Epithelial to mesenchymal transition in renal fibrogenesis: pathologic significance, molecular mechanism, and therapeutic intervention. *J Am Soc Nephrol* 15: 1-12.
60. Kalluri R, Neilson EG (2003) Epithelial-mesenchymal transition and its implications for fibrosis. *J Clin Invest* 112: 1776-1784.
61. Lortat-Jacob H, Grosdidier A, Imberty A (2002) Structural diversity of heparan sulfate binding domains in chemokines. *Proc Natl Acad Sci U S A* 99: 1229-1234.
62. Gesemann M, Cavalli V, Denzer AJ, Brancaccio A, Schumacher B et al. (1996) Alternative splicing of agrin alters its binding to heparin, dystroglycan, and the putative agrin receptor. *Neuron* 16: 755-767.

63. O'Toole JJ, Deyst KA, Bowe MA, Nastuk MA, McKechnie BA et al. (1996) Alternative splicing of agrin regulates its binding to heparin alpha-dystroglycan, and the cell surface. *Proc Natl Acad Sci U S A* 93: 7369-7374.
64. Kawashima H, Watanabe N, Hirose M, Sun X, Atarashi K et al. (2003) Collagen XVIII, a basement membrane heparan sulfate proteoglycan, interacts with L-selectin and monocyte chemoattractant protein-1. *J Biol Chem* 278: 13069-13076.
65. Malek P, Vrabel J (1968) Lymphatic system and organ transplantation. *Lymphology* 1: 4-22.
66. Kerjaschki D, Regele HM, Moosberger I, Nagy-Bojarski K, Watschinger B et al. (2004) Lymphatic neoangiogenesis in human kidney transplants is associated with immunologically active lymphocytic infiltrates. *J Am Soc Nephrol* 15: 603-612.
67. Stuht S, Gwinner W, Franz I, Schwarz A, Jonigk D et al. (2007) Lymphatic neoangiogenesis in human renal allografts: results from sequential protocol biopsies. *Am J Transplant* 7: 377-384.
68. Colvin RB (2004) Emphatically lymphatic. *J Am Soc Nephrol* 15: 827-829.
69. Thauat O, Kerjaschki D, Nicoletti A (2006) Is defective lymphatic drainage a trigger for lymphoid neogenesis? *Trends Immunol* 27: 441-445.
70. Kerjaschki D, Huttary N, Raab I, Regele H, Bojarski-Nagy K et al. (2006) Lymphatic endothelial progenitor cells contribute to de novo lymphangiogenesis in human renal transplants. *Nat Med* 12: 230-234.
71. van Goor H, Leuvenink HG (2009) The goddess of the waters. *Kidney Int* 75: 767-769.
72. Sakamoto I, Ito Y, Mizuno M, Suzuki Y, Sawai A et al. (2009) Lymphatic vessels develop during tubulointerstitial fibrosis. *Kidney Int* 75: 828-838.
73. Rutkowski JM, Boardman KC, Swartz MA (2006) Characterization of lymphangiogenesis in a model of adult skin regeneration. *Am J Physiol Heart Circ Physiol* 291: H1402-H1410.
74. Labropoulou VT, Theocharis AD, Ravazoula P, Perimenis P, Hjerpe A et al. (2006) Versican but not decorin accumulation is related to metastatic potential and neovascularization in testicular germ cell tumours. *Histopathology* 49: 582-593.
75. Celie JW, Beelen RH, van den Born J (2009) Heparan sulfate proteoglycans in extravasation: assisting leukocyte guidance. *Front Biosci* 14: 4932-4949.

Chapter 3

Renal Heparan Sulfate Proteoglycans Modulate FGF2 Signaling in Experimental Chronic Transplant Dysfunction

Submitted

Kirankumar Katta
Miriam Boersema
Heleen Rienstra
Saritha Adepu
Johanna W.A.M. Celie
Grietje Molema
Harry van Goor
Jo H.M. Berden
Gerjan Navis
Jan-Luuk Hillebrands
Jacob van den Born

Abstract

Depending on the glycan structure, proteoglycans can act as co-receptors for growth factors thereby contributing to cell survival, proliferation and fibrosis. Chronic transplant dysfunction is characterized by extensive fibrotic tissue remodeling including glomerulosclerosis and neointima formation in arteries. We hypothesize that proteoglycans and their growth factor ligands orchestrate tissue remodeling in chronic transplant dysfunction. Therefore, in a rat renal transplantation model, we studied proteoglycan and growth factor expression in glomeruli, arterial mediae and neointimae by qRT-PCR and immunofluorescence. To this end, laser microdissection of glomeruli, arterial mediae and neointimae followed by low density qRT-PCR was performed. Uniform upregulation of collagen I, IV, and TGF- β 1 in the allografted kidneys was observed. However, spatial differences in proteoglycan expression and ligand binding properties were detected. In glomeruli and neointimae of allografts we found induction of the matrix heparan sulfate proteoglycan perlecan along with massive accumulation of FGF2. Profiling the heparan sulfate polysaccharide side chains of renal heparan sulfate proteoglycans revealed conversion from a non-FGF2-binding heparan sulfate phenotype in control and isografted kidneys towards a FGF2-binding phenotype in allografts. The functional significance of these findings was evidenced by *in vitro* experiments with rat mesangial cells showing that FGF2-induced proliferation is dependent on sulfation and can be inhibited by exogenously added heparan sulfate. These data indicate that heparan sulfate proteoglycans such as perlecan serve as docking platforms for FGF2 in various renal compartments in chronic transplant dysfunction. We speculate that heparin-like glycomimetica could be a promising intervention to retard development of chronic transplant dysfunction.

Introduction

Renal chronic transplant dysfunction (CTD) is the leading cause of long-term loss of transplanted kidneys (1,2). CTD is the result of tissue remodeling in the intrarenal arteries, glomeruli and tubulointerstitium leading to transplant vasculopathy, focal glomerulosclerosis (FGS), interstitial fibrosis and tubular atrophy (2-4). These lesions are characterized by accumulation of extracellular matrix, activation of mesangial cells, interstitial myofibroblasts and tubular epithelial cells, and chronic inflammation. To date, due to the lack of knowledge on the pathogenetic mechanisms leading to the development of these lesions, no effective therapies are available to prevent or treat renal CTD. Progressive loss can only be retarded by anti-hypertensive and anti-proteinuric treatment in combination with lipid lowering drugs.

Recently, we showed accumulation of the heparan sulfate proteoglycans (HSPGs) collagen type XVIII and perlecan during tissue remodeling in CTD in rats (5). However, whether and how these proteoglycans mediate tissue remodeling in CTD is as yet unknown. In native kidney diseases and ischemia-reperfusion injury we have already shown that HSPGs are involved in leukocyte influx and proteinuria-mediated renal injury (6-8).

The carbohydrate side chains (i.e. the glycosaminoglycans) are attached to proteoglycan core proteins and can bind a variety of ligands depending on their highly variable composition, mainly variations in N- and O-sulfation patterns (9). Along with chondroitin sulfate- and dermatan sulfate proteoglycans, HSPGs form the large majority of the proteoglycan family. Potential ligands are chemokines (9) and growth factors such as basic fibroblast growth factor (bFGF/FGF2; 10,11). Proteoglycans are highly involved in morphogenesis and tissue remodeling processes (12-17).

Studies in non-transplantation models of renal and vascular disease have shown potential roles of FGF2 in FGS and neointima formation (18-22). These data led us to hypothesize that interaction of FGF2 with proteoglycans also affects tissue remodeling processes in CTD. To test this hypothesis we used an experimental rat CTD model, from which we microdissected glomeruli, the arterial media as well as the neointima followed by low density qRT-PCR analysis for matrix and cell surface proteoglycans and FGF2. In addition, we profiled the heparan sulfate (HS) polysaccharide side chains by anti-HS mAbs and their binding capacity for FGF2. Finally, we investigated the HSPG involvement of FGF2-driven mesangial proliferation. Our data indeed indicate spatial proteoglycan involvement in CTD, which might be a potential target for future intervention therapy.

Materials and Methods

Rats

Inbred female (175-210 gram) Dark Agouti (DA) rats were obtained from Harlan (Horst, The Netherlands) and inbred male Wistar Furth (WF) rats (240-295 gram) from Charles River Laboratories Inc. (l'Arbresle, Cedex, France). All animals received care in compliance with the Principles of Laboratory Animal Care (NIH Publication No.86-23, revised 1985), the University of Groningen guidelines for animal husbandry and the Dutch Law on Experimental Animal Care.

Kidney transplantation and experimental groups

Female DA kidney allografts were orthotopically transplanted into male Wistar Furth recipients as described previously (5,23). Cold ischemic time ranged from 16 to 38 minutes. Warm ischemic time ranged from 19 to 32 minutes. Recipients received cyclosporine A (5 mg/kg bodyweight) (Sandimmune, Novartis, Arnhem, the Netherlands) subcutaneously for 10 days posttransplantation. The native kidney was removed after 8 to 14 days. Total follow-up was 12 weeks or shorter in case animals had to be sacrificed due to renal failure. Allografts used in this study had developed severe CTD (n=5). Further characteristics of the model are described elsewhere (5,18). Non-transplanted DA kidneys (n=5) and DA to DA isografted kidneys (n=5) served as controls.

Laser Microdissection and Gene Expression Analysis

Laser microdissection, RNA isolation and qRT-PCR were performed essentially according to Asgeirsdottir et al. (39). Briefly, frozen kidneys were sectioned at 9 μm and mounted on UV pretreated slides (PALM Micro Laser Technology, Bernried, Germany). Sections were quickly fixed in acetone and air-dried for 3 min. Sections were subsequently stained with Mayer's hematoxylin (Merck, Darmstadt, Germany) for 1 min and rinsed in diethyl pyrocarbonate (DEPC) treated tap water for 20 s. Slides were then used for microdissection using the Leica Microdissection microscope (Leica Microsystems, Houston, Texas). Glomeruli and various layers (including media and neointima) of larger arteries were separately dissected from 9 serial sections per kidney. An average of 194 [range 71-308] glomeruli and 63 [range 25-117] arteries were dissected from each kidney.

Total RNA was isolated from microdissected structures by using the RNeasy Micro Kit (Qiagen, Hilden, Germany). Reverse transcription was carried out using Superscript III reverse transcriptase (Invitrogen, Breda, the Netherlands) and random hexamer primers (Promega, Leiden, the Netherlands). Gene expression was analyzed with a custom made microfluidic card-based low density array (Applied Biosystems, Nieuwerkerk a/d IJssel, the Netherlands) using the ABI Prism 7900HT Sequence Detection System (Applied

Chapter 3

Biosystems, Nieuwerkerk a/d IJssel, the Netherlands). Composition of the low density array is indicated in Table 1. Relative mRNA levels were calculated as $2^{-\Delta CT}$, in which ΔCT is $CT_{\text{gene of interest}} - CT_{\beta\text{-actin}}$. CT-values that were beyond detection level were set manually to 50.

Table 1. Composition of low-density array

Gene name	General name	Gene symbol	Assay ID
Matrix molecules			
collagen, type I, alpha 1	Collagen I	<i>Coll1a1</i>	Rn01463848_m1
collagen, type IV, alpha 1	Collagen IV	<i>Col4a1</i>	Rn01482925_m1
Proteoglycans			
perlecan	Perlecan	<i>LOC313641</i>	Rn01515780_g1
agrin	Agtrin	<i>Agrn</i>	Rn00598349_m1
versican	Versican	<i>Vcan</i>	Rn01493755_m1
biglycan	Biglycan	<i>Bgn</i>	Rn00567229_m1
syndecan 1	Syndecan 1	<i>Sdc1</i>	Rn00564662_m1
syndecan 4	Syndecan 4	<i>Sdc4</i>	Rn00561900_m1
Growth factors			
fibroblast growth factor 2	FGF2	<i>Fgf2</i>	Rn00570809_m1
transforming growth factor, beta 1	Tgf-b1	<i>Tgfb1</i>	Rn01475963_m1
Reference genes			
beta actin	Beta-actin	<i>Actb</i>	Rn00667869_m1
beta 2 microglobulin	B2m	<i>B2m</i>	Rn00560865_m1
Eukaryotic 18S rRNA	18S	<i>18s</i>	Hs99999901_s1

Immunofluorescence on rat kidney sections

Four μm frozen sections were fixed in acetone or 4% formaldehyde and were blocked for endogenous peroxidase activity with 0.03% H_2O_2 if appropriate. Sections were blocked with normal goat or rabbit serum. Sections were incubated for 1h with the following primary antibodies: mouse anti-human FGF2 (Peprotech, London, UK), mouse anti-HS mAb JM-403, which recognizes low sulfated heparan sulfate domains with N-unsubstituted glucosamine residues (25), mouse anti-HS stub mAb 3G10 (epitope becomes expressed after heparitinase I digestion of HS; Seikagaku, Tokyo, Japan; ref. 26) and mouse anti-rat perlecan (clone10B2 kindly provided by Prof. dr. J.R. Couchman, Copenhagen, Denmark).

Binding of primary antibodies was detected by incubating the sections for 30 min with secondary antibodies diluted in PBS with 5% normal rat serum: goat anti-mouse IgG1 HRP (Southern Biotech, Birmingham, AL, USA), rabbit anti-mouse IgM HRP (DAKO, Heverlee, Belgium,), or goat anti-mouse IgG1 Alexa488 (Invitrogen-Molecular Probes, Breda, the Netherlands). HRP-activity was visualized using the TSATM Tetramethylrhodamine System (PerkinElmer LAS Inc.). All fluorescence microscopy was performed using a Leica DMLB microscope (Leica Microsystems, Rijswijk, the Netherlands) equipped with a Leica DC300F camera and Leica QWin 2.8 software.

Ligand binding assays on rat kidney sections

To detect capacity of renal proteoglycans to bind FGF2, formalin-fixed rat renal sections were incubated with recombinant human FGF2 (Peprotech) for 60 min. After washing, the staining was continued according to the FGF2 staining protocol described above. Formalin fixation essentially avoids recognition of endogenous renal FGF2 by anti-FGF2 antibodies. To confirm that the observed binding pattern was mediated by HS proteoglycans, the sections were pretreated with 0.05 U/ml heparitinase I (Flavobacterium heparinum, EC 4.2.2.8; Seikagaku, Tokyo, Japan) for 1h at 37°C in a humidified chamber.

FGF2 stimulation assay on rat mesangial cells

Rat mesangial cells (Thy 1.1 and α -smooth muscle actin positive, passage 11-15) were cultured in 24 well plates in Dulbecco's modified Eagle's medium (DMEM) supplemented with 25 mM HEPES, 4.5 mg/ml glucose, pyridoxine, 1 mM pyruvate, 50 ng/ml insulin, and 10% fetal bovine serum. Before stimulation with FGF2 cells were grown until confluency, serum deprived (0.5% serum) for 24 h and subsequently incubated with different concentrations (0.031 – 8 ng/ml) of FGF2 for 24 h. Proliferation was measured by adding 0.5 μ Ci/ml 3H-thymidine (Amersham, Buckinghamshire, UK) for 24 h to the cultures. After 24 h, 5% trichloric acid precipitable material was dissolved in 0.1% SDS, Optiphase "HiSafe 3" was added and radioactivity was counted in a 1214 Rackbeta liquid scintillation counter. To study whether FGF2-induced proliferation of mesangial cells was reduced in the presence of exogenous HS, mesangial cells were stimulated with 0.5 ng/ml FGF2 for 24 hours in the presence of various concentrations (0, 8, 32 and 128 μ g/ml) exogenous HS from bovine kidney [HSBK] (Seikagaku, Tokyo, Japan). Proliferation was measured as described above. To study whether proteoglycan sulfation was reduced by chlorate, mesangial cells were cultured for 24 hrs in the presence of various concentrations (5-25 mM) Na-chlorate (Sigma) and 35S-sulfate (2 μ Ci/ml; Amersham, Buckinghamshire, UK). Incorporation of 35S-sulfate into proteoglycans was quantified similarly as described above for 3H-thymidine incorporation. Finally, to analyze whether chlorate impairs FGF2-induced

proliferation of mesangial cells, cells were stimulated with FGF2 (0.5 ng/ml) for fixed times (0, 0.5, 1, 2, 4 and 24 hrs) in the presence or absence of 25 mM Na-chlorate and in the presence of 0.5 μ Ci/ml 3H-thymidine. Total culture time was 24 hrs. Proliferation was determined as described above.

Statistics

mRNA expression levels were analyzed using a one-way ANOVA with Turkey's post-hoc test. P values of <0.05 were considered statistically significant (SPSS® software package). Mesangial cell culture data were expressed as mean \pm standard error of the mean (SEM) and analyzed by one-way ANOVA. If overall $p < 0.05$, Bonferroni's Multiple Comparison Test was performed (GraphPad Prism 5.0, GraphPad Software, Inc.).

Results

Development of chronic transplant dysfunction in renal allografts

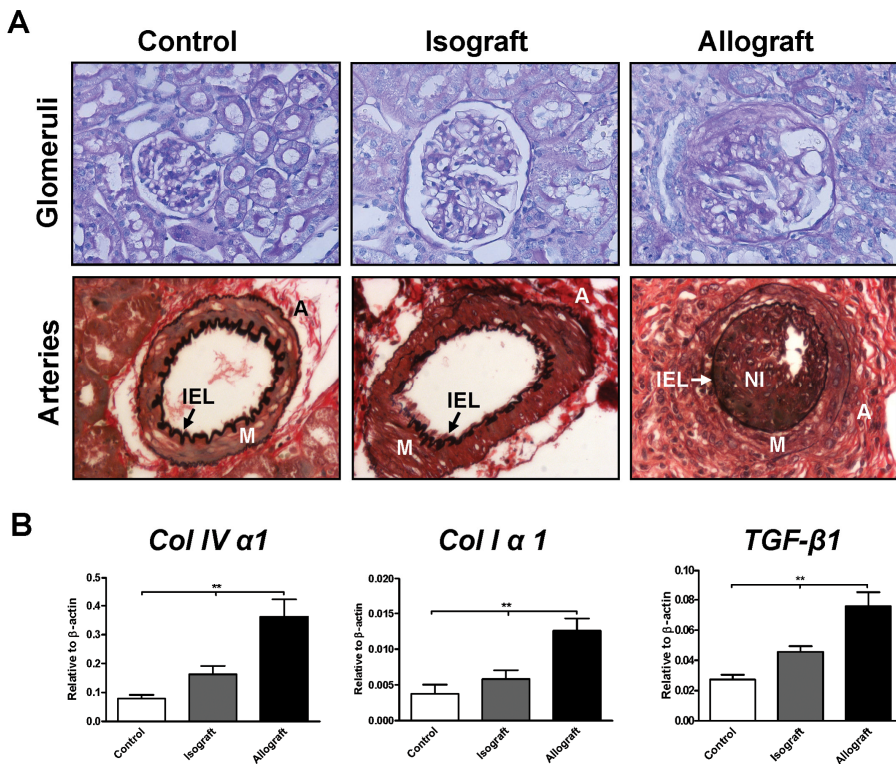


Figure 1. Chronic transplant dysfunction in renal allografts. A: Representative photomicrographs showing development of glomerulosclerosis in allografted kidneys, in contrast to isografted and control kidneys (upper row; PAS staining). Neointima formation was observed in allografts but not in isografts and controls (lower row, Verhoeff staining). Magnification: 400x. B: qRT-PCR analysis performed on RNA isolated from microdissected glomeruli from non-transplanted control tissue, isografts and allografts (n=5/group). Expression levels of *Coll1 α 1*, *Coll3 α 1* and *TGF- β 1* are expressed relative to the expression level of β -actin. ** p<0.01 vs. isografts and non-transplanted control tissue. Abbreviations: IEL: internal elastic lamina, M: media, A: adventitia, NI: neointima

Progressive renal function loss was evidenced in the allografted kidneys by a \approx 50% loss in creatinine clearance and a \approx 15-fold rise in urinary protein excretion at 8 weeks after transplantation, both of which were not observed in isografted kidneys, as we showed before in this model (5,23). The rat renal allografts showed development of severe CTD with FGS and arterial neointima formation (Figure 1A). In isografts, development of FGS was minimal and no neointima formation was observed (5,23). The development of FGS coincided with significantly increased expression of the pro-fibrotic factors *Col 1 α 1*, *Col 3 α 1* and *TGF- β 1* as determined by qRT-PCR on microdissected glomeruli (Figure 1B). These molecular responses were also observed in RNA isolated from microdissected arterial medial and neointimal tissue as well as in whole kidney material (not shown). These data confirm development of CTD in our rat transplantation model.

Induction of glomerular and neointimal perlecan expression in CTD

Proteoglycans can modulate growth factor responses by virtue of their glycosaminoglycan side chains. Therefore, we profiled the matrix HS proteoglycans agrin and perlecan, the matrix chondroitin sulfate- and dermatan sulfate proteoglycans versican and biglycan, and the major epithelial cell surface proteoglycans syndecan-1 and -4 by qRT-PCR. PCR analysis showed the expression of the basement membrane HSPG perlecan to be upregulated mainly in the glomeruli (Figure 2A), and mediae and neointimae (Figure 2B) of the allografts. This spatial upregulation of perlecan by qRT-PCR in glomeruli, mediae and neointimae was however not observed when performing qRT-PCR analysis on whole kidney RNA isolates (Figure 2C), which clearly stresses the power, and need, of using microdissection of specific structures to demonstrate differential proteoglycan expression in specific renal compartments. Using immunofluorescence, expression of perlecan was virtually absent in the glomerular basement membranes of non-transplanted control kidneys. In the glomerular basement membranes of isografts, perlecan expression was increased compared with control kidneys, but to a far lesser extent than the increase observed in allografts (Figure 2D, left column). In glomeruli with FGS in allografts a strong expression of perlecan was observed in the glomerular basement membranes and mesangial areas (Figure 2D, left column). In control tissue, isografts and allografts the Bowmans capsule was positive for perlecan. Immunofluorescence also showed perlecan expression in the newly-formed neointimae present in allografts (Figure 2D, right column). No significant

differences in expression levels were found for syndecan-1 and -4, agrin, and biglycan, although these proteoglycans were expressed in the neointimae based on qRT-PCR data (Figure 3A-E).

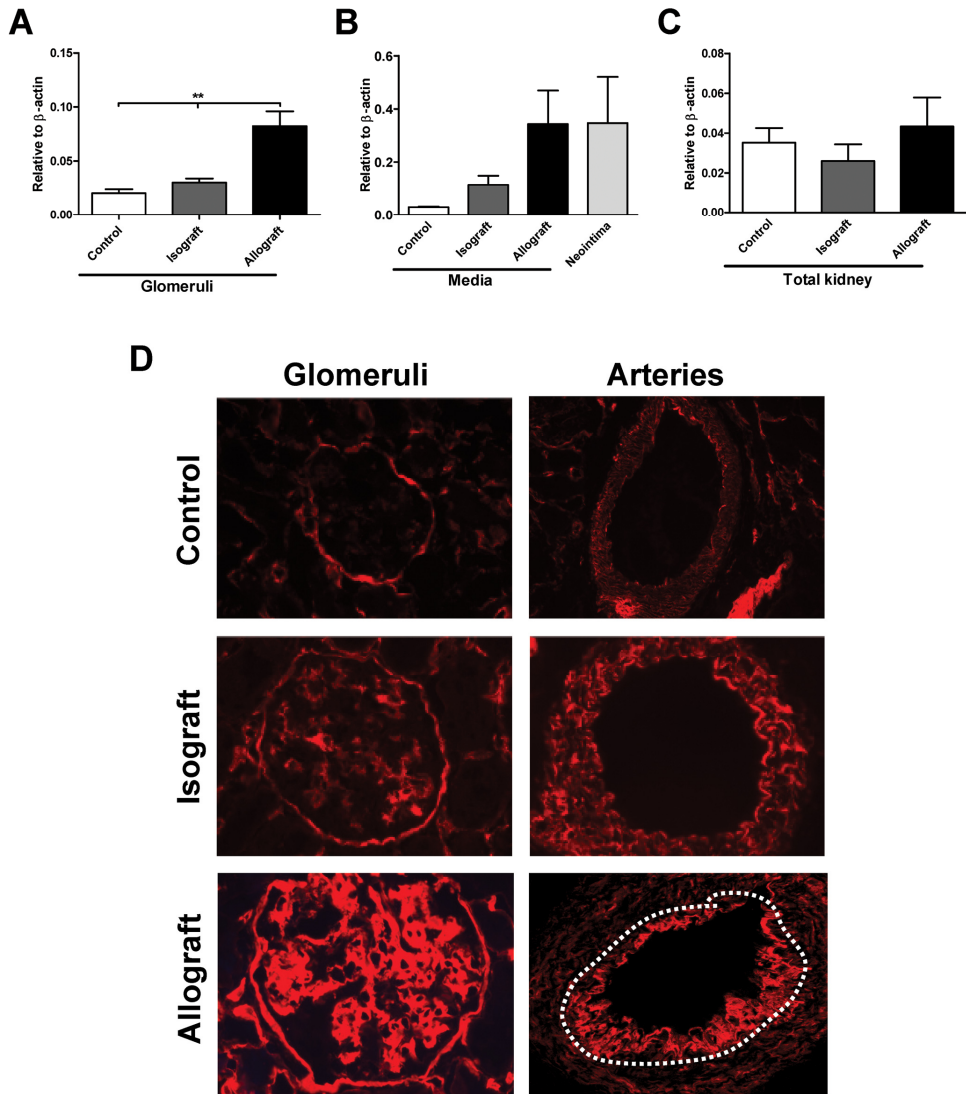


Figure 2. Upregulation of perlecan in glomeruli and neointimae of renal allografts with CTD. A-C. Perlecan expression measured by qRT-PCR in glomeruli (n=5/group) (A), arteries (n=4-5/group) (B), and whole kidney tissue (n=3/group) (C). D: Immunofluorescence demonstrating perlecan accumulation in glomeruli (left column) and neointimae (right column) of allografts with CTD. In isografted kidneys a minor increase of perlecan was seen in glomeruli and arterial media compared to control tissue. Dotted line represents the internal elastic lamina. Magnification: 640x except for the lower right panel (artery of allograft) which was taken at 320x. Expression levels of perlecan are expressed relative to the expression level of β -actin. ** p<0.01 vs. isografts and non-transplanted control tissue

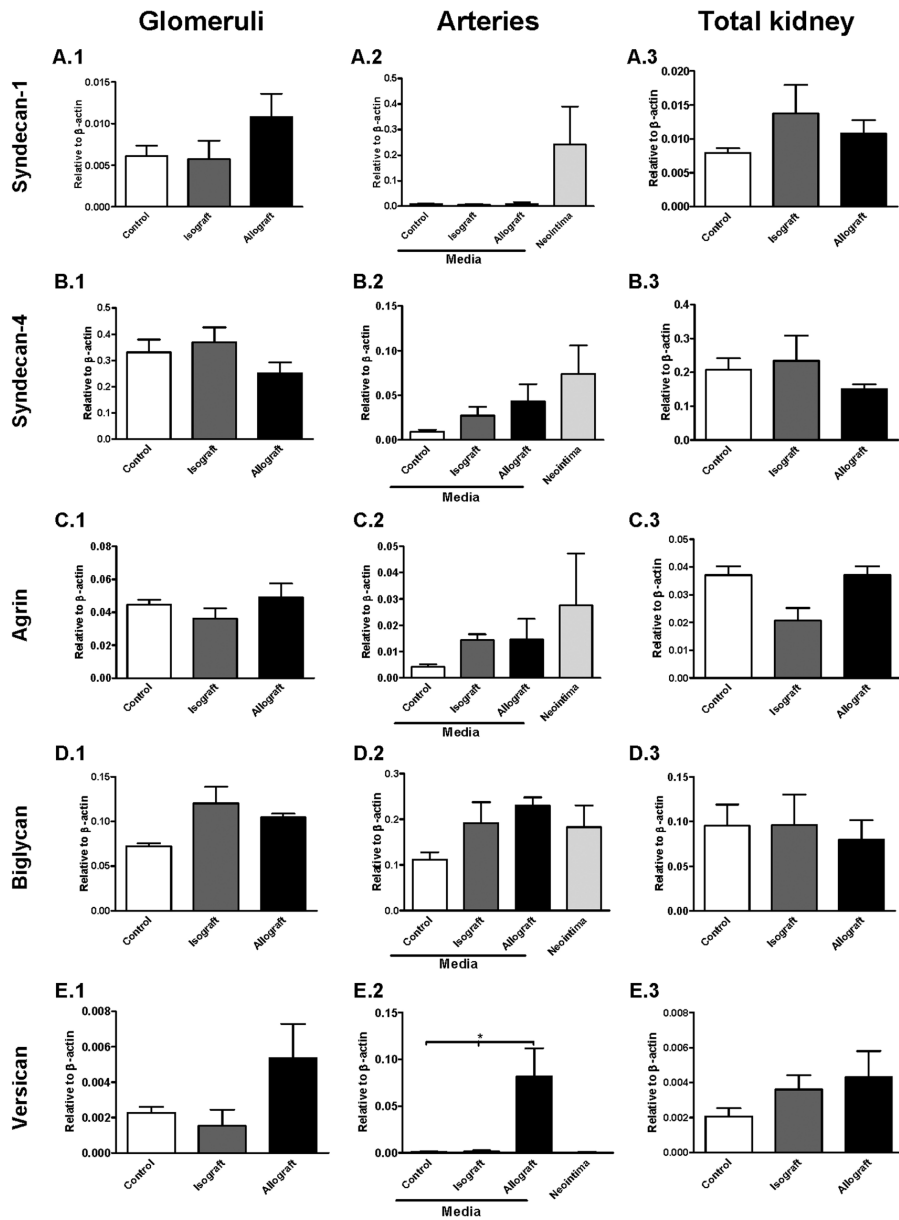


Figure 3. Proteoglycan mRNA expression profiles in microdissected glomeruli (A.1-E.1), arteries (A.2-E.2) and total kidney lysates (A.3-E.3) of non-transplanted control tissue, isografts and allografts with CTD.

Expression of syndecan-1 (A), syndecan-4 (B), agrin (C), biglycan (D) and versican (E) was analyzed using qRT-PCR (n=3-5/group). Expression levels of the respective genes are expressed relative to the expression level of β -actin. Transcripts for the various proteoglycans were adjusted for the expression of β -actin. * p<0.05 vs. isografts and non-transplanted control tissue

Versican expression was significantly upregulated in the media of the allografted kidneys (Figure 3E.2), which is in line with a pro-migratory phenotype of the vascular smooth muscle cells. This proteoglycan profiling led us to conclude that glomerular and neointimal perlecan is upregulated in renal allografts at both the mRNA and protein level.

Heparan sulfate profiling

Since HS proteoglycans are involved in morphogenesis and tissue remodeling mainly by their HS glycosaminoglycan side chains, we profiled HS polysaccharide structures in renal sections. To this end we visualized HS epitopes by anti-HS mAbs JM-403 and 3G10, and by a ligand binding assay using the HS-binding growth factor FGF2. Characteristics of the corresponding HS-epitopes are detailed in Table 2.

Table 2. Basic characteristics of the HS epitopes recognized by the anti-HS mAbs and FGF2

Anti-HS mAb or HS-binding protein	Basic characteristics of the HS epitope
Anti-HS mAb JM-403	GlcUA-rich sequences with N-unsubstituted GlcN units in low sulfated HS (24)
Anti-HS mAb 3G10	Desaturated Uronate residues after digestion with heparitinase (GlcNAc/NS α 1-4 GlcA linkage; ref.25)
FGF2	2-O sulfation in heparin and heparan sulfates (26)

Anti-HS mAb JM-403 demonstrated a clear staining of the glomerular basement membranes in control (Figure 4A.1) and isografted (Figure 4A.2) kidneys. Mesangial staining was weak for mAb JM-403. In allografts however, glomerular JM-403 HS staining is partly or completely lost in sclerotic areas (Figure 4A.3), likely due to increased HS sulfation. The 3G10 HS epitope, which becomes available after heparitinase cleavage of HS, is absent in the glomerular basement membranes of control kidneys (Figure 4B.1), becomes weakly expressed in the isografted kidneys (Figure 4B.2), and is strongly upregulated in glomerular basement membranes and sclerotic areas in the allografts (Figure 4B.3). The 3G10 staining nicely paralleled perlecan stainings (see Figure 2D), suggesting this HS epitope to be expressed by perlecan. FGF-2 binding is completely HS-dependent as evidenced by control experiments on heparitinase pretreated sections, where all binding of FGF-2 was lost (not shown). In glomeruli of control kidneys (Figure 4C.1) and isografts (Figure 4C.2) FGF-2 binding to HS was absent or only weakly present. In allografts,

increased binding of FGF-2 was observed (Figure 4C.3). These data indicate changes in glomerular HS composition in CTD as evidenced by an increased FGF2 binding capacity, which occurred most likely due to increased sulfation.

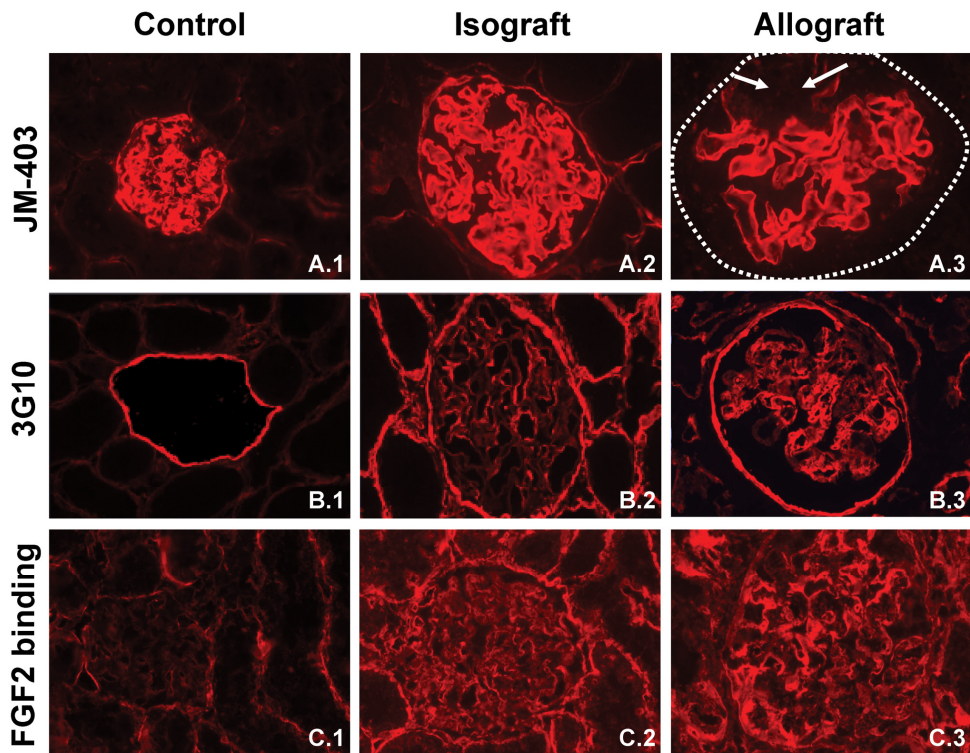


Figure 4. Modification of glomerular HS structure in allografts with CTD. Glomerular expression of HS was evaluated by two anti-HS mAbs (JM-403 [A] and 3G10 [B]) as well as by the binding of FGF2 (C) In allografts, glomerular JM-403 staining is partly lost in sclerotic areas (arrows). On the, contrary HS expression as evidenced by 3G10 (B.3) and FGF2 binding capacity (C.3) was increased in glomeruli in allografts. Dotted line represents Bowmans capsule. Arrows indicate sclerotic area. Magnification: 640x.

In the arterial media of control and isografted kidneys moderate staining for anti-HS mAbs JM-403 (Figure 5A.1,2) and 3G10 (Figure 5B.1,2) was observed, however binding capacity for FGF2 was absent (Figure 5C.1,2). Compared to the mediae of control and isografted kidneys, in allografts JM-403 staining was lost in the media (Figure 5A.3), whereas 3G10 staining was increased (Figure 5B.3). Moreover, FGF2 binding capacity was increased in the allograft media (Figure 5C.3). In the neointimae strong binding of anti-HS mAbs JM-403 (Figure 5A.3) and 3G10 (Figure 5B.3) as well as binding of FGF2 (Figure 5C.3) was observed.

Collectively, these data show changes in glomerular and arterial HS composition in allografts with CTD, with loss of JM-403 staining and increased FGF2 binding capacity, which can be explained by increased HS sulfation.

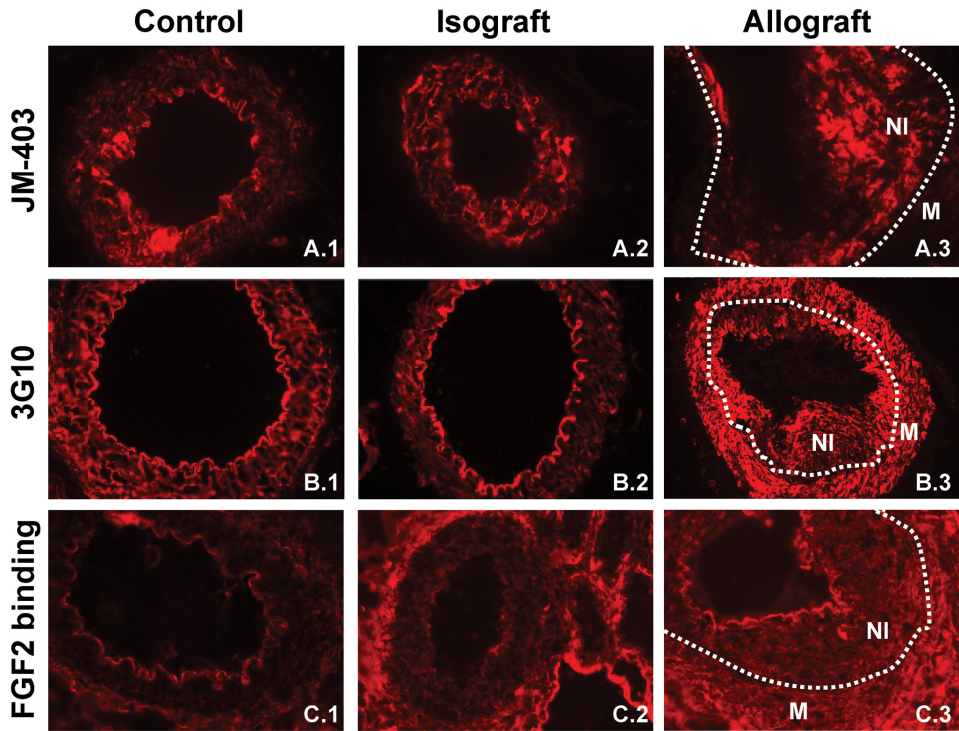


Figure 5. Modification of arterial HS structure in allografts with CTD. Medial and neointimal expression of HS was evaluated by two anti-HS mAbs (JM-403 [A] and 3G10 [B]) as well as by the binding of FGF2 (C). In the media of allografted kidneys, JM-403 staining was largely lost, whereas in the neointima this epitope was clearly expressed (A.3). Both the media and neointima of the allografts expressed the 3G10 HS epitope (B.3). The media but not neointima bound FGF2 (C.3). Magnification: 640x except for B.3 which was taken at 320x.

Endogenous expression of FGF-2 in allografts with CTD

After showing an upregulation of glomerular and neointimal perlecan expression accompanied by increased binding capacity for FGF2 in renal allografts, we next evaluated endogenous expression levels of FGF2. In control kidneys, we only observed weak segmental FGF2 expression in the glomeruli (Figure 6A.1), the tubulointerstitium (Figure 6A.1) and arteries (Figure 6B.1) being devoid of any FGF2 expression. In isografts, a slight upregulation of FGF2 expression in glomeruli was observed (Figure 6A.2), with the arteries remaining devoid of any FGF2 expression (Figure 6B.2). However, in the allografts, FGF2 was strongly and homogeneously accumulated throughout the glomeruli, and present mainly in the glomerular capillary wall and mesangium (Figure 6A.3). PCR analysis

showed no significant differences in glomerular FGF2 expression, although a tendency towards higher expression was observed in the allografts (Figure 6C). We suggest that this discrepancy may be explained by plasma-derived FGF2 being trapped in the glomeruli by perlecan endowed with HS chains able to bind FGF2 (as shown in Figure 4) during ultrafiltration. This would cause local accumulation of FGF2 protein in the absence of an increase in mRNA expression. In addition, in the neointimae of allografts increased FGF2 expression was observed both at the protein and mRNA level (Figures 6B.3 and 6D, respectively).

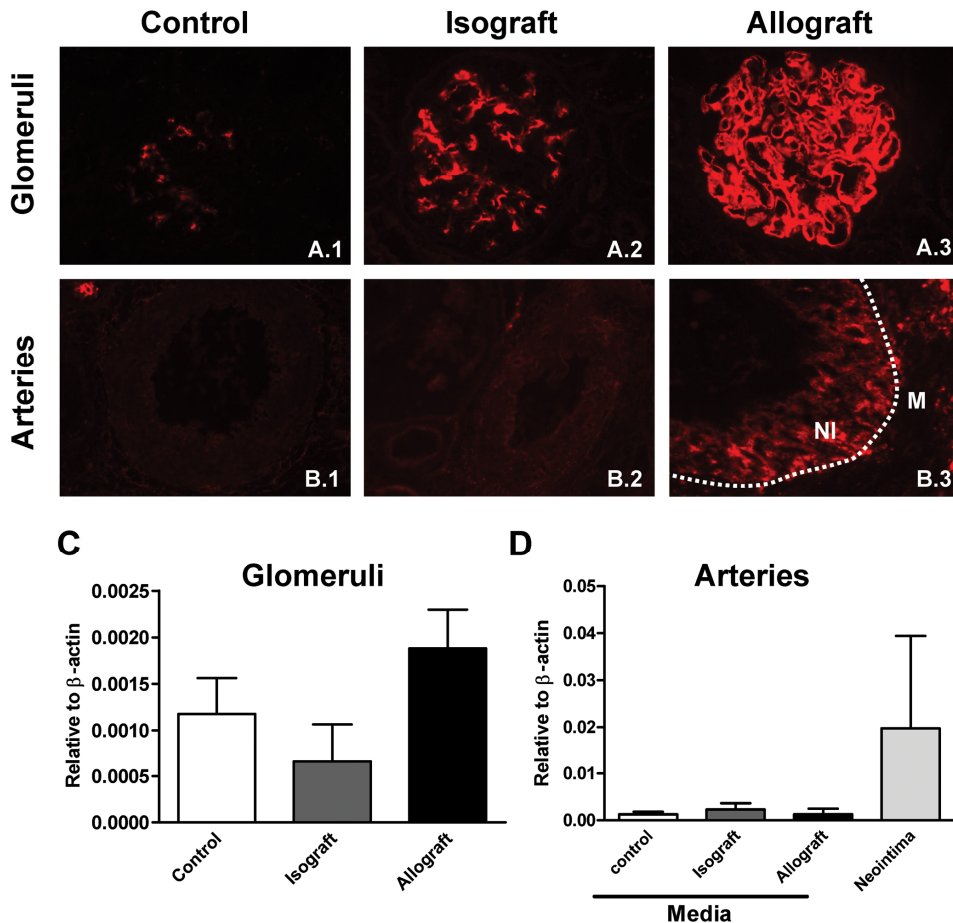


Figure 6. Glomerular and arterial expression of FGF2 in allografts with CTD. Endogenous expression of FGF2 was evaluated by immunofluorescence (A-B) and qRT-PCR (C-D). In allografts with CTD, a strong expression of FGF2 was exclusively found in glomeruli (A.3) and neointimae (B.3). In glomeruli of isografts a slight increase in FGF2 expression was found (A.2). The dotted line represents the internal elastic lamina. qRT-PCR analysis revealed an increase in FGF2 expression in the glomeruli in allografts, which did however reach the level of statistical significance when compared with isografts and non-

transplanted control tissue (C). Neointimal expression of FGF2 was clearly present (D) although again not being significantly different from isografts and non-transplanted control tissue (n=4-5/group). Magnification of the photomicrographs: 640x.

Involvement of proteoglycans in FGF2-driven proliferation of mesangial cells

As described above, we showed an upregulation of the HS proteoglycan perlecan in the glomeruli of allografts, which coincided with increased FGF2 binding capacity and FGF2 expression. We next hypothesized that the upregulation of perlecan and FGF2 may be involved in mesangial expansion and formation of FGS. To explore a possible mechanistic relation between mesangial HSPGs and FGF2 in more detail, we conducted a number of *in vitro* experiments. Primary rat mesangial cells were cultured until confluency, serum starved for 24 h followed by 24 h stimulation with FGF2. Figure 7A shows a dose-dependent increase in proliferation of mesangial cells in response to FGF2.

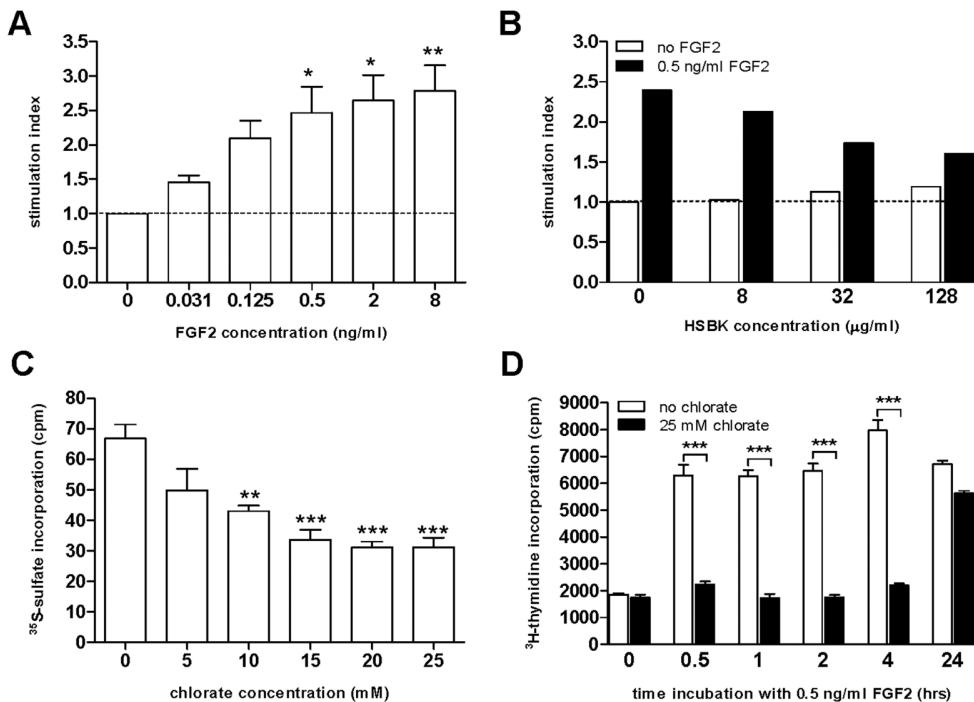


Figure 7. FGF2-induced proliferation of mesangial cells depends on sulfated proteoglycans. A: Rat mesangial cells were stimulated with various concentrations of FGF2 for 24 h. Proliferation was measured by ³H-thymidine incorporation. Data are expressed as the stimulation index, i.e. fold increase in proliferation + FGF2 / proliferation – FGF2 (n=4; *p<0.05, **p<0.01 vs. no FGF2 added). B: Exogenous HS from bovine kidney (HSBK) hampers FGF2-induced mesangial cell proliferation in a dose-dependent manner (n=2). C: Proteoglycan sulfation of mesangial cells is reduced by chlorate in a dose-dependent manner (**p<0.01, ***p<0.001 vs. no chlorate added). D: Chlorate impairs FGF2-induced proliferation of mesangial cells which is dependent on the duration of FGF2 stimulation (***p<0.001 vs. no chlorate at the respective duration of FGF2 stimulation).

Based on these data we used the FGF2 concentration of 0.5 ng/ml in the subsequent *in vitro* experiments. The FGF2-induced proliferative response was blunted by the addition of exogenous competitive bovine kidney-derived HS (Figure 7B). This was due to reduced binding of FGF2 to the cells as demonstrated by reduced binding of 125I-labeled FGF2 to the mesangial cells (not shown).

These data suggest that due to competition between mesangial and exogenous HS for binding of FGF2, less FGF2 was bound to the endogenous HS proteoglycans, resulting in decreased proliferation of the mesangial cells. To show that proliferation of the mesangial cells was dependent on active FGF2 binding by endogenous HS, cells were cultured in the presence of chlorate. Chlorate inhibited the sulfation of the side chains of the proteoglycans in a dose-dependent manner (Figure 7C) which should lead to loss of binding sites for growth factors including FGF2. Indeed, chlorate prevented the FGF2-induced proliferative response of mesangial cells, which appeared to be dependent on the duration of FGF2 stimulation (Figure 7D). These results indicate that the proliferation of mesangial cells is dependent on FGF2 binding to endogenous HS proteoglycans. The interaction between FGF2 and HS proteoglycans on mesangial cells may therefore play a key role in the development of FGS.

Discussion

In this study we provide evidence that HSPGs such as perlecan serve as functional docking platforms for FGF2 and contribute to glomerular and arterial tissue remodeling in experimental CTD. The concept of extracellular regulation of growth factors by proteoglycans has been studied predominantly in tissue remodeling related to embryonic development (12,13), ontogenesis (14,15) and angiogenesis (16,17). Our data indicate that HSPGs modulate growth factors in the renal transplant setting as well. This is an important finding that opens the possibility to target proteoglycans by therapeutic intervention to ameliorate the development of CTD.

Development of CTD in renal allografts is the result of tissue remodeling affecting all functional-structural compartments of the kidney including the tubulointerstitium (tubular atrophy and interstitial fibrosis), glomeruli (focal glomerulosclerosis), and larger arteries (neointima formation) (2-4). We recently demonstrated compositional changes of the HSPGs collXVIII, perlecan and agrin in tissue remodeling in experimental CTD by immunofluorescence (5). We now investigated functional aspects of proteoglycans in experimental CTD as well as in renal cell culture assays. Depending on their highly variable composition, HS carbohydrate side chains can bind a variety of ligands including FGF2 (10), which is known to be involved in renal tissue remodeling. In experimental allografts with CTD, a massive increase in matrix HSPG-mediated binding capacity for FGF2 was observed. Enhanced binding capacity for this growth factor was the result of

increased HSPG expression, and modified HS sulfation [most likely increased 2-O sulfation leading to loss of JM-403 staining (24,25) and increased FGF2 binding (26)]. This finding suggests that upon allo-transplantation the kidney mobilizes matrix HSPGs to become docking molecules for heparin-binding growth factors such as FGF2. This was also reported by Morita et al. (27) showing increased FGF2 binding in fibrotic areas of native kidney diseases.

The laser microdissection approach on isolated glomeruli, arterial mediae and neointimae revealed spatial differences in HSPG expression, which were not seen, and would have been missed, in whole kidney homogenates. We observed increased glomerular and neointimal perlecan expression in allografted kidneys. This regional HSPG regulation opposes the uniform induction of pro-fibrotic pathways (Coll I, Coll IV, TGF- β 1) seen in glomeruli, mediae and whole kidney tissue, which probably reflects a more generalized response upon allo-transplantation. Like perlecan, FGF2 showed a restricted glomerular and neointimal expression pattern as well. The marked FGF2 and perlecan expression observed in glomeruli of allografted kidneys suggests a role in the proliferative response of mesangial cells. In other settings perlecan/FGF2 has been shown to induce proliferation in a number of cell types including chondrocytes, neural stem cells, retinal pigmental epithelial cells and vascular smooth muscle cells (17, 28-30). In the kidney FGF2 has been shown to be proliferative for fibroblasts and mesangial cells (29,30). *In vitro* studies showed that the expression of cell surface HSPG was a prerequisite for the proliferation of renal fibroblasts in response to FGF2 (31). We therefore studied the functional role of the FGF2-proteoglycan interaction in mesangial cell proliferation *in vitro*. FGF2 was shown to induce mesangial cell proliferation in a dose- and sulfation-dependent manner indeed favoring for a role of the FGF2-proteoglycan interaction in mesangial cell proliferation. Although FGF2 binding on allograft sections was shown to be heparitinase-sensitive (indicating that FGF2 interacts with HSPGs), the exact identity of the FGF2-binding HSPG(s) is as yet unknown. Since both collXVIII and perlecan are upregulated in FGS (5 and this study) we propose that FGF2 binds to (one of) these proteoglycans. The exact mechanism by which HSPGs enhance FGF2-induced mesangial cell proliferation is unknown. We propose that binding of FGF2 to mesangial (matrix) HSPGs facilitates the interaction between FGF2 and its surface receptor on mesangial cells, as has been demonstrated for other cell types (28-33). This is supported by our observation that removing the FGF2 binding capacity of proteoglycans on mesangial cells by chlorate treatment resulted in a significant delay, but not complete abrogation of FGF2-induced proliferation.

Based on our data, HSPGs could be interesting therapeutic targets to limit CTD, especially focusing on the potential of inhibiting growth factor signaling. To study the possibility that exogenous glycosaminoglycans may hamper growth factor responses, heparin(oids) have been shown to reduce progressive renal failure in experimental renal diseases, including renal transplantation (34-36). Increasing research interest is focusing on the possibility to produce small HS-mimetics, which may more specifically target a particular component of

HS/heparin bioactivity (37). The use of HSPGs as targets, for example using antibodies that recognize and thereby block specific HS-motifs/domains, may also have clinical potential. This strategy has been exemplified *in vitro* by the demonstration that 6-O-sulfate specific anti-HS antibodies produced in a phage-display library can inhibit leukocyte rolling and firm adhesion to glomerular endothelial cells, whereas anti-HS antibodies with different specificities do not (38). Mutant growth factors, which are made incapable of glycosaminoglycan binding, could be used to specifically inhibit cell survival/proliferation. In addition, small inactive growth factor fragments could be generated that block the HSPG-binding sites of their *in vivo* active counterparts. Together, there are various options for the use of HSPGs in therapeutic strategies, but further proof of efficacy *in vivo* needs to be provided.

Acknowledgements

This study was financially supported by the Dutch Kidney Foundation (C03.6015, MB, HR and JLH) and the Graduate School of Medical Sciences (GSMS) of the University Medical Center Groningen (KK). We thank Peter Zwiers, Marian Bulthuis, André Zandvoort and Annemieke Smit-van Oosten for their excellent technical assistance.

Competing financial interests

None

References

1. Kouwenhoven EA, IJzermans JN, de Bruin RW: Etiology and pathophysiology of chronic transplant dysfunction. *Transpl Int* 13: 385-401, 2000
2. Chapman JR, O'Connell PJ, Nankivell BJ: Chronic renal allograft dysfunction. *J Am Soc Nephrol* 16: 3015-26, 2005
3. Solez K, Colvin RB, Racusen LC, Haas M, Sis B, Mengel M, Halloran PF, Baldwin W, Banfi G, Collins AB, Cosio F, David DS, Drachenberg C, Einecke G, Fogo AB, Gibson IW, Glotz D, Iskandar SS, Kraus E, Lerut E, Mannon RB, Mihatsch M, Nankivell BJ, Nিকেleit V, Papadimitriou JC, Randhawa P, Regele H, Renaudin K, Roberts I, Seron D, Smith RN, Valente M: Banff 07 classification of renal allograft pathology: updates and future directions. *Am J Transplant* 8: 753-60, 2008
4. Solez K, Colvin RB, Racusen LC, Sis B, Halloran PF, Birk PE, Campbell PM, Cascalho M, Collins AB, Demetris AJ, Drachenberg CB, Gibson IW, Grimm PC, Haas M, Lerut E, Liapis H, Mannon RB, Marcus PB, Mengel M, Mihatsch MJ, Nankivell BJ, Nিকেleit V, Papadimitriou JC, Platt JL, Randhawa P, Roberts I, Salinas-Madriga L, Salomon DR, Seron D, Sheaff M, Weening JJ: Banff '05 Meeting Report: differential diagnosis of chronic allograft injury and elimination of chronic allograft nephropathy ('CAN'). *Am J Transplant* 7: 518-26, 2007
5. Rienstra H, Katta K, Celie JW, van Goor H, Navis G, van den Born J, Hillebrands JL: Differential expression of proteoglycans in tissue remodeling and lymphangiogenesis after experimental renal transplantation in rats. *PLoS One* 5: e9095, 2010
6. Celie JW, Reijmers RM, Slot EM, Beelen RH, Spaargaren M, Ter Wee PM, Florquin S, van den Born J: Tubulointerstitial heparan sulfate proteoglycan changes in human renal diseases correlate with leukocyte influx and proteinuria. *Am J Physiol Renal Physiol* 294: F253-63, 2008
7. Celie JW, Rutjes NW, Keuning ED, Soininen R, Heljasvaara R, Pihlajaniemi T, Dräger AM, Zweegman S, Kessler FL, Beelen RH, Florquin S, Aten J, van den Born J: Subendothelial heparan sulfate proteoglycans become major L-selectin and monocyte chemoattractant protein-1 ligands upon renal ischemia/reperfusion. *Am J Pathol* 170: 1865-78, 2007
8. Zaferani A, Vives RR, van der Pol P, Hakvoort JJ, Navis GJ, van Goor H, Daha MR, Lortat-Jacob H, Seelen MA, van den Born J: Identification of tubular heparan sulfate as a docking platform for the alternative complement component properdin in proteinuric renal disease. *J Biol Chem* 286: 5359-67, 2011
9. Lortat-Jacob H: The molecular basis and functional implications of chemokine interactions with heparan sulphate. *Curr Opin Struct Biol* 19: 543-8, 2009
10. Guimond S, Maccarana M, Olwin BB, Lindahl U, Rapraeger AC: Activating and inhibitory heparin sequences for FGF-2 (basic FGF). Distinct requirements for FGF-1, FGF-2, and FGF-4. *J Biol Chem* 268: 23906-14, 1993
11. Gallagher JT, Turnbull JE: Heparan sulphate in the binding and activation of basic fibroblast growth factor. *Glycobiology* 2: 523-8, 1992
12. Schwabiuk M, Coudiere L, Merz DC: SDN-1/syndecan regulates growth factor signaling in distal tip cell migrations in *C. elegans*. *Dev Biol* 334: 235-42, 2009
13. Olivares GH, Carrasco H, Aroca F, Carvallo L, Segovia F, Larraín J: Syndecan-1 regulates BMP signaling and dorso-ventral patterning of the ectoderm during early *Xenopus* development. *Dev Biol* 329: 338-49, 2009
14. Menashe I, Maeder D, Garcia-Closas M, Figueroa JD, Bhattacharjee S, Rotunno M, Kraft P, Hunter DJ, Chanock SJ, Rosenberg PS, Chatterjee N: Pathway analysis of breast cancer genome-wide association study highlights three pathways and one canonical signaling cascade. *Cancer Res* 70: 4453-9, 2010
15. Götte M, Kersting C, Radke I, Kiesel L, Wülfing P: An expression signature of syndecan-1 (CD138), E-cadherin and c-met is associated with factors of angiogenesis and lymphangiogenesis in ductal breast carcinoma in situ. *Breast Cancer Res* 9: R8, 2007
16. Iozzo RV, Zoeller JJ, Nyström A: Basement membrane proteoglycans: modulators Par Excellence of cancer growth and angiogenesis. *Mol Cells* 27: 503-13, 2009

17. Aviezer D, Hecht D, Safran M, Eisinger M, David G, Yaron A: Perlecan, basal lamina proteoglycan, promotes basic fibroblast growth factor-receptor binding, mitogenesis, and angiogenesis. *Cell* 79: 1005-13, 1994
18. Nakamura T, Ebihara I, Fukui M, Osada S, Nagaoka I, Horikoshi S, Tomino Y, Koide H: Messenger RNA expression for growth factors in glomeruli from focal glomerular sclerosis. *Clin Immunol Immunopathol* 66: 33-42, 1993
19. Floege J, Kriz W, Schulze M, Susani M, Kerjaschki D, Mooney A, Couser WG, Koch KM: Basic fibroblast growth factor augments podocyte injury and induces glomerulosclerosis in rats with experimental membranous nephropathy. *J Clin Invest* 96: 2809-19, 1995
20. Kriz W, Hähnel B, Rösener S, Elger M: Long-term treatment of rats with FGF-2 results in focal segmental glomerulosclerosis. *Kidney Int* 48: 1435-50, 1995
21. Chan J, Prado-Lourenco L, Khachigian LM, Bennett MR, Di Bartolo BA, Kavurma MM: TRAIL promotes VSMC proliferation and neointima formation in a FGF-2-, Sp1 phosphorylation-, and NFkappaB-dependent manner. *Circ Res* 106: 1061-71, 2010
22. Camozzi M, Zacchigna S, Rusnati M, Coltrini D, Ramirez-Correa G, Bottazzi B, Mantovani A, Giacca M, Presta M: Pentraxin 3 inhibits fibroblast growth factor 2-dependent activation of smooth muscle cells *in vitro* and neointima formation *in vivo*. *Arterioscler Thromb Vasc Biol* 25: 1837-42, 2005
23. Waanders F, Rienstra H, Boer MW, Zandvoort A, Rozing J, Navis G, van Goor H, Hillebrands JL: Spironolactone ameliorates transplant vasculopathy in renal chronic transplant dysfunction in rats. *Am J Physiol Renal Physiol* 296: F1072-9, 2009
24. van den Born J, Gunnarsson K, Bakker MA, Kjellén L, Kusche-Gullberg M, Maccarana M, Berden JH, Lindahl U: Presence of N-unsubstituted glucosamine units in native heparan sulfate revealed by a monoclonal antibody. *J Biol Chem* 270: 31303-9, 1995
25. David G, Bai XM, Van der Schueren B, Cassiman JJ, Van den Berghe H: Developmental changes in heparan sulfate expression: in situ detection with mAbs. *J Cell Biol* 119: 961-75, 1992
26. Maccarana M, Casu B, Lindahl U: Minimal sequence in heparin/heparan sulfate required for binding of basic fibroblast growth factor. *J Biol Chem* 268: 23898-905, 1993
27. Morita H, Shinzato T, David G, Mizutani A, Habuchi H, Fujita Y, Ito M, Asai J, Maeda K, Kimata K: Basic fibroblast growth factor-binding domain of heparan sulfate in the human glomerulosclerosis and renal tubulointerstitial fibrosis. *Lab Invest.* 71(4):528-35, 1994
28. Smith SM, West LA, Govindraj P, Zhang X, Ornitz DM, Hassell JR: Heparan and chondroitin sulfate on growth plate perlecan mediate binding and delivery of FGF-2 to FGF receptors. *Matrix Biol* 26: 175-84, 2007
29. Guillonneau X, Tassin J, Berrou E, Bryckaert M, Courtois Y, Mascarelli F : *In vitro* changes in plasma membrane heparan sulfate proteoglycans and in perlecan expression participate in the regulation of fibroblast growth factor 2 mitogenic activity. *J Cell Physiol* 166: 170-87, 1996
30. Park Y, Rangel C, Reynolds MM, Caldwell MC, Johns M, Nayak M, Welsh CJ, McDermott S, Datta S: Drosophila perlecan modulates FGF and hedgehog signals to activate neural stem cell division. *Dev Biol* 253: 247-57, 2003
31. Clayton A, Thomas J, Thomas GJ, Davies M, Steadman R: Cell surface heparan sulfate proteoglycans control the response of renal interstitial fibroblasts to fibroblast growth factor-2. *Kidney Int* 59(6): 2084-94, 2001
32. Francki A, Uciechowski P, Floege J, von der Ohe J, Resch K, Radeke HH: Autocrine growth regulation of human glomerular mesangial cells is primarily mediated by basic fibroblast growth factor. *Am J Pathol* 147: 1372-82, 1995
33. Strutz F: The role of FGF-2 in renal fibrogenesis. *Front Biosci* 1: 125-31, 2009
34. van Bruggen MC, Walgreen B, Rijke TP, Corsius MJ, Assmann KJ, Smeenk RJ, van Dedem GW, Kramers K, Berden JH: Heparin and heparinoids prevent the binding of immune complexes containing nucleosomal antigens to the GBM and delay nephritis in MRL/lpr mice. *Kidney Int* 50: 1555-64, 1996
35. Gottmann U, Mueller-Falcke A, Schnuelle P, Birck R, Nিকেleit V, van der Woude FJ, Yard BA, Braun C: Influence of hypersulfated and low molecular weight heparins on ischemia/reperfusion: injury and allograft rejection in rat kidneys. *Transpl Int* 20: 542-9, 2007

36. Ceol M, Gambaro G, Sauer U, Baggio B, Anglani F, Forino M, Facchin S, Bordin L, Weigert C, Nerlich A, Schleicher ED: Glycosaminoglycan therapy prevents TGF-beta1 overexpression and pathologic changes in renal tissue of long-term diabetic rats. *J Am Soc Nephrol* 11: 2324-36, 2000
37. Ashikari-Hada S, Habuchi H, Sugaya N, Kobayashi T, Kimata K: Specific inhibition of FGF-2 signaling with 2-O-sulfated octasaccharides of heparan sulfate. *Glycobiology* 19: 644-54, 2009
38. Rops AL, van den Hoven MJ, Baselmans MM, Lensen JF, Wijnhoven TJ, van den Heuvel LP, van Kuppevelt TH, Berden JH, van der Vlag J: Heparan sulfate domains on cultured activated glomerular endothelial cells mediate leukocyte trafficking. *Kidney Int* 73: 52-62, 2008
39. Asgeirsdottir SA, Werner N, Harms G, Van Den Berg A, Molema G: Analysis of *in vivo* endothelial cell activation applying RT-PCR following endothelial cell isolation by laser dissection microscopy. *Ann N Y Acad Sci* 973: 586-9, 2002.

Chapter 4

Non-anticoagulant heparinoid reduces renal inflammation in experimental renal transplant dysfunction

In preparation

Kirankumar Katta
Saritha Adepu
Ditmer Talsma
Pramod Kumar Agarwal
Saleh Yazdani
Annamaria Naggi
Giangiacomo Torri
Gerjan Navis
Jan-Luuk Hillebrands
Jacob van den Born

Abstract

The pathogenesis of chronic transplant dysfunction (CTD) is multifactorial and is histologically characterized by interstitial fibrosis and tubular atrophy, transplant vasculopathy and focal segmental glomerulosclerosis, and is also associated by an inflammatory component. To date, no effective therapies are available to treat renal CTD. Via their heparan sulfate polysaccharide side chains, heparan sulfate proteoglycans are crucial players in tissue homeostasis. We hypothesized that heparan sulfate proteoglycans could be promising therapeutic targets to limit CTD, by their involvement in inflammation and chemokine/growth factor signaling cascades. To test this hypothesis, in a rat model for renal CTD, by daily subcutaneous injections we intervened with vehicle, unfractionated heparin, and the non-anticoagulant heparinoids N-acetyl heparin and periodate-oxidized, borohydrate-reduced (RO-) heparin for 9 weeks. Both these non-anticoagulant heparinoids have been described to exert similar anti-inflammatory and anti-proliferative properties as heparin. Compared to the vehicle group, RO-heparin ameliorates the cortical tubulo-interstitial accumulation of CD45+ inflammatory cells (week 9: 0.8% surface area in RO-heparin group versus 1.8% surface area in vehicle group; $p < 0.02$). Additionally, a tendency for lower proteinuria was present. Regular heparin adversely increased neointima formation in arteries $< 200 \mu\text{m}$ (week 9: heparin vs vehicle group: $p = 0.006$), whereas both non-anticoagulant heparinoids did not provoke this arterogenic response and did not differ from vehicle group. Heparin(oid) treatment did not affect body weight, graft survival, blood pressure, and renal function, and neither reduced glomerular and interstitial tissue remodeling, although glomerulosclerosis score was non-significantly reduced in the RO-heparin group. These data demonstrate that specifically modified heparinoids can reduce inflammation in experimental CTD, and suggest that carefully selected non-anticoagulant heparan sulfate glycomimetics could have protective effects as adjunct therapy for CTD.

Introduction

Chronic transplant dysfunction (CTD) is characterized by decline in kidney function over time and is related to progressive tissue remodeling in the transplanted kidney. CTD is the second leading risk for graft loss (after death) and has a histological incidence of >70% already 2 years after transplantation. The pathogenesis of CTD is multifactorial and is clinically associated by progressive hypertension, proteinuria and increased values of triglycerides (1-3). At present, besides immunosuppressive therapy, progressive loss of transplant function is only symptomatically treated by anti-hypertensive and anti-proteinuric treatment in combination with lipid lowering drugs. Histologically, CTD is characterized by chronic lesions such as interstitial fibrosis and tubular atrophy (IF/TA), transplant vasculopathy (TV) and focal segmental glomerulosclerosis (FSGS) (1,4,5). To date, due to lack of knowledge on tissue remodeling and development of these lesions, no effective therapies are available to treat renal CTD.

Recently, we showed increased expression of heparan sulfate proteoglycans (HSPGs) during tissue remodeling in experimental CTD (6). We also showed that renal HSPGs modulate FGF2 signaling in mesangial cells in culture (chapter 3 of this thesis). In native kidney diseases and ischemia-reperfusion injury we demonstrated that HSPGs are critically involved in leukocyte influx and proteinuria-mediated renal injury (7-9). However, the precise mechanism behind the involvement of proteoglycans in CTD-associated progressive renal failure is still not unraveled.

In general, via their heparan sulfate (HS) glycosaminoglycan side chains, HSPGs act as co-receptors for a number of growth factors resulting in the formation of active signaling complexes that lower the concentration of growth factor necessary to initiate signaling through its receptor and extend the duration of the response (10,11). Moreover, after injury HSPGs can also act as ligands for adhesion molecules such as L- and P-selectin, MAC-1 and VLA-4, and also as docking molecules for complement factors and chemokines. By doing so HSPGs play pivotal roles in cellular activation, and leukocyte adhesion, activation and extravasation (12). Thus, HSPGs are crucial players in inflammation, cell survival and proliferation, fibrosis, regeneration and repair. Based on these functions, HSPGs are potential targets for intervention in order to reduce leukocyte recruitment and fibrotic processes. Heparin is well known for its anti-coagulant activity and used in the prevention and treatment of thromboembolic complications. In addition heparin has anti-inflammatory, anti-proliferative and anti-oxidative properties.

Non-anticoagulant heparins and various other heparin derivatives (low-molecular weight heparins, synthetic heparin mimetics and anti-HS antibodies) are regarded as agonists or antagonists of HS function (13-16). Non-anticoagulant heparins are obtained from regular heparin by removing and/or changing residues that are essential for high affinity binding to antithrombin (17,18).

Beneficial effects of exogenously administered (non-anticoagulant) heparinoids is thought to be associated with altered molecular processes involving HS chains of cell surface and extracellular matrix HSPGs on one hand, and growth factors and their receptors, chemokines and adhesion molecules on the other hand. Thus, these (non-anticoagulant) heparinoids most likely intervene in several processes that include blocking selectins, preventing chemokine presentation, interruption of chemokine gradient formation, and down modulation of growth factor signaling cascades.

Previously, it has been shown that treatment with LMWH reviparin reduces signs of progressive renal failure in experimental renal transplantation (19,20). Human renal allograft recipients, receiving unfractionated heparin therapy early after transplantation showed increased risk of hemorrhagic complications (21). Moreover, heparin therapy can have side effects that include heparin-induced thrombocytopenia type II, a potentially harmful threat to patient and graft survival (22). In experimental renal ischemia-reperfusion injury (a non-transplant renal disease), it has been demonstrated that treatment with a synthetic and non-anticoagulant heparin showed reduced inflammation and neutrophil accumulation(23,24).

Based on our previous data and other heparinoids intervention studies, we hypothesize that HSPGs could be promising therapeutic targets to limit CTD, especially focusing on the potential to inhibit inflammation and growth factor signaling cascades. To test this hypothesis, in a well established rat model for renal chronic transplant dysfunction (25), we intervened with vehicle, with unfractionated heparin, and with two different non-anticoagulant heparinoids (N-desulfated/reacetylated (NAc-) heparin and periodate-oxidized/borohydride-reduced (RO-)heparin). Both these non-anticoagulant heparinoids exert similar anti-inflammatory and anti-metastatic properties as heparin. In addition biostability, activity and specificity of these heparinoids were properly controlled and also showed beneficial effects in several experimental model (18,26,27). Lastly, these heparinoids can be produced in larger quantities within affordable costs and limited time. Our studies demonstrate significant beneficial effects of RO-heparin on the development of triglyceride levels and renal influx of inflammatory cells along with a tendency to lower proteinuria in an experimental CTD model.

Material & methods

Animals

In this study 52 ten weeks old female inbred Dark Agouti (DA) rats (donors) and 52 ten weeks old male inbred Wistar Furth (WF) rats (recipients) were used. DA and WF rats were obtained from Harlan Nederland (Zeist, The Netherlands) and Charles River Laboratories (I'Arbresle, Cedex, France) respectively. Animals were kept in a temperature controlled room, with a 12:12-h light:dark cycle and fed standard rodent chow and water ad libitum.

The local animal ethics committee of the University of Groningen approved all the procedures used in the study and the Principles of Laboratory Animal Care (National Institute of Health publication no. 86-23) were followed.

Kidney transplantation

Kidney allotransplantation was performed from female DA donors to male WF recipients according to standard procedures as described previously (25). Cold and warm ischemia times were 15 ± 3 (mean \pm SD) and 25 minutes, respectively. After transplantation the recipients were placed in an incubator at 28°C for approximately 6 hours and caged individually. After transplantation all recipients subcutaneously received Cyclosporine A (5 mg/kg BW/day) for 10 days. The native kidney was removed after 12 to 14 days after transplantation. Total follow up was 65 ± 4 days (mean \pm SD). Fourteen rats were excluded from the study because of technical surgery failure (n=3) or acute rejection (n=11) which became evident by inspection of the graft during nephrectomy procedure. Thus 38 transplanted rats were included in the study.

Experimental groups

In this experiment, an intervention was done with regular, unfractionated heparin (Hep; n=9) and two non-anticoagulant heparinoids derived from regular unfractionated heparin: N-desulfated, N-reacetylated heparin (NAc-Hep; n=10) and periodate-oxidized, borohydride-reduced heparin (RO-Hep; n=9). Production and characterization of these heparinoids have been described before (28). The control transplanted group (Con; n=10) received daily vehicle (physiological saline) injections. One day before transplantation, treatment with the respective formulations was started. The above mentioned groups daily received heparin(oids) between 9.00 and 12.00 AM dissolved in physiological salt, injected subcutaneously at 2 mg/kg BW/day until sacrifice. The treatment dose was chosen according to previous studies (19,20) and is in the physiological range normally used for the treatment of thrombotic complications.

Clinical variables

Animals were weighed every day and observed for signs of decreasing animal welfare reflecting their clinical condition. Upon weight loss of >15% compared to highest measured body weight, animals were sacrificed and regarded as drop outs. Blood pressure was measured non-invasively with tail cuff method (CODA; Kent Scientific, Torrington, CT). Two weeks before transplantation the rats were trained to undergo blood pressure measurements. Rats were placed individually in metabolic cages to obtain 24h urines, food and water intake measurements. Blood pressure, 24h urine sampling and non-fasting blood

sampling by orbital puncture were taken before transplantation (baseline), four and eight weeks after transplantation. Urine was analyzed for urea, creatinine and total protein. Blood was analyzed for urea, creatinine and triglycerides. Analyses were performed on a multi-test analyzer system (Roche Modular; F.Hoffmann-La Roche Ltd, Basel, Switzerland) at the central clinical laboratory of the University Medical Center Groningen. Creatinine clearance was calculated from 24h urinary volume, plasma and urinary creatinine.

Quantification of glomerulosclerosis and neo-intima formation

Kidneys were perfused with saline prior to sacrifice. Half of the kidney was fixed in 4% formaldehyde and processed for paraffin embedding and other half was cryopreserved. Paraffin sections (4 μ m) were stained with periodic acid-Schiff (PAS) and Verhoeff's stain to evaluate focal glomerulosclerosis (FGS) and transplant vasculopathy, respectively. The sections were semi-quantitatively scored for focal glomerulosclerosis in a blinded fashion by determining the level of mesangial expansion and focal adhesion in each quadrant in a glomerulus and expressed on a scale from 0 to 4. If the glomerulus was unaffected, it was scored as 0; if one quadrant of the glomerulus was affected, it was scored as 1, two affected quadrants as 2, three affected quadrants as 3 and 4 affected quadrants as 4. In total, 50 glomeruli per kidney were analyzed, and the total FGS score was calculated by multiplying the score by the percentage of glomeruli with the same FGS score. The sum of these scores gives the total FGS score with a maximum of 400.

To investigate the transplant vasculopathy, neo-intima formation was determined using a Verhoeff staining. Neo-intima formation was scored at 200x magnification (Olympus BX 50 (Olympus Europa, Hamburg, Germany) by determining the percentage of luminal occlusion. All the identifiable elastin positive intra renal vessels were evaluated in a blinded fashion. Lumen of vessels was the mean lengths of two straight lines drawn from the internal elastic lamina (IEL) and passing through the center of vessel. The areas enclosed by lumen, internal elastic lamina and external lamina were measured. The area between the lumen and internal elastic lamina was described as neointimal area. The percentage of neo-intima area to the area enclosed by IEL (total lumen) is described as percentage of luminal occlusion.

Immunohistochemistry

Renal tissue was processed for immunohistochemistry. Details on fixation, antigen retrieval, antibodies and conjugates are given in Table 1. After the staining procedure, quantification was done in cortical tissue by using the MacBiophotonics ImageJ program (Rasband, W.S., ImageJ, U.S. National Institute of Health, Bethesda, Maryland, USA).

Chapter 4

Table 1. Immunohistochemical procedures for various fibrotic, inflammatory and lymphatic cell types

Cell type	Tissue processing	Marker	Antibody	Conjugate	Quantification
Myofibroblasts	Cryosections, Acetone fixed	α -smooth muscle actin (α - SMA)	Mouse anti- α - SMA; clone 1A4; (DAKO, Glostrup, Denmark) 1:100.	Goat anti-mouse IgG2a-PO (Southern Biotech, Birmingham, USA); 1:100. Tetramethylrhodamine System (PerkinElmer LAS Inc)	30 photomicrographs randomly selected at 200 x magnification. Digital image analysis by ImageJ
Leukocytes	Cryosections, Acetone fixed	CD45	Mouse anti-rat CD45 antibody (clone OX- 1)(ref.29) 1:2	Goat anti-mouse IgG PO(Southern Biotech, Birmingham, USA); 1:100, Tetramethylrhodamine System (PerkinElmer LAS Inc)	30 photomicrographs randomly selected at 200 x magnification. Digital image analysis by ImageJ
Macrophages	Cryosections, Acetone fixed	CD68	mouse anti-rat CD68 antibody (clone ED-1), (ab serotech, Oxford, UK), 1:500.	Rabbit anti-mouse Ig PO (DAKO); 1:100 3-amino- 9-ethyl-carbazole (AEC) (DAKO)	30 photomicrographs randomly selected at 200 x magnification. Digital image analysis by ImageJ
T-cells	Cryosections, Acetone fixed	CD3	Rabbit anti- human CD3; (DAKO, Glostrup, Denmark) 1:100.	Goat anti-rabbit Ig PO (DAKO); 1:100, tetramethylrhodamine System (PerkinElmer LAS Inc)	30 photomicrographs randomly selected at 200 x magnification. Digital image analysis by ImageJ
Lymphatic endothelium	Formaldehyde fixed, paraffin embedded, deparafinization, Tris/EDTA (pH 9.0)	Podoplanin	Mouse anti-rat Podoplanin, (Angiobio, Huissen, Netherlands) 1:100	Goat anti mouse Ig PO (Southern Biotech, Birmingham, USA); 1:100, 3,3'-Diaminobenzidine (DAB) (DAKO)	30 photomicrographs randomly selected at 200 x magnification. Manual quantification

Data are expressed as % positive stained surface areas. Lymph vessels were counted manually and expressed as number/ high power field.

Statistics

Differences among the groups were tested with a Mann-Whitney U test, $p < 0.05$ was considered statistically significant. The graphs and statistics were done by GraphPad Prism 5.00 for Windows (GraphPad Software Inc., La Jolla, CA, USA).

Results

Development of CTD-related renal failure

This study included 38 male WF rats that were transplanted with a female DA kidney. During follow-up from 2-9 weeks, pre-term graft loss occurred in 3 rats in the vehicle treated group ($n=10$), 5 rats in the normal unfractionated heparin ($n=9$), 5 rats in the N-acetyl heparin ($n=10$) and 2 rats in the RO-heparin group ($n=9$). Renal graft loss was evidenced by clinical signs such as pilo-erected fur, severe body weight loss, disoriented behaviour and high blood creatinine values. Graft loss among the various heparinoid groups was statistically not significantly different. The rats that had to be sacrificed before the end of the experiment (before 9 weeks after transplantation) were excluded from all histological and biochemical analyses described later. Accordingly, the following groups with mentioned group size were studied: Allografts treated with Vehicle ($n=7$), with unfractionated heparin ($n=4$), with N-acetyl heparin ($n=5$) and with RO-heparin ($n=7$). In the plasmas of the rats taken at 8 weeks after renal transplantation, four hours after heparin(oid) injection, we measured the activated partial thromboplastin time. In the saline treated transplanted rats this was 75 sec (median value). In the heparin(oid) groups this time was 173 sec in regular heparin group (saline versus regular heparin: $p < 0.05$), 73 sec in the RO-heparin group, and 69 sec in the N-acetyl heparin group (both non-anticoagulant heparinoids being not different from saline treated rats). These data show that both chemically modified heparin preparations indeed were non-anticoagulant, and clearly different from regular heparin, and not from the saline-treated rats.

No effects of (non-)anticoagulant heparin(oids) on body weight, blood pressure, food and water intake, and urine output

Treatment with heparin and non-anticoagulant heparins had no effect on body weight of the WF recipient rats. In accordance with our previous transplantation data, during the follow-up, the mean arterial pressure increased gradually in recipient WF rats until the end of the

experiment without statistical significances among the groups. Similarly, food and water intake and urine output in all the groups were not affected by the treatment (Table 2).

Effects of (non-)anticoagulant heparin(oids) on renal function, proteinuria and plasma triglycerides

Vehicle treated groups developed CTD-related renal failure according to previous findings (30), as evidenced by rise in plasma urea and creatinine, rise in urinary protein excretion and blood pressure, and rise in plasma triglycerides (Table 2). The plasma creatinine and urea levels increased in all the groups over time. Although plasma creatinine and urea levels in the RO-heparin group at 8 weeks seems to be higher compared to all other groups, these values were not significantly different. In addition, at 8 weeks, unfractionated heparin and RO-heparin treated groups have significantly lower plasma triglycerides compared to vehicle and N-acetyl heparin treated groups (week 8: $0,4\pm 0,26$ mmol/l in RO-heparin group versus $0,8\pm 0,2$ mmol/l in vehicle group; $p < 0.02$). RO-heparin treated group showed less urinary protein excretion after 8 weeks follow-up compared to untreated rats (Table 2); however, without reaching the level of statistical significance. Taken together, heparinoids had no effect on renal function and RO-heparin had a tendency to reduce proteinuria; regular heparin and R-O-heparin prevented the rise of plasma triglycerides

(Non-)anticoagulant heparin(oids) are not effective in reducing CTD associated tissue remodeling

Glomerulosclerosis - FGS was determined by the PAS staining and is abundantly present in all the groups. Whereas non-transplanted rats have a FGS score close to zero (not shown), animals that are treated with unfractionated heparin and N-Acetyl heparin showed FGS score comparable to the vehicle treated group. These groups approximately scored median value of 3, indicating FGS in three out of four glomerular quadrants. The RO-heparin group however showed a lower FGS, scoring median value of 2.5; however, without reaching the level of statistical significance (Figure 1A).

Tubulo-interstitial changes: pre-fibrotic lesions (α -SMA) and lymphangiogenesis - In the tubulo-interstitial areas of the cortex, heparin and non-anticoagulant heparins treated groups did not show any statistical difference in α -SMA positive cell density compared to the vehicle treated group as shown in the figure 1B, suggesting comparable degree of interstitial fibrosis.

In the tubulo-interstitium of the transplanted rats, lymphangiogenesis occurred to ~5 lymph vessels/high power field. In vehicle treated rats this ranged from 3 to 8 and neither of the heparinoids changed the lymphangiogenic response, although lymph vessel density appeared to be a bit lower in the regular heparin group, however without reaching the level of statistical significance (Figure 1C).

Chapter 4

Table 2. Clinical variables from recipients at baseline (pre-Tx) and at 4 and 8 weeks after transplantation. Data shown as Median (25%-75% interquartile range)

		DA-to-WF allograft			
		Vehicle (n=7)	Unfractionated Heparin (n=4)	RO-Heparin (n=7)	N-acetyl Heparin (n=5)
Body weight (g)	Baseline	290(285-296)	283(274-291)	270(263-284)	271(270-276)
	4 weeks after Tx	293(281-313)	299(292-302)	284(281-302)	285(276-290)
	8 weeks after Tx	323(298-347)	311(300-320)	298(280-326)	303(299-313)
Food intake (g/24h)	Baseline	9(5-11)	5(5-7)	5(4-7)	5(4-7)
	4 weeks after Tx	5(4-8)	7(6-9)	2(1-5)	5(5-11)
	8 weeks after Tx	3(3-6)	1,5(1-4)	4(1-7)	2(1-6)
Water intake (ml/24h)	Baseline	17(17-20)	14(12-17)	13(10-16)	12(8-15)
	4 weeks after Tx	25(21-27)	29(19-37)	18(16-24)	19(17-23)
	8 weeks after Tx	27(24-30)	28(24-31)	22(17-46)	18(9-33)
Urinary output(ml/24h)	Baseline	14(13-17)	15(15-15)	12(11-14)	11(11-12)
	4 weeks after Tx	26(18-30)	24(20-28)	15(13-28)	19(19-20)
	8 weeks after Tx	33(29-34)	32(28-35)	31(18-44)	30(21-30)
Plasma creatinine (µmol/L)	Baseline	19(18-21)	19(19-21)	15(14-17)	15(15-19)
	4 weeks after Tx	73(59-120)	64(52-73)	65(54-168)	81(53-84)
	8 weeks after Tx	96(73-139)	72(58-99)	136(70-207)	73(58-122)
Creatinine Clearance (ml/min)	Baseline	3,0(2,8-3,8)	2,6(2,5-3,0)	3,5(2,7-3,7)	3,0(2,3-3,0)
	4 weeks after Tx	0,7(0,4-1,1)	1,0(1,0-1,3)	1,0(0,5-1,2)	0,7(0,1-0,8)
	8 weeks after Tx	0,6(0,3-1,0)	0,8(0,5-1,2)	0,4(0,2-0,9)	0,9(0,4-1,0)
Plasma urea (mmol/L)	Baseline	6(5-7)	6(5-7)	6(5-6)	6(5-6)
	4 weeks after Tx	20(18,3-36)	18(16-20)	20(14-39)	19(15-24)
	8 weeks after Tx	28(21-51)	22(18-37)	43(21-64)	27(24-40)
Total urinary protein (mg/24h)	Baseline	10(8-11)	7(6-8)	9(7-10)	9(6-9)
	4 weeks after Tx	8(7-12)	8(7-11)	9(7-13)	8(7-10)
	8 weeks after Tx	56(34-93)	61(57-74)	33(23-43)	94(90-184)
Plasma triglycerides (mmol/L)	Baseline	0,6(0,5-0,6)	0,7(0,6-0,7)	0,6(0,5-0,6)	0,6(0,4-0,7)
	4 weeks after Tx	0,6(0,5-0,7)	0,5(0,5-0,5)	0,7(0,5-0,8)	0,6(0,5-0,6)
	8 weeks after Tx	0,8(0,8-1,0)	0,3(0,3-0,4)*	0,4(0,2-0,5)*	1,0(1,0-1,0)
Mean arterial pressure (mmHg)	Baseline	118(111-121)	118(111-121)	118(111-121)	118(111-121)
	4 weeks after Tx	110(104-123)	118(106-132)	141(121-148)	146(135-148)
	8 weeks after Tx	138(131-165)	143(138-150)	149(135-154)	166(153-171)

Abbreviation: Tx-transplantation, *P<0.05 compared to vehicle treated control group

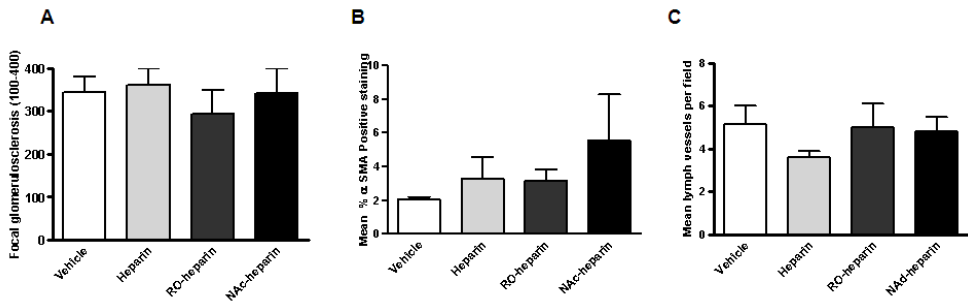


Figure 1. Heparin(oid) treatment did not affect glomerular and interstitial tissue remodeling, and lymphangiogenesis. A. glomerulosclerosis score was non-significantly reduced in the RO-heparin group. B. Mean area of interstitial myofibroblasts (positive for α -SMA showing pre-fibrotic lesions) in cortical regions. C. Mean number of podoplanin positive lymph vessels per microscopic cortical field (200x). Graphs represent mean±SE at 9 weeks.

Development of transplant vasculopathy (TV) - All the treated groups showed the formation of occlusive neointima in arteries, indicative of TV. In the arteries with a diameter <200 μ m a significant increase in lumen occlusion was found in unfractionated heparin treated group compared to the other groups ($p < 0.02$; Figure 2A-C). In the arteries with diameter ≥ 200 μ m, no differences among the groups was observed in arterial occlusion due to neointima formation (not shown). In conclusion (non-anticoagulant) heparin(oids) are not very effective in reducing CTD-associated tissue remodeling, at least not in this fully HLA-mismatched model with severe renal damage

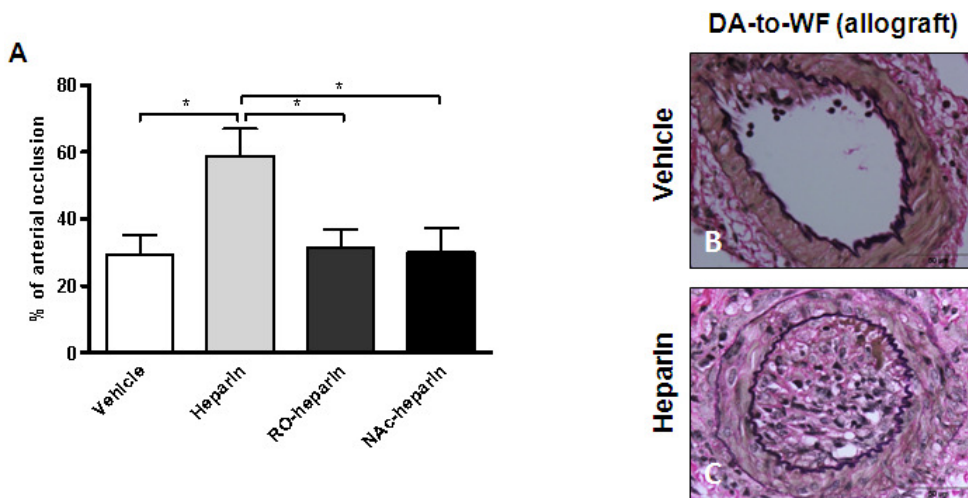


Figure 2. A. Heparin treatment showed significant increase in the arterial occlusion compared to the other treated groups. Graphs represent mean±SE at 9 weeks in arteries ≤ 200 μ m diameter. B-C. Photomicrograph showing less neointima formation in renal arteries of vehicle treated animals compared to heparin treated animals (400x magnification).

RO-heparin is effective in reducing CTD associated inflammation

Cortical CD45 staining revealed that the leukocyte influx was significantly decreased by ~50% in RO-heparin group compared to the vehicle treated group ($p=0.0175$; Figure 3A-C). In order to investigate the subtypes of the leukocytes that are reduced in RO-heparin group, we analyzed the macrophage and T-cell influx by morphometric analysis. Glomerular and tubulo-interstitial monocyte/macrophage density (ED1 positive) were analyzed separately. In the vehicle treated group, the glomerular macrophage influx was substantially lower than in the tubulo-interstitial compartment. Overall, both in glomeruli and in the interstitial areas, there were no major differences among the groups regarding the ED-1 influx(not shown). We next analyzed T-cell infiltration by CD3 staining and quantification. The data suggest a lower T-cell infiltration in the RO-heparin group compared to the other groups, however, no statistical significance was reached. We conclude that RO-heparin reduced the influx of inflammatory cells into the transplanted kidney, most likely partly T-cells (Figure 4).

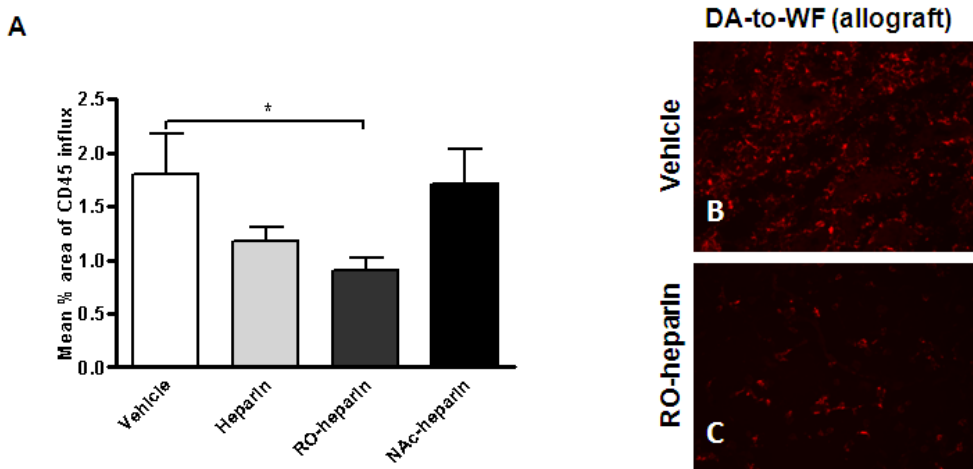


Figure 3. RO-heparin treatment significantly reduced leukocyte influx. A. Graph represents leukocyte quantification (CD45 positive area, mean \pm SE) at 9 weeks. B-C. Photomicrographs showing less leukocyte (CD45) influx in renal tissue of RO-heparin treated animals. (200x magnification)

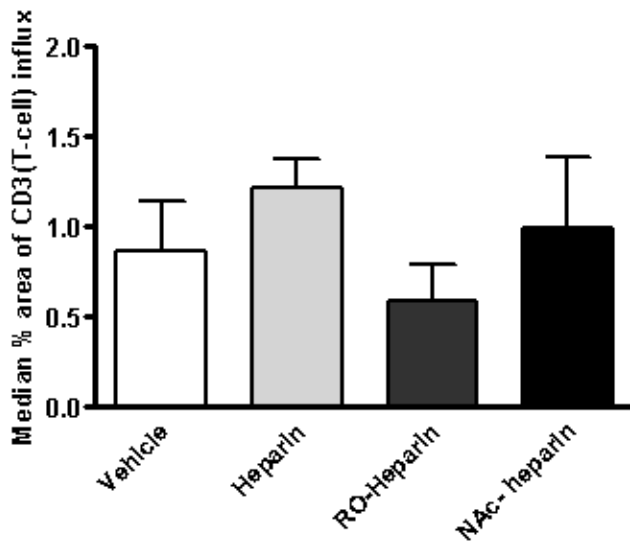


Figure 4. RO-heparin treatment non-significantly reduced the T-cell (CD3) influx. Graphs represent mean \pm SE at 9 weeks

Discussion

In this study we show that a non-anticoagulant heparinoid (RO-heparin) reduced renal inflammation, and plasma triglycerides and exerted modest reducing effects on proteinuria. However, this heparinoid is not effective in reducing kidney function, graft survival and renal scarring in experimental renal transplantation. One of the most striking findings of our study was the fact that the non-anticoagulant RO-heparin was the most active compound with respect to proteinuria, inflammation and triglycerides, even more active than regular heparin. This might be related to the opening of the ring structure of non-sulfated glucuronic acid units in heparin, which results in more flexibility of the polysaccharide chain and consequently a more efficient interaction with most heparin-binding proteins(15). This is an interesting finding, since RO-heparin lacks anti-thrombotic activity, however, is more effective in reducing proteinuria and inflammation. N-acetyl heparin on the contrary, lost one of the sulfate groups by the N-desulfation procedure, and thereby most likely reduces its binding properties to a number of heparin-binding proteins, and consequently did not display any beneficial effects in our study.

Although our study does not explain how the heparinoids exerted their effects, we propose the following mechanisms to be involved. The role of HSPGs in inflammatory leukocyte recruitment is well established (7,8) and is in particular due to the binding of HSPGs to L- and P-selectins on leukocytes and endothelial cells and the presentation and gradient formation of chemokines. Intervention by heparinoids thus will reduce endothelium – leukocyte interactions (selectin block), and reduces activation and migration of leukocytes

by disturbing chemokines. This finding is in line with a number of other studies showing the anti-inflammatory effects of heparin-related compounds(23,31). Our data furthermore suggest that T-cell recruitment is inhibited to a larger extent than monocyte influx. At present we do not have an explanation for this finding, which however might be related to interruption of certain chemokines such as RANTES (CCL5), that specifically attracts T-cells. The reduction of plasma triglycerides by regular heparin and RO-heparin is most likely explained by the release of lipoprotein lipase, which cleaves plasma triglycerides. This is a well-known and described effect of heparin (32). Due to a lower degree of sulfation, N-acetyl heparin seems not able to release lipoprotein lipase. The apparent attenuation of proteinuria development by RO-heparin coincides with the small reduction in FGS by RO-heparin. We speculate RO-heparin to interrupt glomerular growth factor signaling, resulting in less FGS and improved glomerular filtration function. We finally found that regular heparin increased neointima formation in the smaller arteries, which however was not found in both non-anticoagulant heparinoids. This suggests neointima formation in this model to be associated with reduced coagulation and/or platelet function, which however is not clear yet and requires further studies.

Our study had a number of limitations that should be taken into consideration. First of all, from histopathology (e.g. influx of T-cells) it became evident that our model in fact is a combination of CTD with transplant rejection and not a pure CTD model. Secondly, because of the full HLA mismatch between the donor and recipient there was severe damage to the transplanted kidney, resulting in a high number of dropouts in all the groups independent of treatment which seriously hampered the power of our study to find differences between the groups. We neither can exclude a certain selection bias in the surviving animals.

It remains a question why the heparin(oids) turned out to be ineffective with regard to renal function, graft survival and tissue remodeling. In other experimental models, treatment with non-anticoagulant LMWH showed prolonged skin, cardiac and renal allograft survival with beneficial outcomes (19,33-35). In addition, LMWH decreases mesangial proliferation and matrix expansion (36,37). Moreover RO-heparin have been described to inhibit FGF2 and VEGF mediated pathways and to reduce tumor growth(14). We suggest that the full HLA-mismatch of our DA to Wistar Furth model, without any immunosuppression after day 10 might explain this. The progressive tissue remodeling in our model might be simply too strong to show (partial) down modulation by heparinoids. It also could be that a number of non-heparin binding growth factors such as insulin-like growth factors, plasminogen activator inhibitor-1, and angiotensin II are involved that cannot be regulated via heparinoids. Besides to that, it is known that the half-life of unfractionated heparin(oids) as used in our study, is shorter compared to LMW heparinoids. Based on these consideration we propose a future experiment using LMW-heparinoids (including LMW-RO-heparin), in combination with the immunosuppressive agent cyclosporine A.

In conclusion, based on our data we speculate that heparin-like glycomimetics might be promising add- on therapeutic modalities next to immunosuppressants, and blood-pressure and lipid lowering medication. Future studies in experimental models and in human renal transplantation setting have to prove efficacy of this assumption.

References

1. Chapman JR, O'Connell PJ, Nankivell BJ. Chronic renal allograft dysfunction. *J Am Soc Nephrol* 2005 Oct;16(10):3015-3026.
2. Solez K, Vincenti F, Filo RS. Histopathologic findings from 2-year protocol biopsies from a U.S. multicenter kidney transplant trial comparing tacrolimus versus cyclosporine: a report of the FK506 Kidney Transplant Study Group. *Transplantation* 1998 Dec 27;66(12):1736-1740.
3. McLaren AJ, Fuggle SV, Welsh KI, Gray DW, Morris PJ. Chronic allograft failure in human renal transplantation: a multivariate risk factor analysis. *Ann Surg* 2000 Jul;232(1):98-103.
4. Solez K. Making global transplantation pathology standards truly global. *Am J Transplant* 2007 Dec;7(12):2834.
5. Solez K, Colvin RB, Racusen LC, Haas M, Sis B, Mengel M, et al. Banff 07 classification of renal allograft pathology: updates and future directions. *Am J Transplant* 2008 Apr;8(4):753-760.
6. Rienstra H, Katta K, Celie JW, van Goor H, Navis G, van den Born J, et al. Differential expression of proteoglycans in tissue remodeling and lymphangiogenesis after experimental renal transplantation in rats. *PLoS One* 2010 Feb 5;5(2):e9095.
7. Celie JW, Rutjes NW, Keuning ED, Soininen R, Heljasvaara R, Pihlajaniemi T, et al. Subendothelial heparan sulfate proteoglycans become major L-selectin and monocyte chemoattractant protein-1 ligands upon renal ischemia/reperfusion. *Am J Pathol* 2007 Jun;170(6):1865-1878.
8. Celie JW, Reijmers RM, Slot EM, Beelen RH, Spaargaren M, Ter Wee PM, et al. Tubulointerstitial heparan sulfate proteoglycan changes in human renal diseases correlate with leukocyte influx and proteinuria. *Am J Physiol Renal Physiol* 2008 Jan;294(1):F253-63.
9. Zaferani A, Vives RR, van der Pol P, Hakvoort JJ, Navis GJ, van Goor H, et al. Identification of tubular heparan sulfate as a docking platform for the alternative complement component properdin in proteinuric renal disease. *J Biol Chem* 2011 Feb 18;286(7):5359-5367.
10. Mohammadi M, Olsen SK, Goetz R. A protein canyon in the FGF-FGF receptor dimer selects from an a la carte menu of heparan sulfate motifs. *Curr Opin Struct Biol* 2005 Oct;15(5):506-516.
11. Forsten-Williams K, Chua CC, Nugent MA. The kinetics of FGF-2 binding to heparan sulfate proteoglycans and MAP kinase signaling. *J Theor Biol* 2005 Apr 21;233(4):483-499.
12. Parish CR. The role of heparan sulphate in inflammation. *Nat Rev Immunol* 2006 Sep;6(9):633-643.
13. Lindahl U, Li JP. Interactions between heparan sulfate and proteins-design and functional implications. *Int Rev Cell Mol Biol* 2009;276:105-159.
14. Casu B, Vlodavsky I, Sanderson RD. Non-anticoagulant heparins and inhibition of cancer. *Pathophysiol Haemost Thromb* 2008;36(3-4):195-203.
15. Casu B, Naggi A, Torri G. Heparin-derived heparan sulfate mimics to modulate heparan sulfate-protein interaction in inflammation and cancer. *Matrix Biol* 2010 Jul;29(6):442-452.
16. Rops AL, van den Hoven MJ, Baselmans MM, Lensen JF, Wijnhoven TJ, van den Heuvel LP, et al. Heparan sulfate domains on cultured activated glomerular endothelial cells mediate leukocyte trafficking. *Kidney Int* 2008 Jan;73(1):52-62.
17. Naggi A, Casu B, Perez M, Torri G, Cassinelli G, Penco S, et al. Modulation of the heparanase-inhibiting activity of heparin through selective desulfation, graded N-acetylation, and glycol splitting. *J Biol Chem* 2005 Apr 1;280(13):12103-12113.
18. Gao Y, Li N, Fei R, Chen Z, Zheng S, Zeng X. P-Selectin-mediated acute inflammation can be blocked by chemically modified heparin, RO-heparin. *Mol Cells* 2005 Jun 30;19(3):350-355.
19. Braun C, Schultz M, Fang L, Schaub M, Back WE, Herr D, et al. Treatment of chronic renal allograft rejection in rats with a low-molecular-weight heparin (reviparin). *Transplantation* 2001 Jul 27;72(2):209-215.
20. Gottmann U, Mueller-Falcke A, Schnuelle P, Birck R, Nickeleit V, van der Woude FJ, et al. Influence of hypersulfated and low molecular weight heparins on ischemia/reperfusion: injury and allograft rejection in rat kidneys. *Transpl Int* 2007 Jun;20(6):542-549.

21. Kusyk T, Verran D, Stewart G, Ryan B, Fisher J, Tsacalos K, et al. Increased risk of hemorrhagic complications in renal allograft recipients receiving systemic heparin early posttransplantation. *Transplant Proc* 2005 Mar;37(2):1026-1028.
22. Anderegg BA, Baillie GM, Lin A, Lazarchick J. Heparin-induced thrombocytopenia in a renal transplant recipient. *Am J Transplant* 2005 Jun;5(6):1537-1540.
23. Frank RD, Holscher T, Schabbauer G, Tencati M, Pawlinski R, Weitz JI, et al. A non-anticoagulant synthetic pentasaccharide reduces inflammation in a murine model of kidney ischemia-reperfusion injury. *Thromb Haemost* 2006 Dec;96(6):802-806.
24. Frank RD, Schabbauer G, Holscher T, Sato Y, Tencati M, Pawlinski R, et al. The synthetic pentasaccharide fondaparinux reduces coagulation, inflammation and neutrophil accumulation in kidney ischemia-reperfusion injury. *J Thromb Haemost* 2005 Mar;3(3):531-540.
25. Rienstra H, Boersema M, Onuta G, Boer MW, Zandvoort A, van Riezen M, et al. Donor and recipient origin of mesenchymal and endothelial cells in chronic renal allograft remodeling. *Am J Transplant* 2009 Mar;9(3):463-472.
26. Chen Z, Jing Y, Song B, Han Y, Chu Y. Chemically modified heparin inhibits *in vitro* L-selectin-mediated human ovarian carcinoma cell adhesion. *Int J Gynecol Cancer* 2009 May;19(4):540-546.
27. Nakamura T, Vollmar B, Winning J, Ueda M, Menger MD, Schafers HJ. Heparin and the nonanticoagulant N-acetyl heparin attenuate capillary no-reflow after normothermic ischemia of the lung. *Ann Thorac Surg* 2001 Oct;72(4):1183-8; discussion 1188-9.
28. Harenberg J, Casu B. Heparin and its derivatives - present and future. *Thromb Haemost* 2009 Nov;102(5):801-803.
29. Sunderland CA, McMaster WR, Williams AF. Purification with monoclonal antibody of a predominant leukocyte-common antigen and glycoprotein from rat thymocytes. *Eur J Immunol* 1979 Feb;9(2):155-159.
30. Waanders F, Rienstra H, Boer MW, Zandvoort A, Rozing J, Navis G, et al. Spirinolactone ameliorates transplant vasculopathy in renal chronic transplant dysfunction in rats. *Am J Physiol Renal Physiol* 2009 May;296(5):F1072-9.
31. Johnson Z, Kosco-Vilbois MH, Herren S, Cirillo R, Muzio V, Zaratin P, et al. Interference with heparin binding and oligomerization creates a novel anti-inflammatory strategy targeting the chemokine system. *J Immunol* 2004 Nov 1;173(9):5776-5785.
32. Cole RP. Heparin treatment for severe hypertriglyceridemia in diabetic ketoacidosis. *Arch Intern Med* 2009 Aug 10;169(15):1439-1441.
33. Shapira OM, Rene H, Lider O, Pfeffermann RA, Shemin RJ, Cohen IR. Prolongation of rat skin and cardiac allograft survival by low molecular weight heparin. *J Surg Res* 1999 Jul;85(1):83-87.
34. Braun C, Schultz M, Schaub M, Fang L, Back WE, Herr D, et al. Effect of treatment with low-molecular-weight heparin on chronic renal allograft rejection in rats. *Transplant Proc* 2001 Feb-Mar;33(1-2):363-365.
35. Spirig R, Gajanayake T, Korsgren O, Nilsson B, Rieben R. Low molecular weight dextran sulfate as complement inhibitor and cytoprotectant in solid organ and islet transplantation. *Mol Immunol* 2008 Oct;45(16):4084-4094.
36. Coffey AK, Karnovsky MJ. Heparin inhibits mesangial cell proliferation in habu-venom-induced glomerular injury. *Am J Pathol* 1985 Aug;120(2):248-255.
37. Floege J, Eng E, Young BA, Couser WG, Johnson RJ. Heparin suppresses mesangial cell proliferation and matrix expansion in experimental mesangioproliferative glomerulonephritis. *Kidney Int* 1993 Feb;43(2):369-380.

Chapter 5

Local Medial Microenvironment Directs Phenotypic Modulation Of Smooth Muscle Cells After Experimental Renal Transplantation

Am J Transplant. 2012 Mar 15.

doi: 10.1111/j.1600-6143.2012.04001.x.

Miriam Boersema
Kirankumar Katta
Heleen Rienstra
Grietje Molema
Tri Q. Nguyen
Roel Goldschmeding
Gerjan Navis
Jacob van den Born
Eliane. R. Popa
Jan-Luuk Hillebrands

Abstract

Smooth muscle cells (SMCs) play a key role in the pathogenesis of occlusive vascular diseases, including transplant vasculopathy. Neointimal SMCs in experimental renal transplant vasculopathy are graft-derived. We propose that neointimal SMCs in renal allografts are derived from the vascular media resulting from a transplantation-induced phenotypic switch. We examined the molecular changes in the medial microenvironment that lead to phenotypic modulation of SMCs in rat renal allograft arteries with neointimal lesions.

Dark Agouti donor kidneys were transplanted into Wistar Furth recipients and harvested at day 65. Neointimal and medial layers were isolated using laser-microdissection. Gene expression was analyzed using low-density arrays and confirmed by immunostaining. In allografts, neointimal SMCs expressed increased levels of *Tgfb1* and *Pdgfb*. In medial allograft SMCs, gene expression of *Ctgf*, *Tgfb1* and *Pdgfrb* was upregulated. Gene expression of *Klf4* was upregulated as well, while expression of *Sm22a* was downregulated. Finally, PDGF-BB-stimulated phenotypically modulated SMCs as evidenced by reduced contractile function *in vitro* which was accompanied by increased *Klf4* and *Colla1*, and reduced *α -Sma* and *Sm22a* expression.

In transplant vasculopathy, neointimal PDGF-BB induces phenotypic modulation of medial SMCs, through upregulation of KLF4 in the media to contribute to (further) expansion of the neointima.

Keywords: media, neointima, smooth muscle cell, transplantation

Abbreviations

CTD	Chronic transplant dysfunction
DA	Dark Agouti
ECM	Extracellular matrix
IEL	Internal elastic lamina
IF/TA	Interstitial fibrosis and tubular atrophy
SMA	Smooth muscle cells
MYH11	Smooth muscle myosin heavy chain 11 (MYH11)
TV	Transplant vasculopathy
WF	Wistar Furth

Introduction

Vascular remodeling comprises of structural changes of the arterial wall in response to various stimuli including shear stress, hypoxia, and immunological or mechanical injury. The structural changes of the arterial wall lead to changes in vessel size and luminal width (1). Vascular remodeling has various clinical and pathological manifestations, including transplant vasculopathy (TV), (in-stent) restenosis and spontaneous (native) atherosclerosis. Hallmark of these obliterative vascular pathologies is neointima formation resulting from both an increase in the number of cells in the subendothelial intima as well as deposition extracellular matrix (ECM) (2). Narrowing, thickening and stiffening of the vessel wall by neointima formation results in reduced blood flow and subsequent ischemia in downstream tissues.

TV in renal allografts is a histopathologic feature observed in addition to transplant glomerulopathy, interstitial fibrosis and tubular atrophy (IF/TA) in patients with chronic renal transplant dysfunction (CTD). Development of CTD is a major cause of renal allograft loss, only second to patient death with a functioning graft (3). Development of TV in transplanted kidneys presumably contributes to graft deterioration. In support of this, we recently demonstrated that TV severity is indeed associated with premature graft loss in a renal transplant model in rats (4). As yet, no adequate preventive or curative therapies for TV are available.

Neointima formation in TV is the accumulation of α -smooth muscle actin (α -SMA)-positive smooth muscle cells (SMCs) between the endothelial lining and the internal elastic lamina (IEL), forming an occlusive neointima (5). Neointimal SMCs secrete ECM leading to arterial stiffness, luminal stenosis and, eventually, ischemic graft failure. The overall concept of neointima formation in general and in TV in particular, is that local inflammatory responses of the vessel wall trigger SMC migration and proliferation (6). Until a decade ago, the general dogma was that neointimal SMCs in TV are graft-derived as proposed in the response-to-injury hypothesis for atherosclerosis (7). However, this response-to-injury hypothesis has been challenged as various research groups, including our own, showed recipient-origin of neointimal SMCs in TV in predominantly experimental arterial-segment and cardiac transplant models in rodents (5,8,9). Until recently the anatomical origin of neointimal SMCs in TV in renal allografts was largely unknown. Knowing the anatomical origin of neointimal SMCs is key to the development of new therapeutic modalities to attenuate TV development that should lead to prolonged graft survival. We therefore determined host vs. graft origin of neointimal SMCs in both an experimental renal transplant model in rats as well as in human renal allografts with TV. In both experimental renal transplantation in rats as well as in human renal transplantectomy samples neointimal SMCs turned out to be of graft origin with only a relatively small proportion of host-derived SMCs being detected in human renal allografts (4),(10). Graft origin of neointimal SMCs fits with the response-to-injury hypothesis which states that

medial SMCs migrate across the internal elastic lamina in response to arterial injury (7). However, formal proof for medial origin (rather than recruitment of adventitial or interstitial (myo)fibroblasts or SMC precursor cells) still needs to be delivered. Based on our previous results on graft origin of neointimal SMCs in renal allografts we hypothesize that these cells are indeed derived from the vascular media. Due to the lack of markers specific for medial-derived SMCs, it is however not possible to track medial SMCs during neointima development using lineage tracing.

Medial SMCs can only contribute to neointima formation after undergoing a phenotypic switch from a contractile to a synthetic state (11). Synthetic SMCs have migratory and proliferative capacities and secrete ECM molecules. We hypothesize that the combination of ischemia/reperfusion injury and ongoing alloreactivity towards the allograft induces medial SMCs to switch to synthetic SMCs. Synthetic SMCs can migrate to the subendothelial space which will eventually lead to neointima formation. To test this hypothesis, we investigated the spatiotemporal expression of factors in the neointimal and medial microenvironment known to influence phenotypic modulation of SMCs. Furthermore, we investigated genes indicative of phenotypic modulation of medial SMCs in rat renal allografts with TV as well as in isografts and non-transplanted control kidneys without TV. To not disturb the location nor the status of the cellular content, neointimal and medial layers were isolated using laser dissection microscopy after which gene expression was analyzed in these different compartments with a low density array. Results were confirmed at protein level in tissue sections and functionally analyzed in an *in vitro* SMC function assay.

Methods

Kidney Transplantation and Experimental Groups

Animals were handled in compliance with the Principles of Laboratory Animal Care (NIH Publication No. 86-23, revised 1985), the University of Groningen guidelines for animal husbandry (University of Groningen, the Netherlands), and the Dutch Law on Experimental Animal Care.

Female Dark Agouti (DA) kidneys were orthotopically transplanted into male DA or Wistar Furth (WF) recipients as described previously (4). The following experimental groups were included: control (non-transplanted) DA kidneys (n = 5), DA-to-DA isografts (n = 5), and DA-to-WF allografts (n = 5). Isograft recipients were sacrificed at day 81 (range 70–84 days) and allograft recipients at day 65 (range 54–84 days) after transplantation.

Laser Dissection Microscopy and Gene Expression Analysis

The neointima and media were separately laser microdissected from nine serial kidney sections per animal. Per renal allograft, an average of 75 (range 25 – 117) arteries was dissected (Supplemental Table 1). An average of 46 (range 37 – 52) arteries was dissected from renal isografts and an average of 69 (range 47 – 100) was dissected from arteries of non-transplanted kidneys (Supplemental Table 1).

Total RNA was isolated from microdissected vascular structures and gene expression of genes known to influence fibrosis and SMC phenotype were analyzed with a custom made micro fluidic card-based low density array (Supplemental Table 2). Relative mRNA levels were calculated as $2^{-\Delta CT}$, in which ΔCT is $CT_{\text{gene of interest}} - CT_{\beta\text{-actin}}$. CT values that were below detection level were set at 50.

For gene expression analysis of cultured rat aortic SMCs, total RNA was isolated after 24 hours of stimulation with PDGF-BB or TGF- β 1 (PreproTech EC LTD. London, UK). Relative mRNA levels were normalized against β -actin expression as described above.

Immunohistochemistry

Sections were stained for Masson's trichrome, Verhoeff-van Gieson, TGF- β 1, CTGF, PDGF-B and smooth muscle myosin heavy chain 11 (MYH11). The degree TV (i.e., obliteration in arteries) was measured in all arteries with a clearly visible IEL (Verhoeff-van Gieson staining) within a section.

Collagen gel contraction assay

Gel contraction assay of 3D collagen gels were performed using a solution of rat tail collagen I (BD Bioscience, Breda, the Netherlands). Aliquots of 50 μ L (containing 50,000 rat aortic SMCs and 0.25 mg Collagen type I) were added to a 96 wells plate that had been preincubated with 0.1% BSA. After solidification, collagen gels were further cultured with or without additional PDGF-BB or TGF- β 1 (PreproTech EC LTD. London, UK). Collagen gels were imaged using a common flatbed-scanner (ScanJet 5370C; HP, CA, USA) and gel contraction was measured after 24 hours (12).

Statistics

Data are expressed as mean \pm standard error of the mean (SEM). Differences between contralateral kidneys, isografts and allografts were analyzed using a one-way ANOVA with Tukey's posthoc test. Differences between unstimulated SMCs and TGF- β 1- or PDGF-BB-stimulated SMCs were analyzed using a one-way ANOVA with Dunnett's posthoc test. $p < 0.05$ was considered statistically significant. Statistical analysis were performed using SPSS (version 16.0.2; IBM Nederland B.V., Nieuwegein, the Netherlands).

Detailed methods can be found as online Supporting information.

Results

Chronic transplant dysfunction after experimental renal transplantation

We first confirmed the development of CTD in allograft recipients by renal function analysis and histological evaluation of the graft.

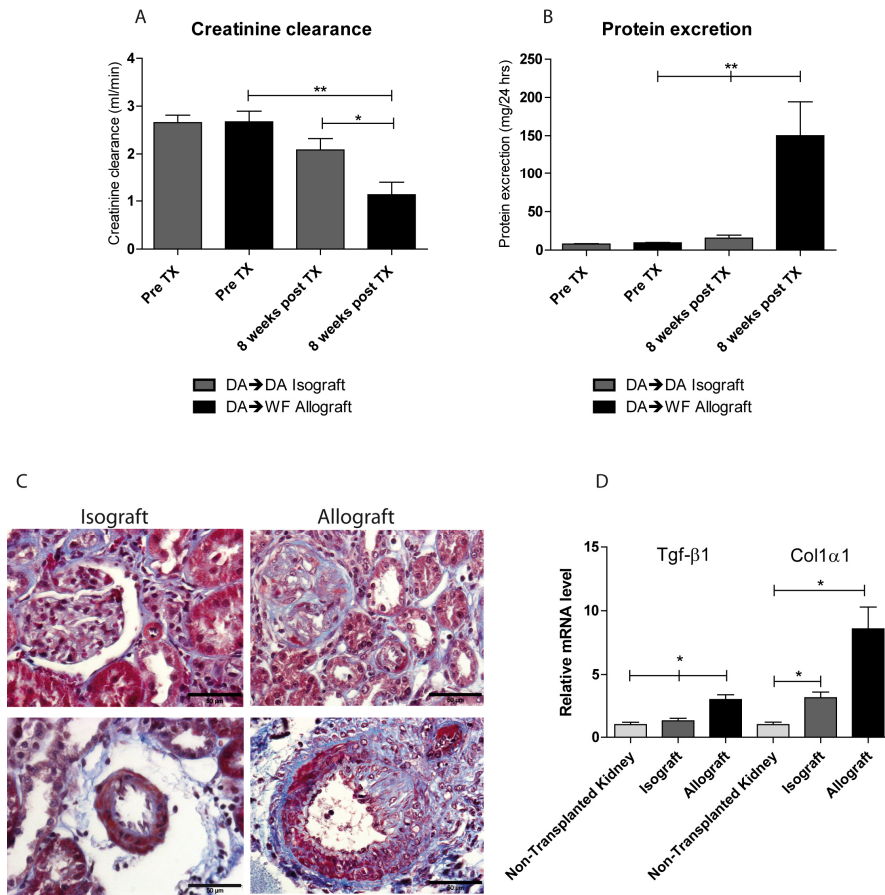


Figure 1. CTD development after renal allograft transplantation. (A) Creatinine clearance in allografts (n=3) and isografts (n=5) before and 8 weeks after transplantation. (B) Protein excretion in allografts (n=3) and isografts (n=5) before and 8 weeks after transplantation. (C) Renal allografts developed IF, glomerulosclerosis and TV (Masson's trichrome staining [collagen: blue]). Scale bar represents 50 μ m. (D) Gene expression analysis of fibrosis-related genes *Tgfβ1* and *Col1α1* in total kidney samples from renal allografts, isografts and non-transplanted control kidneys (n=5). Data are presented as mean \pm SEM. * $p < 0.05$, ** $p < 0.01$. Abbreviation: TX; transplantation

Creatinine clearance was similar in allograft and isograft recipients before transplantation (2.7 mL/min [2.1–3.1 mL/min] (mean [range]) vs. 2.7 mL/min [2.3–2.8 mL/min], respectively) (Figure 1A). Eight weeks after transplantation, creatinine clearance in isograft recipients did not differ from pre-transplantation levels (2.1 mL/min [1.4–2.8 mL/min]), whereas allograft recipients had significantly lower creatinine clearance rates compared with pre-transplantation levels and isograft recipients 8 weeks after transplantation (1.1 mL/min [0.9–1.6 mL/min]) (Figure 1A). In addition, allograft but not isograft recipients developed proteinuria as determined 8 weeks after transplantation (150 mg/day [90–237 mg/day] vs. 18 mg/day [9–26 mg/day], respectively) (Figure 1B).

Functional deterioration observed in allografts was accompanied by histopathological changes indicative of CTD, including interstitial fibrosis, glomerulosclerosis and TV (Figure 1C). Isografts developed some interstitial fibrosis as well, however, to a significantly lesser extent than allografts (Figure 1C), corroborating our previous observations (4). These histological changes were associated with significantly upregulated mRNA expression levels of fibrosis-related genes *Tgf β 1* and *Colla1* in renal allografts compared to isografts and non-transplanted contralateral kidneys (Figure 1D).

Neointimal Tgf- β 1, Ctgf and Pdgfb mRNA expression

TV in rat renal allografts developed neointima formation (Figure 2A). Luminal occlusion of measured arteries in renal allografts was 37% [range 7–88%], whereas luminal occlusion in isografts and non-transplanted kidneys was 15% [1–28%] and 6% [0–11%], respectively. Luminal occlusion detected in non-transplanted control kidneys was comprised of endothelial cells covering the IEL and was considered as the basal surface intima (not shown). The neointima consisted predominantly of SMCs, as shown by expression of smooth muscle myosin heavy chain (MYH11, (13)) (Figure 2C). Staining for CD45 revealed only a few infiltrating leukocytes in the neointima (data not shown).

Since we previously showed donor origin of neointimal SMCs in this model we hypothesized that neointimal SMCs are derived from the media by migration and proliferation. To test whether the microenvironment within the arterial neointima and media in allografts support this hypothesis, we determined gene expression levels in the vascular media and neointima using a low density array. Genes included in this array were associated with SMC phenotype, growth factors and their receptors and ECM molecules as summarized in Supplemental table 2. Medial and neointimal tissues were isolated using laser microdissection (Figure 2D) and processed for gene expression analysis. Per allograft, a mean of 74 (range 25–117) neointimae were microdissected (Table 1). Medial tissue from a non-transplanted kidney (i.e., control medial tissue) contained fully differentiated contractile SMCs and was used for comparison. When compared with control medial tissue, SMCs in the allograft neointima displayed increased *Tgf- β 1* (~7 fold) and *Ctgf* (~2 fold)

gene expression levels (Figure 2E). Both genes are known for their profibrotic actions (reviewed in (14)) which would stimulate SMC accumulation in the neointima.

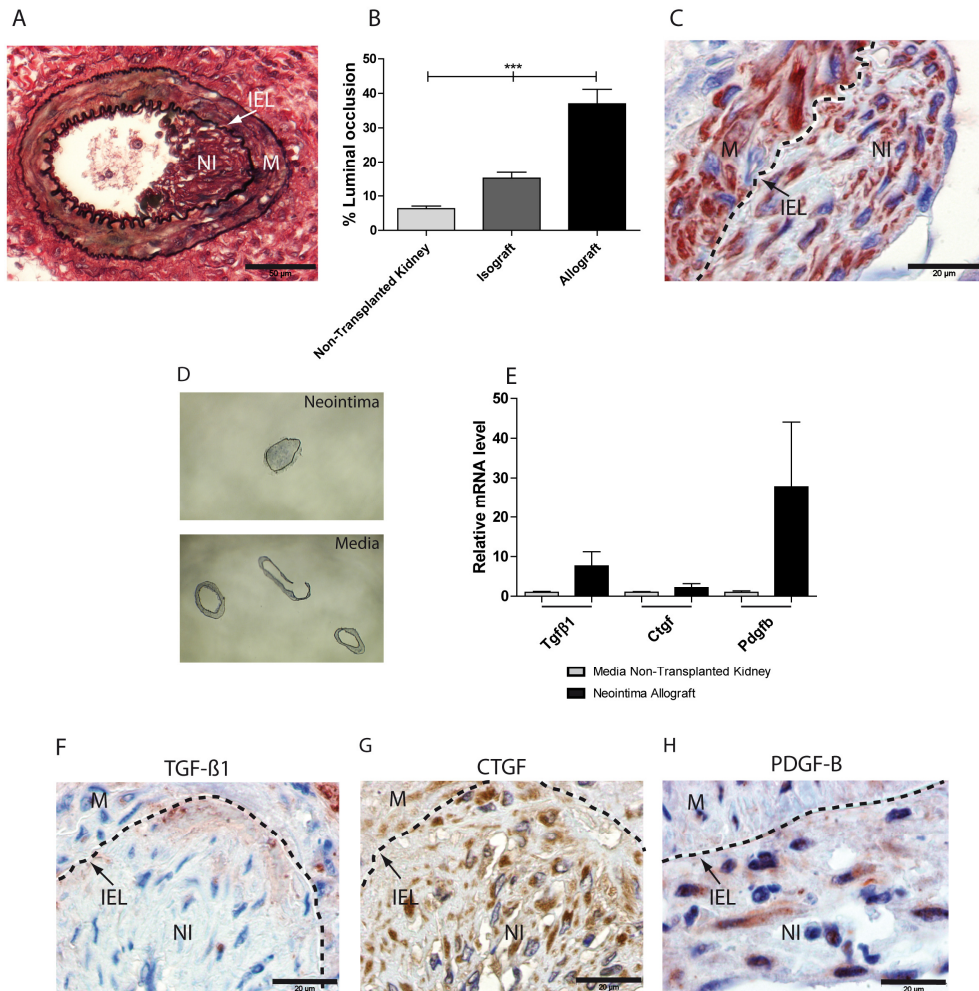


Figure 2. Characteristics of transplant vasculopathy in renal allografts. (A) Artery with neointima in a renal allograft (Verhoeff staining [elastin: black; collagen: red]). Scale bar represents 50 μ m. (B) Luminal obliteration due to neointima formation in renal allografts, isografts and non-transplanted control kidneys. (C) Smooth muscle cells (Myh11, red staining) in the neointima of renal allografts. Scale bar represents 20 μ m. (D) Laser microdissected neointima (upper photo) and medial (lower photo) layers. (E) Gene expression of *Tgfbf1*, *Ctgf* and *Pdgfb* in laser microdissected neointimal tissue normalized to their expression in medial tissue of non-transplanted control kidneys. Detection of (F) Tgf- β 1, (G) CTGF and (H) PDGF-B protein in the neointima. Scale bar represents 20 μ m. IEL = internal elastic lamina; M = media; NI = neointima. Dotted line indicates the IEL. Data are presented as mean \pm SEM (n=5). ***p < 0.001

Furthermore, expression of *Pdgfb* was ~27 fold upregulated in the neointima compared with control medial tissue (Figure 2E), suggesting that the neointimal microenvironment is

capable of attracting SMCs to the neointima. PDGF-BB is known to act as a mitogen and chemoattractant for SMCs in intimal thickening (15). Due to a relatively high variation in neointimal gene expression levels between the different allografts, differences in gene expression levels between the neointima and control media were not statistically significant although marked differences were observed. Presence of *Tgfb1*, *Ctgf* and *Pdgfb* mRNA transcripts in the neointima was confirmed at the protein level by immunohistochemistry (Figure 2F, 2G and 2H). TGF- β 1 protein was mainly associated with neointimal SMCs close to the internal elastica lamina (Figure 2F), whereas CTGF and PDGF-B protein was distributed across the entire neointima (Figure 2G and 2H).

Increased medial Tgf- β 1, Ctgf and Pdgfrb mRNA expression

In a healthy artery, medial SMCs are fully differentiated and have a contractile phenotype. In contrast, synthetic SMCs have a decreased expression of contractile proteins and show a high degree of proliferation and the ability to migrate, which can potentially lead to neointima formation (11). Since we found increased expression of profibrotic growth factors in the neointima (Figure 2E-G), we subsequently investigated whether the medial microenvironment is characterized by increased expression of profibrotic growth factors and growth factors known to induce phenotypic modulation of SMCs.

To this end we analyzed gene expression of *Tgfb1*, *Ctgf* and *Pdgfb* in laser-microdissected medial tissue from iso- and allografts. Gene expression of *Tgfb1* and *Ctgf* was increased in medial SMCs in allografts compared to isografts and non-transplanted control kidneys (~7 fold ($p < 0.01$) and ~8 fold ($p < 0.05$), respectively) (Figure 3A and 3B). No differential expression of *Pdgfb* was observed in medial tissue from all groups (Figure 3C). However, gene expression of *Pdgfrb* was ~4 fold ($p < 0.05$) increased in the media of allografts when compared to isografts and non-transplanted control kidneys (Figure 3D). The increased mRNA expression of *Tgfb1* and *Ctgf* in the media of allografts was confirmed at the protein level (Figure 3E and 3F, respectively). TGF- β 1 and CTGF protein expression were not detected in the media of non-transplanted kidneys and isografts (upper and middle panels, respectively in Figure 3E and 3F). In allografts, TGF- β 1 expression was associated with SMCs at sites in the media adjacent to neointima formation. Protein expression of PDGF-B was similar in the media of allografts, isografts and non-transplanted control kidneys (Figure 3H).

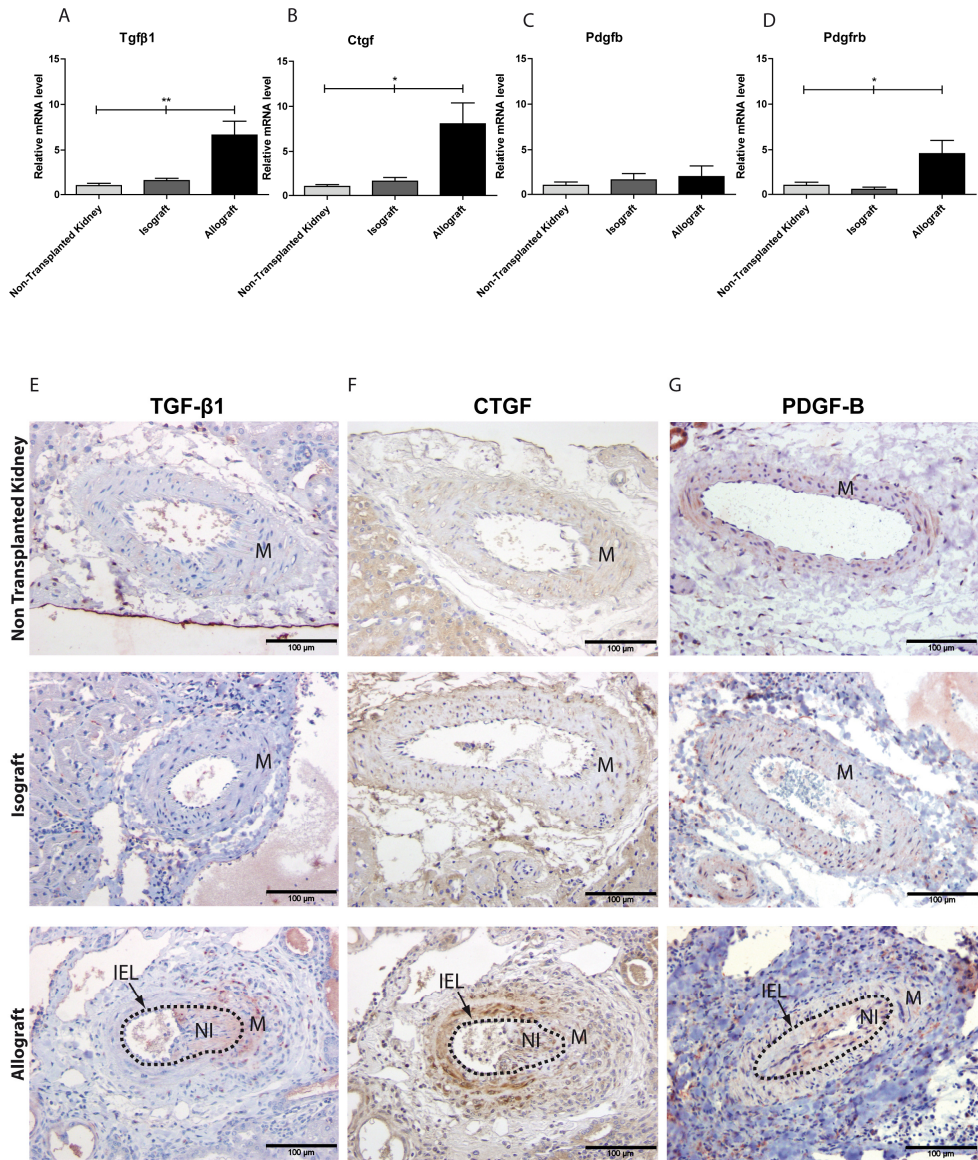


Figure 3. Microenvironment of laser microdissected medial tissues. The medial microenvironment was assessed by low-density arrays in laser microdissected media from allografts, isografts and non-transplanted control kidneys. (A-D) Gene expression of (A) *Tgfb1*, (B) *Ctgf*, (C) *Pdgfb* and (D) *Pdgfrb* in laser-dissected medial tissue of allografts and isografts normalized to non-transplanted control medial tissue. (E-G) Protein expression of (E) TGF-β1, (F) CTGF and (G) PDGF B in arteries from a non-transplanted control kidney, an isograft and an allograft. Scale bar represents 100 μm. IEL = internal elastic lamina; M = media; NI = neointima. Dotted line indicates the IEL. Data are presented as mean ± SEM (n=5). *p < 0.05, **p < 0.01

Allograft medial SMCs are phenotypically modulated

Next, we investigated whether medial SMCs indeed switch to a synthetic phenotype after allogeneic transplantation. In non-transplanted donor-type (DA) kidneys, medial SMCs had a relatively high gene expression of *Sm22 α* (Figure 4A). Since the expression of *Sm22 α* is required for modulation of vessel contractility (16), this marker is indicative of a contractile SMC phenotype. In medial SMCs from isografts, *Sm22 α* gene expression was reduced (~1.5 fold) but not significantly different compared with medial tissue from non-transplanted control kidneys (Figure 4A). When compared to medial SMCs from non-transplanted control kidneys, expression of *Sm22 α* was significantly reduced in allograft medial SMCs (~3 fold, $p < 0.001$) (Figure 4A). In line with the downregulation of *Sm22 α* expression in the allograft media, *Klf4*, which is a transcription factor known to downregulate mRNA transcription of SMC genes such as *SM22 α* (17), was significantly increased (~8 fold, $p < 0.05$) in allograft medial SMCs compared to medial SMCs from isografts and non-transplanted kidneys (Figure 4B). We also investigated the expression of myocardin, a transcriptional co-activator for serum response factor (SRF), and SRF which regulate the expression of SMC differentiation genes (18). Gene expression of *Srf* and *Myocardin* was not altered in allograft medial SMCs compared to medial SMCs in isografts and non-transplanted control kidneys (Figure 4C and 4D). A hallmark of synthetic SMCs is the production of extracellular matrix components. In allograft medial SMCs the expression of the ECM molecules *Colla1* and *Col4a1* was significantly increased (~8 fold and ~18 fold, respectively, both $p < 0.05$) compared with medial SMCs in isografts and non-transplanted control kidneys (Figure 4E and 4F). The question remains what the source is of PDGF-BB when there is no neointima formed yet. Therefore, a staining was performed for PDGF-B on isografts and allografts harvested 16 days after transplantation. PDGF-B protein was found in the arterial media of allografts whereas the arterial media of isografts only showed relatively low expression of PDGF-B protein (Supplemental Figure S1).

PDGF-BB-induced synthetic rat aortic SMCs display reduced contractility *in vitro*

To investigate whether synthetic SMCs display less contractility *in vitro*, we performed a collagen type 1 gel contraction assay. To induce phenotypic modulation, SMCs were stimulated with PDGF-BB and TGF- β 1, growth factors of which the expression was increased within the neointima (Figure 3E). Rat aortic SMCs were prestimulated with PDGF-BB (20 ng/mL or 60 ng/mL) or TGF- β 1 (5 ng/mL or 15 ng/mL) for 24 hours to induce phenotypic modulation followed by subsequent culture in a collagen gel allowing contractile function measurements.

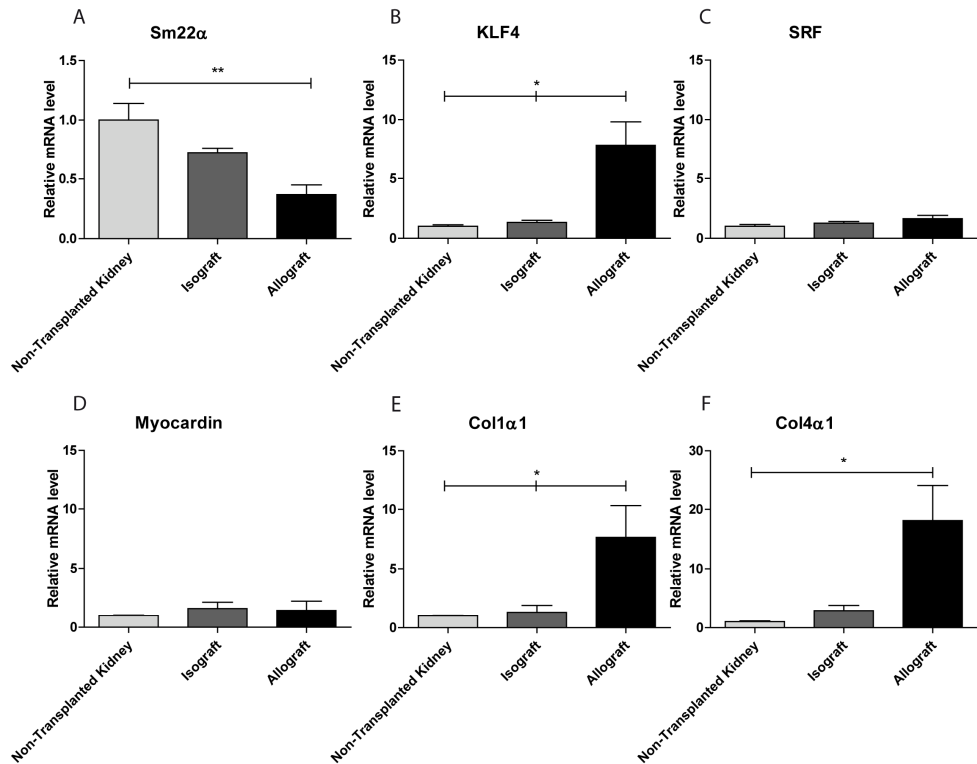


Figure 4. Allograft medial SMCs are phenotypically modulated. Medial SMCs were characterized by low-density arrays in laser-dissected medial tissue from allografts, isografts and non-transplanted control kidneys. (A-F) Gene expression of (A) *Sm22α*, (B) *Klf4*, (C) *Srf*, (D) *Myocardin*, (E) *Col1α1* and (F) *Col4α1* in laser-dissected media of allografts and isografts normalized to laser-dissected non-transplanted control kidneys. Data are presented as mean \pm SEM (n=5). * $p < 0.05$, ** $p < 0.01$

After one hour of stimulation with PDGF-BB (both 20 and 60 ng/mL), expression of *Klf4* was increased \sim 2-3 fold ($p < 0.001$) compared with unstimulated and TGF- β 1-stimulated SMCs (Figure 5A). Stimulation of SMCs with TGF- β 1 did not upregulate gene expression of *Klf4* (Figure 5A). Stimulation of SMCs for 1 hour with either PDGF-BB or TGF- β 1 did not affect gene expression levels of *Srf* and *Myocardin* (Figure 5B and 5C). After 24 hours of stimulation with PDGF-BB, a significant decrease in gene expression of α -*Sma* and *Sm22α* was detected compared with unstimulated and TGF- β 1-stimulated SMCs (Figure 5D and 5E). Stimulation with 60 ng/mL PDGF-BB resulted in a \sim 2 fold ($p < 0.001$) decrease in α -*Sma* gene expression compared with unstimulated and TGF- β 1-stimulated SMCs. Stimulation with 20 ng/mL PDGF-BB resulted in a \sim 1.5 fold decrease ($p < 0.01$) in *Sm22α* gene expression, which was further reduced (\sim 2 fold ($p < 0.001$) following stimulation with 60 ng/mL PDGF-BB. Gene expression of α -*Sma* and *Sm22α* after stimulation with TGF- β 1 (5 ng/mL and 15 ng/mL) was similar to unstimulated SMCs. Furthermore, stimulation of

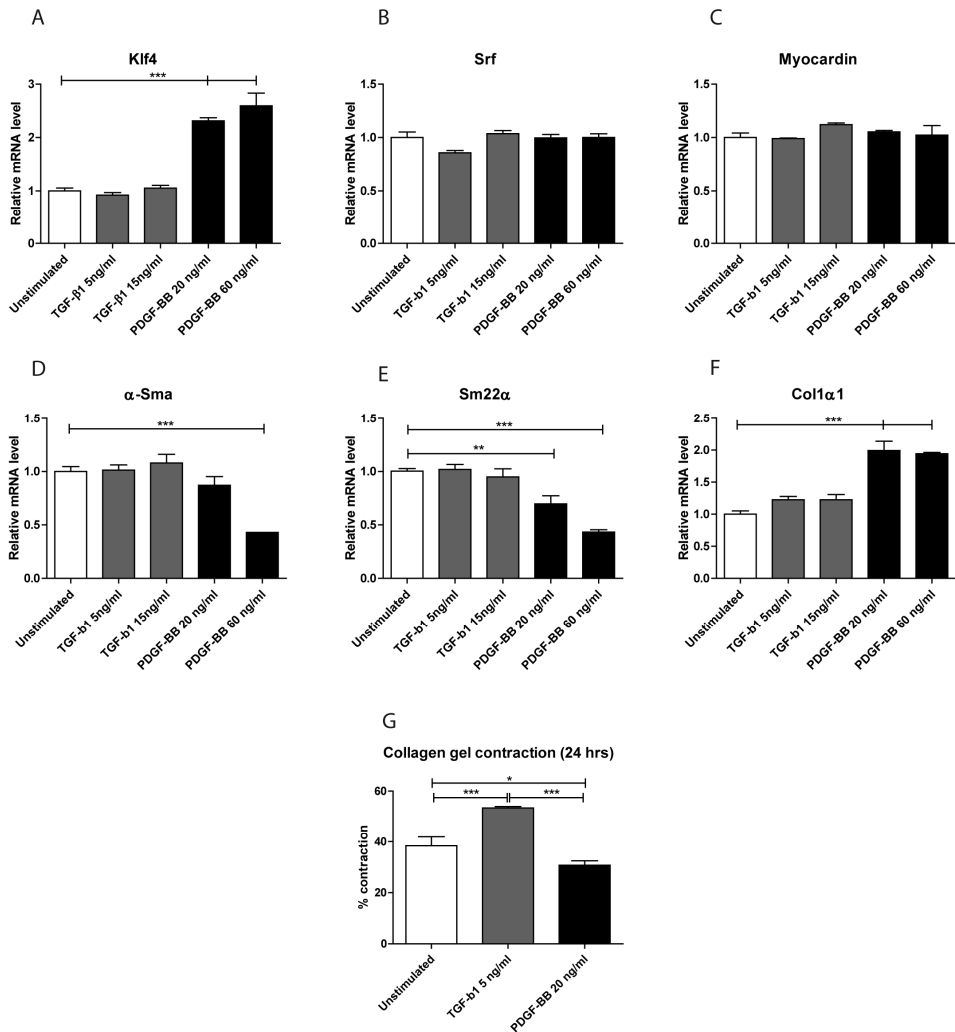


Figure 5. PDGF-BB-induced phenotypically modulated rat aortic SMCs display reduced contractility *in vitro*. Rat aortic SMCs were stimulated with TGFβ1 and PDGF-BB. Unstimulated SMCs were used as control. (A-C) Gene expression of (A) *Klf4*, (B) *Srf* and (C) *Myocardin* after stimulation for 1 hour with TGF-β1 (5 ng/mL or 15 ng/mL) or PDGF-BB (20 ng/mL or 60 ng/mL), normalized to unstimulated SMCs. (D-F) Gene expression of (D) *α-Sma*, (E) *Sm22α* and (F) *Col1α1* after stimulation for 24 hours with TGF-β1 (5 ng/mL or 15 ng/mL) or PDGF-BB (20 ng/mL or 60 ng/mL), normalized to unstimulated SMCs. To investigate functional consequences of phenotypic modulation of SMCs, rat aortic SMCs were stimulated with PDGF-BB (20 ng/mL) after which SMCs and collagen I gels were admixed. (G) Collagen I gel contraction assay with unstimulated SMCs or SMCs prestimulated with PDGF-BB (20 ng/ml) or TGF-β1 (5 ng/mL). SMCs were allowed to contract for 24 hours in the presence of TGF-β1 or PDGF-BB. Data are presented as mean ± SEM (n=3). *p < 0.05, **p < 0.01, ***p < 0.001

SMCs with PDGF-BB (both concentrations) led to increased gene expression of *Col1α1* (~2 fold, p<0.001), whereas stimulation with TGF-β1 did not have an effect (Figure 5F).

After stimulation for 24 hours, SMCs and collagen type 1 gels were admixed and cultured for an additional 24 hours in the presence of PDGF-BB (20 ng/mL) or TGF- β 1 (5 ng/mL). Reduction of collagen gel size by contraction of unstimulated SMCs was $38\pm 4\%$ (Figure 5G). Contraction of collagen gels by SMCs prestimulated with PDGF-BB was $30\pm 2\%$, which was significantly less compared to unstimulated SMCs ($p < 0.05$) (Figure 5G). SMCs prestimulated with TGF- β 1 were able to contract the collagen gels by $53\pm 1\%$ (Figure 5G), which was significantly more compared to either unstimulated or PDGF-BB-stimulated SMCs ($p < 0.001$).

Discussion

Neointima formation plays an important role in the pathogenesis of TV, restenosis and atherosclerosis. Neointima formation is the luminal narrowing of arteries by SMC accumulation which leads to downstream ischemic injury. For the development of new treatment modalities to attenuate TV, it is important to know the anatomical origin of neointimal SMCs and the molecular mechanisms that lead to the formation of TV. We recently showed in a rat kidney transplantation model that all neointimal SMCs were of graft origin (4). The results of the present study indicate that medial SMCs are phenotypically modulated during neointima formation after rat renal transplantation, and are the most likely source for neointimal SMCs in TV.

According to the response-to-injury hypothesis (7), medial SMCs migrate to the subendothelial intimal space in response to transplantation-induced vascular injury, culminating in the formation of an occlusive neointima. Due to the lack of markers specific for differentiated medial SMCs, it is not (yet) feasible to investigate if medial SMCs are truly the anatomical origin of neointimal cells using lineage tracing. Medial SMCs can only contribute to neointima formation after a phenotypic switch from a contractile to a synthetic phenotype which is induced by growth factors and cytokines produced in response to vascular injury (11). To investigate the neointimal microenvironment and presence of factors indicative of medial phenotypic modulation of SMCs after allogeneic kidney transplantation, we analyzed the gene expression profile in laser microdissected neointimal and medial tissue. Within the allograft neointima we observed enhanced gene expression of *Pdgfb* when compared with the normal (non-transplanted) vascular media. Enhanced expression of *Pdgfb* in the neointima was accompanied by increased expression of *Pdgfrb* in the allograft media. This raises the question what the source is of PDGF-BB when a neointima has not yet been formed. Protein expression analysis of PDGF-B in arteries without a neointima 16 days after transplantation showed the presence of PDGF-B in the media of allografts. This suggests that injury to medial SMCs shortly after transplantation induces the expression of endogenous PDGF-B which might contribute to initiation of SMC phenotypic modulation. PDGF-BB is well documented to act as a potent mitogen and chemoattractant for SMCs, leading to intimal thickening (19,20). PDGF-BB is also a

known mediator of SMC phenotypic modulation (21). Our observations support a role of PDGF-BB in phenotype switching of medial SMCs after allogeneic transplantation resulting in subsequent chemoattraction to the developing neointima.

Phenotypically modulated SMCs are characterized by a decreased expression of SMC-specific proteins and show a high degree of proliferation and the ability to migrate. We found reduced expression of the SMC-specific gene *Sm22 α* and increased expression of ECM molecules in medial SMCs from arteries with a neointima. Consistent with the downregulation of *Sm22 α* , *Klf4*, a transcription factor known to downregulate mRNA transcription of SMC genes, was increased in allograft medial SMCs. To study whether this *in vivo* observation might be PDGF-BB driven, as PDGF-BB was highly expressed in the developing neointima, *in vitro* experiments using rat SMCs were performed. PDGF-BB indeed reduced the expression of *Sm22 α* and *α -Sma* which was accompanied by increased *Klf4* and *Colla1* expression indicating phenotypic modulation of SMCs. Stimulation with TGF- β 1 did not induce phenotypic modulation of SMCs. KLF4 can repress myocardin-induced activation of SMC genes by selectively decreasing binding of SRF to DNA within intact chromatin (22). It is well established that virtually all SMC differentiation genes characterized to date are SRF/myocardin-dependent (23). Our observations are in line with data reported by Yu et al (24) who showed that stimulation of SMCs with PDGF-BB resulted in a downregulation of *Sm22 α* expression which was mediated via KLF4. Also KLF5 has been suggested to have a role in phenotype modulation of SMCs. However, we did not find any differences in *Klf5* expression between the different experimental groups analyzed (data not shown). We thus demonstrate for the first time a potential role for KLF4 in phenotype switching of medial SMCs after transplantation-related injury.

To further study whether PDGF-BB induced phenotypic modulation of SMCs resulted in reduced contractile function, *in vitro* collagen 1 contraction assays with rat aortic SMCs were performed. SMCs stimulated with PDGF-BB showed indeed impaired contractile function when compared with unstimulated SMCs, whereas stimulation with TGF- β 1 enhanced contractile function. The stimulating effect of TGF- β 1 on SMC contractility is probably unrelated to SMC phenotype as TGF- β 1 is shown to induce activation of Rho-GTPase and subsequent contraction of SMCs without interfering with the phenotype of SMCs (25,26).

This is the first study showing an upregulation of *Klf4* and a downregulation of *Sm22 α* in medial SMCs after renal transplantation thereby indicating phenotypic modulation of medial SMCs during neointima formation. One of the questions that can be raised is at what time-point after allogeneic transplantation phenotypic modulation SMC is initiated. This knowledge will provide valuable information required for the design of interventional strategies to attenuate neointima formation using phenotypic modulation of SMC as a target. In addition, we need to know whether phenotypic modulation of medial SMCs *in vivo* is associated with the enhanced proliferation rather than migration or vice versa. To address this issue Ki67 stainings were performed, revealing only few proliferating

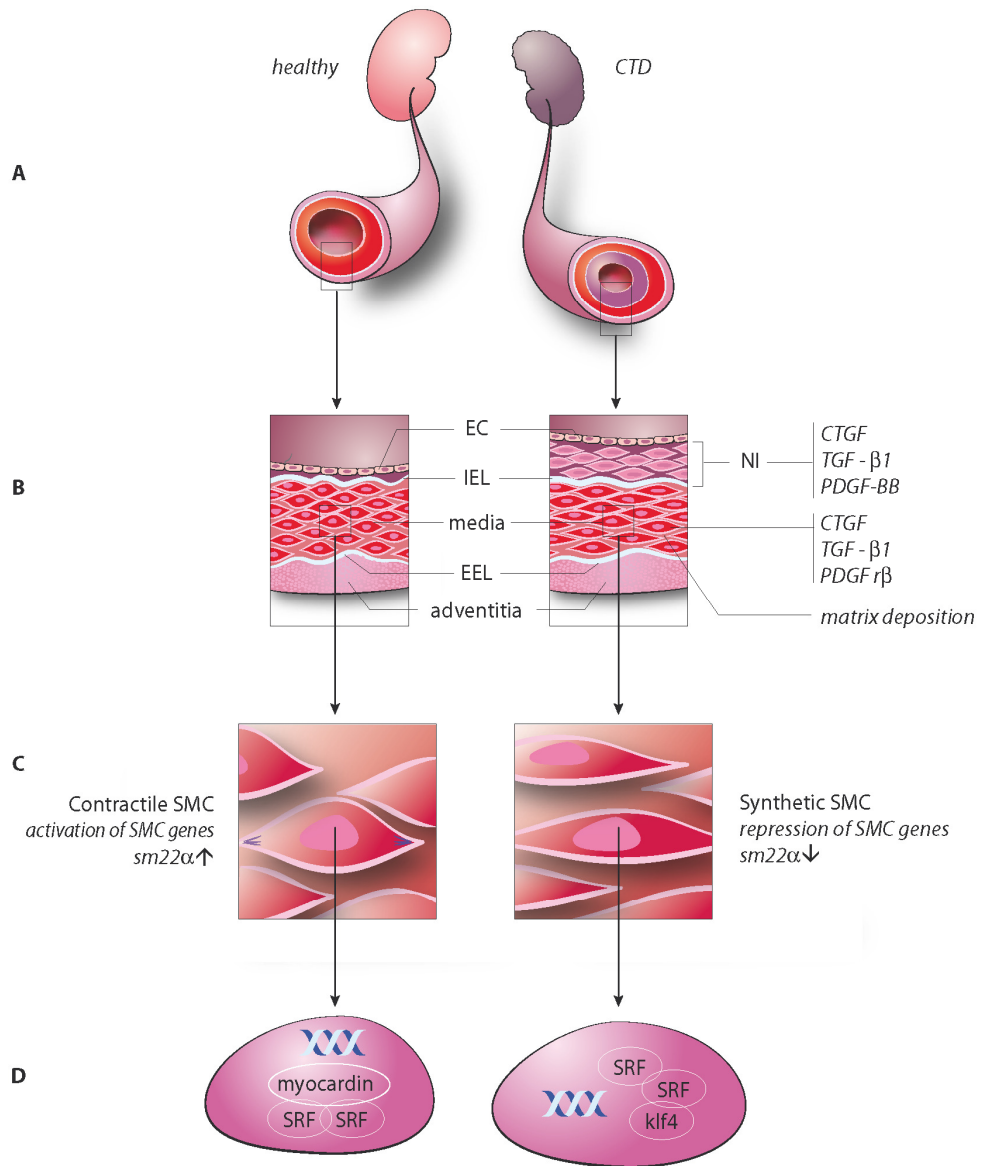


Figure 6. Scheme illustrating the molecular mechanisms of NI formation after renal transplantation. (A) One of the histopathologic features of CTD after renal transplantation is the development of TV. (B) Luminal narrowing of TV by neointima formation is the result of SMC accumulation between the endothelial cells and the IEL. Profibrotic growth factors CTGF and TGF- β 1 stimulate matrix production and are found in the neointima and media of arteries with TV. PDGF-BB is present in the neointima and may act as a chemoattractant for medial SMCs that express PDGFr β . (C) Medial SMCs modulate their phenotype after transplantation-related injury and switch from a contractile to a synthetic phenotype, characterized by a lower expression of SMC genes. (D) In synthetic SMCs, KLF4 abrogates myocardin-induced expression of SMC genes such as Sm22 α .

neointimal and medial SMCs 12 weeks after transplantation (data not shown). Neointima formation after transplantation-related injury seems to be more dependent on migration than enhanced proliferation of synthetic SMCs. The pathways involved in increasing *Klf4* expression in our model needs to be determined but we propose an important role for PDGF-BB-induced signaling on medial SMCs. miRNAs might be involved as well as it has been shown that specific miRNAs (in particular miR-145) influence SMC phenotype by targeting *KLF4* (27),(28). Local perfusion with miR-145 was indeed shown to reduce neointima formation after balloon injury (29). The potential role of miR-145 in the development of TV needs to be determined.

Based on the data described in this study we propose the following cascade of events leading to the development of TV in renal allografts (illustrated in Figure 6). Medial SMCs in renal allografts have increased expression of growth factors leading to ECM deposition and subsequently fibrosis. Furthermore, medial SMCs modulate their phenotype after transplantation-related injury and switch from a contractile to a synthetic phenotype, which is characterized by a reduced *Sm22 α* and increased *KLF4* and ECM expression. PDGF-BB, which is expressed in the developing neointima, may act as a chemoattractant for medial SMCs that express PDGFR β . Phenotypically modulated medial SMCs will migrate into the subendothelial intimal space followed by proliferation, culminating in the formation of an occlusive neointima.

In conclusion, our results indicate that in a rat model for CTD after renal transplantation, medial SMCs phenotypically modulated and are the most likely source for neointimal cells. Prevention of phenotypic modulation of medial SMCs may provide a novel strategy to reduce occlusive neointima formation, including transplant vasculopathy.

Acknowledgements

We thank Peter Zwiers, Marian Bulthuis, Andre Zandvoort en Annemieke Smit- van Oosten for their excellent technical assistance.

Disclosure

The authors of this manuscript have no conflicts of interest to disclose as described by the American Journal of Transplantation.

Sources of funding

This work was supported by a Career Stimulation Program Grant from the Dutch Kidney Foundation (C03.6015, MB, HR and JLH) and Graduate School GUIDE from the University Medical Center Groningen (KK).

Online supporting information

Additional Supporting Information may be found in the online version of this article.

- Detailed methods.
- Supplemental table 1: Characteristics of arteries collected by laser dissection microscopy.
- Supplemental table 2: Composition of low-density array.
- Supplemental table 3: Primer sequences used for real-time RT-PCR
- Supplemental figure 1: Expression of PDGF B in the media of isografts and allografts 16 days after transplantation.

References

1. Ward MR, Pasterkamp G, Yeung AC, Borst C. Arterial remodeling. Mechanisms and clinical implications. *Circulation* 2000 Sep 5;102(10):1186-1191.
2. Newby AC, Zaltsman AB. Molecular mechanisms in intimal hyperplasia. *J Pathol* 2000 Feb;190(3):300-309.
3. Chapman JR, O'Connell PJ, Nankivell BJ. Chronic renal allograft dysfunction. *J Am Soc Nephrol* 2005 Oct;16(10):3015-3026.
4. Rienstra H, Boersema M, Onuta G, Boer MW, Zandvoort A, van Riezen M, et al. Donor and recipient origin of mesenchymal and endothelial cells in chronic renal allograft remodeling. *Am J Transplant* 2009 Mar;9(3):463-72.
5. Hillebrands JL, Klatter FA, Rozing J. Origin of vascular smooth muscle cells and the role of circulating stem cells in transplant arteriosclerosis. *Arterioscler Thromb Vasc Biol* 2003 Mar 1;23(3):380-387.
6. Ross R. Atherosclerosis--an inflammatory disease. *N Engl J Med* 1999 Jan 14;340(2):115-126.
7. Ross R, Glomset J, Harker L. Response to injury and atherogenesis. *Am J Pathol* 1977 Mar;86(3):675-684.
8. Hillebrands JL, Klatter FA, van den Hurk BM, Popa ER, Nieuwenhuis P, Rozing J. Origin of neointimal endothelium and alpha-actin-positive smooth muscle cells in transplant arteriosclerosis. *J Clin Invest* 2001 Jun;107(11):1411-1422.
9. Hillebrands JL, Onuta G, Rozing J. Role of progenitor cells in transplant arteriosclerosis. *Trends Cardiovasc Med* 2005 Jan;15(1):1-8.
10. Boersema M, Rienstra H, van den Heuvel M, van Goor H, van Luyn MJ, Navis GJ, et al. Donor and recipient contribution to transplant vasculopathy in chronic renal transplant dysfunction. *Transplantation* 2009 Dec 27;88(12):1386-1392.
11. Owens GK, Kumar MS, Wamhoff BR. Molecular regulation of vascular smooth muscle cell differentiation in development and disease. *Physiol Rev* 2004 Jul;84(3):767-801.
12. Krenning G, Moonen JR, van Luyn MJ, Harmsen MC. Vascular smooth muscle cells for use in vascular tissue engineering obtained by endothelial-to-mesenchymal transdifferentiation (EnMT) on collagen matrices. *Biomaterials* 2008 Sep;29(27):3703-3711.
13. Iwata H, Manabe I, Fujii K, Yamamoto T, Takeda N, Eguchi K, et al. Bone marrow-derived cells contribute to vascular inflammation but do not differentiate into smooth muscle cell lineages. *Circulation* 2010 Nov 16;122(20):2048-2057.
14. Boor P, Floege J. Special Series: Chronic Kidney Disease Growth Factors in Renal Fibrosis. *Clin Exp Pharmacol Physiol* 2011 Jan 29.
15. Bornfeldt KE, Raines EW, Nakano T, Graves LM, Krebs EG, Ross R. Insulin-like growth factor-I and platelet-derived growth factor-BB induce directed migration of human arterial smooth muscle cells via signaling pathways that are distinct from those of proliferation. *J Clin Invest* 1994 Mar;93(3):1266-1274.
16. Zeidan A, Sward K, Nordstrom I, Ekblad E, Zhang JC, Parmacek MS, et al. Ablation of SM22alpha decreases contractility and actin contents of mouse vascular smooth muscle. *FEBS Lett* 2004 Mar 26;562(1-3):141-146.
17. Liu Y, Sinha S, McDonald OG, Shang Y, Hoofnagle MH, Owens GK. Kruppel-like factor 4 abrogates myocardin-induced activation of smooth muscle gene expression. *J Biol Chem* 2005 Mar 11;280(10):9719-27.
18. Du KL, Ip HS, Li J, Chen M, Dandre F, Yu W, et al. Myocardin is a critical serum response factor cofactor in the transcriptional program regulating smooth muscle cell differentiation. *Mol Cell Biol* 2003 Apr;23(7):2425-37.
19. Jiang B, Yamamura S, Nelson PR, Mureebe L, Kent KC. Differential effects of platelet-derived growth factor isoforms on human smooth muscle cell proliferation and migration are mediated by distinct signaling pathways. *Surgery* 1996 Aug;120(2):427-31; discussion 432.
20. Myllarniemi M, Calderon L, Lemstrom K, Buchdunger E, Hayry P. Inhibition of platelet-derived growth factor receptor tyrosine kinase inhibits vascular smooth muscle cell migration and proliferation. *FASEB J* 1997 Nov;11(13):1119-1126.
21. Chen PY, Simons M, Friesel R. FRS2 via fibroblast growth factor receptor 1 is required for platelet-derived growth factor receptor beta-mediated regulation of vascular smooth muscle marker gene expression. *J Biol Chem* 2009 Jun 5;284(23):15980-15992.

22. Liu Y, Sinha S, McDonald OG, Shang Y, Hoofnagle MH, Owens GK. Kruppel-like factor 4 abrogates myocardin-induced activation of smooth muscle gene expression. *J Biol Chem* 2005 Mar 11;280(10):9719-9727.
23. Miano JM. Serum response factor: toggling between disparate programs of gene expression. *J Mol Cell Cardiol* 2003 Jun;35(6):577-593.
24. Yu K, Zheng B, Han M, Wen JK. ATRA activates and PDGF-BB represses the SM22alpha promoter through KLF4 binding to, or dissociating from, its cis-DNA elements. *Cardiovasc Res* 2011 Jun 1;90(3):464-474.
25. Meyer-ter-Vehn T, Sieprath S, Katzenberger B, Gebhardt S, Grehn F, Schlunck G. Contractility as a prerequisite for TGF-beta-induced myofibroblast transdifferentiation in human tenon fibroblasts. *Invest Ophthalmol Vis Sci* 2006 Nov;47(11):4895-4904.
26. Fukata Y, Amano M, Kaibuchi K. Rho-Rho-kinase pathway in smooth muscle contraction and cytoskeletal reorganization of non-muscle cells. *Trends Pharmacol Sci* 2001 Jan;22(1):32-39.
27. Cordes KR, Sheehy NT, White MP, Berry EC, Morton SU, Muth AN, et al. miR-145 and miR-143 regulate smooth muscle cell fate and plasticity. *Nature* 2009 Aug 6;460(7256):705-10.
28. Albinsson S, Suarez Y, Skoura A, Offermanns S, Miano JM, Sessa WC. MicroRNAs are necessary for vascular smooth muscle growth, differentiation, and function. *Arterioscler Thromb Vasc Biol* 2010 Jun;30(6):1118-1126.
29. Elia L, Quintavalle M, Zhang J, Contu R, Cossu L, Latronico MV, et al. The knockout of miR-143 and -145 alters smooth muscle cell maintenance and vascular homeostasis in mice: correlates with human disease. *Cell Death Differ* 2009 Dec;16(12):1590-1598.

Supplemental material

Detailed Methods

Rats

Inbred female (175–210 gram) and male (200–225 gram) Dark Agouti (DA) rats were obtained from Harlan (Horst, the Netherlands) and inbred male Wistar Furth (WF) rats (240–295 gram) from Charles River Laboratories Inc. (l'Arbresle, Cedex, France). Animals were handled in compliance with the Principles of Laboratory Animal Care (NIH Publication No. 86-23, revised 1985), the University of Groningen guidelines for animal husbandry (University of Groningen, the Netherlands), and the Dutch Law on Experimental Animal Care.

Kidney Transplantation

Female DA kidneys were orthotopically transplanted into male DA or WF recipients (1). Donor rats were anesthetized with isoflurane/O₂, and left kidneys were flushed in situ with saline and removed. The donor rats were then killed by exsanguination, warm ischemia time varied between 0 to 15 min. Kidneys were preserved in ice-cold saline (range 16-38 min) and then transplanted into the recipient from which the left kidney was removed under isoflurane/O₂ anesthesia. The graft renal vein, artery, and ureter were anastomosed end-to-end to the recipients' left renal vein, artery, and ureter, respectively, using 10-0 prolene sutures. Vascular clamps were released after a warm ischemia time of 25 to 30 min. Both adrenal glands of the recipient remained in situ. All transplanted rats were given buprenorphine (Temgesic; 0.01 mg/kg) subcutaneously directly after transplantation and for 8–10 h and 24 h after transplantation for pain relief. Recipients received cyclosporine A (5 mg/kg bodyweight) (Sandimmune, Novartis, the Netherlands) subcutaneously during the first 10 days after transplantation. The recipients' contralateral kidney was removed 8 to 14 days after transplantation. Total follow-up was time 12 weeks unless animals had to be sacrificed earlier due to graft failure.

Laser Dissection Microscopy and Gene Expression Analysis

Frozen kidneys were sectioned at 9 μ m and mounted on UV-pretreated slides (PALM Micro Laser Technology, Bernried, Germany). Sections were fixed in acetone and air-dried. Sections were subsequently stained with Mayer's hemalum (Merck, Darmstadt, Germany) and rinsed in diethyl pyrocarbonate (DEPC)-treated tap water. Slides were then used for laser dissection microscopy using a Leica Microdissection System (Leica Microsystems). The neointima and media were separately dissected from nine serial sections per kidney.

Total RNA was isolated from microdissected vascular structures using the RNeasy Micro Kit (Qiagen, Hilden, Germany). Reverse transcription was carried out using Superscript III reverse transcriptase (Invitrogen, Breda, the Netherlands) and random hexamer primers (Promega, Leiden, the Netherlands). Gene expression was analyzed with a custom made microfluidic card-based low density array (Table 2, full manuscript) using the ABI Prism 7900HT Sequence Detection System (Applied Biosystems, Nieuwerkerk a/d IJssel, the Netherlands). Micro fluidic cards consists of 384 wells pre-loaded with oligos including 3 endogenous controls, for high-throughput, low reaction volume, real-time PCR. For each micro fluidic card, 10 μ l cDNA was diluted in 40 μ l of double distilled water and mixed with 50 μ l of Taqman PCR master mix (Applied Biosystems). Standard recommended PCR protocols were performed (50°C for 2 minutes, 94.5°C for 10 min, 97°C for 30 s, 59.7°C for 1 min, with steps 3 and 4 repeated for 50 cycles). Relative mRNA levels were calculated as $2^{-\Delta CT}$, in which ΔCT is CTgene of interest – CT β -actin. CT values that were below detection level were set at 50.

For gene expression analysis of cultured rat aortic SMCs, total RNA was isolated after 24 hours of stimulation with PDGF-BB or TGF- β 1 (PreproTech EC LTD. London, UK) using the RNeasy Micro Kit (Qiagen Inc., CA, USA). Subsequently, 1 μ g of total RNA was reverse transcribed using the FirstStrand cDNA synthesis kit (Fermentas UAB, Lithuania). Real time RT-PCR analysis was performed in a final reaction volume of 10 μ L, consisting of 4.5 μ L SYBR Green Supermix (Bio-Rad, Veenendaal, The Netherlands), 0.5 μ L primer-mix (Table 3, 0.5mmol/L), and 5 μ L cDNA (1ng/ μ L) using the ABI Prism 7900HT Sequence Detection System (Applied Biosystems, the Netherlands). Reactions were performed at 95°C for 15s, 60°C for 30s, and 72°C for 30s, for 40 cycles. Relative mRNA levels were normalized against β -actin expression as described above.

Immunohistochemistry

Immunohistochemistry was performed on 2 μ m paraffin sections. Sections were stained for Masson's trichrome, Verhoeff-van Gieson, Tgf- β 1, Ctgf, Pdgfb and Myh11. Sections were dewaxed and antigen retrieval was performed for Tgf- β 1 and Pdgfb staining by incubation in 0.1 mol/L citric acid buffer for 8 minutes in a microwave. Endogenous peroxidase was blocked with 0.1% H₂O₂ for 10 min at room temperature. Sections were incubated for 1 h with primary antibodies i.e. rabbit anti Tgf- β 1 (Santa Cruz, Heidelberg, Germany), rabbit anti Ctgf (Santa Cruz, Germany), rabbit anti Pdgfb (Abcam, Cambridge, UK) or rat anti Myh11 (Abnova, Heidelberg, Germany). Goat anti rabbit-horseradish peroxidase (HRP), rabbit anti goat-HRP, Goat anti rabbit-biotin, rabbit anti goat-biotin and rabbit anti rat-HRP conjugates were used as secondary antibodies. Detection of biotinylated antibody complex was done by incubation with a streptavidin-HRP conjugate. Color development was performed with 3-amino-9-ethylcarbazole substrate dissolved in N,N-dimethylformamide and 0.5 mol/L acetate buffer (pH 4.9) or with 3,3'-diaminobenzidine tetrachloride. Sections

were counterstained with Mayer's hemalum (Merck) and mounted in Kaiser's glycerol gelatin (Merck).

The degree TV (i.e. obliteration in arteries) was measured in all arteries within a section with a clearly visible internal elastic lamina (IEL) in the Verhoeff-van Gieson stained sections. The total surface area lying at the luminal side of the IEL (lumen + neointima), was measured and set at 100%. Subsequently, the luminal area was subtracted from this total area, to obtain the neointimal area. Luminal occlusion was expressed as mean percentage \pm SEM. Arteries cut diagonally, i.e. arteries with a compressed lumen, were excluded from this measurement.

Collagen gel contraction assay

Gel contraction assay of 3D collagen gels were performed using a solution of rat tail collagen I (BD Bioscience, Breda, the Netherlands). Rat aortic SMCs (prestimulated for 24 hours with PDGF-BB or TGF- β 1, passage 3) (Lonza Benelux BV, Breda, The Netherlands) were resuspended in a mixture of collagen I, 10X DMEM, 1.5 mg/mL NaHCO₃ and 25 mmol/L HEPES at a concentration of 3.0×10^6 cells/mL. Aliquots of 50 μ L (containing 50,000 cells and 0.25 mg collagen type I) were added to a 96 wells plate, that had been preincubated with 0.1% BSA, and allowed to solidify at 37°C in a humidified incubator with 5% CO₂ for 1 hour. After solidification, collagen gels were further cultured in DMEM/F12 (Lonza) containing 2% FCS with or without additionally added PDGF-BB or TGF- β 1 (PreproTech EC LTD. London, UK). Collagen gels were imaged using a common flatbed-scanner (ScanJet 5370C; HP, CA, USA) and gel contraction was measured after 24 hours. The degree of gel contraction was determined by dividing the total gel area before contraction (i.e. surface area of a 96 well) by the gel area after 24 hours of contraction.

Supplemental References

1. Rienstra H, Boersema M, Onuta G, Boer MW, Zandvoort A, van Riezen M, et al. Donor and recipient origin of mesenchymal and endothelial cells in chronic renal allograft remodeling. *Am J Transplant* 2009 Mar;9(3):463-72.

Supplemental Tables

Table 1. Characteristics of arteries collected by laser dissection microscopy

	Number of arteries collected per animal (n=5)	NI surface area (μm^2) mean [range]	Media surface area (μm^2) mean [range]
Allograft kidneys	74 [25-117]	1,092,834 [136,748-3,961,874]	1,064,410 [239,821-3,607,250]
Isograft kidneys	46 [37-52]	NP	596,368 [338,924-913,221]
Contralateral kidneys	69 [47-100]	NP	1,603,483 [436,477-5,207,341]

NI=neointima
NP=not present

Table 2. Composition of low-density array

Gene name	General name	Gene symbol	Assay ID
Smooth muscle phenotype			
calponin 1, basic, smooth muscle	Calponin 1	<i>Cnn1</i>	Rn00582058_m1
krüppel-like factor 4	KLF4	<i>Klf4</i>	Rn00821506_g1
krüppel-like factor 5	KLF5	<i>Klf5</i>	Rn00821442_g1
myocardin	Myocardin	<i>Mycd</i>	Rn01786178_m1
serum response factor	Srf	<i>Srf</i>	Rn01757240_m1
transgelin	SM22a	<i>Tagln</i>	Rn00580659_m1
Growth factors and receptors			
connective tissue growth factor	CTGF	<i>Ctgf</i>	Rn00573960_g1
platelet-derived growth factor beta polypeptide	PDGFB	<i>Pdgfb</i>	Rn01502596_m1
platelet derived growth factor receptor, beta polypeptide	PDGFRb	<i>Pdgfrb</i>	Rn00709573_m1
transforming growth factor, beta 1	Tgf-b1	<i>Tgfb1</i>	Rn01475963_m1

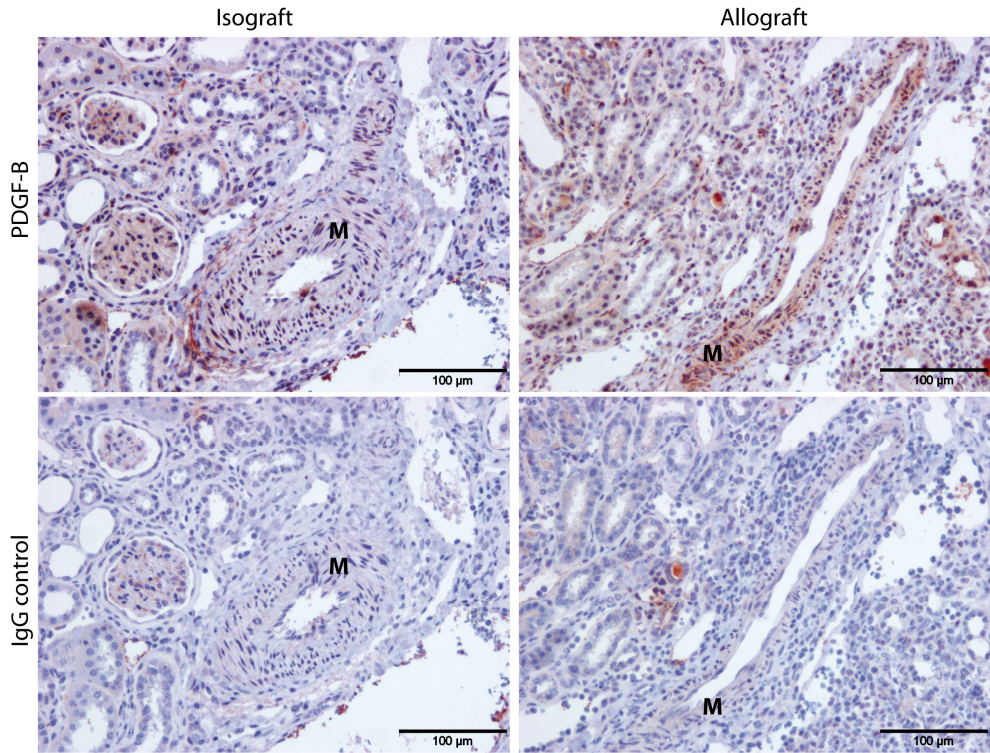
Chapter 5

Matrix molecules			
collagen, type I, alpha 1	Collagen I	<i>Col1a1</i>	Rn01463848_m1
collagen, type IV, alpha 1	Collagen IV	<i>Col4a1</i>	Rn01482925_m1
Reference genes			
β -actin	Beta-actin	<i>Actb</i>	Rn00667869_m1
β 2-microglobulin	B2m	<i>B2m</i>	Rn00560865_m1
Eukaryotic 18S rRNA	18S	<i>18s</i>	Hs99999901_s1
cadherin 5	VE-cadherin	<i>Cdh5</i>	Rn01536708_m1

Table 3. Primer sequences used for real-time RT-PCR

Gene	Forward (5'-3')	Reverse (5'-3')
Coll α 1	catgttcagctttgtggacct	gcagctgactcagggatgt
KLF4	ccgtccttetccacgttc	gagttcctctcgccaacg
Myocardin	ccgtgaaaaggctataaaagg	ctgtcatcttcaaggcaaatg
Sm22a	agtgtggccctgatgtgg	tcaccaacttgctcagaatca
α -Sma	tgccatgtatgtggctattca	accagttgtacgtccagaagc
Srf	gcacagacctcacgcaga	atgtggcccccacagtt
β -actin	cccgcgagtacaaccttct	cgtcacatggcgaact

Supplemental Figure Legends



Supplemental Figure 1: Expression of PDGF B in the media of isografts and allografts 16 days after transplantation. Protein expression of PDGF-B was assessed in the media from allografts and isografts 16 days after transplantation. Polyclonal rabbit IgG replaced the PDGF-B antibody and was used as a negative control. Scale bar represents 100 µm. M = media.

Tubular epithelial syndecan-1 maintains renal function in murine ischemia/reperfusion and human transplantation

Kidney Int. 2012 Apr;81(7):651-61

Johanna W.A.M. Celie#

Kirankumar Katta#

Saritha Adepu

Wynand B.W.H. Melenhorst

Rogier M. Reijmers

Edith M. Slot

Robert H.J. Beelen

Marcel Spaargaren

Rutger J. Ploeg

Gerjan Navis

Jaap J. Homan van der Heide

Marcory C.R.F. van Dijk

Harry van Goor

Jacob van den Born

#contributed equally

Abstract

Syndecan-1, a heparan sulfate proteoglycan, plays an important role in wound healing by binding several growth factors and cytokines. As these processes are also crucial in damage and repair after renal transplantation, we examined syndecan-1 expression in human control kidneys, renal allograft protocol biopsies, and renal allograft biopsies taken at indication and non-transplant interstitial fibrosis. Syndecan-1 expression was increased on tubular epithelial cells in renal allograft biopsies compared to control kidneys. Increased epithelial syndecan-1 in allografts correlates with low proteinuria and serum creatinine, less interstitial inflammation, less tubular atrophy, and prolonged allograft survival. Knockdown of syndecan-1 on tubular epithelial cells *in vitro* reduces cell proliferation. Selective binding of growth factors suggests that syndecan-1 may promote epithelial restoration. Bilateral renal ischemia/reperfusion in syndecan-1 deficient mice resulted in increased initial (day 1) renal failure and tubular injury compared to wildtype mice. Macrophage and myofibroblast numbers, tubular damage and plasma ureum levels were increased, and tubular proliferation reduced in syndecan-1 deficient over wildtype kidneys at day 14. Our results indicate that syndecan-1 promotes tubular survival and repair upon renal allograft transplantation and ischemia/reperfusion injury. As far as we know syndecan-1 is the first induced tubular marker that is positively associated with graft function and survival.

Introduction

Renal allograft transplantation is the treatment of choice for chronic kidney failure. Although significant advances have been made in the limiting (hyper) acute renal allograft rejection, chronic transplant dysfunction poses a serious risk of renal allograft loss at months to years after transplantation. Many factors are known to affect graft function and survival. For example, peri-operative ischemia/reperfusion injury (IRI) causes severe damage to the tubular epithelial cells (TECs) of the donor organ, and tubular injury due to ischemia can persist into the chronic phase as a result of vascular changes (1-4). The number and severity of immune-mediated acute allograft rejection episodes, and especially chronic transplant dysfunction, characterized by tubular atrophy, interstitial fibrosis and transplant glomerulopathy, can result in graft loss. Clearly, repair of tubular damage is a crucial step in restoration of renal function upon transplantation, and the balance between functional repair of tubular epithelium versus chronic inflammation and non-functional scarring, i.e. fibrosis, is a dominant factor determining renal allograft function in the long run(5).

In previous studies, we showed that renal inflammatory responses can be affected by changes in heparan sulfate proteoglycans (HSPGs), as observed in experimental renal IRI as well as in primary human kidney diseases(6;7). HSPGs are glycoconjugates which consist of a core protein to which a number of linear carbohydrate side chains (glycosaminoglycans; GAGs) are linked(8;9). HS-GAG chains are typically very heterogeneous due to the coordinated action of various enzymes, which modify the alternating glucuronic acid and N-acetylglucosamine residues, resulting in varying degrees of sulfation and epimerization. HSPGs are involved in diverse biological processes, including angiogenesis, wound healing, development and inflammation(10-12). HSPGs exert their functions predominantly by binding and presenting growth factors, chemokines and cytokines, and facilitating adhesion of inflammatory cells via binding to the leukocyte adhesion molecule L-selectin(6;8;13). Binding of these factors to HSPGs is mediated by the HS-GAG chains, and is dependent on the chemical fine-structure of the GAGs(8;14). We previously showed that within 24h after renal IRI, HSPGs expressed at the abluminal side of peritubular capillaries are induced to bind L-selectin and the monocyte chemoattractant protein-1, and that these HSPGs facilitate monocyte extravasation(6). Similar changes were observed in human primary kidney diseases associated with interstitial inflammation(7). In addition, we noted an increased expression of the cell surface HSPG syndecan-1 on TECs in biopsies of proteinuric patients(7). Syndecan-1 is a transmembrane HSPG involved in re-epithelialization during wound healing and inflammation(10;15;16). Earlier studies have implicated syndecan-1 in epithelial differentiation(17;18). These processes are also very relevant in the context of renal allograft transplantation, i.e. inflammation as a result of IRI and donor-acceptor antigenic mismatching, and tubular re-epithelialization and differentiation to restore the damaged tubular epithelium after IRI. Indeed, a recent review

by Venkatachalam et al. posed the hypothesis that failure of tubular epithelial differentiation and therefore impaired tubular repair upon larger or smaller acute kidney injury episodes may play a significant role in the progression of kidney disease(19).

Based on this background, we hypothesized that syndecan-1 is involved in tubular survival and repair upon renal transplantation. We examined expression of syndecan-1 in human renal allograft biopsies, including protocol biopsies and biopsies taken at indication, and correlated syndecan-1 expression to allograft function and binding of relevant growth factors. To directly study the functional role of syndecan-1, we studied the effect of syndecan-1 knockdown (*in vitro*) on TEC proliferation. In addition, we performed bilateral renal IRI in syndecan-1 versus wildtype mice and studied functional and histological outcome. Based on our data, we propose that syndecan-1 is involved in determining the balance between non-functional scarring and functional repair, and could be a novel marker indicating prolonged renal allograft survival.

Methods

Patient characteristics and histopathology

Renal allograft biopsies used in this study included protocol biopsies taken at one year after transplantation (n=9), or taken upon indication, diagnosed according to BANFF criteria (39-42), representing minor histological alterations (Tx-MHA, n=27; borderline interstitial inflammation and/or borderline tubular atrophy and/or borderline interstitial fibrosis, no tubulitis or vasculopathy), acute allograft rejection (AR, n=23), transplants with interstitial fibrosis and/or tubular atrophy (Tx-IFTA, n=38; includes chronic allograft rejection (n=6)) and non-transplant interstitial fibrosis (non-Tx IF, n=20). Control kidney tissue included histologically normal tissue from kidneys removed because of renal carcinoma (n=12) and donor kidneys unused because of anatomical issues (n=2). Patient characteristics are summarized in Table 1. All patients with a renal allograft used standard immunosuppressive regimens according to institutional guidelines. All procedures and use of anonymized tissue were performed according to national ethical guidelines. Diagnosis and scoring was performed by an experienced nephropathologist according to Banff classification of renal allograft pathology, in which the cell-mediated component of AR is classified based on significant interstitial infiltration with foci of tubulitis (Type IA/B), signs of intimal arteritis (Type IIA/B), or transmural arteritis potentially accompanied by fibrinoid changes and medial smooth muscle cell necrosis (Type III), and the severity of Tx-IFTA is graded based on the amount of interstitial fibrosis and tubular atrophy (Grade I; mild, Grade II; moderate, Grade III, severe). Data on interstitial inflammation, tubulitis, tubular atrophy, acute tubular necrosis, epithelial vacuolization, interstitial fibrosis, vasculopathy, global glomerulosclerosis and C4d staining (anti-human polyclonal, Biomedica, Vienna, Austria) per diagnosis group are provided in suppl. Table 1.

Table 1: Patient characteristics

Diagnosis	n	Age (years)	Sex (m/f)	Time Tx to biopsy (weeks)	MAP (mmHg) ^A	Serum creatinine ($\mu\text{mol/l}$) ^A	Proteinuria (g/24h) ^A
Control	14	67 (29-84)	9/3 ^B				
Tx-Protocol	9	51 (32-66)	7/2	50 (45-53)*	104 (93-129)	102 (47-115)	0.2 (0-0.7)
Tx-MHA	25	48 (18-70)	19/6	3 (1-288)	101 (74-120)	222 (105-1229)**	0.3 (0-1.7)***
Tx-AR	28	45 (25-66)	16/12	2 (0.4-1248)	99 (62-137)	252 (127-1021)**	0.4 (0-11.3)***
Tx-IFTA	33	43 (11-69)	20/13	337 (12-1092)*	106 (80-153)	276 (125-730)**	1.6 (0-9.4)****
NonTx-IFTA	20	57 (20-79)	10/10		104 (84-133)	394 (80-632)**	1.1 (0.3-11.6)****

Values are expressed as median and range

^Adetermined at time of biopsy; MAP= mean arterial pressure

^Bno data were available from two donor kidneys

*p<0.05 Tx-protocol compared to Tx-AR p<0.05 Tx-IFTA compared to Tx-MHA and Tx-AR

**p<0.005 compared to Tx-protocol

***p<0.05 compared to Tx-IFTA and Non-Tx-IFTA

****p<0.001 compared to Tx-protocol

Kruskal-Wallis test with pairwise multiple comparisons (adjusted p-values)

Renal biopsy immunofluorescence and scoring

Formalin-fixed, paraffin-embedded archival renal tissue was used. Staining for syndecan-1 (CD138; Serotec) and anti-HS mAbs JM-403 (43), JM-13 (44), 10E4 (45; Seikagaku) and HK249 (46; Seikagaku) was performed after microwave-citrate antigen retrieval by incubating appropriate dilutions of primary antibodies for 1hr at room temperature (RT; 20°C), followed by incubation of AlexaFluor-labelled anti-mouse IgG and anti-rabbit IgG secondary antibodies (Molecular Probes, Invitrogen) for 45 min at RT. Binding experiments were performed by incubating excess amounts of recombinant human FGF-2 (2.5 $\mu\text{g/ml}$; Peprotech) or HB-EGF (2.5 $\mu\text{g/ml}$; R&D Systems) on tissue sections for 2hr at RT, followed by anti-human basic FGF (Sigma-Aldrich) or anti-human HB-EGF (R&D Systems) for 1 hr, and AlexaFluor-labelled anti-mouse IgG secondary antibodies for 45 min at RT. Isotype matched non-relevant antibodies served as background controls and proved to be negative. In some experiments, tissue sections were pre-treated with heparitinase I (0.05 U/ml; EC4.2.2.8; Seikagaku Corp.) in acetate buffer (50mM C₂H₃O₂Na, 5mM CaCl₂•2H₂O, 5mM MgCl₂•6H₂O, pH 7.0) for 1h at 37°C. Sections were examined using a

Nikon Eclipse E800 fluorescence microscope with digital camera using identical microscopy conditions and exposure time for different samples. Stainings were scored as % of TECs involved in cortical regions of biopsies (typically 5-10 visual fields per biopsy), or non-biopsy tissues (15 visual fields)(200x magnification) without knowledge of diagnosis.

Cell culture

The human TEC cell line HK-2(47) was kindly provided by Dr. C. van Kooten, Leiden University Medical Center, Leiden, the Netherlands. Cells were cultured in Dulbecco's modified Eagle's medium (DMEM)/F-12 (Gibco/Invitrogen) supplemented with 5µg/ml insulin, 5µg/ml transferrin, 5ng/ml selenium, 36ng/ml hydrocortisone, 10ng/ml epidermal growth factor (Sigma-Aldrich), 50U/ml penicillin, 50µg/ml streptomycin and 2mM L-glutamine (Cambrex).

shRNA silencing

shRNAs targeting syndecan-1 (synd1-shRNA; target sequence 3'-GGTGCTTTGCAAGATATCA-5') and renilla luciferase (control vector; target sequence 3'-AAACATGCAGAAAATGCTG-5') were cloned into the pTER expression vector (kindly provided by Prof. H. Clevers, Hubrecht Laboratory, Centre for Biomedical Genetics, Utrecht, the Netherlands). HK-2 cells were transfected with synd1-shRNA vector or control vector using Lipofectamine (Invitrogen) according to manufacturer's protocol and selected based on zeocine resistance(7). Knockdown of syndecan-1 expression was determined by flow cytometry. Cells were detached using EDTA-mix (10mM EDTA, 150mM NaCl, 6mM KCl, 1.2mM KH₂PO₄, 20mM Hepes, 5mM glucose, 0.5% BSA; pH 7.4), washed with PBS/0.5%BSA (PBA) and incubated with anti-syndecan-1 (CD138) antibody in PBA (30min on ice). After washing, cells were incubated with FITC-labeled anti-mouse IgG (30 min on ice), washed and analysed (FACSCalibur, Becton Dickinson). Non-relevant mouse IgG served as isotype control.

Standardized scratch assay

Control vector or synd1-shRNA HK-2 cells were grown to confluency in a 24-well plate. A standardized scratch was made in all wells, and digital images were taken at indicated time-points using a time-lapse microscopy stage (37°C; 5% CO₂). Scratch area was calculated using AnalySIS (SIS Pro) software.

MTT assay

Control vector or synd1-shRNA HK-2 cells were seeded in a 96-well plate at 6000 cells/well. Cell proliferation was determined at indicated time-points by adding 10µl MTT

(5mg/ml; 3-[4,5-dimethylthiazol-2-yl]-2,4 diphenyltetrazolium bromide) per well and incubating for 2h at 37°C. Supernatant was removed, 100µl/well DMSO/glycine (7:1 v/v) was added to dissolve the formed formazan crystals, and absorbance at 540nm was measured. Data are expressed as % MTT activity, with input at t=0 set at 100%.

ELISA-based growth factor binding assay

Nunc maxisorp ELISA plates were coated overnight with 2.5µg/ml heparin-albumin (Sigma) in PBS. After blocking (PBS/5%BSA; 2hr RT), wells were incubated for 2hr at RT with indicated concentrations of FGF-2 or HB-EGF in blocking buffer. Wells were washed (PBS/0.05%Tween-20) and incubated with anti-human basic FGF or anti-human HB-EGF diluted in blocking buffer. After washing, wells were incubated with biotinylated anti-mouse IgG (1hr RT) and streptavidin-peroxidase (30min RT) in blocking buffer. Wells were extensively washed and substrate solution (TMB) was incubated for 15 min at RT, after which the reaction was stopped using 10% H₂SO₄. Absorbance was read at 450nm.

Bilateral renal IRI

Syndecan-1 deficient mice(16;26) and wildtype mice (both C57BL/6 background, syndecan-1 deficient mice backcrossed >6 generations) were bred in VU University Medical Center facilities, the Netherlands. Age and sex-matched mice were used in all experiments. The animal ethics committee of the VU University Medical Center approved all experiments. Briefly, renal pedicles were clamped for 25 min using microaneurysm clamps through a midline abdominal incision under anesthesia (0.07 ml/10 g mouse of fentanyl citrate fluanisone midazolam mixture containing 1.25 mg/ml midazolam [Roche Diagnostics Corp.], 0.08 mg/ml fentanyl citrate, and 2.5 mg/ml fluanisone [Janssen Pharmaceutical]). After 25 min of ischemia, clamps were removed and kidneys were inspected for restoration of blood flow. The abdomen was closed in 2 layers, mice received s.c. analgesic (50 µg/kg buprenorphin [Temgesic; Schering-Plough]) and were allowed to recover from surgery under a warm lamp. Sham-operated mice underwent the same procedure without clamping and were sacrificed 1 day after surgery. IRI mice were sacrificed at indicated time points and blood was taken by cardiac puncture. Kidneys were removed, and one half was snap-frozen, one half was formalin-fixed, paraffin-embedded for (immuno)histology.

Renal IRI histology and scoring

Formalin-fixed kidney sections (4 µm) were stained with periodic acid Schiff's (PAS) reagent and hematoxylin according to routine protocol to determine tubular damage. For specific detection of monocytes/macrophages, acetone-fixed (10 min RT) tissue sections

were rehydrated in PBS, blocked with PBS+5% normal goat serum (10 min RT), incubated with anti-monocyte/macrophage F4/80 (1h RT), and subsequently with anti-rat Alexa 488-labeled secondary antibody. For specific detection of myofibroblasts, α -SMA staining was performed by incubating the sections with mouse anti-smooth muscle actin (1h RT), and subsequently with Goat anti-Mouse IgG2a peroxidase labeled secondary antibody, followed by the TSATM tetramethylrhodamine system (PerkinElmer LAS Inc., Waltham, MA, USA). Immunofluorescence stainings were scanned by using TissueFAXS (TissueGnostics GmbH, Vienna, Austria) and 15 digital photographs were made (magnification 200x) from renal cortex and outer medulla per kidney (30 photos for left and right kidney together), using n=7 mice per group per time-point. The total area stained was quantified using ImageJ 1.41 (Rasband, W.S., ImageJ, U.S. National Institutes of Health, Bethesda, Maryland, USA) which was downloaded from <http://rsb.info.nih.gov/ij/download.html>. Ki67 (Ab 15580, Abcam) staining was done on 4% formaldehyde fixed cryosections. Endogenous peroxidase activity was blocked by 0.01% H₂O₂ in PBS, followed by blocking with 10% normal mouse serum. Primary antibody was incubated overnight at 4°C, followed by peroxidase-labeled goat anti-rabbit IgG, and peroxidase-labeled rabbit anti-goat IgG, and 3-Amino-9-Ethyl-Carbozol. Quantification was done on 10 cortical fields/kidney at 20x magnification. Indicated is the mean number of Ki67 positive tubular nuclei/high power field per mice (left and right kidney together).

Statistical analysis

Data were analysed using Kruskal-Wallis test with pairwise comparisons (p-values adjusted for multiple comparisons), Spearman's rank correlation test, Student's t-test or survival analysis by log-rank test as indicated (PASW 18 statistics software). For Kaplan-Meier analysis with log rank test, groups of normal (as in control kidneys; <30%) versus increased (30-100%) TEC syndecan-1 were compared. Loss of graft was defined by graft failure requiring dialysis treatment or explantation of renal allograft. p-values of <0.05 were considered to be statistically significant.

Results

Increased syndecan-1 expression on TECs in a subset of renal allograft biopsies

In 13 out of 14 control kidneys, weak staining for syndecan-1 protein was detected in a limited percentage of TECs (Fig.1A,B). In contrast, very prominent TEC syndecan-1 staining was observed in all Tx-protocol biopsies (taken according to protocol at one year after transplantation), and a large subset of Tx-MHA (minor histological alterations; borderline interstitial inflammation and/or borderline tubular atrophy and/or borderline

intersitial fibrosis, no tubulitis or vasculopathy), acute allograft rejection biopsies (Tx-AR), and Tx-IFTA biopsies (interstitial inflammation/tubular atrophy)(Fig.1B). This increased syndecan-1 staining showed distinct localization to the basolateral side of TECs (Fig.1A). Syndecan-1 staining was not observed in glomeruli or interstitial vasculature in any of the biopsies examined.

Within the Tx-AR and Tx-IFTA group, the percentage of syndecan-1 positive TECs was heterogeneous throughout the different pathological types/grades (Fig.1B-D), and there was a trend towards a lower percentage of syndecan-1 positive TECs in the more severe Tx-IFTA grades, which was however not statistically different. To further characterize the pathological status of transplant biopsies included in this study, we scored for interstitial inflammation, tubulitis, tubular atrophy, C4d status, glomerulosclerosis, vasculopathy, acute tubular necrosis, epithelial vacuolization and interstitial fibrosis according to BANFF criteria (as indicated in Suppl. Table 1). Correlation analysis across the whole panel of biopsies revealed that increased TEC syndecan-1 is associated with lower scores for interstitial fibrosis (Spearman's $\rho=-0.356$, $p<0.001$), interstitial inflammation (Spearman's $\rho=-0.305$, $p<0.005$) and tubular atrophy (Spearman's $\rho=-0.262$, $p<0.01$).

Increased TEC syndecan-1 is associated with better graft function and prolonged allograft survival

We next examined whether the percentage of syndecan-1 positive TECs was associated with clinical parameters, including time between transplantation and biopsy (time Tx to biopsy), markers for renal function (proteinuria, serum creatinine) and graft survival. A negative correlation was found between the percentage of syndecan-1 positive TECs and time Tx to biopsy (Spearman's $\rho=-0.254$, $p=0.016$; analysed over Tx-protocol, Tx-MHA, Tx-AR and Tx-IFTA groups together), indicating that a longer time between transplantation and biopsy is associated with lower percentage syndecan-1 positive TECs. However, in subgroups of Tx-MHA and Tx-IFTA which were matched according to similar time Tx to biopsy (Fig.2A; time Tx to biopsy between 32 to 288 weeks; Tx-MHA $n=6$, median 216 weeks, range 32-288 vs. Tx-IFTA $n=12$, median 188 weeks, range 40-265), the percentage of syndecan-1 positive TECs was significantly higher in the Tx-MHA subgroup compared to Tx-IFTA subgroup (Fig.2B; $p=0.032$). Within the Tx-MHA or Tx-IFTA groups no statistical correlation was observed between time Tx to biopsy and the percentage syndecan-1 positive TECs (Spearman's $\rho=0.150$, $p=0.495$ for Tx-MHA; Spearman's $\rho=0.193$, $p=0.315$ for Tx-IFTA). These data suggest that TEC syndecan-1 expression is initially increased upon transplantation and decreases over time, although expression remains higher over time in biopsies with relatively mild histological abnormalities (e.g. Tx-MHA).

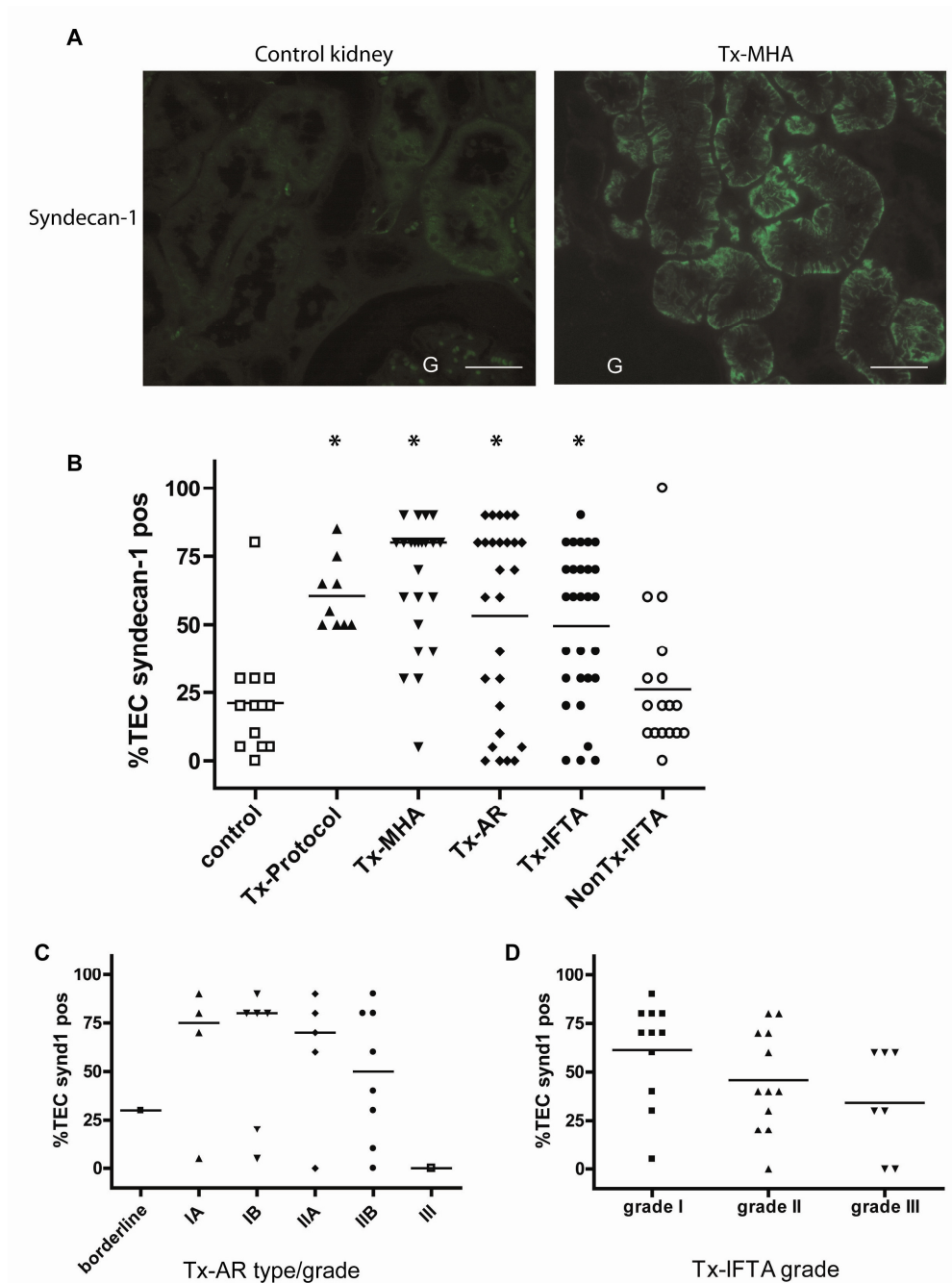


Figure 1. Increased syndecan-1 expression on TECs in a subset of renal allograft biopsies. (A) Immunostaining of human control kidney and Tx-MHA biopsy for syndecan-1 protein expression. G=glomerulus, bar=50µm. (B) Scoring for syndecan-1 positive TECs in control kidney, Tx-protocol, Tx-MHA, Tx-AR, Tx-IFTA and nonTx-IFTA biopsies. *Kruskal-Wallis test $p<0.001$; $p<0.05$ control vs. Tx-protocol, Tx-MHA, Tx-AR and Tx-IFTA, $p<0.05$ nonTx-IFTA vs. Tx-IFTA (p-values adjusted for multiple comparison using Bonferroni) (C) Scoring for the percentage of syndecan-1 positive TEC in biopsies with different types/grades AR according to Banff-classification; not statistically different (Kruskal-Wallis). (D) Scoring for the percentage of syndecan-1 positive TEC in biopsies diagnosed as Tx-IFTA grade I, II and III according to Banff-classification; not statistically different (Kruskal-Wallis).

We next investigated whether TEC syndecan-1 expression in the allografts was related to clinical markers indicative of allograft function (determined at time of biopsy). A statistically significant negative correlation was found between the percentage of syndecan-1 positive TECs and proteinuria (as indicated in Fig.2C; Spearman's $\rho=-0.315$, $p<0.005$) and serum creatinine (as indicated in Fig.2D; Spearman's $\rho=-0.334$, $p<0.001$; both analysed across Tx-protocol, Tx-MHA, Tx-AR and Tx-IFTA groups). These data demonstrate that increased TEC syndecan-1 expression is associated with improved renal allograft function.

In control kidneys, 13 out of 14 biopsies showed syndecan-1 expression in 30% or less of TECs, which we therefore regarded as a relevant cut-off for survival analysis. There was a statistically significant correlation between an increased percentage of syndecan-1 positive TECs and renal allograft survival (Fig.2E; $<30\%$ TEC syndecan-1 mean survival= 405 weeks, $>30\%$ TEC syndecan-1 mean survival=862 weeks; log-rank test $p<0.001$). As expected, increased proteinuria was associated with decreased graft survival (log-rank test $p=0.039$).

Together, these data show that TEC syndecan-1 is differentially expressed in renal allografts, and increased TEC syndecan-1 is associated with better renal allograft function and prolonged graft survival.

Silencing of syndecan-1 in TEC cell line results in reduced proliferation

We next examined the effect of shRNA mediated silencing of syndecan-1 in the human TEC cell line HK-2 on short-term *in vitro* re-epithelialization and more long-term proliferation. As shown in Fig.3A, shRNA mediated silencing of syndecan-1 (synd1-shRNA) reduced cell-surface syndecan-1 expression to background levels, whereas transfection with a control vector did not affect syndecan-1 expression. In the standardized scratch assay, no difference was observed between control vector and synd1-shRNA TECs in short-term re-epithelialisation (Fig.3B,C). However, the more long-term proliferation of synd1-shRNA TECs was significantly reduced compared to control vector TECs (Fig.3D). Together, these data show that although knockdown of syndecan-1 in TECs does not affect short-term (likely predominantly migration-induced) *in vitro* re-epithelialization, syndecan-1 expression seems to be a prerequisite for proper TEC proliferation.

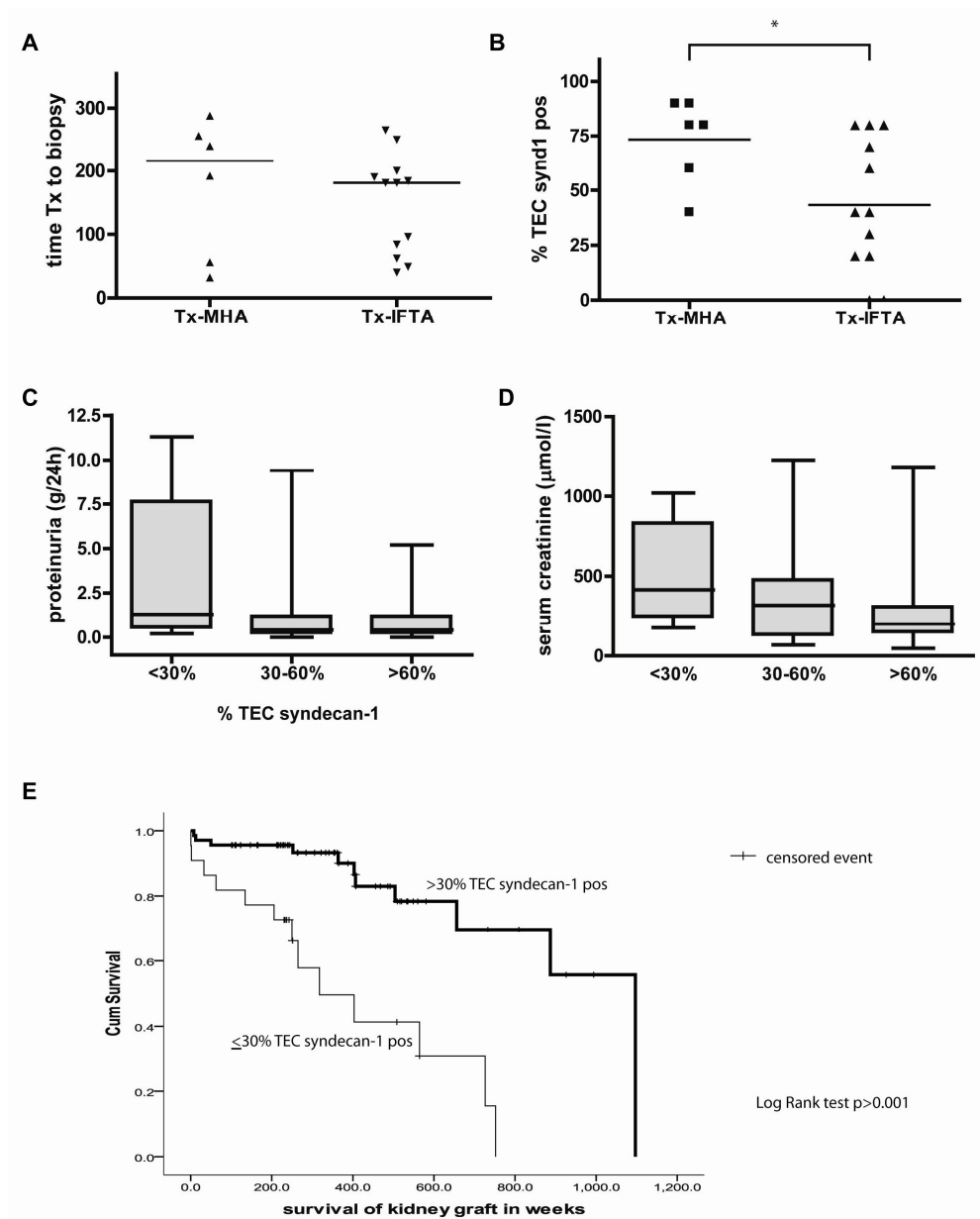


Figure 2 Increased TEC syndecan-1 expression is associated with time Tx to biopsy, renal allograft function and survival. (A) Subgroups of Tx-MHA and Tx-IFTA were matched based on similar time Tx to biopsy. (B) Scoring for the percentage of syndecan-1 positive TEC in Tx-MHA and Tx-IFTA subgroups; *p=0.032 (Mann-Whitney test). (C&D) Graphic representation of the association between TEC syndecan-1 and proteinuria (C) and serum creatinine (D). (E) Kaplan-Meier curve showing the association between TEC syndecan-1 and allograft survival. <30%TEC syndecan-1 n=22 with 13 events, >30% TEC syndecan-1 n=68 with 11 events. Log Rank test p<0.001.

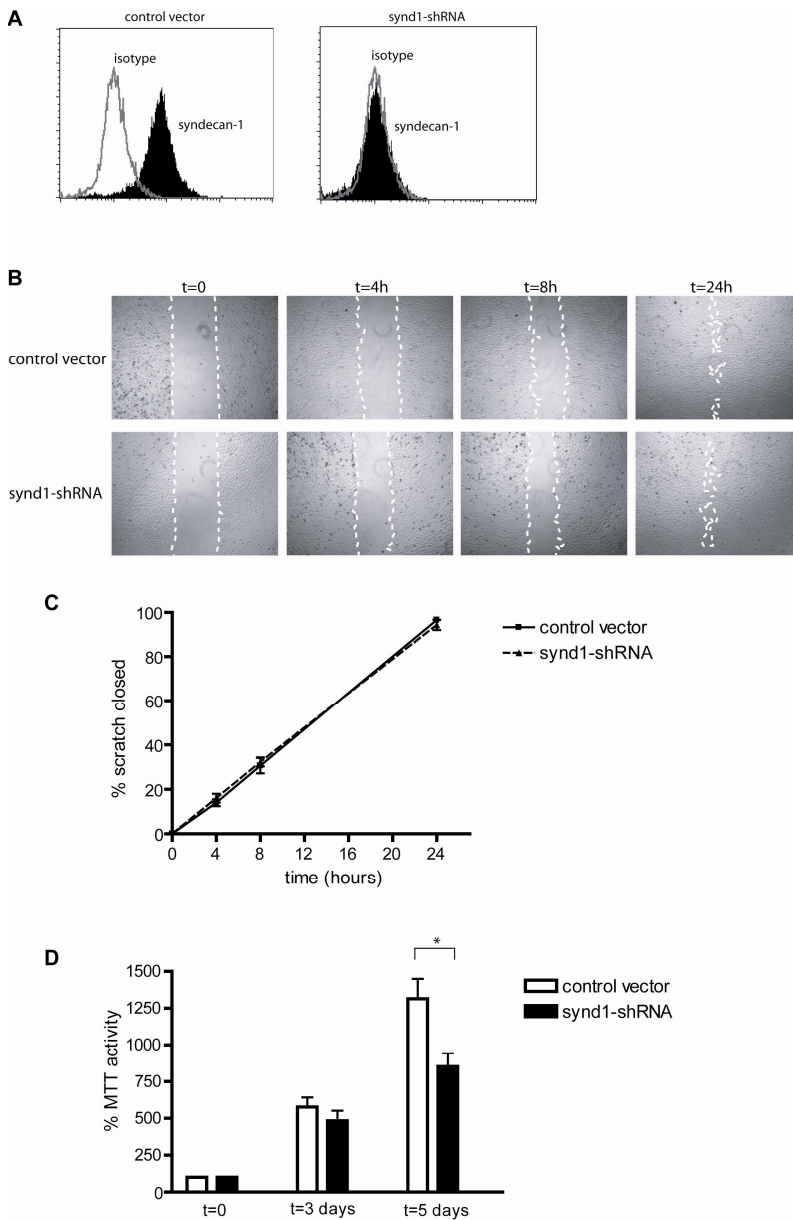


Figure 3 Silencing of syndecan-1 reduces TEC proliferation *in vitro*. (A) Knockdown of cell-surface syndecan-1 expression on the human TEC cell line HK-2 transfected with syndecan-1 specific shRNA (synd1-shRNA) compared to control vector as shown by flow cytometry. (B&C) Knockdown of syndecan-1 does not affect short-term re-epithelialisation of HK-2 cells in a standardized scratch assay. Representative photographs (B), mean and SD of 5 separate experiments (C). (D) Reduced proliferation of synd1-shRNA transfected HK-2 cells as determined by MTT assay. Mean and SEM of 5 separate experiments, * $p=0.013$ (Student's t-test).

Increased TEC syndecan-1 shows specific binding with HB-EGF and anti-HS mAb 10E4, but not FGF-2 and the anti-HS mAbs JM-403, JM-13 and HK249

Knowing that HSPGs, including syndecan-1, can be modified to present growth factors depending on cellular activation status, we explored whether the association between syndecan-1 and TEC proliferation could be attributed to growth factor binding. We chose to use FGF-2 (basic FGF) and HB-EGF, which are both known to bind HSPGs(20-22), although possibly with differences in GAG-chain requirements(20-23). In an ELISA-type binding assay, we were able to detect dose-dependent binding of FGF-2 and HB-EGF to a heparin-albumin coating, which is used as a model molecule for HSPGs (heparin is a highly sulfated HS-GAG chain)(Fig.4A). As shown in Fig.4B and Table 2, no basolateral FGF-2 binding was observed in Tx-MHA biopsies despite high syndecan-1 expression. Limited basolateral TEC binding of FGF-2 was observed in one Tx-IFTA biopsy (Table 2), and binding of FGF-2 to interstitially infiltrated cells was observed in a number of biopsies (predominantly Tx-IFTA and non Tx-IF; likely representing binding to heparin-containing mast cells; not shown). When incubation of FGF-2 was omitted no staining was observed, indicating that binding of the exogenously added FGF-2 was detected rather than endogenously present FGF-2 (not shown). Although FGF-2 is a prototypic HSPG binding growth factor, it is also a pro-fibrotic growth factor, and therefore increased binding and expression in the renal allograft could be harmful/ disadvantageous. We therefore also examined binding of HB-EGF, an epithelial survival factor, which is associated with renal epithelial repair and is expressed in the regeneration phase upon renal injury(24;25). As shown in Fig.4B and Table 2, prominent binding of HB-EGF to the basolateral side of TECs was observed most dominantly in the Tx-MHA group, although it was also observed to different extents in control tissue, Tx-IFTA and non Tx-IF. Pre-treatment of Tx-MHA tissue sections with heparitinase I, an enzyme that specifically degrades HS-GAG chains, completely diminished HB-EGF binding to TECs, showing that HB-EGF binds to basolateral TEC HSPGs (Fig.4C). To explore the structural characteristics of tubular epithelial HS in more detail, we also evaluated four different anti-HS mAbs, namely JM-403, JM-13, 10E4 and HK249. The various epitope requirements of these anti-HS mAbs have been detailed elsewhere (see Materials and Methods section). All four anti-HS mAbs stained subsets of renal basement membranes, however 10E4 in addition stained tubular epithelial cells in a baso-lateral fashion in a number of biopsies. Sub-group analysis revealed a close colocalization of anti-HS mAb 10E4 and syndecan-1 (Table 2 and Fig.5). Together, our data show increased binding of HB-EGF, but not FGF-2, to basolateral TEC HSPGs, colocalizing with syndecan-1 and 10E4 HS expression, in a subset of renal allograft biopsies. Syndecan-1 positive tubules however failed to bind with FGF-2, and anti-HS mAbs JM-403, JM-13 and HK249. These data highlight two levels of regulation by

Chapter 6

which the cells modulate growth factor affinity, namely syndecan-1 protein expression and the formation of specific sulfation motifs in the HS polysaccharide side chains.

Table 2: Scoring for TEC syndecan-1 protein expression and binding of FGF-2, HB-EGF, and anti-HS mAb 10E4 in a subset of renal biopsies.

Case	Diagnosis	Syndecan-1 ^A	FGF-2 binding ^A	HB-EGF binding ^A	Anti-HS mAb 10E4 ^A
1	Control	5	0	5	nd ^B
2	Control	20	0	30	nd
3	Control	10	0	0	nd
4	Control	0	nd	0	8
5	Control	20	nd	nd	46
6	Control	5	nd	nd	10
7	Control	30	nd	nd	3
8	Tx-MHA	80	0	70	nd
9	Tx-MHA	60	0	70	72
10	Tx-MHA	90	0	80	nd
11	Tx-MHA	80	0	nd ^B	77
12	Tx-MHA	80	0	40	73
13	Tx-MHA	90	nd	nd	82
14	Tx-IFTA	60	0	30	53
15	Tx-IFTA	30	0	0	1
16	Tx-IFTA	20	10	10	13
17	Tx-IFTA	0	0	0	nd
18	Non-Tx IFTA	10	0	0	2
19	Non-Tx IFTA	30	0	30	22
20	Non-Tx IFTA	60	0	0	nd
21	Non-TxIFTA	60	nd	nd	36

^A percentage of TECs positive for expression/binding

^B nd= not determined

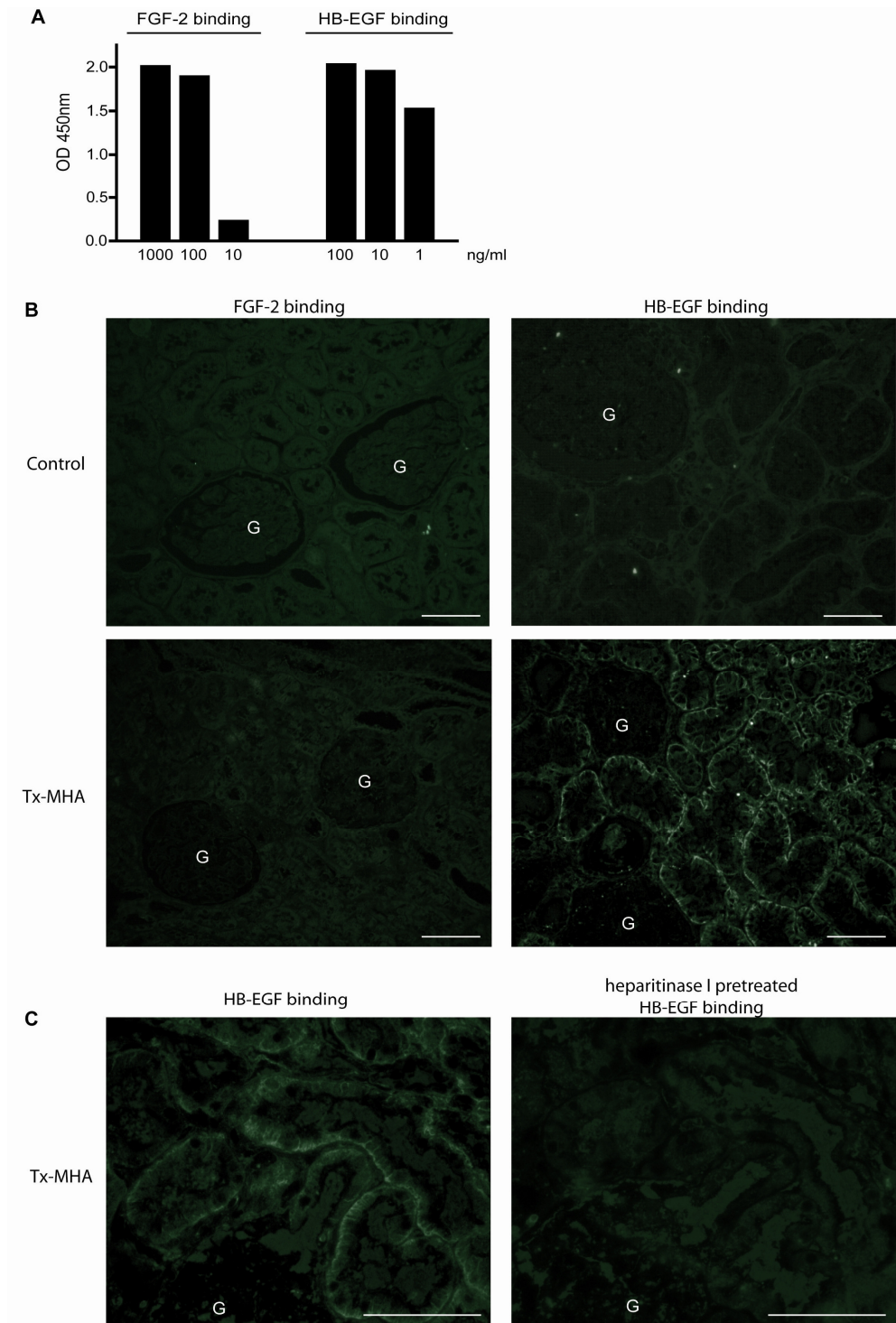


Figure 4. Specific binding of HB-EGF, but not FGF-2, to basolateral TEC HSPGs in Tx-MHA biopsies. (A) Dose-dependent binding of HB-EGF and FGF-2 to heparin-albumin *in vitro*. (B) Binding of FGF-2 (left) or HB-EGF (right) to control kidney (upper panels) and Tx-MHA biopsies (lower panels). (C) Basolateral TEC binding of HB-EGF in Tx-MHA binding is lost after pre-incubation of a sequential tissue section with heparitinase I. G=glomerulus, bar=50µm.

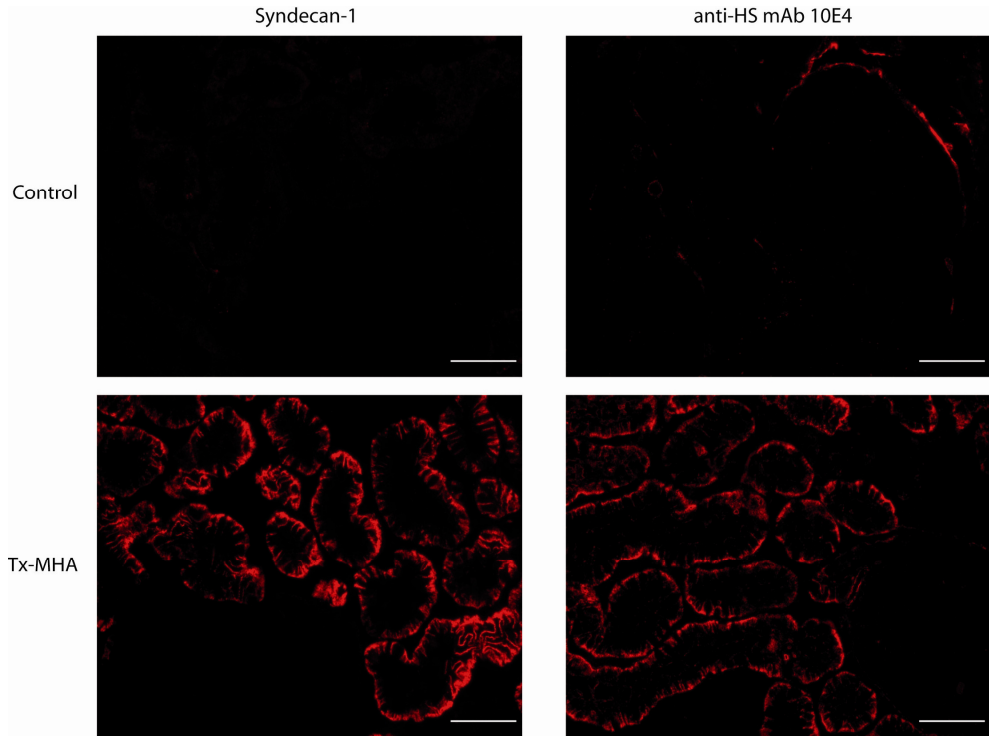


Figure 5. Specific binding of anti-HS mAb 10E4 in syndecan-1 positive biopsies. Staining of syndecan-1 (left) and HS 10E4 epitope (right) in control kidney (upper panel) and Tx-MHA biopsy (lower panel). Note the absence of syndecan-1 and 10E4 HS staining in control tissue, whereas 10E4 HS positivity co-localizes with baso-lateral syndecan-1 in representative Tx-MHA biopsy. Bar = 50 µm.

Syndecan-1 deficient mice are more susceptible to renal IRI and show repair skewed to fibrosis

To determine the *in vivo* importance of syndecan-1 in renal IRI, we next performed bilateral warm IRI in syndecan-1 deficient mice (16;26). Anticipating a more severe phenotype in syndecan-1^{-/-}, we used a relatively mild IRI model (25 min bilateral warm ischemia, followed by bilateral reperfusion). Induction of syndecan-1 in the WT mice was evidenced from day 1 onwards, which by definition was not observed in the syndecan-1 KO mice (Fig 6A-E). Compared to wildtype mice, syndecan-1^{-/-} proved to be more susceptible to IRI-induced renal damage (Fig.6&7).

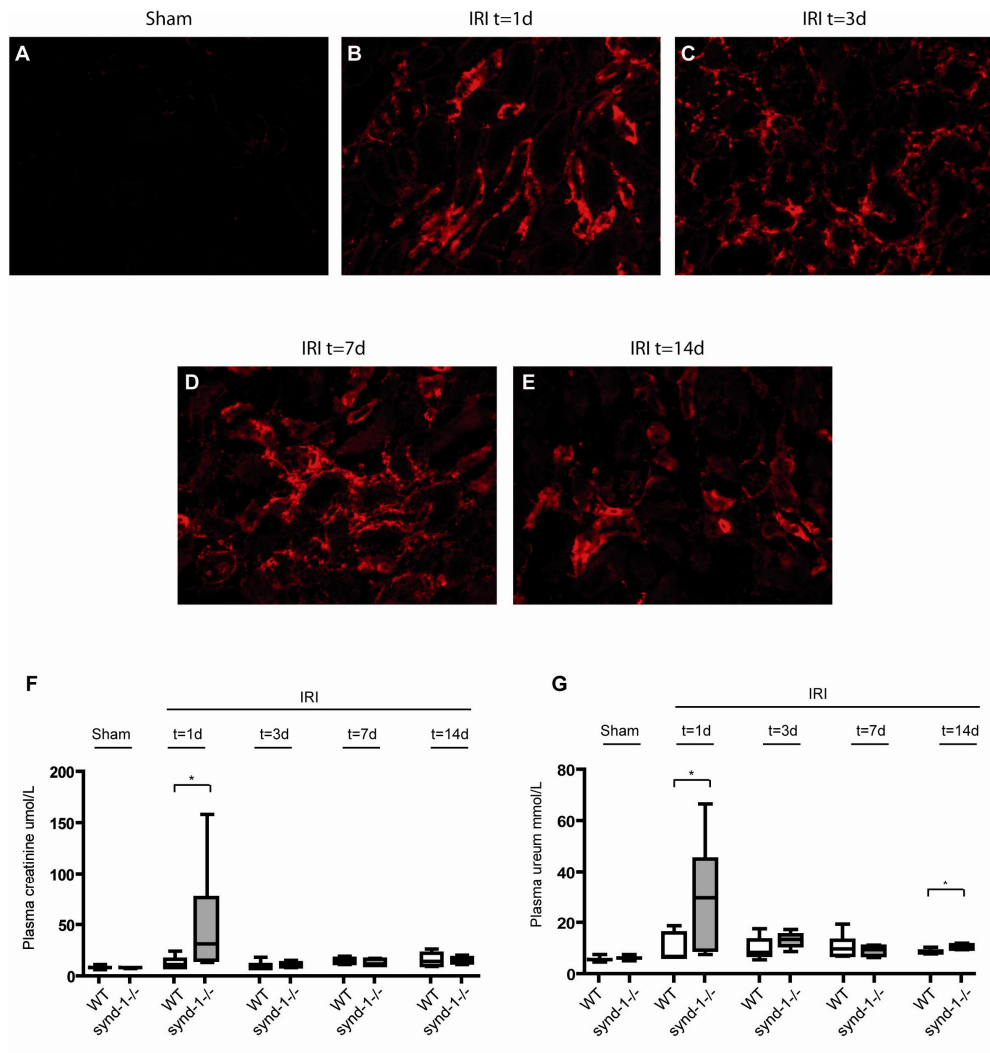


Figure 6. Impaired renal function upon bilateral IRI in syndecan-1^{-/-} compared to wildtype mice. Renal IRI was performed by bilateral clamping of renal pedicles for 25 min (warm ischemia), followed by bilateral reperfusion. (A) Syndecan-1 expression is nearly absent in sham-operated wildtype animals, whereas tubular syndecan-1 is clearly induced in cortical regions upon I/R from (B) day 1, (C) day 3, (D) day 7 to (E) day 14. Plasma creatinine (F) and ureum (G) were determined at indicated timepoints, and were increased compared to wildtype at day 1 and 14 (for plasma ureum). *p<0.05 (Mann-Whitney test)

At day 1 after IRI, plasma creatinine and ureum levels were significantly increased in syndecan-1^{-/-} compared to wildtype mice (Fig.6F and G). Histologically, clearly more tubular damage was observed in syndecan-1^{-/-} kidneys at day 1 after IRI (Fig.7A,C). Interestingly, tubular damage appeared to remain constant over time in syndecan-1^{-/-} kidneys, while damage was largely restored in wildtype kidneys at day 14 after IRI

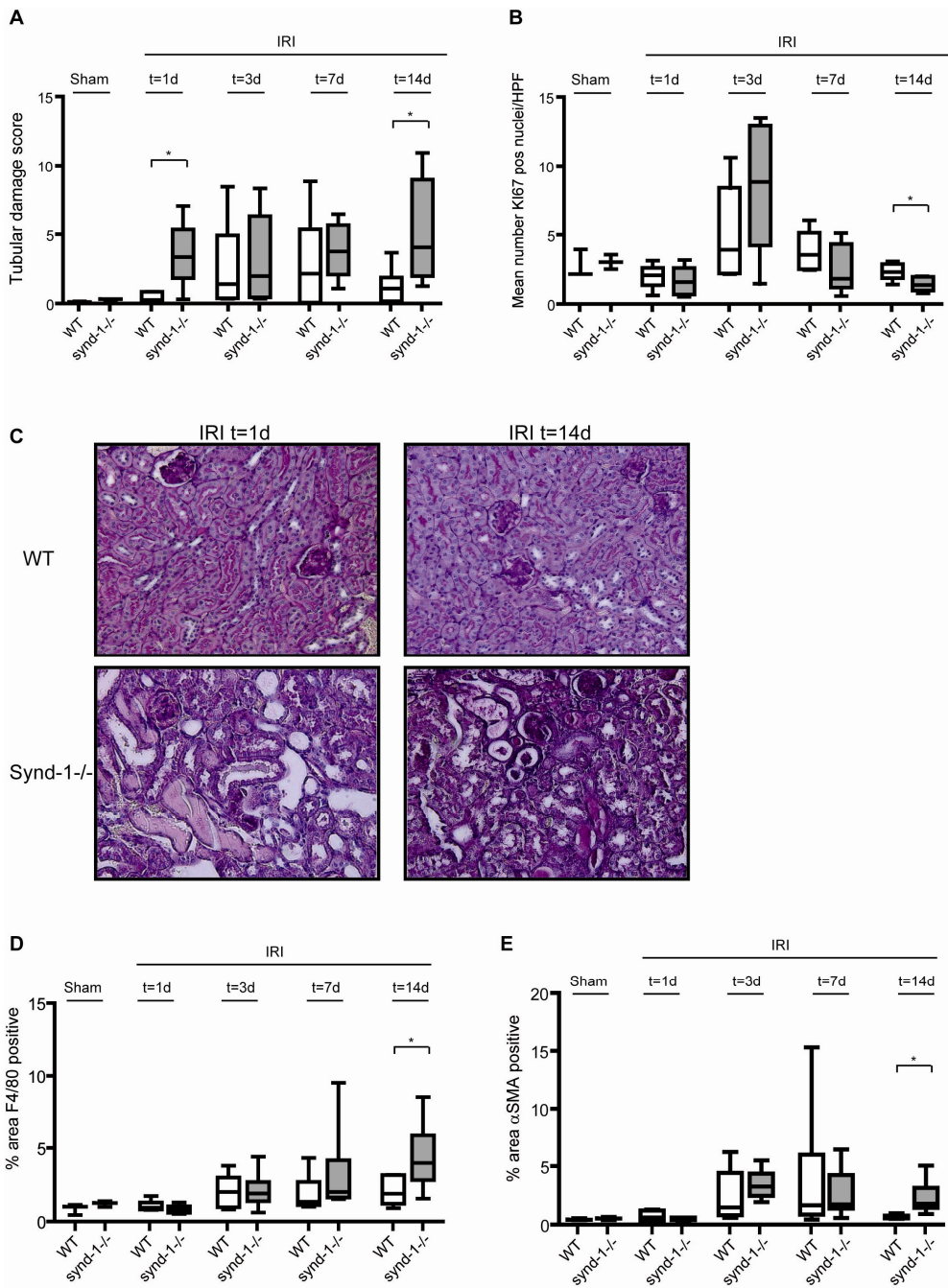


Figure 7. Increased tubular damage, reduced proliferation, and increased amounts of macrophages and myofibroblasts in syndecan-1^{-/-} kidneys upon bilateral IRI. Renal IRI was performed by bilateral clamping of renal pedicles for 25 min (warm

ischemia), followed by bilateral reperfusion. (A) Increased tubular damage was observed at day 1 and 14 after IRI, whereas (B) reduced tubular proliferation (Ki67 positive tubular cells) was observed at day 14 in the syndecan-1 KO mice. (C) Representative photographs of PAS-stained kidney sections of wildtype and syndecan-1^{-/-} at day 1 and 14 after IRI. (D) Monocytes/macrophages (F4/80 staining) appear to accumulate over time upon IRI in syndecan-1^{-/-} compared to wildtype, with significantly more monocyte/macrophages in syndecan-1^{-/-} kidneys at day 14. (E) Myofibroblasts (α SMA staining) are increased in syndecan-1^{-/-} kidneys compared to wildtype at day 14 after IRI. *p<0.05 (Mann-Whitney test)

(Fig.7A,C). By Ki67 staining we evaluated the proliferative response of the tubular epithelium both in wildtype and syndecan-1 KO mice. Although there is quite some proliferation at day 3 after I/R (not different between both groups), at day 7 and 14 of the regeneration phase the syndecan-1 KO mice revealed lower proliferation rates compared to the WT (day 14: p=0.0411; Fig.7B).

Both macrophages and myofibroblasts are known to play an important role in renal IRI damage/repair responses. We therefore quantified the amounts of these cells by staining for F4/80 (monocytes/macrophages) and α -SMA (myofibroblasts). As shown in Fig.7D, monocytes/macrophages steadily accumulated in syndecan-1^{-/-} compared to wildtype kidneys. Interestingly, also the amount of myofibroblasts was increased in syndecan-1^{-/-} compared to wildtype kidneys at day 14 after IRI (Fig.7E).

Together, these data show that syndecan-1^{-/-} mice have impaired renal function and increased tubular damage upon renal IRI compared to wildtype mice. In addition, our data indicate that tubular damage is restored less efficiently in syndecan-1^{-/-} mice, and repair mechanisms may be skewed towards fibrosis rather than restoration of tubular epithelium.

Discussion

In this study, we show that syndecan-1 protein expression is increased on the basolateral side of TECs after renal transplantation and that the percentage of syndecan-1 positive TECs is significantly associated with better allograft function and survival. We provide evidence that syndecan-1 is involved in TEC proliferation, and that binding of the growth factor HB-EGF to TEC HSPGs is increased on the basolateral side of TECs that also express syndecan-1. Finally, we show that syndecan-1 deficient mice show more impaired renal function, increased tubular damage associated with reduced tubular repair in an experimental IRI model. Based on our data, the role of syndecan-1 in the renal epithelium may be similar to its role in dermal wound healing(10;16). Indeed, we show that shRNA mediated knockdown of syndecan-1 expression in a TEC cell line significantly reduces cell proliferation, affirming a role of syndecan-1 in tubular re-epithelialization and repair. The involvement of HB-EGF in TEC proliferation and renal epithelial repair has been proposed earlier(24;25). Moreover, in a murine I/R experiment we show that syndecan-1 promotes survival (day 1) and proliferation/repair (day 14) of injured epithelial cells, probably by acting as co-receptors for survival/growth factors such as hepatocyte growth factor, stromal derived factor and HB-EGF.

Tubular induction of syndecan-1 likely reflects a certain degree of de-differentiation of the tubular cells in order to be responsive after transplantation and permanent immunological attack. Thus, renal tubular syndecan-1 expression probably reflects a meaningful early epithelial mesenchymal transition response and mirrors syndecan-1 expression of the developing kidney (18). The presence of syndecan-1 on epithelial cells brings the cells in a mobilized condition, now able to respond effectively to growth factors such as HB-EGF. We speculate that the loss of syndecan-1 in a number of transplantation biopsies is due to further de-differentiation and/or more advanced epithelial mesenchymal transition. These fully de-differentiated epithelial cells are not able to respond to survival/growth factors anymore and will contribute to chronic inflammation and IFTA. In our opinion, this interpretation nicely corresponds to the concept of Venkatachalam et al. (19), that prolonged deep de-differentiation of tubular cells contribute to progression in chronic kidney disease. Our data are also in line with the findings of Halloran et al. (5), who showed that impaired renal function in transplantation biopsies is correlated with increased expression of tissue injury gene sets and decreased expression of kidney transcripts, indicating de-differentiation of renal epithelial cells. We thus conclude that the tubular induction of syndecan-1 reflects a physiological response of the epithelium in order to maintain/restore tubular integrity and regeneration/repair.

The mechanism behind increased expression of syndecan-1 protein was not specifically addressed in this study. There are indications that syndecan-1 transcription can be regulated by the pro-inflammatory transcription factor NF- κ B, as well as by an FGF-inducible response element located upstream of the syndecan-1 promoter(27-29). Both pathways are relevant in the context of renal transplantation(30;31). Furthermore, both TGF- β and EGF have been shown to induce syndecan-1 mRNA expression *in vitro*, and expression/activation of these factors is enhanced upon renal transplantation, although especially TGF- β has been associated with fibrosis, and EGF with proliferation(28;32-34). Apart from transcriptional regulation, increased staining for syndecan-1 protein could be a result of reduced syndecan-1 shedding from the cell surface.

From a clinical point of view, it would be interesting to assess whether syndecan-1 concentration and binding properties in urine of patients after renal allograft transplantation are of diagnostic value to predict allograft status and survival (ongoing, van den Born et al.). In addition, since immunosuppressive drugs used in the context of renal transplantation are typically anti-proliferative, it would be interesting to investigate their effect on syndecan-1 expression and/or growth factor binding.

As far as we know syndecan-1 is the first tubular marker that is positively associated with graft function and survival. Other tubular markers such as KIM-1 (35;36) and NGAL (37) or typical tubular EMT markers such as vimentin and S100A4 (38) are negatively associated with graft function and graft loss. Therefore, larger studies with protocol biopsies have to show whether tubular syndecan-1 might be a novel independent, prognostic marker able to predict graft function and survival on long term.

In conclusion, our data provide evidence for a role of syndecan-1 in tubular epithelial survival and repair in the renal allograft. We propose that syndecan-1 can help shift the balance in the renal allograft towards functional restoration, rather than non-functioning scarring (fibrosis).

Acknowledgements

We thank Dr. P.D. Bezemer and Dr. D.J. Kuik (Dept. Clinical Epidemiology and Biostatistics, VU University Medical Center) for statistical advice and A. Kuil and M. Bulthuis (Depts. Pathology, Academic Medical Center, Amsterdam and University Medical Center Groningen, respectively) for technical assistance.

Disclosures

None to be declared

References

1. Grinyo JM. Role of ischemia-reperfusion injury in the development of chronic renal allograft damage. *Transplant Proc* 2001, 33: 3741-3742
2. Lien YH, Lai LW, and Silva AL. Pathogenesis of renal ischemia/reperfusion injury: lessons from knockout mice. *Life Sci* 2003, 74: 543-552
3. Hoffmann SC, Kampen RL, Amur S, et al. Molecular and immunohistochemical characterization of the onset and resolution of human renal allograft ischemia-reperfusion injury. *Transplantation* 2002, 74: 916-923
4. Nankivell BJ and Chapman JR. Chronic allograft nephropathy: current concepts and future directions. *Transplantation* 2006, 81: 643-654
5. Bunnag S, Einecke G, Reeve J, et al. Molecular correlates of renal function in kidney transplant biopsies. *J Am Soc Nephrol* 2009, 20: 1149-1160
6. Celie JW, Rutjes N, Keuning ED, et al. Subendothelial heparan sulfate proteoglycans become major L-selectin and MCP-1 ligands upon renal ischemia/reperfusion. *Am J Pathol* 2007, 170: 1865-1878
7. Celie JW, Reijmers RM, Slot EM, et al. Tubulointerstitial heparan sulfate proteoglycan changes in human renal diseases correlate with leukocyte influx and proteinuria. *Am J Physiol Renal Physiol* 2008, 294: F253-F263
8. Esko JD and Selleck SB. Order out of chaos: assembly of ligand binding sites in heparan sulfate. *Annu Rev Biochem* 2002, 71: 435-471
9. Prydz K and Dalen KT. Synthesis and sorting of proteoglycans. *J Cell Science* 2000, 113: 193-205
10. Alexopoulou AN, Multhaupt HA, and Couchman JR. Syndecans in wound healing, inflammation and vascular biology. *Int J Biochem Cell Biol* 2007, 39: 505-528
11. Parish CR. The role of heparan sulphate in inflammation. *Nat Rev Immunol* 2006, 6: 633-643
12. Whitelock JM and Iozzo RV. Heparan sulfate: a complex polymer charged with biological activity. *Chem Rev* 2005, 105: 2745-2764
13. Wang L, Fuster M, Sriramarao P, et al. Endothelial heparan sulfate deficiency impairs L-selectin- and chemokine-mediated neutrophil trafficking during inflammatory responses. *Nat Immunol* 2005, 6: 902-910
14. Kreuger J, Spillmann D, Li JP, et al. Interactions between heparan sulfate and proteins: the concept of specificity. *J Cell Biol* 2006, 174: 323-327
15. Elenius K, Vainio S, Laato M, et al. Induced expression of syndecan in healing wounds. *J Cell Biol* 1991, 114: 585-595
16. Stepp MA, Gibson HE, Gala PH, et al. Defects in keratinocyte activation during wound healing in the syndecan-1-deficient mouse. *J Cell Sci* 2002, 115: 4517-4531
17. Kato M, Saunders S, Nguyen H, et al. Loss of cell surface syndecan-1 causes epithelia to transform into anchorage-independent mesenchyme-like cells. *Mol Biol Cell* 1995, 6: 559-576
18. Vainio S, Lehtonen E, Jalkanen M, et al. Epithelial-mesenchymal interactions regulate the stage-specific expression of a cell surface proteoglycan, syndecan, in the developing kidney. *Dev Biol* 1989, 134: 382-391
19. Venkatachalam MA, Griffin KA, Lan R, et al. Acute kidney injury: a springboard for progression in chronic kidney disease. *Am J Physiol Renal Physiol* 2010, 298: F1078-1094
20. Guerrini M, Hricovini M, and Torri G. Interaction of heparins with fibroblast growth factors: conformational aspects. *Curr Pharm Des* 2007, 13: 2045-2056
21. Chu CL, Goerges AL, and Nugent MA. Identification of common and specific growth factor binding sites in heparan sulfate proteoglycans. *Biochemistry* 2005, 44: 12203-12213
22. Raab G and Klagsbrun M. Heparin-binding EGF-like growth factor. *Biochim Biophys Acta* 1997, 1333: F179-F199
23. Clayton A, Thomas J, Thomas GJ, et al. Cell surface heparan sulfate proteoglycans control the response of renal interstitial fibroblasts to fibroblast growth factor-2. *Kidney Int* 2001, 59: 2084-2094
24. Zhuang S, Kinsey GR, Rasbach K, et al. Heparin-binding epidermal growth factor and Src family kinases in proliferation of renal epithelial cells. *Am J Physiol Renal Physiol* 2008, 294: F459-F468

25. Sakai M, Zhang M, Homma T, et al. Production of heparin binding epidermal growth factor-like growth factor in the early phase of regeneration after acute renal injury. Isolation and localization of bioactive molecules. *J Clin Invest* 1997, 99: 2128-2138
26. Alexander CM, Reichsman F, Hinkes MT, et al. Syndecan-1 is required for Wnt-1-induced mammary tumorigenesis in mice. *Nat Genet* 2000, 25: 329-332
27. Watanabe A, Mabuchi T, Satoh E, et al. Expression of syndecans, a heparan sulfate proteoglycan, in malignant gliomas: participation of nuclear factor-kappaB in upregulation of syndecan-1 expression. *J Neurooncol* 2006, 77:25-32
28. Jaakkola P and Jalkanen M. Transcriptional regulation of Syndecan-1 expression by growth factors. *Prog Nucleic Acid Res Mol Biol* 1999, 63: 109-138
29. Jaakkola P, Vihinen T, and Jalkanen M. Proximal promoter-independent activation of the far-upstream FGF-inducible response element of syndecan-1 gene. *Biochem Biophys Res Commun* 2000, 278: 432-439
30. Loverre A, Ditunno P, Crovace A, et al. Ischemia-reperfusion induces glomerular and tubular activation of proinflammatory and antiapoptotic pathways: differential modulation by rapamycin. *J Am Soc Nephrol* 2004, 15: 2675-2686
31. Villanueva S, Cespedes C, and Vio CP. Ischemic acute renal failure induces the expression of a wide range of nephrogenic proteins. *Am J Physiol Regul Integr Comp Physiol* 2006, 290: R861-R870
32. Hayashida K, Johnston DR, Goldberger O, et al. Syndecan-1 expression in epithelial cells is induced by transforming growth factor beta through a PKA-dependent pathway. *J Biol Chem* 2006, 281: 24365-24374
33. Liu Y. Renal fibrosis: new insights into the pathogenesis and therapeutics. *Kidney Int* 2006, 69: 213-217
34. Stein-Oakley AN, Tzanidis A, Fuller PJ, et al. Expression and distribution of epidermal growth factor in acute and chronic renal allograft rejection. *Kidney Int* 1994, 46: 1207-1215
35. van Timmeren MM, Vaidya VS, van Ree RM, et al. High urinary excretion of kidney injury molecule-1 is an independent predictor of graft loss in renal transplant recipients. *Transplantation* 2007, 84: 1625-1630
36. Malyszko J, Koc-Zorawska E, Malyszko JS, et al. Kidney injury molecule-1 correlates with kidney function in renal allograft recipients. *Transplant Proc* 2010, 42: 3957-3959
37. Nauta FL, Bakker SJ, van Oeveren W, et al. Albuminuria, proteinuria, and novel urine biomarkers of long-term allograft outcomes in kidney transplant recipients. *Am J Kidney Dis* 2011, 57: 733-743
38. Vongwiwatana A, Tasanarong A, Rayner DC, et al. Epithelial to mesenchymal transition during late deterioration of human kidney transplants: the role of tubular cells in fibrogenesis. *Am J Transplant* 2005, 5: 1367-1374
39. Racusen LC, Solez K, Colvin RB, et al. The Banff 97 working classification of renal allograft pathology. *Kidney Int* 1999, 55: 713-723
40. Racusen LC, Halloran PF, and Solez K. Banff 2003 meeting report: new diagnostic insights and standards. *Am J Transplant* 2004, 4: 1562-1566
41. Solez K, Colvin RB, Racusen LC, et al. Banff '05 Meeting Report: differential diagnosis of chronic allograft injury and elimination of chronic allograft nephropathy ('CAN'). *Am J Transplant* 2007, 7: 518-526
42. Solez K, Colvin RB, Racusen LC, et al. Banff 07 classification of renal allograft pathology: updates and future directions. *Am J Transplant* 2008, 8: 753-760
43. van den Born J, Gunnarsson K, Bakker MA, et al. Presence of N-unsubstituted glucosamine units in native heparan sulfate revealed by a monoclonal antibody. *J Biol Chem* 1995, 270: 31303-31309
44. van den Born J, van den Heuvel LP, Bakker MA, et al. Production and characterization of a monoclonal antibody against human glomerular heparan sulfate. *Lab Invest* 1991, 65: 287-297
45. David G, Bai XM, Van der Schueren B, Cassiman JJ, et al. Developmental changes in heparan sulfate expression: in situ detection with mAbs. *J Cell Biol* 1992, 119: 961-975
46. Snow AD, Mar H, Nochlin D, et al. Early accumulation of heparan sulfate in neurons and in the beta-amyloid protein-containing lesions of Alzheimer's disease and Down's syndrome. *Am J Pathol* 1990, 137: 1253-1270
47. Ryan MJ, Johnson G, Kirk J, et al. HK-2: an immortalized proximal tubule epithelial cell line from normal adult human kidney. *Kidney Int* 1994, 45: 48-57.

Suppl. Table 1: Histological characteristics per diagnosis group (according to BANFF criteria).

Diagnosis	n	Acute tubular necrosis	Epithelial vacuolisation	Vasculopathy	C4d staining	Tubular atrophy	Tubulitis	Interstitial inflammation	Intersitial fibrosis	Global glomerulosclerosis
Control	14	0	0	0	0	0	0	0	1	0
Tx-Protocol	9	0	0	0	0	0	0	0	0	0
Tx-MHA	25	2	0	0	1	4	0	4	7	4
Tx-AR	28	6	1	14	5	12	24	26	20	9
Tx-IFTA	33	1	0	0	2	27	2	27	24	20
Non-Tx IFTA	20	0	0	0	0	17	0	17	15	13

Values are expressed as number of cases showing indicated pathology

.

Chapter 7

General discussion and future perspectives

In this thesis, studies were designed and performed to increase our knowledge on the role of proteoglycans in tissue remodeling associated with chronic renal transplant dysfunction (CTD). CTD is characterized by decline in kidney function over time and is histologically characterized by focal glomerulosclerosis (FGS), interstitial fibrosis and tubular atrophy (IF/TA), and transplant vasculopathy.

To better understand the pathogenesis of CTD and identify targets of intervention, we investigated the expression and involvement of various proteoglycans in a rat CTD model. Numerous studies have shown that proteoglycans, especially HSPGs, are able to bind a myriad of proteins that include growth factors, cytokines and adhesion molecules and act as co-receptors and thereby involved in various cell functions. The role of HSPGs in remodeling of the various functional compartments of the kidney after transplantation is discussed below.

Involvement of HSPGs in glomerulosclerosis

After renal transplantation, glomerulosclerosis is one of the histopathological hallmarks which is associated with development of proteinuria. The data presented in chapters 2 and 3, showed glomerular upregulation of the HSPG perlecan in renal allografts at both mRNA and protein levels. Similarly, the pro-fibrotic heparin binding growth factor FGF2 accumulated in the glomeruli of the allografted kidneys. Data presented in chapters 2 and 3 furthermore showed a massive increase in matrix HSPG-mediated binding capacity for FGF2. Enhanced binding capacity for this growth factor was the result of increased HSPG (like perlecan) expression, and modified HS sulfation [most likely increased 2-O sulfation leading to loss of JM-403 staining (1) and increased FGF2 binding (2)]. This finding suggests that upon allo-transplantation the kidney mobilizes matrix HSPGs to become docking molecules for heparin-binding growth factors such as FGF2. This was also reported by Morita et al. (3) showing increased FGF2 binding in fibrotic areas in native kidney diseases. *In vitro* studies reported in chapter 3 support that the FGF2-driven proliferation of mesangial cells crucially depends on the sulfation of mesangial HSPGs, indicating that the observed differential expression of perlecan and FGF2 in the renal allografts most likely also have functional consequences.

Involvement of HSPGs in neo-intima formation

Neo-intima formation is a central event in the pathogenesis of transplant vasculopathy. Neo-intimal tissue consists of migrated smooth muscle cells (SMCs), infiltrated immune cells and extracellular matrix components. In chapter 5 we focused on the molecular pathways in the arterial media which facilitate neointima formation. Enhanced expression of *Pdgfb* in the neointima was accompanied by increased expression of *Pdgfrb* in the allograft media. PDGF-BB is well documented to act as a potent mitogen and

chemoattractant for SMCs, leading to intimal thickening (4,5). PDGF-BB is also a known mediator of SMC phenotypic modulation (6). Our observations support a role of PDGF-BB in phenotype switching of medial SMCs after allogeneic transplantation resulting in subsequent chemoattraction towards the developing neointima. PDGF-BB is known to be a heparin-binding growth factor. It has been shown in vascular development that PDGF-BB-dependent pericyte recruitment and migration is critically dependent on HSPGs (7). Recently it has been shown that neointima formation is attenuated in syndecan-4 KO mice, and that PDGF-BB- and FGF2-induced proliferation of vascular SMCs is impaired in syndecan-4 KO cells (8).

In chapter 2 we showed abundant expression of basement membrane (BM) HSPGs collagen type XVIII and perlecan and interstitial chondroitin/dermatan sulfate (CS/DS) PGs versican in the neo-intimas of CTD kidneys. Upregulated Collagen type XVIII expression in neointima has not been reported before and the potential role of this proteoglycan is as yet unknown. Previously it has been shown that perlecan expression in arteries is associated with inhibition of SMC proliferation and reduced intimal hyperplasia (9-12) which favors for a role of perlecan in neointima stabilization. However, data reported by others indicate that arterial HSPGs can actually activate SMC proliferation by modulating the function of basic fibroblast growth factor (FGF2) (13). Based on these results from chapters 2 and 5 we speculate arterial HSPGs to be involved in PDGF-BB- and possibly FGF2-mediated proliferation and migration of the VSMCs and thereby contribute to neointima formation. Future experiments targeting PDGF-B and/or FGF2 pathways in HS mutated versus wild type animals might reveal the impact of our findings.

Involvement of HSPGs in inflammation and tubulo-interstitial fibrosis

As shown in chapter 2 there is an increase of perlecan in the endothelial BM of peritubular capillaries in rat renal allografts when compared to the non-transplanted controls and isografts. The upregulated expression upon transplantation suggests that these molecules are involved in inflammatory leukocyte influx, since our group previously showed perlecan and collagen XVIII to be involved in leukocyte recruitment upon renal ischemia/reperfusion (14). Recently, we extended these studies in mice deficient for collagen XV, collagen XVIII and the compound double mutant mice. These yet unpublished results indeed confirm the crucial role of subendothelial BM HSPGs in leukocyte recruitment. Related to this finding, in chapter 5 we documented a reduced influx of CD45+ leukocytes in allograft kidneys upon treatment with RO-heparin. This indicates that heparin-like polysaccharides, most likely heparan sulfates, are indeed involved in leukocyte recruitment.

The increased Collagen XVIII and perlecan in the tubular BM of allograft kidneys could play a role in the EMT process by binding of chemokines and growth factors resulting in a

concentration gradient over the tubular BM (15). This gradient might then direct migration of tubular epithelial cells into the interstitium during EMT. Recently it has been demonstrated that heparanase is crucially involved in induction of EMT by FGF-2 in proximal tubular epithelial cells (16). In addition to tubular atrophy and EMT, proteoglycan expression in the tubular BM could be involved in binding of L-selectin and chemokines such as MCP-1, thereby facilitating inflammatory responses in tubules (14,17). We also showed expression of versican in interstitial fibrosis (IF) (chapter 2), which is likely involved in leukocyte recruitment and infiltration by its L-selectin-binding capacity (14,18). The abundant versican expression in IF supports our previous finding that L-selectin in the interstitium binds to CS/DS side chains and not HS side chains (19). Moreover, the high L-selectin-binding capacity of CS/DSPGs in IF fits well with our observation that most leukocyte infiltration was observed in interstitial regions and to a far lesser extent in neointimal lesions and within the glomeruli, suggesting that these interstitial GAGs form a retention motif for infiltrated leukocytes.

Involvement of HSPGs in lymphangiogenesis

In chapter 2 we showed a marked increase of lymph angiogenesis in allografts, which was accompanied by the expression of perlecan at the abluminal side of lymphatic endothelium. This expression of perlecan in close proximity of lymphatic endothelial cells suggests a functional role for perlecan in lymph angiogenesis. This is supported by results from studies performed in a mouse model for regenerating skin which suggest that perlecan is involved in lymphatic endothelial cell migration, lymphatic organization and maturation (20). In addition, also versican, which was abundantly present in the interstitium of CTD kidneys, might play a role in lymph angiogenesis (21). Recently it has been shown that lymphatic endothelial heparan sulfate is required for the lymphatic endothelial cell growth and sprouting by binding to key lymphangiogenic growth factor VEGF-C (22). Indeed, preliminary data in our heparinoids intervention study (chapter 5) suggest a reduction in lymph vessel density upon treatment with heparin. In our study in chapter 2, increased lymph angiogenesis correlated with reduced graft function. The existence of a causal relation between lymph angiogenesis and loss of graft function, however, needs to be established in future studies.

Involvement of HSPGs in epithelial survival and repair

Syndecan-1, a transmembrane cell surface proteoglycan, is known to be involved in epithelial regeneration and repair upon wound healing (23-25). In chapter 6 we show that syndecan-1 protein expression increased in tubular epithelial cells at the basolateral side after human renal transplantation, which is significantly associated with better allograft function and survival. We confirmed a fundamental role of syndecan-1 in tubular cell

survival and repair by *in vitro* studies and by *in vivo* experiments in syndecan-1 KO mice. These data highlight the importance of the epithelial compartment for renal function. Our data suggest that promoting epithelial syndecan-1 might be a promising way to improve renal function in transplanted kidneys and possibly in native renal diseases as well. The mechanism behind increased expression of syndecan-1 protein was not specifically addressed in this study. There are indications that syndecan-1 transcription can be regulated by the pro-inflammatory transcription factor NF- κ B, as well as by an FGF-inducible response element located upstream of the syndecan-1 promoter (26-28). Both pathways are relevant in the context of renal transplantation (29,30). Furthermore, both TGF- β and EGF have been shown to induce syndecan-1 mRNA expression *in vitro*, and expression/activation of these factors is enhanced upon renal transplantation, although especially TGF- β has been associated with fibrosis, and EGF with proliferation (27,31-33). Apart from transcriptional regulation, increased staining for syndecan-1 protein could be a result of reduced syndecan-1 shedding from the cell surface. Down-modulation of syndecan-1 shedding might be an interesting therapeutic target point. Syndecan-1 ectodomain can be shedded by a number of MMPs and other proteolytic enzymes (34,35), most promising candidate being ADAM17/TACE (36). We recently described a role for ADAM17 in renal transplant dysfunction (37), not known however is whether preserved syndecan-1 accounted for the results.

From a clinical point of view, it would be interesting to assess whether syndecan-1 concentration and binding properties in urine of patients after renal allograft transplantation are of diagnostic value to predict allograft status and survival (ongoing, van den Born et al.). As far as we know syndecan-1 is the first tubular marker that is positively associated with graft function and survival. Other tubular markers such as KIM-1(38,39) and NGAL (40) or typical tubular EMT markers such as vimentin and S100A4 (41) are negatively associated with graft function and graft loss. Prospective studies with protocol biopsies could have the potential to show whether tubular syndecan-1 might be a novel independent, player in tubular repair processes. Accordingly, it would be interesting to investigate whether urinary syndecan-1 excretion could be a non-invasive marker of renal tubular repair, and whether it has independent prognostic power for renal outcome.

HSPGs as therapeutic target

Although the advances in immunosuppressive treatment resulted in a sharp decline in the incidence of acute rejection, the long term graft survival rates have hardly or not improved over the last decade. Over time the graft develops CTD associated with massive tissue remodeling. In addition to the immunosuppressive regimen, current treatment in the renal transplant recipients targets common risk factors for renal function loss and cardiovascular complications, such as proteinuria, hypertension and hyperlipidemia but until now there is no therapy available to retard tissue remodeling in CTD. Accordingly, novel therapeutic

modalities to retard tissue remodeling in the process of CTD, that includes inflammation, unlimited proliferation and fibrosis, might provide novel perspectives to improve outcome. Based on previous research on the involvement of HSPGs in inflammation, proliferation and fibrosis, these glycoconjugates could be interesting target molecules to retard CTD. Especially in the field of oncology, HSPGs are considered as therapeutic molecules or targets (42). Exogenously administered heparin-like glycomimetica interfere with the growth factor signaling and inflammation (43-45). This would be especially relevant in developing CTD. As long term heparin administration will chronically inhibit the coagulation system, this might result in severe complications (46). This led to the invention of various heparin derivatives that include non-anti-coagulant heparins, low molecular weight heparins (LMWH), HS mimetics, chemically prepared oligosaccharides and synthetic heparins(43,44,47-49). LMWH has been shown to be effective in binding inflammatory cytokines and down regulating expression of MHC (class I and class II) and ICAM-1, independently of anticoagulant capacity (50). In experimental models, treatment with non-anticoagulant LMWH showed prolonged skin, cardiac and renal allograft survival with beneficial outcomes (48,51-53). In addition, LMWH decreases mesangial proliferation and matrix expansion (54,55). Human data after renal transplantation suggest that LMWH may possess renoprotective properties in human renal transplantation as well (56). In chapter 4, it has been shown that treatment with non-anticoagulant heparin, RO-heparin, reduces the clinical parameters such as urinary protein, serum triglycerides and in addition ameliorates renal inflammation. Recently it has been demonstrated that intervention with a LMWH, sulodexide, was not renoprotective in patients with type 2 diabetes, renal impairment, and macroalbuminuria (57). Although sulodexide has similar structure as unfractionated heparin, it has a lower degree of sulfation and shorter polysaccharide length compared to normal unfractionated heparin and RO-heparin (58). Altogether, these data provide a rationale for clinical studies in renal transplant recipients using a non-anticoagulant heparinoid as add on drug next to standard immunosuppressive medication, eventually with graft survival as hard endpoint, and GFR loss over time and proteinuria development as intermediate endpoints.

Alternative approaches to use HSPGs as targets could be the use of antibodies that recognize and thereby block specific HS-motifs/domains. It was demonstrated by *in vitro* experiments that 6-O-sulfate specific anti-HS antibodies produced in a phage-display library can inhibit leukocyte rolling and firm adhesion to glomerular endothelial cells (59). In addition, generation of non-GAG binding chemokines can interfere with chemokine receptor signaling (60). Recently, a novel approach was presented using biologically inactive CXCL8 with however significantly increased binding affinity for GAGs, thereby competing of endogenous CXCL8 from endothelial GAGs resulting signaling down modulation of the corresponding chemokine receptor (61). Together, there are many options for the use of HSPGs in therapeutic strategies, although many need further development and proof of efficacy *in vivo*.

Conclusions

The data presented in this thesis show the involvement of PGs in CTD tissue remodeling. We showed an upregulation of the HSPGs, collagen type XVIII and perlecan and CSPG versican in rat renal allografts. The binding properties of the upregulated PGs has increased upon renal allo transplantation. Perlecan and FGF2 were found to be upregulated in renal allografts. The functional and mechanistical role of these HSPGs were studied *in vitro* using rat mesangial cells. The results showed that HSPGs mediated FGF2-dependent proliferation of mesangial cells. Treatment with non-anti-coagulant heparin (RO-heparin) showed beneficial effects after rat renal transplantation. Considering the molecular mechanisms behind neointima formation, we showed that in response to allogeneic transplantation there will be medial dedifferentiation, probably mediated by PDGF-B. Lastly we showed that syndecan-1, a trans-membrane cell surface proteoglycan, is involved in tubular regeneration and repair after renal transplantation and ischemia/reperfusion which correlated with better graft function and survival. Overall PGs are crucially involved in tissue remodeling after transplantation and promising intervention molecules to retard CTD.

References

1. van den Born J, Gunnarsson K, Bakker MA, Kjellen L, Kusche-Gullberg M, Maccarana M, et al. Presence of N-unsubstituted glucosamine units in native heparan sulfate revealed by a monoclonal antibody. *J Biol Chem* 1995 Dec 29;270(52):31303-31309.
2. Maccarana M, Casu B, Lindahl U. Minimal sequence in heparin/heparan sulfate required for binding of basic fibroblast growth factor. *J Biol Chem* 1993 Nov 15;268(32):23898-23905.
3. Morita H, Shinzato T, David G, Mizutani A, Habuchi H, Fujita Y, et al. Basic fibroblast growth factor-binding domain of heparan sulfate in the human glomerulosclerosis and renal tubulointerstitial fibrosis. *Lab Invest* 1994 Oct;71(4):528-535.
4. Jiang B, Yamamura S, Nelson PR, Mureebe L, Kent KC. Differential effects of platelet-derived growth factor isoforms on human smooth muscle cell proliferation and migration are mediated by distinct signaling pathways. *Surgery* 1996 Aug;120(2):427-31; discussion 432.
5. Myllarniemi M, Calderon L, Lemstrom K, Buchdunger E, Hayry P. Inhibition of platelet-derived growth factor receptor tyrosine kinase inhibits vascular smooth muscle cell migration and proliferation. *FASEB J* 1997 Nov;11(13):1119-1126.
6. Chen PY, Simons M, Friesel R. FRS2 via fibroblast growth factor receptor 1 is required for platelet-derived growth factor receptor beta-mediated regulation of vascular smooth muscle marker gene expression. *J Biol Chem* 2009 Jun 5;284(23):15980-15992.
7. Abramsson A, Kurup S, Busse M, Yamada S, Lindblom P, Schallmeiner E, et al. Defective N-sulfation of heparan sulfate proteoglycans limits PDGF-BB binding and pericyte recruitment in vascular development. *Genes Dev* 2007 Feb 1;21(3):316-331.
8. Ikesue M, Matsui Y, Ohta D, Danzaki K, Ito K, Kanayama M, et al. Syndecan-4 deficiency limits neointimal formation after vascular injury by regulating vascular smooth muscle cell proliferation and vascular progenitor cell mobilization. *Arterioscler Thromb Vasc Biol* 2011 May;31(5):1066-1074.
9. Segev A, Nili N, Strauss BH. The role of perlecan in arterial injury and angiogenesis. *Cardiovasc Res* 2004 Sep 1;63(4):603-610.
10. Kinsella MG, Tran PK, Weiser-Evans MC, Reidy M, Majack RA, Wight TN. Changes in perlecan expression during vascular injury: role in the inhibition of smooth muscle cell proliferation in the late lesion. *Arterioscler Thromb Vasc Biol* 2003 Apr 1;23(4):608-614.
11. Bingley JA, Hayward IP, Campbell JH, Campbell GR. Arterial heparan sulfate proteoglycans inhibit vascular smooth muscle cell proliferation and phenotype change *in vitro* and neointimal formation *in vivo*. *J Vasc Surg* 1998 Aug;28(2):308-318.
12. Tran PK, Agardh HE, Tran-Lundmark K, Ekstrand J, Roy J, Henderson B, et al. Reduced perlecan expression and accumulation in human carotid atherosclerotic lesions. *Atherosclerosis* 2007 Feb;190(2):264-270.
13. Kinsella MG, Irvin C, Reidy MA, Wight TN. Removal of heparan sulfate by heparinase treatment inhibits FGF-2-dependent smooth muscle cell proliferation in injured rat carotid arteries. *Atherosclerosis* 2004 Jul;175(1):51-57.
14. Celie JW, Rutjes NW, Keuning ED, Soininen R, Heljasvaara R, Pihlajaniemi T, et al. Subendothelial heparan sulfate proteoglycans become major L-selectin and monocyte chemoattractant protein-1 ligands upon renal ischemia/reperfusion. *Am J Pathol* 2007 Jun;170(6):1865-1878.
15. Lortat-Jacob H, Grosdidier A, Imberty A. Structural diversity of heparan sulfate binding domains in chemokines. *Proc Natl Acad Sci U S A* 2002 Feb 5;99(3):1229-1234.
16. Masola V, Gambaro G, Tibaldi E, Brunati AM, Gastaldello A, D'Angelo A, et al. Heparanase and syndecan-1 interplay orchestrates FGF-2-induced epithelial-mesenchymal transition in renal tubular cells. *J Biol Chem* 2011 Nov 18.
17. Kawashima H, Watanabe N, Hirose M, Sun X, Atarashi K, Kimura T, et al. Collagen XVIII, a basement membrane heparan sulfate proteoglycan, interacts with L-selectin and monocyte chemoattractant protein-1. *J Biol Chem* 2003 Apr 11;278(15):13069-13076.

18. Kawashima H, Li YF, Watanabe N, Hirose J, Hirose M, Miyasaka M. Identification and characterization of ligands for L-selectin in the kidney. I. Versican, a large chondroitin sulfate proteoglycan, is a ligand for L-selectin. *Int Immunol* 1999 Mar;11(3):393-405.
19. Celie JW, Reijmers RM, Slot EM, Beelen RH, Spaargaren M, Ter Wee PM, et al. Tubulointerstitial heparan sulfate proteoglycan changes in human renal diseases correlate with leukocyte influx and proteinuria. *Am J Physiol Renal Physiol* 2008 Jan;294(1):F253-63.
20. Rutkowski JM, Boardman KC, Swartz MA. Characterization of lymphangiogenesis in a model of adult skin regeneration. *Am J Physiol Heart Circ Physiol* 2006 Sep;291(3):H1402-10.
21. Labropoulou VT, Theocharis AD, Ravazoula P, Perimenis P, Hjerpe A, Karamanos NK, et al. Versican but not decorin accumulation is related to metastatic potential and neovascularization in testicular germ cell tumours. *Histopathology* 2006 Dec;49(6):582-593.
22. Yin X, Johns SC, Lawrence R, Xu D, Reddi K, Bishop JR, et al. Lymphatic endothelial heparan sulfate deficiency results in altered growth responses to vascular endothelial growth factor-C (VEGF-C). *J Biol Chem* 2011 Apr 29;286(17):14952-14962.
23. Elenius K, Vainio S, Laato M, Salmivirta M, Thesleff I, Jalkanen M. Induced expression of syndecan in healing wounds. *J Cell Biol* 1991 Aug;114(3):585-595.
24. Alexopoulou AN, Multhaupt HA, Couchman JR. Syndecans in wound healing, inflammation and vascular biology. *Int J Biochem Cell Biol* 2007;39(3):505-528.
25. Stepp MA, Gibson HE, Gala PH, Iglesia DD, Pajoohesh-Ganji A, Pal-Ghosh S, et al. Defects in keratinocyte activation during wound healing in the syndecan-1-deficient mouse. *J Cell Sci* 2002 Dec 1;115(Pt 23):4517-4531.
26. Watanabe A, Mabuchi T, Satoh E, Furuya K, Zhang L, Maeda S, et al. Expression of syndecans, a heparan sulfate proteoglycan, in malignant gliomas: participation of nuclear factor-kappaB in upregulation of syndecan-1 expression. *J Neurooncol* 2006 Mar;77(1):25-32.
27. Jaakkola P, Jalkanen M. Transcriptional regulation of Syndecan-1 expression by growth factors. *Prog Nucleic Acid Res Mol Biol* 1999;63:109-138.
28. Jaakkola P, Vihinen T, Jalkanen M. Proximal promoter-independent activation of the far-upstream FGF-inducible response element of syndecan-1 gene. *Biochem Biophys Res Commun* 2000 Nov 19;278(2):432-439.
29. Loverre A, Ditonno P, Crovace A, Gesualdo L, Ranieri E, Pontrelli P, et al. Ischemia-reperfusion induces glomerular and tubular activation of proinflammatory and antiapoptotic pathways: differential modulation by rapamycin. *J Am Soc Nephrol* 2004 Oct;15(10):2675-2686.
30. Villanueva S, Cespedes C, Vio CP. Ischemic acute renal failure induces the expression of a wide range of nephrogenic proteins. *Am J Physiol Regul Integr Comp Physiol* 2006 Apr;290(4):R861-70.
31. Hayashida K, Johnston DR, Goldberger O, Park PW. Syndecan-1 expression in epithelial cells is induced by transforming growth factor beta through a PKA-dependent pathway. *J Biol Chem* 2006 Aug 25;281(34):24365-24374.
32. Liu Y. Renal fibrosis: new insights into the pathogenesis and therapeutics. *Kidney Int* 2006 Jan;69(2):213-217.
33. Stein-Oakley AN, Tzanidis A, Fuller PJ, Jablonski P, Thomson NM. Expression and distribution of epidermal growth factor in acute and chronic renal allograft rejection. *Kidney Int* 1994 Oct;46(4):1207-1215.
34. Jalkanen M, Rapraeger A, Saunders S, Bernfield M. Cell surface proteoglycan of mouse mammary epithelial cells is shed by cleavage of its matrix-binding ectodomain from its membrane-associated domain. *J Cell Biol* 1987 Dec;105(6 Pt 2):3087-3096.
35. Manon-Jensen T, Itoh Y, Couchman JR. Proteoglycans in health and disease: the multiple roles of syndecan shedding. *FEBS J* 2010 Aug 31.
36. Pruessmeyer J, Martin C, Hess FM, Schwarz N, Schmidt S, Kogel T, et al. A disintegrin and metalloproteinase 17 (ADAM17) mediates inflammation-induced shedding of syndecan-1 and -4 by lung epithelial cells. *J Biol Chem* 2010 Jan 1;285(1):555-564.
37. Mulder GM, Melenhorst WB, Celie JW, Kloosterhuis NJ, Hillebrands JL, Ploeg RJ, et al. ADAM17 up-regulation in renal transplant dysfunction and non-transplant-related renal fibrosis. *Nephrol Dial Transplant* 2011 Oct 19.

38. van Timmeren MM, Vaidya VS, van Ree RM, Oterdoom LH, de Vries AP, Gans RO, et al. High urinary excretion of kidney injury molecule-1 is an independent predictor of graft loss in renal transplant recipients. *Transplantation* 2007 Dec 27;84(12):1625-1630.
39. Malyszko J, Koc-Zorawska E, Malyszko JS, Mysliwiec M. Kidney injury molecule-1 correlates with kidney function in renal allograft recipients. *Transplant Proc* 2010 Dec;42(10):3957-3959.
40. Nauta FL, Bakker SJ, van Oeveren W, Navis G, van der Heide JJ, van Goor H, et al. Albuminuria, proteinuria, and novel urine biomarkers as predictors of long-term allograft outcomes in kidney transplant recipients. *Am J Kidney Dis* 2011 May;57(5):733-743.
41. Vongwiwatana A, Tasanarong A, Rayner DC, Melk A, Halloran PF. Epithelial to mesenchymal transition during late deterioration of human kidney transplants: the role of tubular cells in fibrogenesis. *Am J Transplant* 2005 Jun;5(6):1367-1374.
42. Dredge K, Hammond E, Handley P, Gonda TJ, Smith MT, Vincent C, et al. PG545, a dual heparanase and angiogenesis inhibitor, induces potent anti-tumour and anti-metastatic efficacy in preclinical models. *Br J Cancer* 2011 Feb 15;104(4):635-642.
43. Lindahl U. Heparan sulfate-protein interactions--a concept for drug design? *Thromb Haemost* 2007 Jul;98(1):109-115.
44. Lindahl U, Li JP. Interactions between heparan sulfate and proteins--design and functional implications. *Int Rev Cell Mol Biol* 2009;276:105-159.
45. Fuster MM, Esko JD. The sweet and sour of cancer: glycans as novel therapeutic targets. *Nat Rev Cancer* 2005 Jul;5(7):526-542.
46. Nowak G. Heparin-induced thrombocytopenia (HIT II) - a drug-associated autoimmune disease. *Thromb Haemost* 2009 Nov;102(5):887-891.
47. Gottmann U, Mueller-Falcke A, Schnuelle P, Birck R, Nিকেleit V, van der Woude FJ, et al. Influence of hypersulfated and low molecular weight heparins on ischemia/reperfusion: injury and allograft rejection in rat kidneys. *Transpl Int* 2007 Jun;20(6):542-549.
48. Braun C, Schultz M, Fang L, Schaub M, Back WE, Herr D, et al. Treatment of chronic renal allograft rejection in rats with a low-molecular-weight heparin (reviparin). *Transplantation* 2001 Jul 27;72(2):209-215.
49. Frank RD, Schabbauer G, Holscher T, Sato Y, Tencati M, Pawlinski R, et al. The synthetic pentasaccharide fondaparinux reduces coagulation, inflammation and neutrophil accumulation in kidney ischemia-reperfusion injury. *J Thromb Haemost* 2005 Mar;3(3):531-540.
50. Yard BA, Lorentz CP, Herr D, van der Woude FJ. Sulfation-dependent down-regulation of interferon-gamma-induced major histocompatibility complex class I and II and intercellular adhesion molecule-1 expression on tubular and endothelial cells by glycosaminoglycans. *Transplantation* 1998 Nov 15;66(9):1244-1250.
51. Shapira OM, Rene H, Lider O, Pfeffermann RA, Shemin RJ, Cohen IR. Prolongation of rat skin and cardiac allograft survival by low molecular weight heparin. *J Surg Res* 1999 Jul;85(1):83-87.
52. Braun C, Schultz M, Schaub M, Fang L, Back WE, Herr D, et al. Effect of treatment with low-molecular-weight heparin on chronic renal allograft rejection in rats. *Transplant Proc* 2001 Feb-Mar;33(1-2):363-365.
53. Spirig R, Gajanayake T, Korsgren O, Nilsson B, Rieben R. Low molecular weight dextran sulfate as complement inhibitor and cytoprotectant in solid organ and islet transplantation. *Mol Immunol* 2008 Oct;45(16):4084-4094.
54. Coffey AK, Karnovsky MJ. Heparin inhibits mesangial cell proliferation in habu-venom-induced glomerular injury. *Am J Pathol* 1985 Aug;120(2):248-255.
55. Floege J, Eng E, Young BA, Couser WG, Johnson RJ. Heparin suppresses mesangial cell proliferation and matrix expansion in experimental mesangioproliferative glomerulonephritis. *Kidney Int* 1993 Feb;43(2):369-380.
56. Krzossok S, Birck R, Koepfel H, Schnulle P, Waldherr R, van der Woude FJ, et al. Treatment of proteinuria with low-molecular-weight heparin after renal transplantation. *Transpl Int* 2004 Sep;17(8):468-472.
57. Packham DK, Wolfe R, Reutens AT, Berl T, Heerspink HL, Rohde R, et al. Sulodexide Fails to Demonstrate Renoprotection in Overt Type 2 Diabetic Nephropathy. *J Am Soc Nephrol* 2011 Oct 27.

58. Callas DD, Hoppensteadt DA, Jeske W, Iqbal O, Bacher P, Ahsan A, et al. Comparative pharmacologic profile of a glycosaminoglycan mixture, Sulodexide, and a chemically modified heparin derivative, Suleparoid. *Semin Thromb Hemost* 1993;19 Suppl 1:49-57.
59. Rops AL, van den Hoven MJ, Baselmans MM, Lensen JF, Wijnhoven TJ, van den Heuvel LP, et al. Heparan sulfate domains on cultured activated glomerular endothelial cells mediate leukocyte trafficking. *Kidney Int* 2008 Jan;73(1):52-62.
60. Johnson Z, Proudfoot AE, Handel TM. Interaction of chemokines and glycosaminoglycans: a new twist in the regulation of chemokine function with opportunities for therapeutic intervention. *Cytokine Growth Factor Rev* 2005 Dec;16(6):625-636.
61. Bedke J, Nelson PJ, Kiss E, Muenchmeier N, Rek A, Behnes CL, et al. A novel CXCL8 protein-based antagonist in acute experimental renal allograft damage. *Mol Immunol* 2010 Feb;47(5):1047-1057.

**Nederlandse samenvatting voor niet-
ingewijden**

Written in English by Kirankumar Katta
Translated by Jacob van den Born

Niertransplantatie

Niertransplantatie is de beste behandeling voor patiënten met eindstadium nierfalen met betrekking tot kwaliteit van leven en levensverwachting. Door verschillende oorzaken, waaronder toenemende leeftijd en incidentie van vetzucht en diabetes, neemt het aantal patiënten met nierfalen wereldwijd toe. Als gevolg daarvan is er ook een grotere behoefte aan donornieren. In 2010 werden in Nederland meer dan 800 niertransplantaties uitgevoerd, waarvan de helft met nieren van levende donoren. Daarnaast staan er in Nederland meer dan 900 patiënten op de wachtlijst voor een niertransplantatie; de gemiddelde wachttijd voor een donornier afkomstig van een overleden donor is inmiddels langer dan 4 jaar. Door het gebruik van nieuwe afweeronderdrukkende medicijnen is de incidentie van acute afstoting van getransplanteerde nieren de laatste jaren sterk afgenomen. De langetermijnoverleving van getransplanteerde nieren is echter nauwelijks verbeterd in de afgelopen 30 jaar. Dit heeft vooral te maken met de ontwikkeling van chronisch transplantaatfalen van de getransplanteerde nier. Chronisch transplantaatfalen is geassocieerd met achteruitgang van nierfunctie en toenemende verbindweefseling van de getransplanteerde nier. De oorzaken hiervan zijn multifactorieel en deels immunologisch, en deels niet-immunologisch van aard. De verbindweefseling wordt vooral gezien in de filterorgaantjes, de glomeruli (ontwikkeling glomerulosclerose), aan de binnenzijde van de grote bloedvaten (ontwikkeling transplantatie arteriopathie of neointimavorming) en in het bindweefsel tussen de nierbuisjes (ontwikkeling interstitiële fibrose). Algemeen gesproken speelt een groot aantal mediators een rol bij deze verbindweefseling. Veel van deze mediators zijn uitsluitend werkzaam in de aanwezigheid van proteoglycanen. Proteoglycanen vormen een diverse groep complexe eiwit-suiker verbindingen die als co-receptoren een rol spelen bij de weefsel remodellering. Dit is al langer bekend bij weefselveranderingen zoals die worden gezien bij embryonale ontwikkeling, wondgenezing en tumorgroei, maar of vergelijkbare mechanismen ook optreden bij chronisch transplantaatfalen na niertransplantatie is niet bekend. De meeste biologische effecten van proteoglycanen worden bepaald door de binding van de mediators betrokken bij weefselveranderingen. Daarom lijkt het voor de hand liggend om uit te zoeken of therapeutisch ingrijpen in de proteoglycaan – mediator interactie bescherming kan bieden tegen chronisch transplantaatfalen. Dit onderzochten we in een serie experimenten in een rattenmodel voor chronisch transplantaatfalen, en in nierbiopsieën uit getransplanteerde nieren bij de mens.

In **hoofdstuk 2** tonen wij in dit model aan dat er bij chronisch transplantaatfalen een ophoping van de proteoglycanen perlecan en collageen XVIII plaatsvindt in de glomeruli en neointima's van getransplanteerde nieren. In het bindweefsel tussen de tubuli wordt het proteoglycaan versican verhoogd aangetroffen, alsmede een sterk verhoogd aantal lymfevaten. Het aantal lymfevaten correleert met de mate van interstitiële verbindweefseling en verminderde nierfunctie.

In **hoofdstuk 3** isoleren we met behulp van laserdissectiemicroscopie glomeruli en neointima's uit nierweefsel van getransplanteerde ratten. In dit weefsel worden een aantal mRNA transcripten gekwantificeerd. We ontdekken dat er naast de ophoping van perlecan ook een groeifactor is die op deze locaties verhoogd wordt aangemaakt. Het gaat hier om basic fibroblast growth factor (FGF2). In celkweekexperimenten laten we vervolgens zien dat FGF2 heparansulfaatproteoglycanen nodig heeft om niercellen te laten groeien, maar ook dat therapeutische interventie met aan heparansulfaat gerelateerde polysacchariden deze proliferatieve respons afremt.

De bevindingen in **hoofdstuk 3** gaven ons aanleiding om een interventiestudie met heparinoïden uit te voeren in het chronisch niertransplantatiemodel in de rat. Dit onderzoek staat beschreven in **hoofdstuk 4**. Naast interventie met gewone heparine (een polysaccharide die nauw verwant is aan heparansulfaten) werd geïntervenieerd met twee verschillende non-anticoagulante heparinoïden. Alhoewel de heparinoïdeninterventie geen effecten had op transplantaatoverleving of nierfunctie, werd toch een aantal opmerkelijke bevindingen gedaan. Behandeling met RO-heparine, een van de twee non-anticoagulante heparines, verminderde de instroom van ontstekingscellen in de nier en verbeterde de plasma triglyceridewaarden, die verhoogd waren in de onbehandelde transplantatiegroep. Bovendien was er een tendens tot verminderde eiwitlekage in de urine en vermindering van glomerulosclerose bij behandeling met hetzelfde RO-heparine. Verder onderzoek dient uit te wijzen of het gebruik van laag moleculair gewicht heparinoïden of een verhoging van de dosering tot betere resultaten zal leiden.

In **hoofdstuk 5** proberen we te ontrafelen welke moleculaire processen leiden tot neointimavorming in de nierarteriën na niertransplantatie. Daarom werden in het ratten-niertransplantatiemodel met behulp van laserdissectiemicroscopie de media en neointima geïsoleerd en de transcripten van een groot aantal mediators gekwantificeerd. In vergelijking met controlevaten vertonen de mediale gladde spiercellen minder contractiele kenmerken, en meer synthetische en migratoire kenmerken. Zeer waarschijnlijk spelen de groeifactoren platelet derived growth factor B en transforming growth factor beta hierbij een cruciale rol door inductie van de migratie van deze gladde spiercellen van de media naar de neointima, en dragen ze zo bij aan de transplantatie-arteriopathie.

In **hoofdstuk 6** tenslotte, wordt de brug geslagen naar niertransplantatie bij de mens. Na een evaluatie van verschillende proteoglycanen in humane transplantatiebiopten wordt een uitvoerige studie gedaan naar de expressie van syndecan-1, een epitheliaal celoppervlakgebonden heparansulfaatproteoglycaan. Het blijkt dat in de biopten afkomstig van getransplanteerde patiënten de expressie van syndecan-1 in tubulusepithelcellen correleert met betere transplantaatoverleving, verbeterde nierfunctie en minder histologische afwijkingen in de biopten. Experimenten met gekweekte niercellen tonen aan dat syndecan-1 belangrijk is voor de regeneratie van tubulusepithel. Dit laatste konden we vervolgens ook overtuigend aantonen in een muismodel, waarin expressie van syndecan-1 met behulp van genetische manipulatie werd voorkomen.

Vervolgonderzoek moet duidelijk maken of non-anticoagulante heparinoïden een rol kunnen spelen bij de bescherming van de getransplanteerde nier, naast de gebruikelijke medicatie die wordt gegeven om chronisch transplantaatfalen te voorkomen of af te remmen. Daarnaast moet vervolgonderzoek duidelijk maken of de expressie van syndecan-1 in protocolaire nierbiopten en/of de uitscheiding van syndecan-1 in de urine van niertransplantatie patiënten een voorspellende waarde hebben voor het functioneren van de getransplanteerde nieren op langere termijn.



Dankwoord

Four years of research! Four years of memorable moments in Groningen!

It feels wonderful today to complete this thesis. This would not have been possible without constant support from supervisors, friends and family. I owe my best thanks to all these people, without their help it would have been impossible to compile my works into this thesis.

First and foremost, I extend my sincere gratitude to dr. Jacob van den Born (Jaap) for providing me with constant motivation and nourishing my enthusiasm towards research. Jaap, apart from being a dedicated supervisor you are a very kind and friendly person. Your way of handling any situation with a beaming smile has been a constant support to me during my research and thesis writing. Your thought provoking Wednesday meetings and timely planning were crucial in enabling me to complete my thesis on time. I thank you for introducing me to the wonderful world of proteoglycans. I appreciate your enormous knowledge and passion for these molecules. Your positive problem solving approach and constant encouragement have been a great help to me. You have always been active, energetic and full of novel ideas which helped me a lot throughout my doctoral research. I respect and appreciate the way you make fruitful collaborations. I have learnt a lot from you, of special note are interpretation and right presentation of data. I thank you for the hours you spent on reading, discussing and correcting my manuscripts and this thesis. Apart from research, personally I feel that you take care of your students like a guardian who imbibes positive thinking. I sincerely owe a lot to you.

My sincere thanks to my two promotores prof. dr. Gerjan Navis and prof. dr. Jan-Luuk Hillebrands. Their suggestions and critical comments were helpful and encouraging. The positive comments and appreciations from them were always inspiring and gave me loads of energy and maintained my enthusiasm for research. I thank you for those quick responses to my queries and for comments on my manuscripts. The yearly evaluations and constructive comments significantly gave speed and improved the quality of my research. Special thanks to Jan-Luuk for the help and support I got from you during these four years of research.

I would further like to extend these words of gratitude to the members of the reading committee who readily accepted our request to evaluate my thesis. I thank prof. dr. R.A. Bank, prof. dr. J.H.M. Berden and prof. dr. L. Schaefer for their time and kind support.

Prof. dr. Harry van Goor, thank you for granting me permission to use various precious renal materials for my research. I admire your immense knowledge and experience in renal pathology.

I thank dr. Marc Seelen and prof. dr. Moh Daha for their valuable suggestions and comments which were of great help during my research work.

I would like to thank my colleagues who made my time in the lab pleasant and memorable. I thoroughly enjoyed the discussions we had during Wednesday morning meetings, I appreciate you all for your valuable suggestions which resulted in a significant addition to my research. A special mention to our lab technicians Jelleke, Edis, Wendy and Anita whose presence meant that all the things are well organized in the lab. I would also like to thank technicians from other departments Ali, Annie, Jasper, Linda, Martin, Peter and Silke. It was great fun to work in such an international environment which helped me in getting acquainted with the local environment. I am happy having shared my work place with you all. I will always cherish those wonderful parties, lab dinners, coffee breaks and birthday cakes which we had together. I admire the skills and strengths of all of you: Jelleke, Azi, Anna, Katarina, Carolien, Pramod, Saleh, Shanthi, Maaïke, Leandro, Rianne, Menno, Kim, Willemien, Milton, Eva, Stephanie and Saritha. Your suggestions and complements were quite inspiring for me during tough times. I thank you all for the help that I received whenever necessary. I enjoyed every moment in the lab and share a special bond with each of you. It would be mean to say just thanks!

Thank you Heleen and Patricia, it was great working with both of you. You have contributed a lot to my thesis. I learned a lot from your experience. Also, thanks for your critical comments and suggestions.

I would like to thank my good friend and colleague Miriam Boersema from Groningen for her great help and for always being kind. In the beginning of my PhD, you have helped me with many techniques and explained the basic clinical terms with a lot of patience. I can't forget your help during winter school, my first Nefrologiedagen and the PLAN-dag. I enjoyed working with you and I learned a lot from you.

I would like to thank fellow PhD students from UMCG for the great time we had during conferences and also at the UMCG. Alaa, Arjan, Astrid, Betty, Dorien, Eelke, Else, Esther, Femke, Ferdau, Folkert, Gemma, Hiddo, Hilde, Lieneke, Jan, Jeffrey, Jelena, Leendert, Maartje, Marije, Maaïke, Martin, Merel, Mieneke, Mirjan, Nynke, Pauline, Rutger, Sacha, Sander, Solmaz, Steef, Tsjitske, and Giuseppe (may your soul rest in peace). Beside the PhD students I would like to thank the following people for their contribution to a successful PhD project.

I would like to thank the students who worked with me: Jeroen, Maarten, Edwin, Ditmer, Menno and Jozine. Special thanks to Ditmer for his great help during my animal experiment and for the proper sample organisations.

I would like to thank GUIDE, especially, Riekje, Mathilde, and Maaïke for their great assistance. I am grateful to Anneke Toxopeus (ISD, Groningen) for helping me out with my residence permit and tax queries. Also I would like to thank Winie for assisting me with all the official things in the department. I would also like to thank people from our neighbouring departments Clinical Pharmacology, Experimental Cardiology and Molecular Virology. Marry thank you for the skating lessons and the fun we had together.

Also, I would like to thank all the people from CDL (André, Annemieke, Annemiek, Arie, Alex, Catriene, Flip, Hester, Michel, Miriam, Maurice, Natascha, Pieter, Silvia, Yvonne and Wiebe) for their extensive assistance and help.

Special thanks to my lovely Suriname family: Meena, Vinod, Vinay, Nawina and Vineesh. I can't express in words the love and assistance you gave me during my two and half year stay in Lewenborg. My deepest thanks to Meena and Vinod for being my guardians in the Netherlands and taking care of me with an unflagged love and affection. Vineesh, I really enjoyed the conversation we had during our fitness time. Nawina, thanks for making quesadilla and a lot varieties of cupcakes and desserts. Thanks for treating me as a member of your family.

Groningen gave me many good friends, to start with Pramod, you have always been active in all the social events, inspiring and encouraging all the time. Ganesh, just rocking! I had great party times with you guys. For the first two years we three shared a house, I must say that I had a great time guys (organizing lots of parties and outings). I thank Subha (Ganesh) and Meena (Pramod) better halves of my very good friends for having understood my friendship. Akshay, thank you for introducing me to Indian stores and shopping complexes in Groningen. I can't forget how difficult it was for me to buy my first bicycle but unfortunately within a short while I easily lost it. I wish you a happy married life with Spoorthi. Gopi, thanks for funny talks that we had. You are a good human being and have always treated me as a younger brother by ignoring my kidding nature (but with too much complaining). Not only people from Groningen but also our "Skövde group" including Twinkal sorry dr. Twinkal and Rishi. Our trips to various places in The Netherlands were joyful. Soni, thanks for organizing lot of get-togethers, movie nights and games. Vikram, thank you for your good company. I admire your poetic skills and thanks for writing a song about me. Rajender, Raja and Sunil, I know you guys for a short while but enjoyed being with you guys. Shanthi and Elango thank you for warm and nice dinners during my thesis writing. Last but not least, Saritha, it was great time being with you. Thank you for your caring nature and listening to all my stories with great interest (without complaining). Apart from being a good friend, you also contributed a lot to my research. You were a great help at the stages of my doctoral studies and I enjoyed working with you. My deepest thanks to

all Groningen Indian friends. It was nice meeting you all every now and then in GISA get-togethers. I would also like to extend my thanks to my international friends from the student house (VHL). I would like to thank all my friends from India. You all made my stay in Groningen pleasant and I respect you all for that. I wish you all a great future ahead!

Finally my enormous gratitude goes to my family for their infinite love and affection. Thanks to my Mother, for sharing all my bad and good times in my life and guiding me on right path. I agree that a mother plays an important role in building up her child's future. She has always been caring and at the same time correcting my mistakes in life. Deepest thanks to my dad!!!! I cannot explain in words the support he gave me in life. His motivating and inspiring conversations made my life easier and comfortable. I have been missing them all during my stay abroad, their immense support and love throughout my life have made me a man of integrity and have given me a good foundation to stand for what I believe in. Thanks to my brothers Suresh and Praveen!!! I had a great time with you guys (lot of funny parties and unforgettable happy moments). Many thanks to my fiancée Shruthi for accepting me in her life. A happy ending of my PhD life has brought me joy in my personal and professional front. Shruthi, you make me laugh and bring a smile on my face. Thank you for all the care that you show for me.

I sincerely would like to dedicate this thesis to my parents and honestly, they deserve it. Mom and dad on my defense I will miss you both!

Curriculum vitae

Personal details

Name: Kirankumar Katta
Place of birth: Vemulawada, Andhra Pradesh, India
Email: kirankatta1984@gmail.com
Date of birth: August 15th, 1984

Education and Experience

- 2007-2012 PhD
University of Groningen, The Netherlands
- Project Title: Role of Proteoglycans in renal chronic transplant dysfunction
Supervision: dr. Jacob van den Born, Prof. dr. G.J. Navis and Prof. dr. JL. Hillebrands
Department of Internal medicine (Experimental Nephrology).
- 2006-2007 Master of science (Molecular Biology)
University of Skövde, Sweden
- Master thesis title: Identification of interaction partners of STAT 1
Supervision: Prof. dr. U. Vinkemeier
Leibniz-Institut für Molekulare Pharmakologie
Berlin, Germany
- 2002 – 2005 Bachelor of Science (Biotechnology)
Nizam college, Osmania University,
Hyderabad, India

List of publications

Katta K, Adepu S, Talsma D, Agarwal PK, Yazdani S, Naggi A, Torri G, Navis G, Hillebrands JL, Van den Born J. Role of non-anticoagulant heparinoids in rat chronic renal transplant dysfunction model (in preparation)

Katta K, Boersema M, Rienstra H, Celie JW, van Goor H, Berden J, Navis G, Hillebrands JL, van den Born J. Renal heparan sulfate proteoglycans modulate FGF2 signaling in experimental chronic transplant dysfunction (Submitted to *Journal of American Society of Nephrology* and under revision)

Boersema M, **Katta K**, Rienstra H, Nguyen T, Goldschmeding R, Navis G, Van den Born J, Popa ER, Hillebrands JL. Local medial microenvironment direct smooth muscle cell dedifferentiation after experimental renal transplantation. *Am J Transplant.* 2012 Mar 15. doi: 10.1111/j.1600-6143.2012.04001.x.

Celie JW*, **Katta K***, Adepu S, Melenhorst WBWH, Reijmers RM, Slot EM, Beelen RHJ, Spaargaren M, Ploeg RJ, Navis G, Van der Heide JJH, van Dijk MCRF, Van Goor H, Van den Born J. Tubular epithelial syndecan-1 maintains renal function in murine ischemia/reperfusion and human transplantation. (equally contributed). *Kidney Int.* 2012 Apr;81(7):651-61

Katta K*, Rienstra H*, Celie JW, van Goor H, Navis G, van den Born J, Hillebrands JL. Differential expression of proteoglycans in tissue remodeling and lymphangiogenesis after experimental renal transplantation in rats. *PLoS One* 2010, Feb 5;5(2):e9095 (equally contributed)

